Integrating regulatory mechanisms of Wnt signaling in development and tissue homeostasis

by

Eric Hall

B.Sc, University of British Columbia, 2011

Thesis Submitted in Partial Fulfillment of the
Requirements for the Degree of
Doctor of Philosophy

in the
Department of Molecular Biology & Biochemistry
Faculty of Science

SIMON FRASER UNIVERSITY
Fall 2017

Approval

Name:	**Eric Hall**
Degree:	**Doctor of Philosophy**
Title:	**Integrating regulatory mechanisms of Wnt signaling in development and tissue homeostasis**
Examining Committee:	**Chair: Mark Brockman** Professor
	Esther Verheyen Senior Supervisor Professor
	Nicholas Harden Supervisor Professor
	Michel Leroux Supervisor Professor
	Sharon Gorski Internal Examiner Professor
	William Brook External Examiner Associate Professor Department of Biochemistry and Molecular Biology Department of Medical Genetics University of Calgary
Date Defended/Approved:	October 24, 2017

Abstract

Evolutionarily conserved signal transduction pathways mediate the ability of cells to respond to their environment and coordinate with each other for proper development and homeostasis of an organism. The Wnt/Wingless (Wg) pathway is required for proliferation, differentiation, stem-cell renewal and homeostasis, and when disrupted leads to disease. Wnt signaling does not control all these processes alone, its activity is extensively regulated by interaction with other signaling pathways and cellular mechanisms. This is mediated predominantly through phospho-regulation of the key pathway components by kinases and phosphatases. Our lab conducted an *in vivo* RNAi screen designed to identify novel kinase and phosphatase regulators of the Wnt pathway. In my PhD thesis research I further characterized three potential regulators: Downstream of Raf1 (Dsor1), Protein phosphatase 4 (PP4), and myosin phosphatase.

Knockdown of Dsor1 reduced Wnt target gene expression and decreased stabilized β-catenin, the key effector protein of the Wnt pathway. Dsor1 and β-catenin had a close physical interaction, and catalytically inactive Dsor1 caused a reduction in active β-catenin, suggesting that Dsor1 counteracts destruction of β-catenin. Additionally, Ras-Dsor1 activity was independent of EGFR, and likely activated by the insulin-like receptor to promote Wnt. This work demonstrates novel crosstalk between Insulin and Wnt signaling via Dsor1. The reduction of PP4 inhibited Wg pathway activity, by reducing Notch-driven *wg* transcription. PP4 was found to promote Notch signaling within the nucleus of the receiving cell. Furthermore, PP4 regulates proliferation independently of its Notch interaction. This study identified a new role for PP4 in Notch signaling, and subsequently transcriptional regulation of *wg*. Reduced myosin phosphatase inhibited Wnt signaling by causing increased non-muscle myosin II (NMII) activation and cellular contraction. NMII activation stabilizes cortical F-actin resulting in accumulation of E-cadherin to the adherens junctions (AJ). E-cadherin titrates available β-catenin to the AJs in order to maintain cell-cell adhesion under contraction. The decreased cytoplasmic β-catenin results in insufficient nuclear translocation for full Wnt target gene transcription. This work elucidates that the dynamic activation of actomyosin contractility refines patterning of Wnt target gene expression.

These studies identified three novel regulatory mechanisms for controlling Wnt signaling in development and homeostasis.

Keywords: Wnt; Wingless; Dsor1; PP4; NMII

To my Grandfather, Dr. John V. G. Hall

Your love of the natural world and all it holds, and your drive to foster my curiosity and love of science has guided me here.

Acknowledgements

I wish to express my sincerest thanks and appreciation to my senior supervisor, Dr. Esther Verheyen for all the guidance and support over the years. Esther, you have been an excellent mentor. You have allowed me the freedom to find my way in the lab, while providing guidance and that extra push when I needed it. Your availability to discuss any problems, or share exciting results has made me cherish my time in the lab.

I also want to thank my supervisory committee, Dr. Nicholas Harden and Dr. Michel Leroux for their support and ideas over the years. Whether it was determining a follow up experiment to some results, discussing where to send a manuscript, or sending out reference letters for scholarships, I could always count on a positive response. I also thank my thesis examiners Dr. Sharon Gorski and Dr. William Brook for evaluating my dissertation.

To the members of the Verheyen lab, you all kept me going and sane over the years. To those before me, Sharan Swarup, Tirthadipa Pradhan-Sundd, Vilaiwan Fernandes, and Jessica Blaquiere, your time and expertise taught me how to function and thrive in the lab. I'm here because of your friendship and help. To those who joined after, Nathan Wray, Elizabeth Hoesing, Kenneth Wong, Stephen Kinsey, Nicole Yoo and Endre Sinkovics, your help on experiments, discussions, and fun outside of the lab made the years memorable. I also want to thank all the people and friends in the department who I could shoot the breeze with in the hallways, or trouble shoot any problems on a daily basis.

Finally, thank you to all my friends and family. You always supported me and were proud of me, even if you weren't totally sure what I was doing. Your ability to help me relax and enjoy my time outside of the lab has kept me balanced and brought so much happiness to my life over the past years. To my wife Helen who is always there for me, in the lab late at night, at home, or anywhere you made this happen as well. I love you all.

Table of Contents

List of Figures

List of Acronyms

Wg	Wingless
En	Engrailed
Hh	Hedgehog
EGFR	Epidermal growth factor receptor
HSPG	Heparan sulfate proteoglycan
Arm	Armadillo
Sens	Sensless
Dll	Distal-less
Arr/LRP	Arrow/Low-density lipoprotein receptor-related protein
Fz	Frizzled
APC	Adenomatous polyposis coli
CK	Casein kinase
Gro	Groucho
Dvl/Dsh	Dishevelled
TCF	T-cell factor
LEF	Lymphoid enhancer factor
RTK	Receptor tyrosine kinase
MAPK	Mitogen-activated protein kinase
Sos	Son of sevenless
MEK	MAPK-extracellular signal-regulated kinase
Dsor1	Downstream of Raf1
ERK	Extracellular signal-regulated kinase
Rl	Rolled
Ci	Cubitus interruptus
Dpp	Decapentaplegic
GFP	Green fluorescent protein
RFP	Red fluorescent protein
Bs	Blistered
GPCR	G-protein coupled receptor
InR	Insulin-like growth factor receptor
PLA	Proximity ligation assay
N	Notch

Dl	Delta
D/V	Dorsal/Ventral
A/P	Anterior/Posterior
JNK	c-Jun N-terminal kinase
Flfl	Falafel
SOP	Sensory organ precursor
PP	Protein phosphatase
PH	Phospho-Histone
aPKC	Atypical protein kinase C
ACD	Asymmetrical cell division
AJ	Adherens junction
NMII	Non-muscle myosin II
MYPT	Myosin phosphatase targeting protein
MBS	Myosin binding subunit
Flw	Flapwing
Sqh	Spaghetti squash
Dia	Diaphanous
Shg	Shotgun
GSK3	Glycogen Synthase Kinase 3

Chapter 1. Wnt Signaling

1.1. Cell signal transduction pathways

For cells to grow, replicate and survive they must be able to sense and respond to their environment, and this is compounded in multicellular organisms where cells must also communicate and coordinate with one another. Cells manage this by utilizing a few evolutionarily conserved signal transduction pathways. These pathways are used reiteratively, both spatially and temporally, to form complex signaling networks that guide organismal development and homeostasis. These complex interactions of only a few signaling pathways allows for control of all cellular functions, as well as gives rise to the differentiation of countless cell types and other unique downstream events.

Signal transduction is initiated by a ligand (an environmental stimulus), which may come in the form of a protein, lipid, small molecule, radiation, binding to its receptor (Cooper, 2000a), to induce and relay the signal to the cell, usually resulting in a transcriptional change in expression of target genes. Depending on the complexity of the pathway, the signal from the receptor-ligand interaction may be relayed through multiple secondary messengers and effector molecules, increasing the complexity and specificity of the response. In addition to this, responses may vary depending on the concentration of the ligand, to induce a graded activation, or must overcome a threshold of activation (Affolter et al., 2008; Barolo and Posakony, 2002).

A few of the core signaling pathways that control cell differentiation during development are Wnt, Receptor Tyrosine Kinase (RTK), Hedgehog (Hh), Transforming growth factor-β (TGF- β), Janus kinase (JAK)/ Signal Transducer and Activator of Transcription (STAT), Hippo, Nuclear receptor, and Notch (N) (Barolo and Posakony, 2002; Cooper, 2000b). Combinatory interactions between these pathways drive development, and if disrupted, can lead to innumerable diseases and cancer (reviewed in Akhurst and Hata, 2012; Briscoe and Thérond, 2013; Clevers and Nusse, 2012; Lemmon and Schlessinger, 2010; Sonoda et al., 2008; Talora et al., 2008; Villarino et al., 2015).

1.2. The Wnt protein family

Wnt signaling consists of several distinct pathways, which are all initiated by Wnt proteins. The Wnt protein family comprises of secreted glycoproteins that control a diverse range of functions during development including axis formation, cell fate, proliferation, and migration (Kikuchi et al., 2011). The Wnt name originated from the identification that the *Drosophila* segment polarity gene *wingless* (*wg*) was the homolog of mouse *int-1*, the first known integration site of the Mouse Mammary Tumor Virus (Nusse and Varmus, 1982; Nüsslein-Volhard and Wieschaus, 1980; Rijsewijk et al., 1987). Therefore the hybrid name, Wingless-related integration site (Wnt) family of genes was born (Nusse et al., 1991).

To date, there have been 19 distinct *Wnt* genes identified in most mammalian genomes, falling into 12 of 13 conserved subfamilies (Clevers and Nusse, 2012; Janssen et al., 2010). *Wnt* genes are present in all multicellular organism, but have not been identified in single-cell life, suggesting their key importance for metazoans, in particular their requirement for axis formation (Kusserow et al., 2005).

Wnt proteins are defined by their 22 cysteine residues, which are thought to form disulfide bridges that maintain the secondary structure of the protein (Willert and Nusse, 2012). Wnts are also palmitoylated at a conserved serine residue to promote Wnt secretion (Takada et al., 2006). Wnt proteins are usually glycosylated as well, but the amount varies dramatically across different proteins and even individual Wnts may contain a variable glycosylation affecting its secretion, stability, and signaling outcomes (Doubravska et al., 2011; Komekado et al., 2007; Kurayoshi et al., 2007; Tang et al., 2012). The physical structure of Wnts has been exceedingly difficult to determine. To date only the structure of the *Xenopus* Wnt8 protein, bound to its receptor, has been determined (Janda et al., 2012). *Xenopus* Wnt8 is described as a ‘palm’, and ’thumb’, with ‘index finger’ grasping the receptor at two distinct binding sites (Janda et al., 2012) (Fig. 1.1) It is unclear if this structure is conserved with other Wnt proteins. Although there are several distinct Wnt pathways, there is no known specific sequence, or structure to a Wnt protein that can determine its signaling output (Willert and Nusse, 2012). It is likely that the cellular conditions play an important role in determining the signaling outcome for specific Wnts. i.e. Wnt5a, which is thought to be specific for controlling planar cell polarity (PCP), has also been shown to induce ‘canonical’ Wnt

signaling in certain conditions (He et al., 1997; Mikels and Nusse, 2006). This relatively small group of signaling proteins therefore can provide an immense diversity in controlling cellular responses through several intracellular signaling cascades.

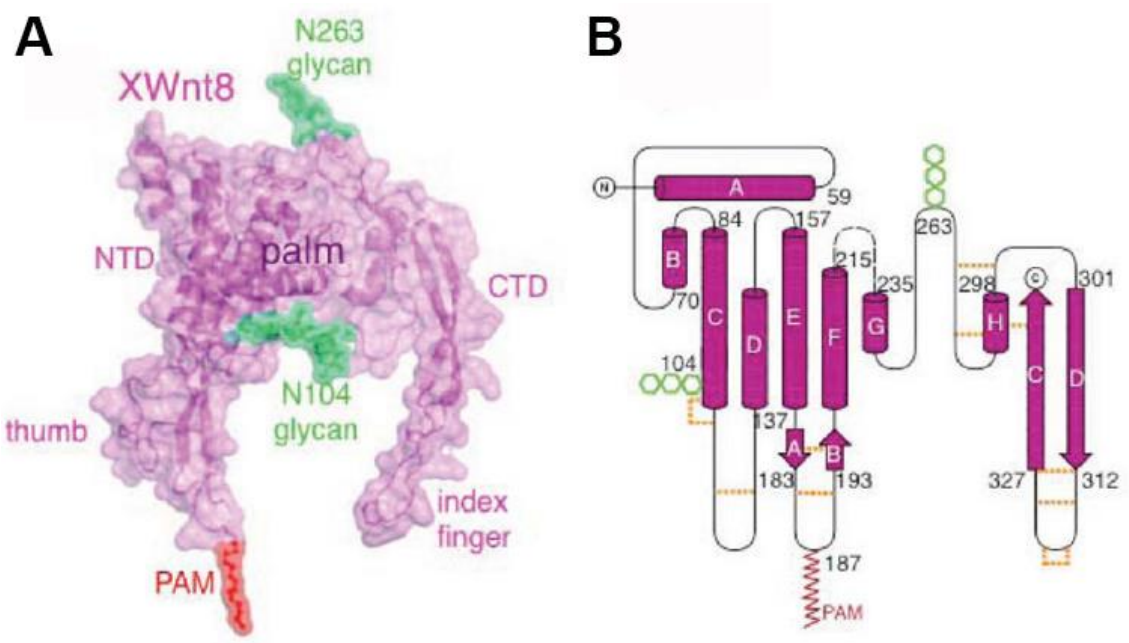

Figure 1.1 Structure of Xenopus Wnt8 when bound to receptor.

(A) Surface representation of XWnt8, when bound in complex with its receptor, Fz8. Fz8 not shown. Conserved palmitoleic acid (PAM) site shown in red, and glycan sites in green. (B) Secondary structure of XWnt8. α-helices and β-sheets shown in pink. Disulphide bonds shown by orange dotted lines. (Taken from Janda et al., 2012 with permission).

1.3. Wnt signaling pathways

Wnt signalling cascades have been traditionally classified as canonical (β-catenin-dependent) and non-canonical (β-catenin-independent), based on the ability of canonical Wnt signaling to induce axis duplication in Xenopus embryos (McMahon and Moon, 1989), or induce transformation in the mouse mammary epithelial cell line C57MG (Nusse and Varmus, 1982; Wong et al., 1994). However, as mentioned in the previous section, this may not be an accurate descriptor of the pathway, as non-canonical Wnt proteins and what was thought to be β-catenin-independent signaling, can promote β-catenin activation in certain cellular contexts (He et al., 1997; Mikels and Nusse, 2006). For the sake of simplicity, I will continue to refer to the traditional β-catenin dependent pathway, as canonical Wnt signaling, and exclude the known non-canonical exceptions. The mechanism and function of the traditional β-catenin-dependent pathway will be described in detail in the next section. β-catenin-independent Wnt signaling can be further broken down into the planar cell polarity (PCP) and Ca^{2+} pathways. Pathway specificity is usually determined by the binding of individual Wnt proteins to specific receptors.

1.3.1. Planar cell polarity pathway

The PCP pathway was first identified in developing *Drosophila*, for its role in determining epithelial polarity to align and orient cells with one other within the plane of cells in order to form an axis of polarity across a tissue (Wong and Adler, 1993). Its function in the orientation of cilia in mammals was later discovered in cochlear development, and many other axis developmental defects and ciliopathies (Butler and Wallingford, 2017; Qian et al., 2007).

PCP signaling is activated by Wnt binding to its receptor Frizzled (Fz) and co-receptor Receptor Tyrosine Kinase (RTK)-like orphan receptor (ROR), or Receptor-like Tyrosine Kinase (RYK) (Green et al., 2008; Lu et al., 2004; Masiakowski and Carroll, 1992; Wang et al., 2006a). This stimulates various small GTPases such as Rho and Rac or Cdc42, which in turn regulate Rho-associated kinase (ROCK) and c-Jun N-terminal kinase (JNK) respectively, leading to control of the cytoskeleton and regulation of migration, cell polarity and even cell survival (Butler and Wallingford, 2017; Zallen, 2007) (Fig. 1.2)

1.3.2. Ca^{2+} pathway

The Wnt/Ca^{2+} pathway is critical for the influx and regulation of intracellular Ca^{2+} concentrations. This subsequently leads to the activation of calmodulin-dependent protein kinase (CaMK) and protein kinase C (PKC), which promotes cell migration for axon guidance as well as inhibition of β-catenin-dependent signaling (Ishitani et al., 2003; O'Connell et al., 2009; Weeraratna et al., 2002). The influx of Ca^{2+} is thought to be generated by Wnt binding to Fz, which can act as a G protein-coupled receptor (GPCR) leading to the stimulation of heterotrimeric G proteins to promote secondary messengers like inositol 1, 4, 5 triphosphate (IP3), by phospholipase C- β (PLC-β) and cyclic-GMP via phosphodiesterase (PDE) and guanylate cyclases (Ahumada et al., 2002; Moon et al., 1997). There are more non-canonical signaling pathways variants, but the models shown in Fig. 1.2 represent the general intracellular signaling pathways.

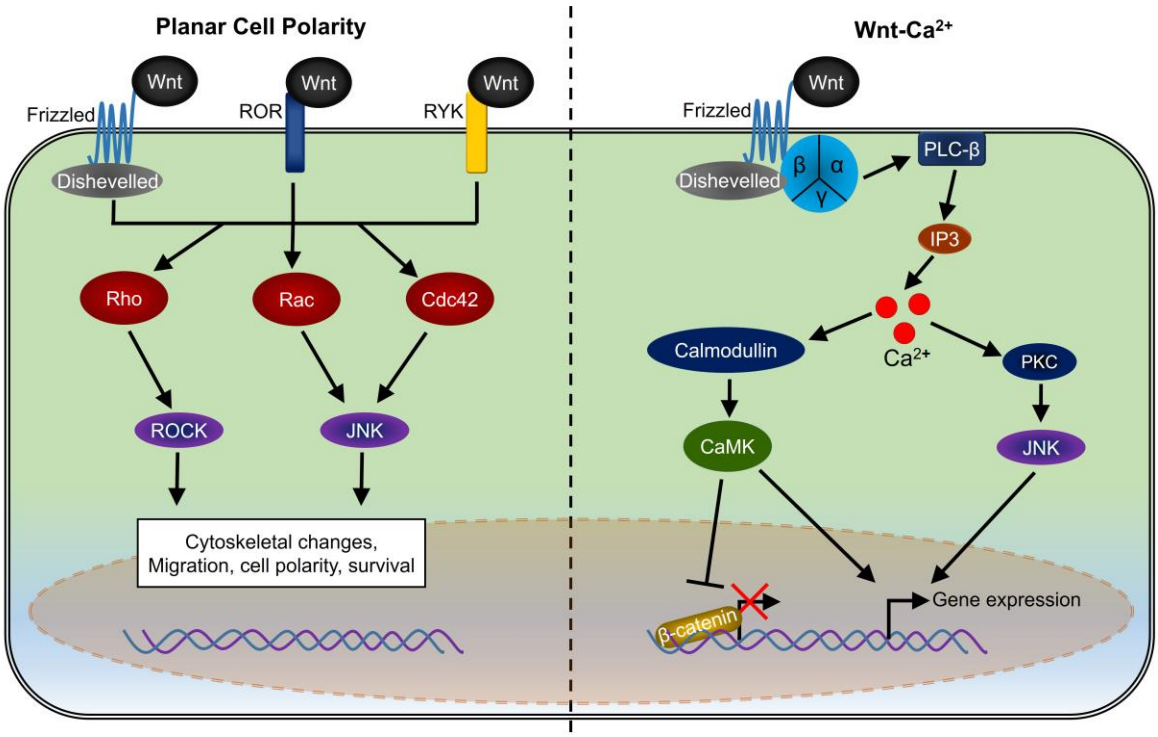

Figure 1.2 Non-canonical Wnt signaling pathways

β-catenin-independent Wnt pathways guide planar cell polarity and Ca^{2+} signaling. Wnt proteins can bind to a number of distinct receptors to induce diverse cellular responses. These include regulation of the cytoskeleton to control cell polarity and migration, cell survival, induction of gene expression and even inhibition of β-catenin-dependent gene expression.

1.4. Mechanism of canonical Wnt signaling

The work in this thesis focuses extensively on the canonical Wnt pathway. Therefore, for ease of reading from this point on the canonical β-catenin signaling pathway will simply be referred to as, 'Wnt' signaling. In addition, as much of my research utilizes developing *Drosophila* and their genetics to study Wnt, genes and proteins will be introduced with their vertebrate nomenclature, followed by the *Drosophila*.

The core components of the canonical β-catenin dependent pathway are highly conserved across metazoans, and at least one group of Wnt proteins that activate it are found in all animals (Janssen et al., 2010). As the name suggests, the pathway revolves around the stabilization and localization of the key effector, β-catenin (β-cat) [the homolog of *Drosophila* Armadillo (Arm)] (Bradley et al., 1993; Pai et al., 1997; Peifer et al., 1994; Salomon et al., 1997). β-cat/Arm is a continuously produced multifunctional protein essential for the formation and maintenance of the adherens junctions as well as for Wnt signaling (Valenta et al., 2012). In the absence of Wnt ligand, cytoplasmic β-cat/Arm is continuously targeted for degradation by a destruction complex consisting of the scaffolding protein Axin (Ikeda et al., 1998), the tumor suppressor Adenomatous polyposis coli (APC) (Rubinfeld et al., 1993; Su et al., 1993) and the kinases, Casein kinase 1 alpha (CK1α), and Glycogen synthase kinase 3β (GSK3β, also known as Shaggy/Zest White in *Drosophila*) (Peifer et al., 1994; Peters et al., 1999).CK1α and GSK3β phosphorylate β-catenin, targeting it for ubiquitination by an E3 Ubiquitin ligase complex and subsequent proteasomal digestion (Aberle et al., 1997; Amit et al., 2002; Hart et al., 1999) (Fig. 1.3). Upon Wnt/Wg binding to its coreceptors Frizzled (Fz) and Low-density lipoprotein receptor-related protein (LRP)5/6 /Arrow (Arr) (Bhanot et al., 1996; DiNardo et al., 2000; He et al., 2000; Skarnes et al., 2000), Dishevelled (Dvl/Dsh) is recruited to the receptors and mediates recruitment of the destruction complex (Klingensmith et al., 1994; Schwarz-Romond et al., 2007; Yanagawa et al., 1995), along with β-cat/Arm, to phosphorylate LRP/Arr, which is localized at the membrane. This disrupts the destruction complex, allowing accumulation of newly synthesized β-catenin, which can then translocate to the nucleus, acting as a co-activator with T-cell factor (TCF)/lymphoid enhancer factor (LEF) to initiate expression of target genes (Behrens et al., 1996; Daniels and Weis, 2005; Molenaar et al., 1996) (Fig. 1.3).

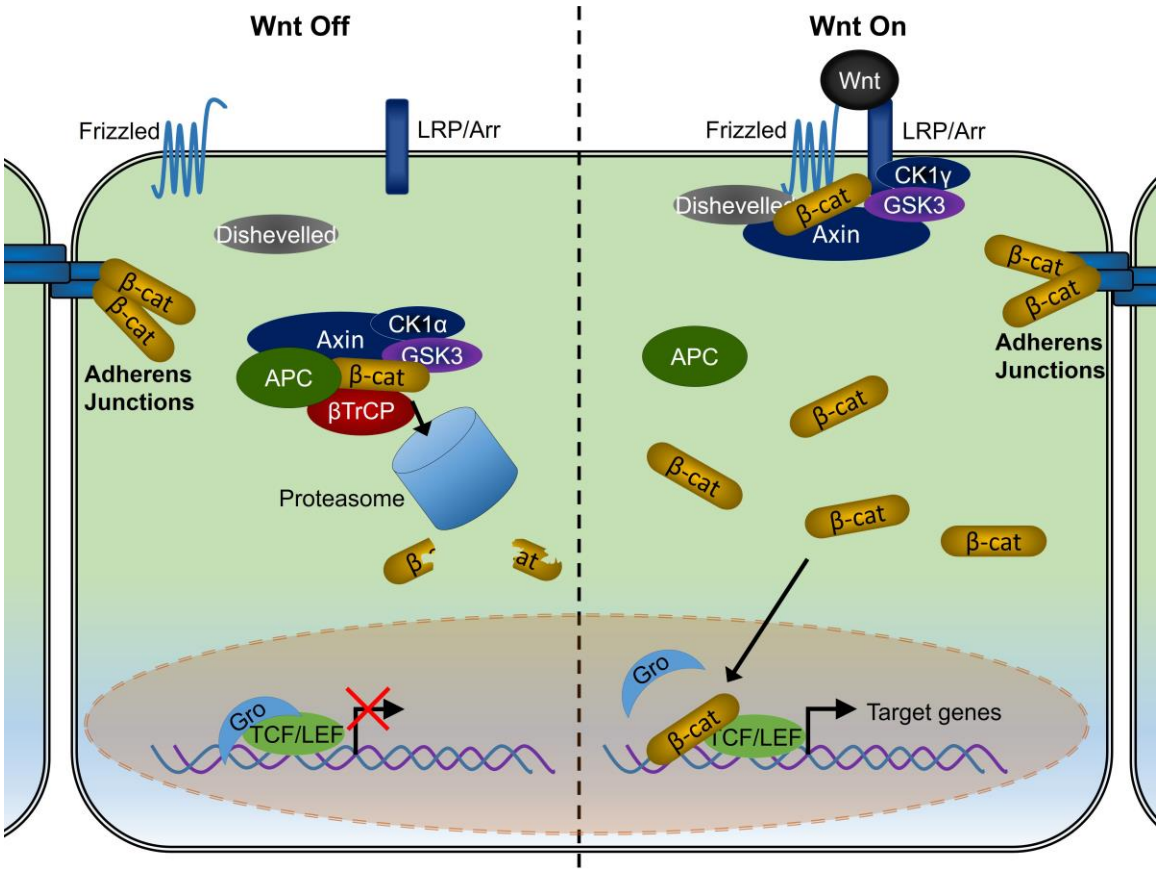

Figure 1.3 Overview of the Wnt/β-catenin signaling pathway

β-catenin is continuously produced in cells for the formation and maintenance of adherens junctions. In the absence of Wnt, cytoplasmic β-catenin is maintained at low concentrations in the cell, by targeting of a multi-protein destruction complex. The destruction complex phosphorylates, and subsequently ubiquitinates β-catenin targeting it for proteasomal degradation. Upon Wnt binding to receptors Frizzled and LRP/Arr the destruction complex becomes recruited to the receptors at the membrane and inactivated. Newly synthesized β-catenin accumulates within the cell, and can enter the nucleus where it displaces the transcriptional repressor protein Groucho (Gro). β-catenin acts as a transcriptional co-activator with TCF/LEF to initiate Wnt target gene expression.

1.4.1. Wnt biogenesis and secretion

After translation, Wnt proteins may undergo multiple post-translational modifications and sorting events, till their final secretion to initiate pathway activity (Fig. 1.4). In the endoplasmic reticulum (ER), Wnt proteins may be glycosylated at several residues. This may occur at variable sites depending on the Wnt protein and individual species. Glycosylation is not considered to be a conserved essential modification of Wnt proteins, as consequences of glycan mutated Wnts range from no effect, minor defects, or major defects, highlighting that this modification may be essential for Wnt activation and secretion, in a species to species and Wnt to Wnt circumstance. (Doubravska et al., 2011; Tang et al., 2012).

Lipidation has been identified as the essential modification to Wnt proteins. The addition of a palmitic acid to Wnt3A at cysteine 77 is required for full activation of Wnt signaling (Willert et al., 2003), while if serine 209 is not palmitoylated, Wnt fails to be secreted altogether and accumulates in the ER (Takada et al., 2006). This is catalyzed by the multipass transmembrane O-acyltransferase Porcupine (van den Heuvel et al., 1993; Kadowaki et al., 1996). Wnts can then be shuttled to the Golgi, by P24 proteins (Buechling et al., 2011; Port and Basler, 2010), where they bind to the transmembrane sorting receptor Wntless (Wls)/Evenness interrupted (Evi) at the essential palymitoylated serine residue (Herr and Basler, 2012). Wls then transports the Wnt in endosomes to the plasma membrane to be secreted in some context or another (Bänziger et al., 2006; Bartscherer et al., 2006). Wls may then be endocytosed and recycled back to the Golgi by a retromer complex consisting of vacuolar protein sorting (Vps)26-Vps29-Vps35 and sorting nexin (Snx) proteins (Belenkaya et al., 2008; Coudreuse et al., 2006; Harterink et al., 2011; Yang et al., 2008). This prevents Wls lysosomal degradation and allows for full normal Wnt secretion.

Upon Wnt reaching the surface of the cell it can be secreted to diffuse to adjacent cells by several routes. Considering that Wnts are palmitoylated and therefore hydrophobic, they cannot easily diffuse outside the cell. This may be overcome by binding to lipoprotein particles stabilizing them for long range signalling (Morrell et al., 2008; Panáková et al., 2005), or by interactions with membrane microdomains could

allow Wnts to form higher order micelle-like multimers, burying the lipidation sites in the interior of the complex (Katanaev et al., 2008; Zeng et al., 2001). Wnt diffusion is also heavily controlled by Heparan sulfate proteoglycan (HSPGs) on the cell-surface. HSPGs have been identified to regulate Wnts diffusion gradient, binding to receptors, and even trancytosis across the cell (Baeg et al., 2001; Han et al., 2005; Perrimon and Lin, 1999; Sarrazin et al., 2011) (Fig. 1.4).

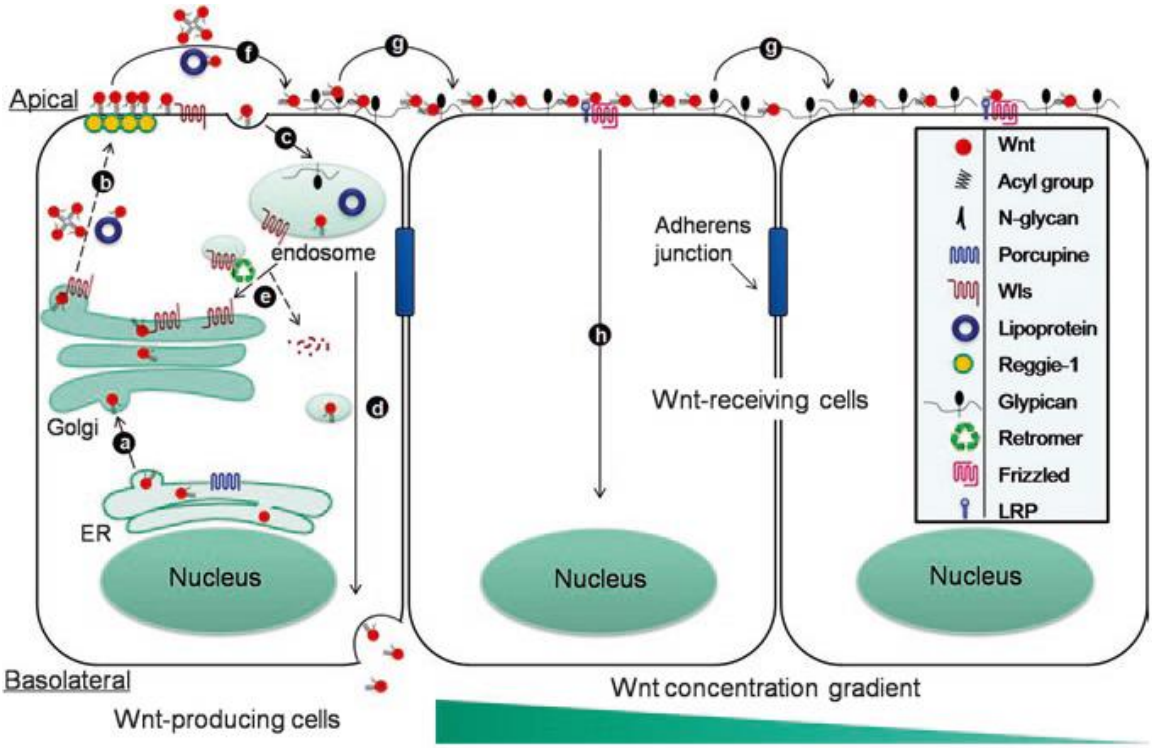

Figure 1.4 Overview of Wnt biogenesis and secretion

(a) Wnt is translated and undergoes glycosylation, and palmytolation by Porcupine in the ER, then transported to the Golgi. (b) Wls binds Wnt and transports it to cell surface. (c) Wnt may then be re-endocytosed, to undergo transcytosis and be secreted basolaterally with the aid of HSPGs (Gypicans) (d). (e) Upon dissociation with Wnt, Wls is endocytosed and may be recycled to the Golgi by the Retromer complex, or targeted for lysosomal degradation. (f) Wnt may be secreted into the extracellular space by formation of oligomer micelles via membrane microdomains (Reggie-1), or binding to lipoprotein particles. (g) HSPGs modulate the spreading of Wnt on cell surfaces, and modulate the interaction with its receptor Fz, to affect signaling outcome (h). (Image taken from Tang et al., 2011, with permission).

1.4.2. Wnt receptor binding interactions

Activation of β-catenin/Wnt signaling requires the Wnt ligand binding to the heterodimeric receptor complex consisting of the seven pass transmembrane protein Frizzled, and Low-density lipoprotein receptor-related protein 5 or 6/Arrow (Arr) (Bhanot et al., 1996; DiNardo et al., 2000). Other secreted proteins also bind these receptors to inhibit, or promote pathway activation (Fig. 1.5).

Fz proteins are members of the G protein-coupled receptor (GPCR) family, and contain containing a conserved extracellular cysteine-rich domain (CRD) (Bhanot et al., 1996). The CRD on Fz also contains a hydrophobic groove allowing strong binding affinity to the palmitoylated residues on Wnt (Bhanot et al., 1996; Janda et al., 2012) Upon Wnt binding to Fz, it allows the single-pass transmembrane protein LRP5/6/Arr to also bind to Wnt through the palmitoylated cysteine residue (Cong et al., 2004; Komekado et al., 2007). Wnt binding pulls the two receptors into close proximity to induce an intracellular response, initiating the Wnt pathway in the receiving cell (Holmen et al., 2005).

Wnt's ability to bind to its co-receptors may be impaired by several different types of inhibitors acting directly upon Wnt or the receptors. Wnt inhibitory factor (WIF) proteins as well as secreted Frizzled-related proteins (sFRPs) can bind extracellular Wnt and impair its ability to bind Fz (Hsieh et al., 1999; Uren et al., 2000; Wang et al., 1997). sFRPs can also bind to the CRD of Fz, inhibiting Wnt binding and subsequent activation (Bafico et al., 1999; Rodriguez et al., 2005). Dickkopf (DKK) proteins are another class of inhibitors that bind to LRP5/6 and prevent proper complex formation with Fz, preventing pathway activation, and can do so by interacting with another transmembrane protein Kremen (Ellwanger et al., 2008; Niehrs et al., 1998; Semënov et al., 2001).

Two more groups of secreted proteins that have been well characterized to promote β-catenin/Wnt signaling by binding to the Wnt receptors are Norrin and R-spondins. These proteins can act independently of Wnt proteins altogether or synergize with them to activate downstream signal transduction (Bell et al., 2008; Kazanskaya et al., 2004; Xu et al., 2004). The cysteine-knot protein Norrin has been shown to bind directly to Fz4 and LRP5 to simulate Wnt binding and activate the pathway (Xu et al.,

2004). R-spondin proteins can bind and synergize with Fz and LRP (Bell et al., 2008; Nam et al., 2006; Wei et al., 2007), but also promote Wnt signaling through another receptor group, Leucine-rich repeat-containing G-protein coupled receptor (Lgr) (Carmon et al., 2011). It should be noted that these are antagonists and agonists of the Wnt receptors and not core conserved components of the Wnt pathway and their presence can vary from species to species.

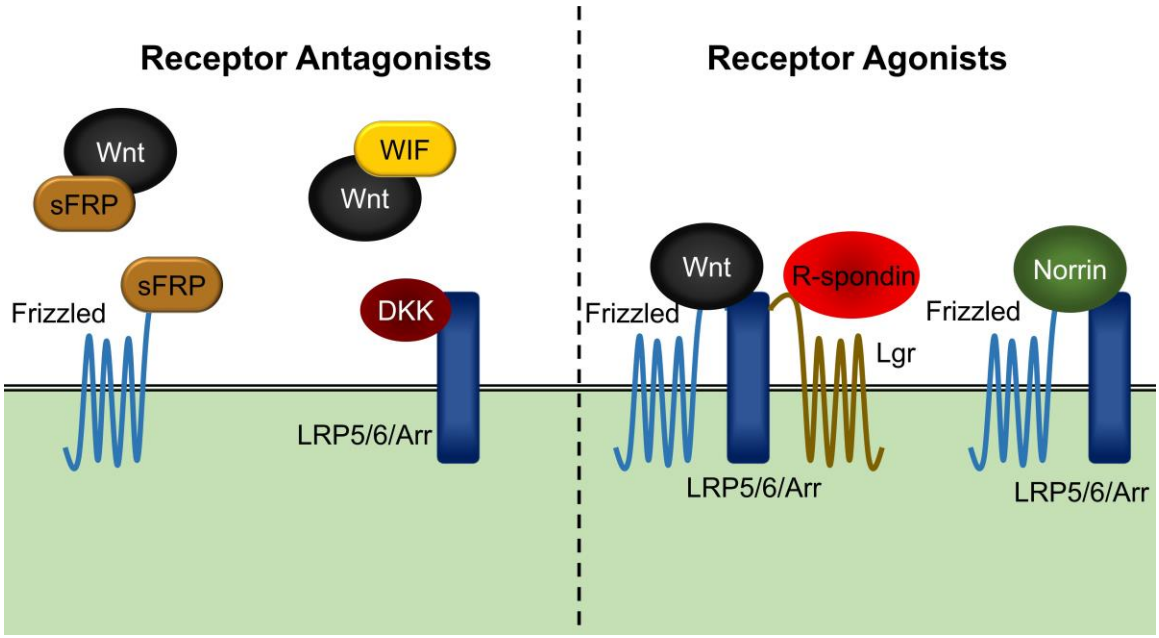

Figure 1.5 Summary of Wnt receptor binding partners regulating signal activation

After Wnt proteins are secreted from the producing cells, their interaction with receptors Fz and LRP5/6/Arr can be antagonized or agonized by interaction with additional proteins. WIF and sFRP bind to Wnts, preventing receptor interactions, sFRP may also bind Fz, preventing Wnt binding. DKK binds LRP5/6/Arr, preventing receptor complex formation. Wnt receptor binding and signal propagation can be up regulated by binding with R-spondin and Lgr proteins to LRP5/6/Arr. Norrin can mimic Wnt binding to receptors, propagating Wnt signaling.

1.4.3. β-catenin regulation in the absence of Wnt

Cytoplasmic β-catenin stability and overall protein levels are tightly regulated by the Axin destruction complex, maintaining the Wnt pathway in a default repressive state (Barolo and Posakony, 2002). This is due to the fact that β-catenin is almost ubiquitously essential for cell-cell adhesion at the adherens junctions (McCrea et al., 1991; Orsulic and Peifer, 1996; Peifer and Wieschaus, 1990; Valenta et al., 2012), and must be constantly produced for their maintenance (Valenta et al., 2012). The core destruction complex consists of the scaffolding protein Axin, tumor suppressor protein APC, kinases GSK3α/β and CK1α, as well as interactions with the Protein Phosphatase 2A (PP2A) protein. The ability of the destruction complex to regulate cytoplasmic β-cat is controlled by a hierarchy of dynamic phosphorylation events leading to the eventual degradation of β-cat (Kimelman and Xu, 2006).

The scaffolding protein Axin binds GSK3 and CK1 at distinct sites (Fagotto et al., 1999; Ikeda et al., 1998). This allows the highly promiscuous GSK3 (Doble and Woodgett, 2003; Xu et al., 2009) to phosphorylate Axin, increasing the binding affinity of Axin for β-cat (Yamamoto et al., 1999). APC is also able to bind both β-cat and Axin (Hamada et al., 1999; Ikeda et al., 1998), allowing for the phosphorylation of the N-terminus of β-cat. β-cat is initially phosphorylated at serine 45 by CK1α; this is essential for subsequent phosphorylation by GSK3 at serine 33, serine 37 and threonine 41 (Amit et al., 2002; Liu et al., 2002).This creates a ‘phosphodegron’ motif on β-cat, specifically the phosphorylated serine 33 and 37, allowing it to be targeted by the F box/WD repeat protein β-TrCP, part of an E3 ubiquitin ligase complex (Hart et al., 1999). APC is also phosphorylated by GSK3, allowing β-TrCP access to β-cat (Fig. 1.6). β-TrCP mediates the poly-ubiquitination of lysine 19 and 49 on β-cat, leading to rapid proteolysis of β-cat by the 26S proteasome (Hart et al., 1999; Winston et al., 1999; Wu et al., 2003). PP2A will then dephosphorylate APC, allowing it to reform the initial β-cat binding and phosphorylation complex (Li et al., 2001; Seeling et al., 1999). This rapid cycling of phosphorylation events allows for continual and rapid degradation of any freely available cytoplasmic β-cat (Fig. 1.6). It should be noted though that the effectiveness of the destruction complex and turn over rate of β-cat can be modulated further by phosphatases countering GSK3. Protein phosphatase 1 (PP1) can dephosphorylate GSK3 phosphorylation sites on Axin, inhibiting complex formation and β-cat binding (Luo

et al., 2007), while PP2A in certain contexts can directly remove the degron motif phosphorylation on β-cat, preventing targeting by β-TrCP (Su et al., 2008).

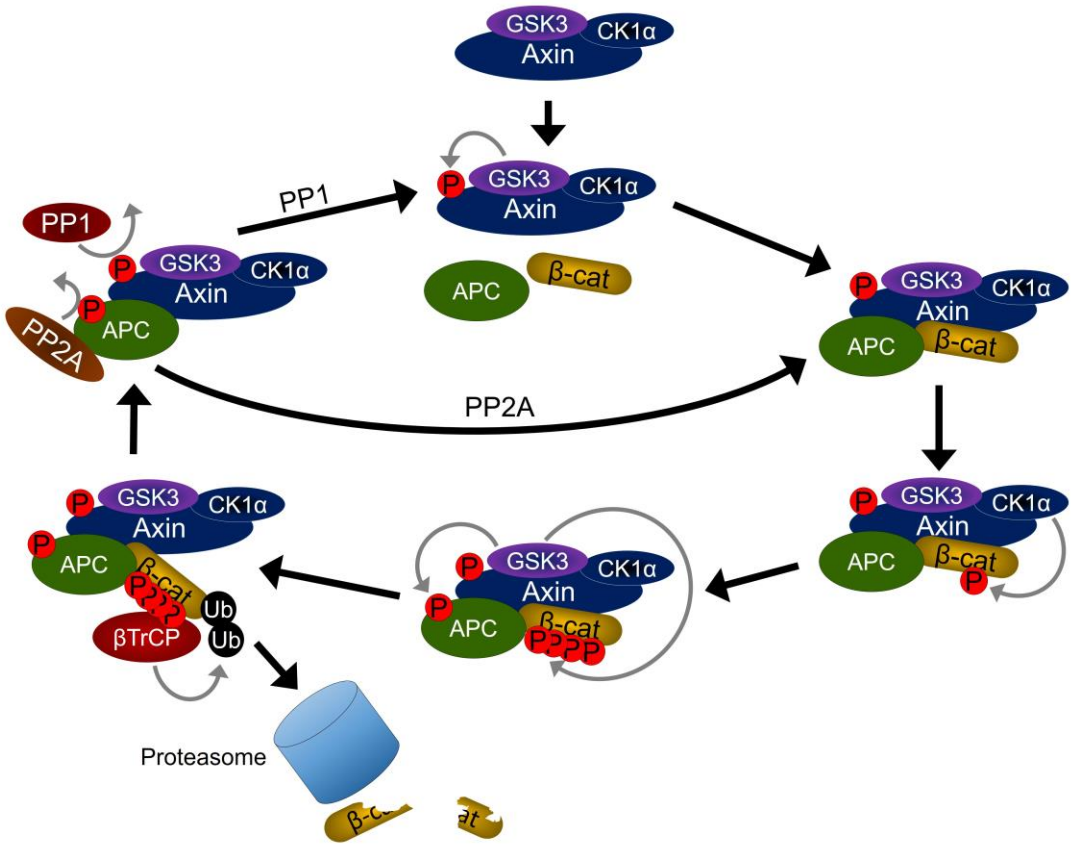

Figure 1.6 Model of destruction complex turnover of β-catenin.

Dynamic phosphorylation cycling of destruction complex proteins, and to some extent β-catenin, allows for rapid and repeated degradation of β-catenin. Phosphorylation of Axin promotes complete complex formation and binding of β-catenin. CK1α phosphorylates and primes β-catenin for subsequent phosphorylation by GSK3. GSK3 also phosphorylates APC to present β-catenin, with its phosphodegron motif, to βTrCP for ubiquitination. Ubiquitinated β-catenin is digested by the proteasome. PP2A may then dephosphorylate APC, allowing for a new capture of β-catenin. Alternatively PP1 may also dephosphorylate Axin, resulting in a partial dissociation of the destruction complex. P: phosphate, Ub: ubiquitin.

1.4.4. β-catenin stabilization

Upon Wnt binding to Fz and LRP/Arr and activating the pathway, a wide range of intracellular responses occur, leading to the eventual inactivation of the destruction complex and stabilization of β-catenin (Fig. 1.7). The formation of the receptor ligand complex initiates the phosphorylation and recruitment of Dishevelled (Dvl/Dsh) to bind to Fz (Lee et al., 1999; Rothbächer et al., 2000; Wong et al., 2003; Yanagawa et al., 1995; Yanfeng et al., 2011). Dvl/Dsh is phosphorylated by various kinases, including CK1ε, CK2, and Par1, to promote its activity (Sun et al., 2001; Willert et al., 1997). The Fz-Dvl/Dsh interaction at the membrane acts as a platform to induce clustering of Dvl/Dsh and receptors (Bilic et al., 2007; Cong et al., 2004; Wong et al., 2003); this recruits and binds Axin to Dvl/Dsh through both proteins DIX domain, resulting in the recruitment of the entire destruction complex to the receptors (Fiedler et al., 2011; Metcalfe et al., 2010; Schwarz-Romond et al., 2007). Axin also interacts with LRP5/6/Arr, allowing GSK3 to come into close proximity to the cytoplasmic tail of LRP5/6/Arr, resulting in the phosphorylation of the PPPSPxS motif on LRP5/6/Arr (Tamai et al., 2004; Zeng et al., 2005). This primes LRP5/6/Arr for subsequent phosphorylation along the cytoplasmic tail, by the membrane bound CK1γ (Davidson et al., 2005; MacDonald et al., 2008; Zeng et al., 2005). These events also create a feed forward loop, recruiting more Axin (and destruction complex components) to the membrane, forming large aggregates of receptor-ligand-destruction complex components, known as the signalosome (Bilic et al., 2007; Feng and Gao, 2015). This effectively inactivates the destruction complex by preferentially targeting LRP5/6/Arr, and sequestering the complex to the membrane (MacDonald et al., 2008; Zeng et al., 2007). The signalosome may then be endocytosed and sequestered to multi vesicular bodies, allowing for sustained signal transduction (Bilic et al., 2007; Feng and Gao, 2015) (Fig. 1.7). These events allows for newly synthesized β-catenin to freely accumulate in the cytoplasm to eventually translocate to the nucleus and initiate transcription.

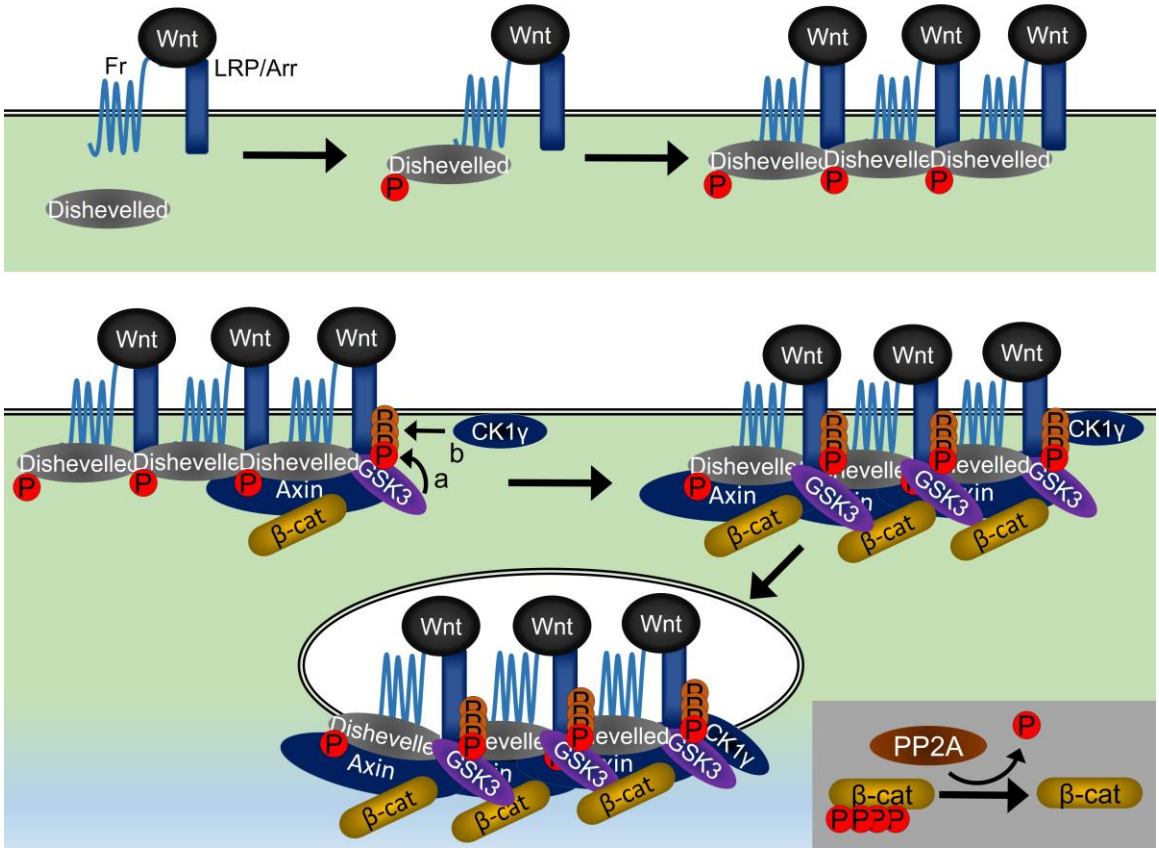

Figure 1.7 Stabilization of β-catenin by destruction complex inactivation and signalosome assembly.

Upon Wnt binding to co-receptors Fz and LRP/Arr, Dishevelled becomes phosphorylated and recruited to the cytoplasmic tail of Fz. Dishevelled then oligomerizes, clustering receptor complexes together, recruiting and binding Axin and the rest of the destruction complex. GSK3 then phosphorylates the PPPSPxS motif on LRP/Arr cytoplasmic tail (a), priming CK1γ for subsequent phosphorylation of LRP/Arr (b). This creates a feed forward loop recruiting and inactivating more destruction complexes, to form a signalosome. The signalosome may then be endocytosed and retained within multivesicular bodies for maintain Wnt signal activation. Phosphodegron marked β-catenin may be dephosphorylated at this time by PP2A, allowing for stabilization protein previously targeted for degradation (inset). P: phosphate.

1.4.5. Transcriptional initiation

The ultimate outcome the Wnt pathway is β-catenin interacting with T-cell factor (TCF)/lymphoid enhancer factor (LEF) to initiate expression of target genes with the cooperation of transcriptional coactivators and histone modifiers (Fig. 1.8). In the absence of β-cat, TCF/LEF is bound to Wnt responsive elements (WREs) (Atcha et al., 2007; Behrens et al., 1996; Hatzis et al., 2008; Molenaar et al., 1996) and the transcriptional repressor Groucho, which promotes histone deacetylation and chromatin compaction (Bejsovec et al., 1998; Clevers et al., 1998). Nuclear β-cat is able is able to displace Groucho. This is aided by extensive post-translational modification of TCF/LEF by various proteins to promote β-cat binding, and diminish Groucho interaction (Daniels and Weis, 2005; Hikasa and Sokol, 2011; Hikasa et al., 2010; Ota et al., 2012). A myriad of different transcriptional coactivators are then recruited to β-cat and TCF/LEF to promote full transcriptional initiation. This includes histone methyltransferases and acetyltransferases, other chromatin modifiers, and binding proteins (Kramps et al., 2002; Mosimann et al., 2006, 2009; Thompson et al., 2002). The transcriptional complex allows for suitable expression of target genes leading to the appropriate biological outcome.

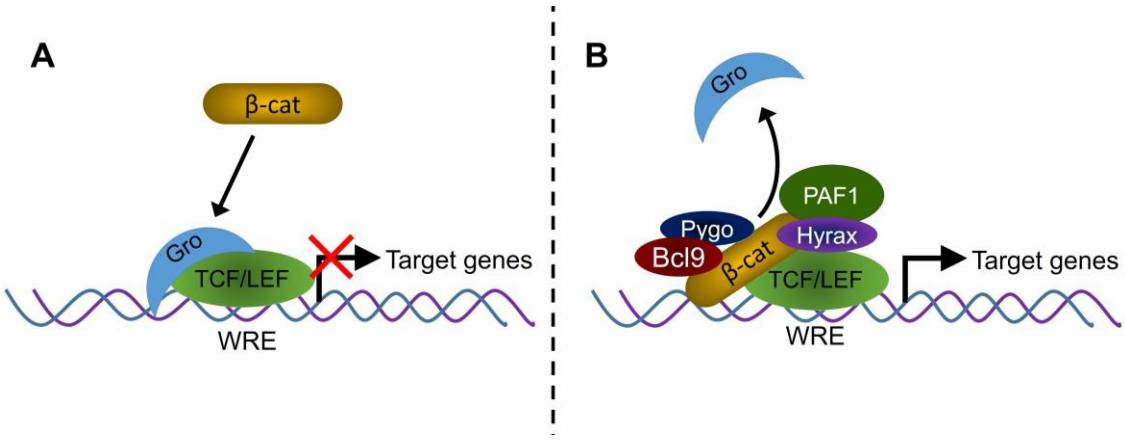

Figure 1.8 Transcriptional initiation of Wnt target genes

(A) Upon stabilization of β-catenin, β-catenin is able to translocate to the nucleus to target WRE-bound TCF/LEF, and transcriptional repressor Gro. (B) β-catenin preferentially binds TCF/LEF and displaces Gro. β-catenin recruits and bind multiple transcriptional coactivators such as Bcl9, Pygo, PAF1, and Hyrax/Parafibromin. This allows for appropriate chromatin remodeling and full transcriptional initiation of Wnt target genes.

1.5. Regulation of Wnt signaling

The Wnt pathway must be extensively regulated in order to maintain a tight control over homeostasis and coordinate normal developmental outcomes. Considering the relative complexity of the pathway involving many proteins, an individual proteins stability, activity, and localization can modulate signaling outputs, ranging from minute adjustments, to constitutively active, or complete loss of overall pathway activity. This is carried out predominantly by post-translational modification of individual Wnt pathway proteins, guided by interactions with other signal transduction pathways. More recent work has started to identify that cell physiology and mechanical forces also play a commanding role in influencing Wnt signaling.

1.5.1. Post-translational modification of Wnt pathway proteins, phosphorylation takes center stage

Post-translational modification (PTM) of Wnt pathway proteins allows for a quick, dynamic, and reversible response system to Wnt stimulation without the need to synthesize new proteins in order to convey signal transduction. To date, several distinct mechanisms of PTM have been identified to regulate Wnt signaling outcomes, including lipidation, glycosylation, sumoylation, ubiquitination, ADP-ribosylation, and phosphorylation (Kadoya et al., 2000; Kaemmerer and Gassler, 2016; Kim et al., 2008; Tauriello and Maurice, 2010; Verheyen and Gottardi, 2010; Willert and Nusse, 2012; Yang et al., 2016). A recent review by Gao et al. (2014), summarized over 72 distinct PTMs of core Wnt proteins that influence pathway activation, indicating the importance of PTM in controlling Wnt. From over three decades of studies, it has become apparent that the phospho-regulation of Wnt pathway components is the most predominant, and well-studied of all these mechanisms (Verheyen and Gottardi, 2010). However from genetic screening, it has become apparent that there are still likely a large number of unidentified phospho-regulators that are critical in regulating the Wnt signaling cascade (Swarup et al., 2015).

Phosphorylation is the reversible covalent attachment or removal of a phosphoryl group (PO_3), mediated by the enzymatic protein family of kinases and phosphatases

respectively. It is speculated that up to three quarters or more of the entire proteome undergoes some form of post translational modification by phosphorylation in eukaryotes, making it the overall most extensively utilised form of PTM in the cell (Krüger et al., 2006; Vlastaridis et al., 2017). Kinases phosphorylate proteins by catalyzing the transfer to the terminal phosphate group off of adenosine triphosphate (ATP), to a hydroxyl group of individual amino acid side chains (Burnett and Kennedy, 1954). This results in the conversion of ATP to adenosine diphosphate (ADP). This process is reversed by dephosphorylation, where phosphatases induce hydrolysis of phosphate group off the amino acid (Fischer and Krebs, 1955; Krebs and Fischer, 1955). The addition of the phosphoryl group to a residue can induce conformational changes in protein structure by allosteric interaction via charge or physical size with other residues in the protein, or binding partners, altering the overall activity, stability, preferred binding partners and localization within the cell (Hunter, 2012; Johnson and Barford, 1993). Phosphorylation affecting signal transduction usually occurs on serine, threonine, and tyrosine residues, but can also target histidine, arginine, aspartate, lysine, and cysteine (Cieśla et al., 2011).

Given the crucial and diverse involvement of phosphorylation in regulating core aspects of Wnt signaling (Verheyen and Gottardi, 2010), it is important to remember that the kinases and phosphatases responsible for these aspects of control must be guided by up upstream signaling cues themselves, by either feedback mechanisms or other signaling pathways.

1.5.2. Signaling pathways and crosstalk regulation of Wnt

The interactions between cellular signaling pathways is a fundamental process that guides complex and diverse cellular responses, and the study of signaling pathway crosstalk is critical in understanding normal cell physiology and, when disrupted, disease progression. The interactions between Wnt signaling and other developmental pathways such as Hippo, TGF-β, MAPK, Notch, Hedgehog, and JAK/STAT, and how they may antagonize or synergize with each other is an ever expanding area of research (Collu et al., 2014; Fragoso et al., 2012; Itasaki and Hoppler, 2010; Kim and Jho, 2014; Song et al., 2015; Zeller et al., 2013).

The interaction between Wnt and any pathway is usually highly context specific. Spatial, temporal and species variations may promote Wnt activity in one condition, while repress it in another, even though the interaction may be mediated through the same protein. For instance, the MAPK protein, Extracellular signal-regulated kinase (ERK) has been identified to phosphorylate and inhibit GSK3 in human liver cells (Ding et al., 2005), while another MAPK protein and direct activator of ERK, MAPK-extracellular signal-regulated kinase (MEK), has been thought to phosphorylate and activate GSK3 in human skin fibroblasts (Takahashi-Yanaga et al., 2004). These specific crosstalk interactions between Wnt and other signaling pathway proteins make it very difficult to come to any consensus on how these interactions generally regulate Wnt. However, it is critical to identify the conserved interactions between pathways that are used reiteratively across species and tissues for a better understanding of how basic cell biology and developmental processes occur, so that they may be possibly applied for mechanisms of disease and medicine (Calil et al., 2007; Collu et al., 2014; Morris and Huang, 2016; Song et al., 2015; Zeller et al., 2013).

1.5.3. Wnt and mechanical forces

Biochemical signal transduction and genetic interactions have been fundamental to understanding development, but increasing evidence has made it apparent that mechanical forces are also involved in directing cell differentiation and growth during this process (Sheehy and Parker, 2011; Sun et al., 2012). Cells are able to respond to mechanical cues and convert them into a biochemical response through the process of mechanotransduction. In a tissue, mechanotransduction predominately occurs either through force sensing at cell-cell adhesion sites like adherens junctions (AJ), or a cells ability to bind to the extracellular matrix (ECM), and overall stiffness of the ECM (Ingber, 2006a). Mechanotransduction has also been identified to occur through forces exerted on nuclear architecture, as well as membranes and mechanosensitive stretch gated ion channels (Ingber, 2006a, 2006b), but they will not be discussed here. In response to physical forces these sensing mechanisms will induce a response from the actomyosin cytoskeleton, as well as potentially induce effects on mechanosensitive pathways, such as Wnt (Mendez and Janmey, 2012) (Fig. 1.9).

To date, the best-characterized and studied mechanism of mechanotransduction is through cell-ECM interactions, specifically through ECM-Integrin signalling at focal

adhesions (Schwartz, 2010). The transmembrane integrin proteins act as a direct mechanical linkage between the ECM and the cytoskeleton (Wang et al., 1993). When clustered together to form focal adhesions, integrins and associated proteins of the focal adhesion complex are able to sense overall stiffness of the ECM, and adjust overall cell-ECM adhesion, while simultaneously convey signaling cues to the cell through various intracellular pathways (Giancotti and Ruoslahti, 1999; Schwartz, 2010). Studies of stem cell niche formation and differentiation have identified that the mechanical microenvironment of the ECM rigidity, can dramatically affect cell differentiation outcomes (Sun et al., 2012). Many of these studies have looked at mesoderm differentiation in cardiomyogenesis, where Wnt signaling is also critical (Happe and Engler, 2016). In mesoderm differentiation, increased matrix rigidity has been identified to promote Wnt signaling by decreasing cell-cell adhesion at the AJs, and releasing more β-catenin into the cytoplasm (Fernández-Sánchez et al., 2015; Przybyla et al., 2016; Samuel et al., 2011).This mechanism is thought to be due to mechanical force balance, where a dynamic equilibrium in a cell between cell-ECM and cell-cell adhesion must be maintained (DuFort et al., 2011; Przybyla et al., 2016; Sheehy and Parker, 2011; Wang et al., 1993). Tissue with a softer matrix is more flexible and contains greater cell-cell adhesion, while a stiff ECM has greater integrin attachment, and less cell-cell adhesion (reviewed in DuFort et al., 2011).

Mechanotransduction across adjacent cells through the AJs is much more relevant and debated mechanism in the regulation of Wnt signaling, considering β-catenin is essential for both the formation and maintenance of adherens junctions as well for transcriptional activation for the Wnt pathway (McCrea et al., 1991; Orsulic and Peifer, 1996; Peifer and Wieschaus, 1990; Valenta et al., 2012) AJs are the major cell-cell adhesion complex, responsible for maintaining tissue integrity by forming an apical-basolateral ring-like structure around cell membranes in polarized cells (reviewed in Harris and Tepass, 2010). AJ form by homophilic interactions between transmembrane cadherin proteins (mainly E-cadherin in epithelia), and several different catenin proteins, p120-catenin, β-catenin, and α-catenin (Aberle et al., 1994; Huber and Weis, 2001; Huber et al., 2001; Ireton et al., 2002; Nagafuchi and Takeichi, 1989). p120 is less critical for mechanotransduction across cells, as it has been identified as dispensable in some cases, and interacts with E-cadherin to mediate its endocytosis rates and interaction with microtubules within the cell (Davis et al., 2003; Delva and Kowalczyk,

2009; Ishiyama et al., 2010; Meng et al., 2008; Pacquelet et al., 2003). β-cat on the other hand is essential for AJs, as it binds to the cytoplasmic tail of cadherin (Huber and Weis, 2001; Ozawa et al., 1989), where it quickly links to α-cat as well (Bajpai et al., 2008), and α-cat is able to attach to the actin cytoskeleton (Benjamin et al., 2010; Kobielak and Fuchs, 2004; Rimm et al., 1995). α-cat is considered to be the mechanosensitive protein of the AJ, it may increase or decrease its interaction and attachment to actin filaments through secondary proteins like vinculin, depending upon the tensile forces exerted on it (Dufour et al., 2013; Yao et al., 2014) These forces are generated by actomyosin contractility within cells, and thus allow AJs to be sites of mechanical force integration across cells and at a tissue level (Lecuit and Yap, 2015) (Fig. 1.10).

AJs are able to maintain cell-cell adhesion and tissue integrity, in response to tensile forces, pulling adjacent cells away from one another by the process of clustering and accumulation to enhance adhesion. Cells under increased lateral contractile forces accumulate AJs to increase adhesion (Engl et al., 2014; Gomez et al., 2011; Lecuit and Yap, 2015) The generation of contractile force, and the adjacent cells ability to respond to it through cadherin clustering is mediated prodominantly by the same major actin-binding motor protein, non-muscle myosin II (NMII), (Cavey et al., 2008; Engl et al., 2014) (Fig. 1.10). NM II is responsible for regulating a diverse range of cellular mechanisms, including cell shape, cadherin clustering, adhesion, migration, cell cycle progression and cell division (reviewed in Vicente-Manzanares et al., 2009) (Fig, 1.11)

It has been debated whether the interactions between mechanotransduction at the AJs can affect Wnt signaling, as traditional models stipulate that β-cat exists in two distinct pools for signaling and adhesion (Heuberger and Birchmeier, 2010). This model has been supported by the fact that a loss of E-cadherin and subsequently AJ, does not affect Wnt signaling in epithelial cancers, and can cause overall decreases in β-cat, presumably from excess cytoplasmic β-cat becoming targeted and degraded via the destruction complex (Caca et al., 1999; Hendriksen et al., 2008; Herzig et al., 2007; van de Wetering et al., 2001). More studies have demonstrated that cadherins can act as stoichiometric inhibitors of Wnt signaling, but this is not associated with any mechanical forces, and additionally requires PTM of β-cat at the AJs to be released to potentiate Wnt signalling in already active conditions (Ciruna and Rossant, 2001; Cox et al., 1996; Huber and Weis, 2001; Przybyla et al., 2016; Sanson et al., 1996). More recent work has started to question this model as several upstream activators of NMII have also been

identified to inhibit Wnt signaling in developing *Drosophila*, through cytoskeleton rearrangement and cellular contraction (Greer et al., 2013). Additionally Wnt inducible proliferation rates can also be modulated by tension exerted on proliferating monolayers (Benham-Pyle et al., 2015), adding support to the influence of mechanotransduction at the AJs can modulate Wnt.

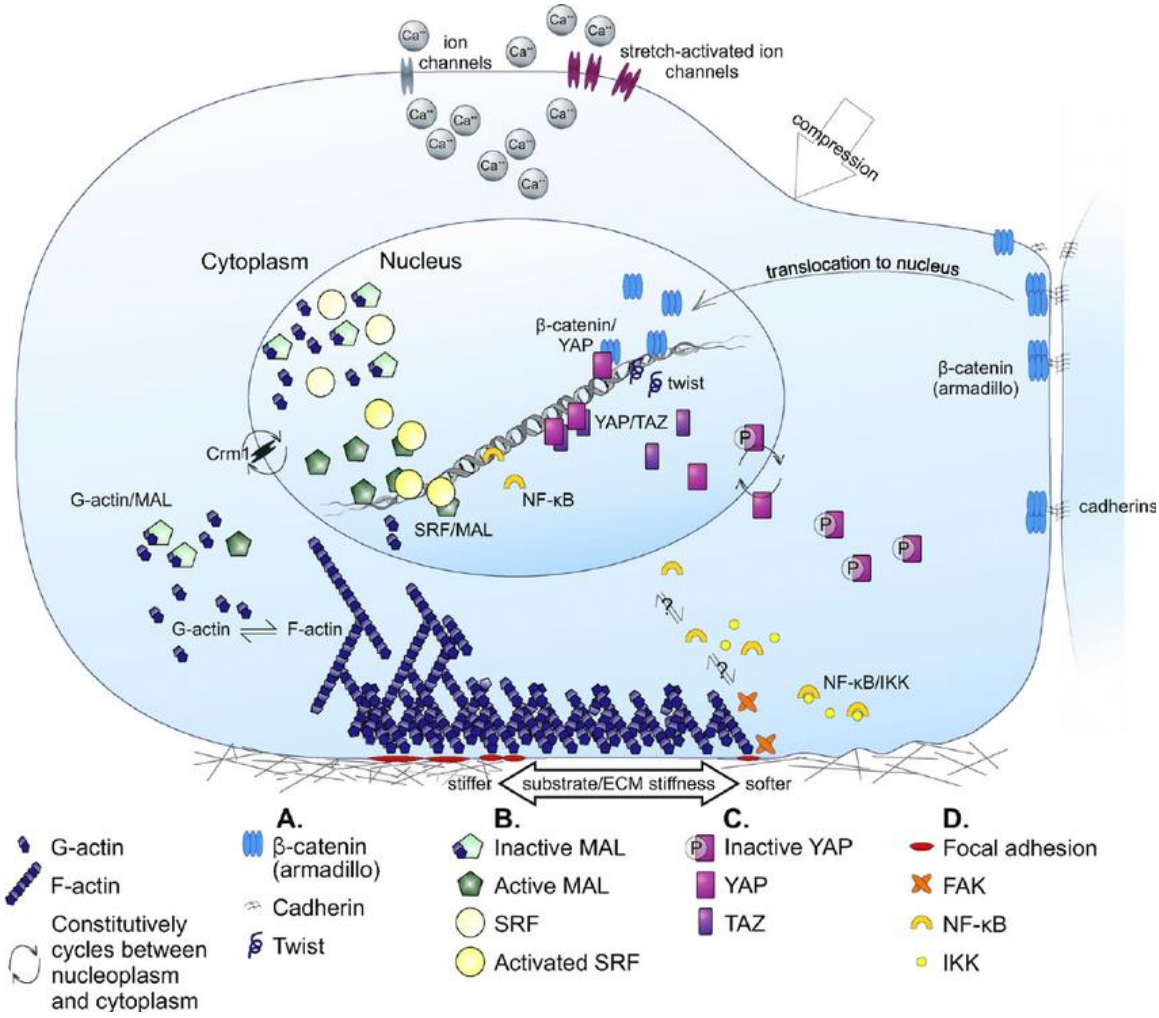

Figure 1.9 Mediators of mechanotransduction, and transcription factor response

Cells are able to sense and respond to mechanical forces through a wide range of signaling pathways, resulting in transcriptional responses. Some of these mechanisms include: adherens junctions and β-catenin nuclear import, ECM stiffness and focal adhesion/integrin signaling, cytoskeletal rearrangement and the levels of F-actin can drive MAL/SRF transcriptional responses, nuclear architecture change drive dynamic responses of YAP and TAZ in Hippo signaling, osmotic pressure and membrane deformation can induce stretch-gated ion channels to promote Ca^{2+} signaling (Image taken with permission from, Mendez and Janmey, 2012)

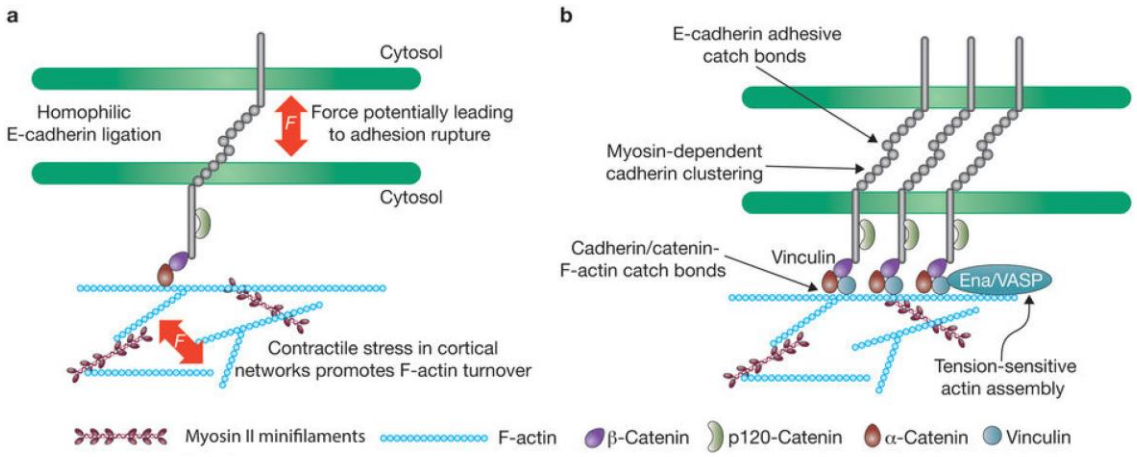

Figure 1.10 Adherens junctions respond to force by clustering to increase adhesion

(a) Adherens junctions consist of homophilic interactions between the transmembrane protein E-cadherin in adjacent cells, and the intracellular proteins β-catenin, p120-catenin, and α-catenin interacting with the cytoplasmic tails of E-cadherin. β-catenin binds to both E-cadherin and α-catenin, and α-catenin binds to F-actin allowing the cytoskeleton to link to cell-cell adhesion sites. (b) In response to intracellular contractile forces or transcellular forces (a), that may break cell-cell adhesion, Myosin II (NMII) induced clustering of adherens junctions occurs. Clustering of adherens junctions increases adhesion across cells. Cells also increase adherens junction attachment to the cytoskeleton by secondary force induced binding proteins like Vinculin. Other proteins such as Ena/VASP promote increased levels of F-actin, allowing for additional attachment sites. This promotes rigidity, and maintenance of adhesion under force. (Image taken with permission from Lecuit and Yap, 2015).

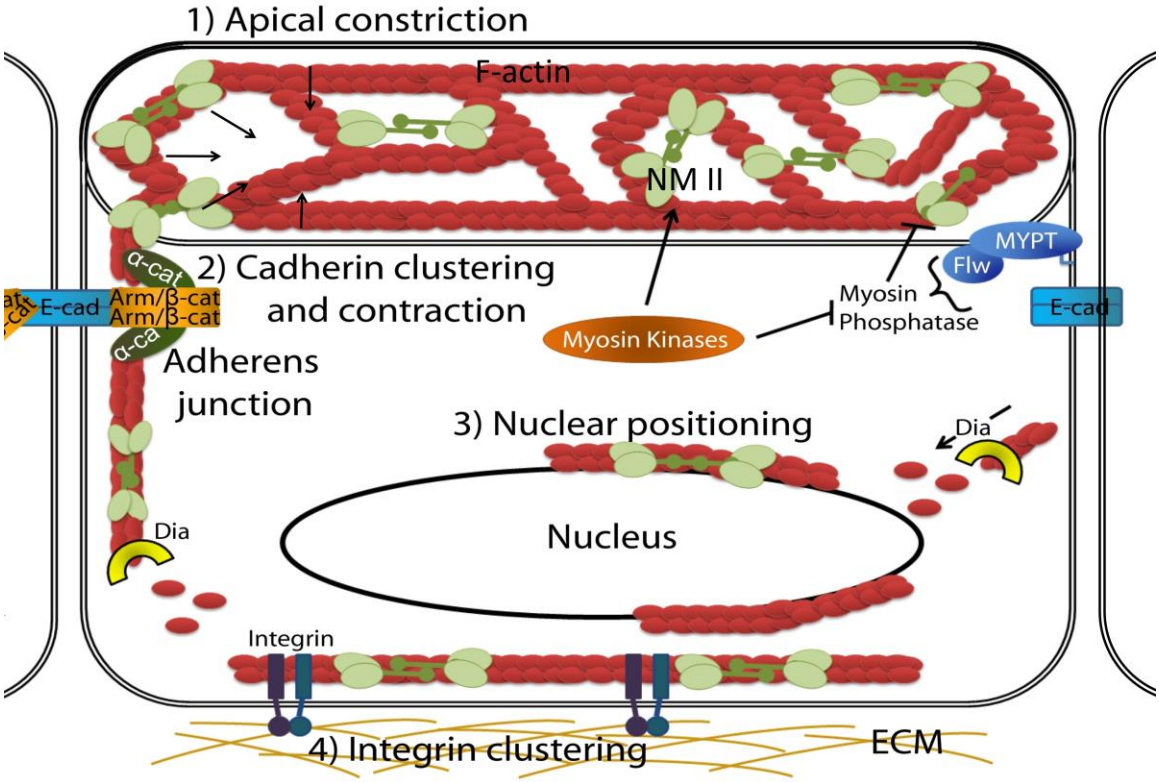

Figure 1.11 Non-muscle myosin II controls a diverse range cell functions.

Non-muscle myosin II (NMII) acts as the master motor protein, controlling many mechanisms by its modulation of the actin-cytoskeleton. NMII minifilaments are activated by multiple myosin kinases and inhibited by myosin phosphatase. Activated NMII binds to actin filaments (F-actin) that are produced by formin proteins like Diaphanous (Dia). NMII constricts adjacent filaments resulting in a wide range of responses, including: (1) apical constriction and cell shape changes: (2) Cadherin clustering, increasing cell-cell adhesion: (3) Nuclear positioning within the cell for and proper progression through the cell cycle, and cell division: (4) Integrin clustering and focal adhesion formation, driving cell-ECM attachment, and migration rates.

1.6. Wnt in development, homeostasis, and disease

Starting at embryogenesis, Wnt signalling is critical for a myriad of developmental processes, ranging from axis formation to cell differentiation and growth. It is then utilized again for the maintenance of many distinct stem cells populations, demonstrating its importance for homeostasis as well. The essential involvement of Wnt signaling in so many distinct biological processes has put it at the forefront for investigating the role of Wnts in genetic diseases, cancers, and as therapeutic targets (Katoh and Katoh, 2017; Tai et al., 2015; Voronkov and Krauss, 2013). It has been identified that mutations of almost every single core component of the pathway have been linked to an incredibly diverse range of diseases, including hereditary colorectal cancer, bone diseases, immune response, defects in angiogenesis, intellectual disability syndromes, metabolic disorders, PCP-related diseases, and many more.

Since the identification of the ability of *int-1* to induce transformation in mouse mammary epithelial cell (Nusse and Varmus, 1982), the study of the Wnt pathway and the involved cellular components required to regulate it in development and homeostatic processes has been a captivating and bustling field of research, utilizing diverse organisms and systems to study it (Nusse and Varmus, 2012).

1.7. Wnt/Wg signaling in developing *Drosophila melanogaster*

Genetic analysis in the fruit fly, *Drosophila melanogaster*, has truly spearheaded the identification and hierarchy of core components of the Wnt pathway, and the diverse role it plays in development. The Drosophila *wnt-1* gene*, wingless (wg*), was first identified as the name suggests, as a hypomorphic allele that resulted in a conversion of the adult wing into thoracic notum tissue (Sharma and Chopra, 1976). Subsequent mutational analysis demonstrated that *wg* is critical for a wide range of developmental processes including brain, leg, wing, mid-gut, and embryonic ectoderm patterning (Bejsovec and Martinez Arias, 1991; Cohen et al., 1991, 1993; Hoppler and Bienz, 1995; Schmidt-Ott and Technau, 1992), and its involvement in development has dramatically expanded since then.

Early mutational screens in Drosophila identified many of the core components of the pathway including *wg, porcupine, dsh, zw3* (GSK3)*, and arm* (Jurgens et al., 1984; Nusslein-Volhard et al., 1984; Nüsslein-Volhard and Wieschaus, 1980; Wieschaus et al., 1984). Later, genetic interaction studies of these genes by combinatorial mutations, allowed for epistatic analysis and the determination of the order of the core pathway proteins (Noordermeer et al., 1994; Siegfried et al., 1994). These studies laid the foundation for our understanding of the Wnt pathway.

1.7.1. Drosophila: a powerful tool for studying Wnt signaling

Drosophila provide an excellent model for studying signal transduction pathways. They have high fecundity with a quick life cycle, and their genomes have relatively low incidence of functional redundancy (Bejsovec, 2006). This allows for clearer interpretation for determining the function of essential genes. For these reasons classical mutational screens were able to identify many core components of individual signaling pathways.

Drosophila geneticists have also developed an incredible number of techniques for studying genetic interactions *in vivo.* The most widely used technique comes from the co-option of the yeast Gal4/UAS transcriptional regulation system, to allow targeted gene expression in Drosophila in a spatial and temporal manner (Brand and Perrimon, 1993; Fischer et al., 1988). cDNA or RNAi of a gene of interest linked to the enhancer like element, Upstream Activating Sequence (UAS), is crossed to a fly strain expressing the Gal4 transcription factor under a tissue specific promoter. In the resulting progeny the Gal4 will bind to the UAS element, inducing expression or knockdown of the gene of interest in the respective Gal4 domain. The Gal4/UAS system has since been diversified and refined for more targeted spatial and temporal experiments, utilizing drug and temperature inducible systems, combining it with FRT-mediated mitotic recombination events, and various reporter systems (reviewed in Duffy, 2002; Blair, 2003). The use of these techniques has become indispensable for studying Drosophila genetics.

1.7.2. Wnt signaling in the developing wing imaginal disc

During *Drosophila* larval development, the primordial adult structures begin to develop from imaginal discs, which initially consist of a few distinct clusters of

undifferentiated cells (Bate and Arias, 1991). These cells form sacs of proliferating epithelium that will undergo morphogenesis during pupation, to eventually give rise to the adult structures and appendages, such as the wings, eyes, antenna, and legs (Cohen et al., 1991; Whittle, 1990). In the wing imaginal disc by the third instar larval stage the refinement of major components of the adult wing have been established, this is regulated in a large part by *wg* expression (Baker, 1988; Phillips and Whittle, 1993). At this stage in development *wg* expression is refined to the dorsal/ventral (D/V) boundary of the wing disc, and in two concentric circles outlining the wing pouch, that will give rise to the presumptive wing margin, blade, and hinge (Couso et al., 1994; Williams et al., 1993). *wg* is also expressed in the notum of the disc, that will form part of the thorax (Phillips and Whittle, 1993)(Fig. 1.12).

wg expression along the D/V boundary of the wing imaginal disc has become a model for studying Wnt signaling in epithelial tissue, as a result the coordinated upstream signaling events that guide Wg refinement have been well established. Expression of the LIM domain containing protein Apterous (Ap), across the entire dorsal section of the wing disc, initiates the patterning refinement of the D/V boundary (Cohen et al., 1992; Diaz-Benjumea and Cohen, 1993; Williams et al., 1993). Ap induces Notch pathway activity along the presumptive D/V boundary by expression of the ligand *serrate* in adjacent cells (de Celis et al., 1996; Diaz-Benjumea and Cohen, 1995). Activated Notch signaling leads to the transcriptional initiation of *wg* along the D/V boundary (de Celis et al., 1996; Rulifson and Blair, 1995). Wg then spreads across the wing pouch inducing nested expression of target genes for wing outgrowth and guiding cell differentiation (Neumann and Cohen, 1997; Zecca et al., 1996).

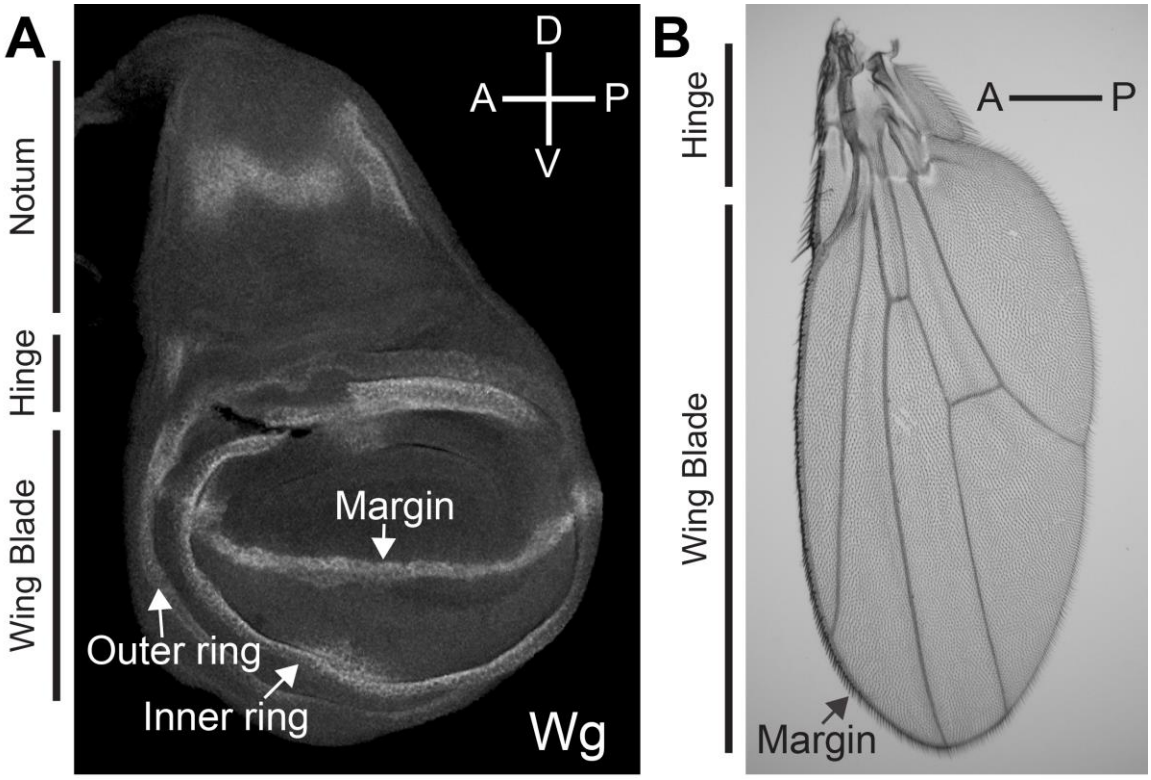

Figure 1.12 Wing imaginal disc Wg pattern guilds adult wing formation.

(A) *wg* expression in a third instar wing imaginal disc. *wg* is expressed in the presumptive notum, along the dorsal/ventral boundary of the disc, and outer and inner concentric circles. (B) Adult wing structure is determined by the expression pattern of *wg* to define the wing margin, blade, and hinge of the adult wing. A: anterior, P: posterior, D: dorsal, V: ventral.

1.8. Aims of the thesis

The purpose of this thesis is to build upon our current knowledge of the Wnt signaling pathway and its regulation and integration with other pathways in order to proceed with normal development and homeostatic regulation. This was done by building on work in our lab by Swarup et al., (2015), where an *in vivo* RNAi screen of the entire *Drosophila* kinome and phosphatome was performed in developing wing imaginal discs in an attempt to uncover novel regulators of the Wnt/Wg pathway. From this screen I have been able to select putative regulators and determine mechanistically how they are involved in promoting or restricting Wnt signaling in developing *Drosophila* and human cells.

The first aim of this thesis is to determine how the kinase and putative Wnt regulator, Downstream of Raf1 (Dsor1), is required for full activation of Wnt signaling, and what upstream signaling events lead to the involvement of Dsor1 in the pathway.

The second aim is to determine how the serine threonine phosphatase, Protein phosphatase 4 (PP4), is crucial for full Wnt signal activation.

The final aim investigates myosin phosphatase and how cellular physiology and mechanical forces are involved in modulating Wnt activity in developing epithelium.

Chapter 2. Ras-activated MEK1/Dsor1 promotes Wnt signaling

This chapter is based off published work from:

Hall E. T., and Verheyen E. M. (2015). Ras-activated Dsor1 promotes Wnt signaling in Drosophila development. Journal of Cell Science 2015 128: 4499-4511; doi: 10.1242/jcs.175240.

2.1. Abstract

Wnt/Wingless (Wg) and Ras/MAPK signaling both play fundamental roles in growth and cell-fate determination, and when dysregulated, can lead to tumorigenesis. Several conflicting modes of interaction between Ras/MAPK and Wnt signaling have been identified in specific cellular contexts, causing synergistic or antagonistic effects on target genes. We find novel evidence that the *Drosophila* homolog of the dual specificity kinases MEK1/2 (also known as MAP2K1/2), Downstream of Raf1 (Dsor1), is required for Wnt signaling. Knockdown of Dsor1 results in loss of Wg target gene expression, as well as reductions in stabilized Armadillo (Arm; *Drosophila* β-catenin). We have identified a close physical association between Dsor1 and Arm, and find that catalytically inactive Dsor1 causes a reduction in active Arm. These results suggest that Dsor1 normally counteracts the Axin-mediated destruction of Arm. We find that Ras-Dsor1 activity is independent of upstream activation by EGFR, and instead it appears to be activated by the insulin-like growth factor receptor to promote Wg signaling. Taken together our results suggest that there is a new crosstalk pathway between Insulin and Wg signaling that is mediated by Dsor1.

2.2. Introduction

The Wnt signaling pathway (Wingless (Wg) in *Drosophila*) plays a crucial role in all metazoans during growth and proliferation, cell-fate determination, and tissue homeostasis (Clevers and Nusse, 2012). Wnt signaling does not control all these processes independently, rather this is achieved by extensive interaction with other signaling pathways, leading to synergistic or antagonistic effects normally resulting in

desirable biological outcomes (reviewed in Zeller et al., 2013; Kim & Jho, 2014; Itasaki & Hoppler, 2010; Collu et al., 2014). Determining how signaling pathways can influence each other through either antagonism or promotion at different levels is essential to understanding disease progression and basic cellular functions.

The canonical Wnt/Wg signaling pathway revolves around the stabilization and localization of the key transducer, β-catenin [Armadillo (Arm) in *Drosophila*]. β-catenin is a continuously produced multifunctional protein essential for the maintenance of the adherens junctions as well as for Wnt signaling (Valenta et al., 2012). In the absence of Wnt ligand, cytoplasmic β-catenin is continuously targeted for degradation by a destruction complex consisting of Axin, Adenomatous polyposis coli (APC) and the kinases, Casein kinase 1 alpha (CK1α), and Glycogen synthase kinase 3β (GSK3β, also known as Shaggy in *Drosophila*).CK1α and GSK3β phosphorylate β-catenin, targeting it for ubiquitination and subsequent proteasomal digestion. Upon Wnt/Wg binding to its coreceptors Frizzled (Fz) and LRP/Arrow (Arr), Dishevelled (Dvl/Dsh) is recruited to the receptors and then mediates recruitment of the destruction complex, along with Arm, to Arr, which is localized at the membrane. This results in the disruption of the destruction complex, allowing accumulation of newly synthesized β-catenin, which can then translocate to the nucleus, acting as a co-activator with T-cell factor (TCF)/lymphoid enhancer factor and (LEF) to initiate expression of target genes (Daniels and Weis, 2005). Perturbations to many of these components or additional regulatory proteins have been implicated in a multitude of cancers and developmental disorders (Clevers and Nusse, 2012).

One signaling pathway that is also crucial for growth, cell fate and tissue homeostasis, and which has been implicated in many of the same diseases as aberrant Wnt signaling, is the receptor tyrosine kinase (RTK)-Ras-mitogen-activated protein kinase (MAPK) pathway, in particular that using the RTK epidermal growth factor receptor (EGFR) (Guturi et al., 2012; Lee et al., 2010; Paul et al., 2013). Pathway activation occurs upon ligand binding to the receptor, leading to the recruitment of Grb2 and the guanine exchange factor, Son of sevenless (Sos). Sos converts the G-protein Ras85D (hereafter referred to as Ras) to an active state, and thereby activates the mitogen-activated protein kinase (MAPK) cascade. The MAPK signaling cascade consists of 3 kinases, Raf (also known as Polehole in *Drosophila*), a MAPK-extracellular signal-regulated kinase family protein (MEK1/2, also known as MAP2K1/2) [Downstream

of Raf1 (Dsor1) in *Drosophila*], and the extracellular signal-regulated kinase (ERK1/2, also known as MAPK3 and MAPK1) family protein [Rolled (Rl) in *Drosophila*]. Ras first activates Polehole, which in turn phosphorylates Dsor1 to activate it. Dsor1 can then dually phosphorylate and activate Rl, which in turn can then phosphorylate and modulate a wide range of substrates throughout the cell, including transcription factors to affect target gene expression (Courcelles et al., 2013). Several proteins from the EGFR-Ras-MAPK pathway have been identified to directly interact with Wnt signaling components, in particular ERK family proteins (Červenka et al., 2011; Hoschuetzky et al., 1994; Krejci et al., 2012; Ding et al., 2005).

Previous studies of Wnt and Ras-MAPK have focused on interactions in various disease states and cancers (Zeller et al., 2013). There is a gap in understanding of how these two key signaling pathways interact in a normal context for proper organismal development. In a kinome and phosphatome RNA interference (RNAi) screen in the developing *Drosophila* larva, multiple components of the EGFR-Ras-MAPK signaling cascade were found to affect Wg signaling (Swarup et al., 2015). Here, we show that Dsor1 plays a crucial conserved function in mammalian cells and *Drosophila* in promoting Wg signaling. We find this is independent of activation of Rolled, and instead that it rather occurs through a new mechanism that involves recruitment and subsequent inhibition of the destruction complex at the membrane. In addition, we show that activation of Dsor1 by Ras in this context is not through EGFR, but most likely the insulin-like growth factor receptor. Taken together, these studies identify a new conserved interaction between RTK–Ras–MAPK and Wg pathways that is mediated by Dsor1 and MEK. This crosstalk is crucial for full Wnt signal propagation for normal development.

2.3. Results

2.3.1. Dsor1 interacts with the Wg pathway to promote target gene expression

Several kinases and phosphatases from the EGFR–Ras–MAPK pathway have been previously identified in an RNAi screen based on their ability to modulate Wg target gene expression (Swarup et al., 2015). We focused our attention on Dsor1, as it was the most terminal protein in the EGFR signaling cascade identified in the screen. In the

developing wing imaginal disc, Wg is secreted from a small stripe of cells marking the dorsoventral boundary, which will eventually form the adult wing margin (Couso et al., 1994). Wg triggers pathway activation and transcriptional response in a concentration-dependent manner in the surrounding cells of the wing pouch (Neumann and Cohen, 1997; Zecca et al., 1996). Sens is only transcriptionally activated in cells flanking the Wg-secreting cells, which have the highest levels of pathway activation (Fig. 2.1A, A″) (Parker et al., 2002). *Dll* is expressed in a much broader domain within the wing pouch (Fig. 2.1B), as it requires lower levels of active Wg signaling to induce its transcription (Zecca et al., 1996). The expression of two independent *dsor1-RNAi* lines in the posterior domain of the disc using engrailed *(en)-Gal4* (marked by GFP; Fig. 2.1C, C′), resulted in a loss of Sens and strong reduction in *Dll* transcription (Fig. 2.1C″,D), suggesting that Dsor1 acts a positive regulator of the Wg pathway.

Wg is a target gene of Notch signaling at the dorsoventral boundary in the wing disc (Klein and Arias, 1998), and crosstalk has been described between Notch and EGFR signaling in *Drosophila* development (Doroquez and Rebay, 2006). To determine whether loss of Dsor1 was affecting Notch signaling upstream of Wg signaling, a *wg* transcriptional reporter, *wg-lacZ* was utilized (Fig. 2.1E). Expression of dsor1-RNAi in the anterior domain of the wing (using *ci-Gal4*) had no effect on *wg* transcription (Fig. 2.1F). Next we assessed whether Wg processing and stability were being affected. Wg is a lipid-modified glycoprotein, and must undergo post translational modifications before being secreted (Franch-Marro et al., 2008; Tanaka et al., 2002). Analyzing total Wg protein levels is a good indicator of defects in Wg stability or processing. Total Wg protein did not differ in control (Fig. 2.1G) and *dsor1-RNAi*-expressing tissue (Fig. 2.1H), suggesting that Dsor1 does not act to regulate *wg* transcription or processing in the secreting cells.

To confirm that reductions in Dsor1 did not critically affect cell viability, and was indeed directly down-regulating Wg signaling, we utilized the apoptotic marker cleaved caspase-3 (C. Casp-3). Small patches of cells within the *dsor1-RNAi* expressing domain did have elevated levels of cleaved Casp-3, indicating that apoptosis was occurring in some areas (Fig. 2.2A, A'). To rule out the effects of apoptosis on Wg signaling, the baculoviral P35 anti-apoptotic protein was co-expressed with *dsor1-RNAi* (Fig. 2.2B, B') (Hay et al., 1994). Co-expression of *p35* and *dsor1-RNAi* still resulted in loss of Sens (Fig. 2.2C, C'), suggesting that the Wg pathway effects are not solely due to cell death.

To validate that the effects of the RNAi lines were a result of a direct reduction in Dsor1, and not due to off target knock down, expression of a *dsor1* transgene was utilized to rescue the *dsor1-RNAi* phenotype. Expression of *dsor1-RNAi* in adult wings resulted in a loss of vein material, indicative of loss of EGFR signaling (Fig. 2.2F)(Diaz-Benjumea and Hafen, 1994). Expression of *dsor1* alone had no effect on the adult wing (Fig. 2.2E), or *Dll* expression in the wing imaginal disc (Fig. 2.2H, I), as Dsor1 is inert unless activated by the rate limiting kinase Raf (Fujioka et al., 2006). *UAS-dsor1* was able to rescue the vein defect and reduction of *Dll* caused by *dsor1-RNAi*, confirming the phenotype seen from RNAi was directly a result of a loss of Dsor1 (Fig. 2.2G, J, K).

To further confirm RNAi results, mitotic clones were generated for a *dsor1* loss of function allele (LOF). Clones of $dsor1^{LOF}$, marked by the presence of GFP (Fig. 2.1I, I'), also resulted in a loss of Sens (Fig. 2.1I" arrow). In addition, the adult wings of flies harbouring small clones at the wing margin exhibited notches, a phenotypic hallmark of reduced Wg signaling (Fig. 2.1J inset). Taken together, these results suggest that Dsor1 is required for Wg target gene transcription.

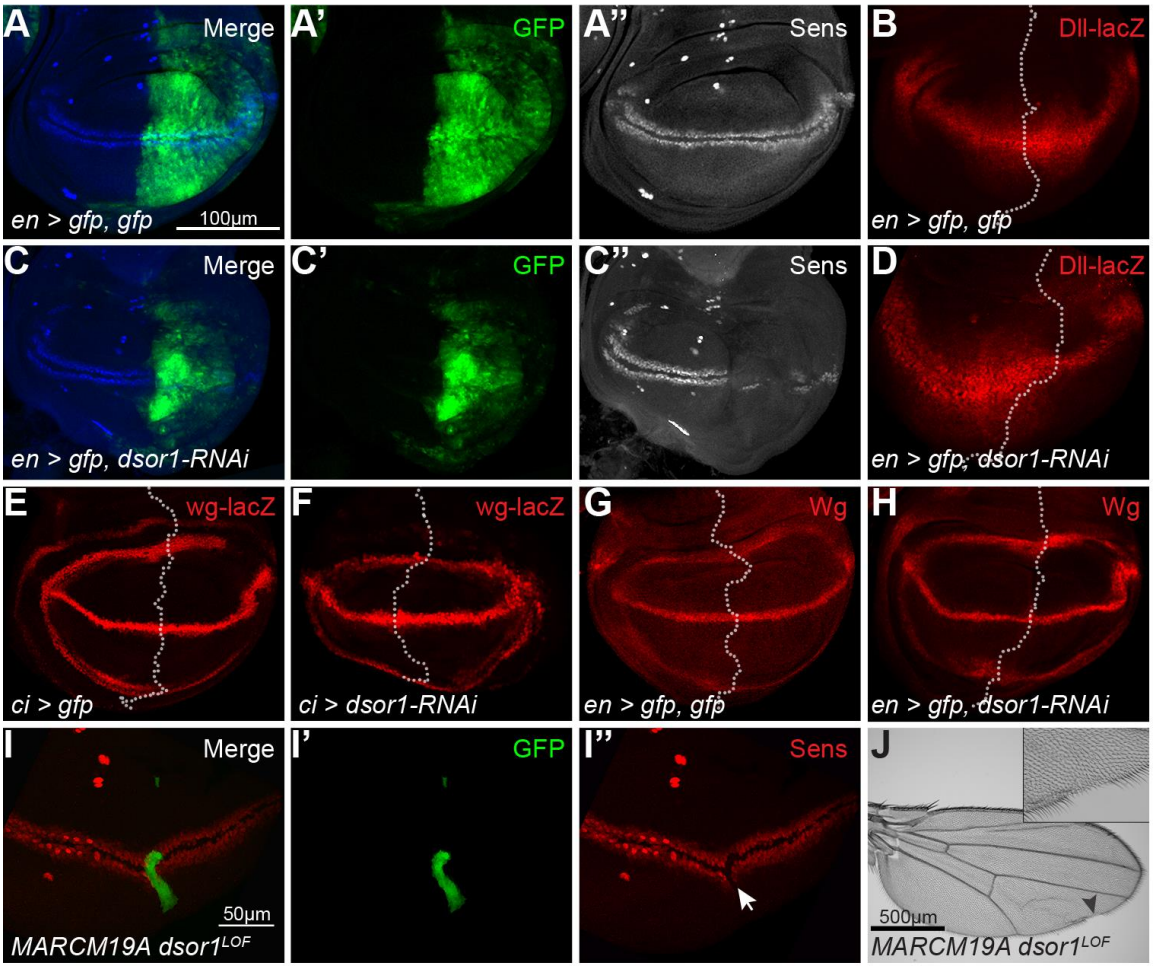

Figure 2.1 Dsor1 is required for Wg signaling

(A-B) Normal expression pattern of *en-Gal4* (A') in the posterior domain of the developing wing disc, shown with the Wg target genes Sens (A'') and *Dll-lacZ* (B). (C,D) The knockdown of Dsor1 via RNAi in the posterior domain (C') causes a loss of Sens (C'') and a strong reduction in *Dll-lacZ* (D). In B and D, the *en-Gal4* domain is to the right of the indicated anterior–posterior boundary (dotted line). (E-F) Utilizing *ci-Gal4*, expressed in the anterior domain (to the left of the dashed line) of the wing imaginal disc, showed no change in *wg* transcription levels (*wg-lacZ*) upon Dsor1 knockdown (F) compared to wild type (E). Total Wg protein levels in wildtype (G) are similar to those seen after Dsor1 knockdown (H). GFP positive *dsor1*^{lof} MARCM clones (I, I') exhibit a loss of Sens (I'' arrow), and induce notches in the adult wing margin (J).

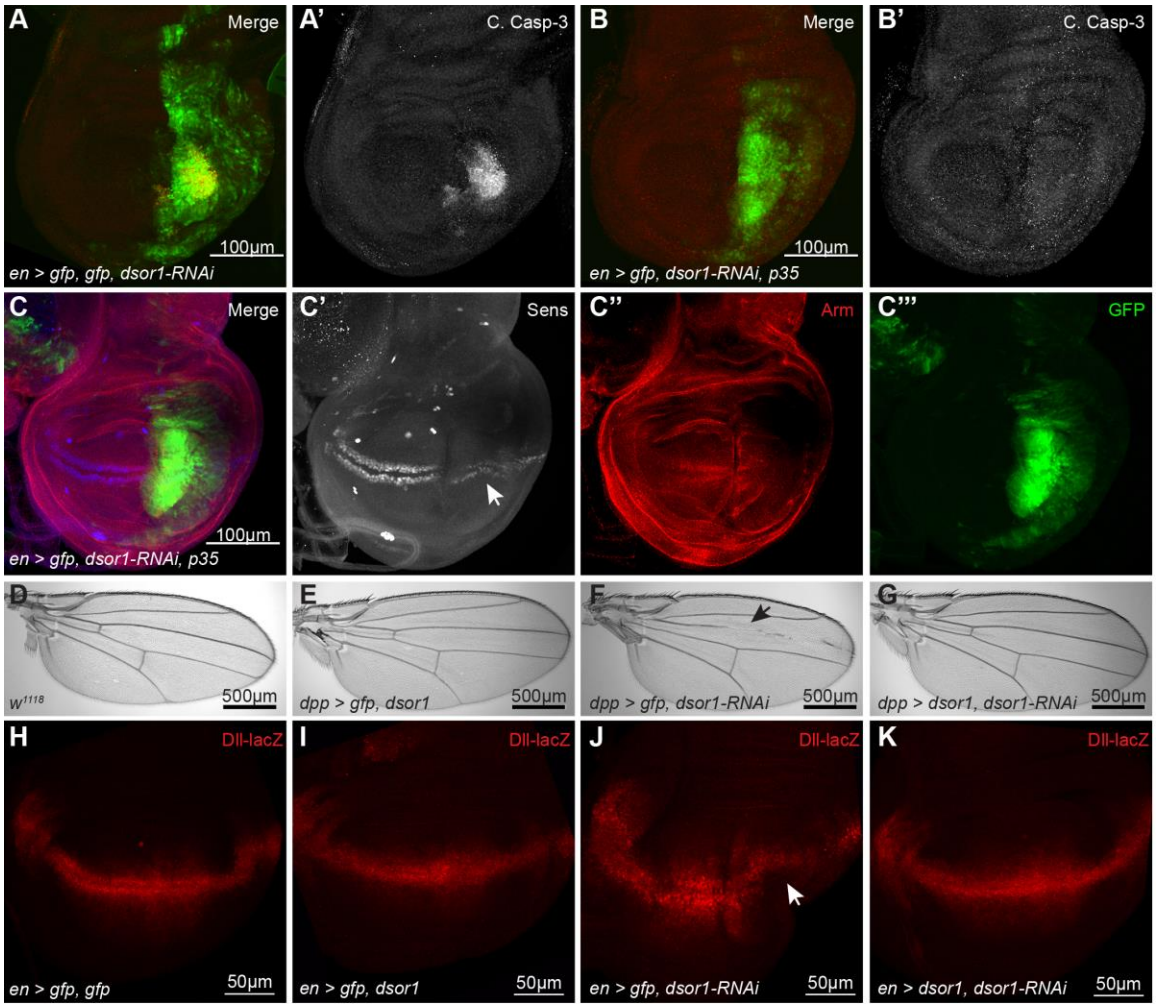

Figure 2.2 Reduction of Dsor1 directly affects Wg signaling.

(A-A') Expression of *dsor1-RNAi* can induce small patches of apoptotic cells marked by cleaved caspase-3(A'). Coexpression of P35 inhibits caspase-3 activation (B-B'). (C-C''') Knockdown of Dsor1 with P35 expression in the posterior domain (C''') results in a loss of Sens (C' arrow), and Arm (C''). Wild type adult wing (D). Over expression of Dsor1 with *dpp-Gal4* expressed between the 3rd and 4th wing veins had no effect (E). The knockdown of Dsor1 using *dpp-Gal4* resulted in a loss of vein material (F arrow). The expression of Dsor1 can rescue the knockdown phenotype from *dsor1-RNAi* (G). Normal expression pattern of Dll-lacZ in the wing imaginal disc (H). *UAS-dsor1* expressed in the posterior domain does not affect Dll-lacZ expression (I). *dsor1-RNAi* expressed in the posterior domain reduces Dll-lacZ (J arrow). The expression of Dsor1 can rescue the Dll-lacZ reduction from *dsor1-RNAi* in the posterior domain (K).

2.3.2. Dsor1 interacts with the Wg pathway prior to destruction complex disruption

To determine at which point Dsor1 acts on the Wg pathway, we first focused on Arm stability as its regulation is key for pathway activation. In the wing imaginal disc, Arm is seen in highest concentrations in two bands flanking the Wg-producing cells at the D/V boundary (Fig. 2.3A) as a result of Arm stabilization allowing high levels in the cytoplasm and nucleus of these cells (Marygold and Vincent, 2003). The expression of *dsor1-RNAi* resulted in a reduction of stabilized Arm, but Arm located in the adherens junction appeared unchanged (Fig. 2.3B, B'). These results were also seen with co-expression of P35 to inhibit any potential cell death (Fig. 2.2C''). Clones of $dsor1^{LOF}$, marked by the presence of GFP (Fig. 2.3C, C'), resulted in a similar loss of stabilized Arm (Fig. 2.3C"). These results suggest that in the absence of Dsor1, Arm is still targeted for proteasomal degradation, even under conditions of active Wg signaling, where the destruction complex would normally be inactivated.

To investigate a link between Dsor1 and the destruction complex, we generated $axin^{null}$ clones and tested for effects on Arm. Axin is a scaffolding protein which acts as the backbone holding the destruction complex together (Zeng et al., 1997). Clones lacking Axin, marked by GFP (Fig. 2.3D, D'''), showed massive accumulations of Arm and resulted in ectopic production of Sens within the clone (Fig. 2.3D', D''). The introduction of *dsor1-RNAi* into an $axin^{null}$ background had no effect on Arm or ectopic Sens (Fig. 2.3E-E'''). Thus, although under normal conditions reduction of Dsor1 caused loss of Arm, in the absence of the destruction complex Dsor1 had no effect. Taken together our findings suggest Dsor1 functions upstream, or at the level of the destruction complex.

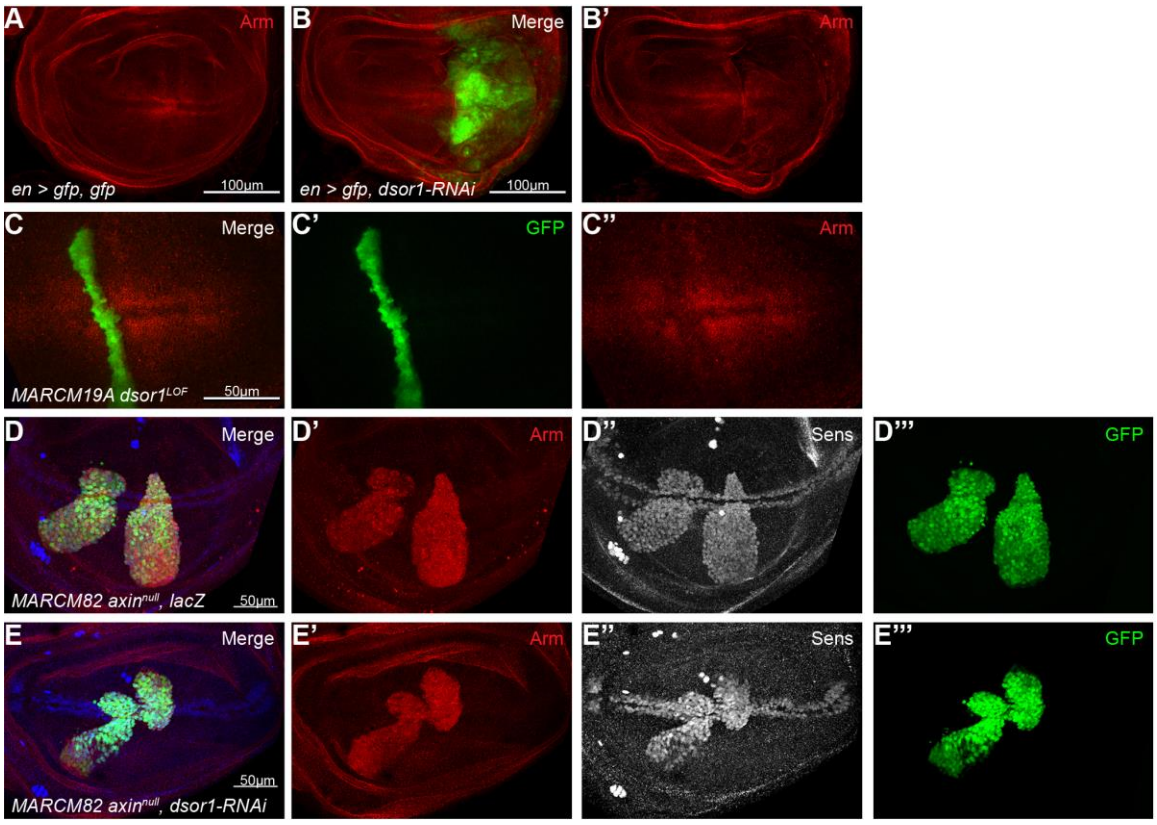

Figure 2.3 Dsor1 acts at or above the level of Arm destruction

Wild type Arm protein stabilization (A). Knockdown of Dsor1 in the posterior domain (marked with GFP) caused a reduction in stabilized Arm (B-B'). GFP positive *dsor1*^{lof} MARCM clones (C, C') show a reduction of stabilized Arm (C''). GFP positive *axin*^{null} MARCM clones (D, D"') show a dramatic accumulation of Arm (D') and Wg target gene product Sens (D''). (E-E"') Expression of *dsor1-RNAi* within *axin*^{null} MARCM clones (E"') showed no change in Arm (E') or Sens (E'') compared to *axin*^{null} clones alone.

2.3.3. Characterization of Wg signaling within the *Drosophila* salivary gland

Regulation of the destruction complex can involve its recruitment and inhibition at the cell membrane following receptor-ligand interaction (Tamai et al., 2004). To investigate whether Dsor1 affects the Wg pathway at the membrane, we looked for effects on protein localization following *dsor1* knockdown. The wing imaginal disc epithelium is composed of tightly packed columnar cells that make it difficult to identify protein localization beyond apical or basal positioning. The *Drosophila* salivary gland, with its giant polyploid cells, offers a much better opportunity to study protein localization *in vivo*, although information about the activity of Wg in this tissue is minimal.

It has been previously shown that Wg is present in the salivary gland where it induces graded ploidy levels (Taniue et al., 2010). We thus set out to characterize Wg pathway activity in this tissue and to use this to study the effects of Dsor1 on Wg signaling. Wg staining revealed that the protein was produced and secreted by cells within the imaginal ring, marked by small nuclei (Fig. 2.4B, B'), and formed a gradient in the proximal cells (Fig. 2.4A). This resulted in the highest levels of cytoplasmic and nuclear Arm within the proximal cells, and transcription of Wg target gene *fz3* (Fig. 2.5B, C; Fig. 2.4C, E, E'). As no suitable anti-Axin antibody was available, we obtained a fly strain that is heterozygous for a mutation in *axin*, while simultaneously expressing FLAG-tagged Axin under the ubiquitous *tubulin* promoter (Petersen-Nedry et al., 2008). In this strain, FLAG-Axin was found at high levels at the membrane in areas with active Wg signaling, and was reduced gradually outside of the zone of active Wg signaling (Fig.2.4G-G"). Membranous Axin localization can be used as an indicator of destruction complex membrane recruitment and disruption (Tamai et al., 2004). In the proximal Wg-receiving cells, a Dsh-GFP fusion protein revealed that Dsh was mainly cytoplasmic with puncta scattered throughout the cytoplasm and at the membrane (Fig. 2.5A, D; Fig. 2.4I, I' arrow) (Axelrod, 2001). Puncta formation is due to the Dsh DIX domain, which allows Dsh polymerization, and anchoring of Axin to the membrane (Bilic et al., 2007; Metcalfe, Mendoza-Topaz, et al., 2010; Schwarz-Romond et al., 2007). As Wg signaling diminishes in the distal cells, cytoplasmic levels of Dsh-GFP dropped dramatically and the protein became mainly nuclear, with moderate levels remaining at the cell membrane (Fig.2.4I''). The model given in Fig. S2K represents expression domains of Wg and several key proteins in the pathway in the salivary gland.

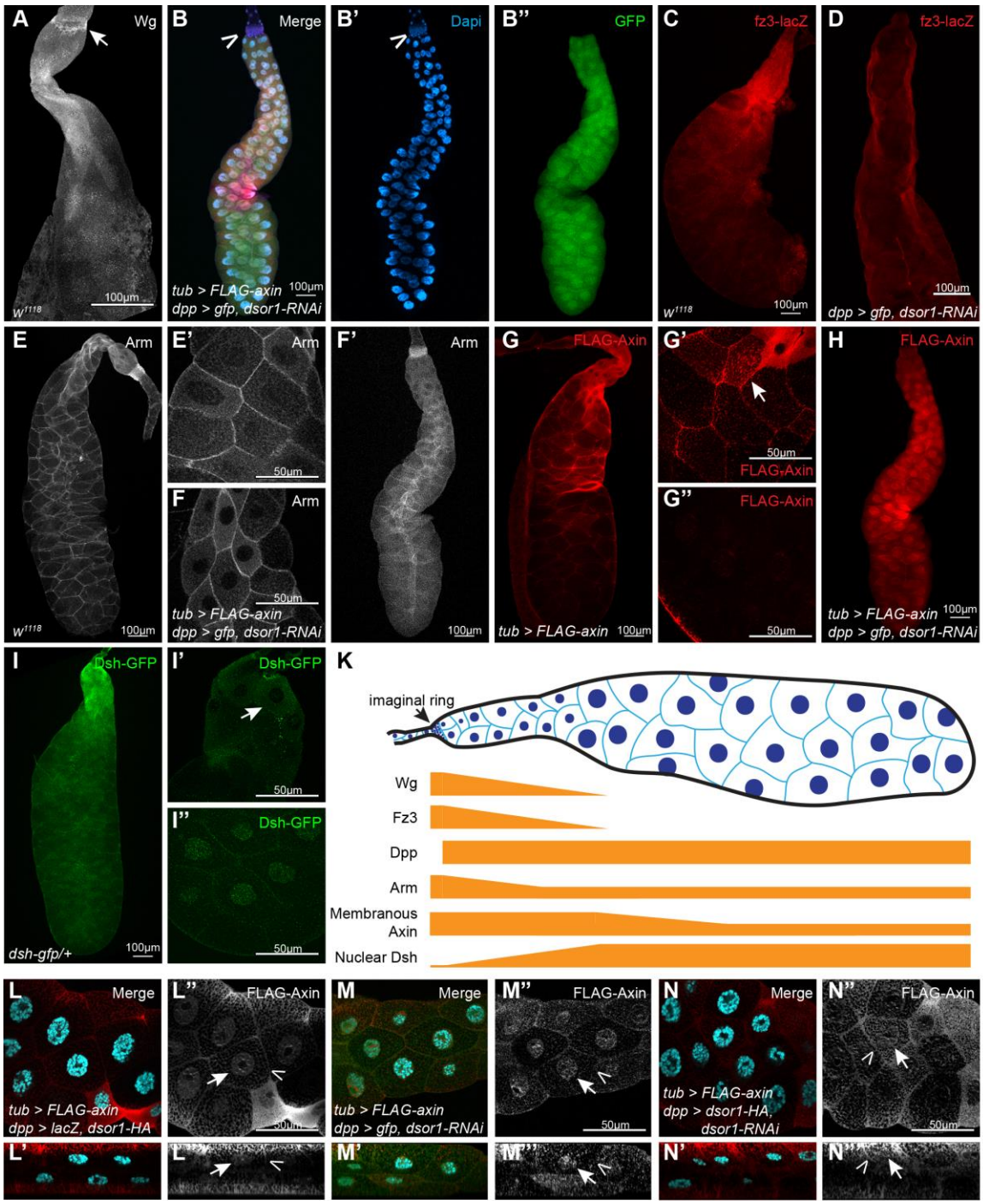

Figure 2.4 Characterization of Wg signaling in the developing salivary glands.

(A) Wg is produced and secrected from the imaginal ring (arrow) to the proximal cells. (B-B') DAPI marks the small diploid nuclei of the imaginal ring (arrow heads). (C) Transcription of the target gene *fz3* occurs in the most proximal cells. Use of *dpp-Gal4* expressed in the Wg-receiving cells (B, B'') to drive *dsor1-RNAi* results in a loss of *fz3* transcription (D). (E-F') Arm levels are highest in the imaginal ring and reduce gradually in the proximal cells (E). Knockdown of Dsor1 causes a reduction in nuclear Arm (F, F'), compared to wild type (E'). (G-G'') FLAG tagged Axin in wild type salivary glands is

highest at the membrane in proximal cell (G' arrow), and gradually reduce to lower levels in the distal cells (G''). Expression of *dsor1-RNAi* causes uniform Axin localization in the salivary gland, with high nuclear enrichment (H). (I-I'') Dsh-GFP is almost entirely membrane associated and cytoplasmic within the proximal cells (I' arrow), and shifts to more nuclear levels in the distal domain (I''). (K) A visual summary of the Wg expression pattern and several key signaling components that respond to Wg ligand. *dpp-Gal4* was used to express transgenes of interest due to the strong expression throughout the salivary gland. (L-N"') Dsor1-HA can rescue the *dsor1-RNAi* phenotype of FLAG tagged Axin localization. Nuclei identified by arrows, and cell mambranes shown by arrow heads. (L-L"') Expression of *dsor1-HA* results in FLAG tagged Axin localization comparable to wild type conditions. (M-M"') Expression of *dsor1-RNAi* results in decreased membranous FLAG tagged Axin (M", M"' arrow heads), and nuclear enrichment (M", M"' arrows). (N-N"') Coexpression of *dsor1-HA* and *dsor1-RNAi,* resuces the *dsor1-RNAi* phenotype, with FLAG tagged Axin localization comparable to wild type or *dsor1-HA* alone (N"-N"').

2.3.4. Dsor1 is required for Axin membrane localization

Having better characterized the distribution of Wg pathway components in the salivary gland, we were able to focus on the effect of Dsor1 on their localization and functionality. A strong potential target for Dsor1 to interact with is Dsh, as it must be phosphorylated to be recruited to Fz and to, in turn, recruit the destruction complex to the membrane (Rothbächer et al., 2000; Umbhauer et al., 2000). The use of *dpp-GAL4* to express *dsor1-RNAi* throughout the salivary gland (Fig. 2.4B'') caused no change in Dsh-GFP puncta and overall localization in proximal cells compared to wild type (Fig. 2.5D, D', G, G'). *dsor1* knock down resulted in a complete absence of the Wg target gene *fz3* (Figs. 2.5E-F', 2.4D), coinciding with a notable reduction in nuclear Arm levels (Fig. 2.4F, F'). From these results, it appears that the role of Dsor1 in the pathway is likely after Dsh phosphorylation and recruitment to Fz, given that Dsh recruitment is normal without Dsor1, but target gene activation is inhibited.

As a reduction in Dsor1 did not perturb Dsh localization, we speculated that Dsor1 interacts with the destruction complex itself. The destruction complex had constitutive activity with the loss of Dsor1, as seen by loss of Arm even in the presence of Wg signaling. The scaffolding protein Axin has diverse roles in the cell in many different contexts and locations (Luo & Lin, 2004). Under active Wg signaling conditions, Axin is found throughout the cell, but with enrichment at the cell membrane (Fig. 2.5H-I'), as a result of destruction complex recruitment (Tamai et al., 2004). This phenotype is also seen upon Dsor1 overexpression (Fig. 2.4L-L'''). Reduction of Dsor1 by RNAi resulted in a striking loss of membranous Axin and a build up of nuclear levels (Fig. 2.5J-K', Fig. 2.4M-M'''). This affect could be rescued by the overexpression of the *dsor1* transgene (Fig. 2.4N-N'''). We propose that the loss of membranous Axin and nuclear accumulation are two independent events. First, the reduction of membranous Axin within the active Wg-receiving cells suggests that Dsor1 is required to recruit the destruction complex to the membrane. Without Dsor1, Axin and the destruction complex remain active in the cytoplasm, where they mediate the degradation of Arm and thus preventing transcription of target genes. Second, we have shown that *dsor1-RNAi* can critically impair cell viability, and induce patches of apoptotic cells (Fig. 2.2A). Axin has been shown to translocate to the nucleus under conditions of cell stress, where it plays a crucial role with p53 in cell viability to initiate cell-cycle arrest or apoptosis (Li et al., 2009). In addition, Lui et al.

(2011) have identified a nuclear role for Axin in promoting Wnt signaling post β-catenin stabilization. Given that we observe reduced Wg signaling due to loss of *dsor1*, our findings suggest that the nuclear Axin associated with Dsor1 knockdown is independent of Wg signaling. Thus we propose that loss of Dsor1 causes both the Wnt-specific loss of Axin membrane recruitment and the unrelated nuclear localization linked to cell stress. This interpretation is bolstered by the appearance of nuclear Axin in every cell in the salivary gland, including the proximal cells distant from active Wg signaling (Fig. 2.4H). Taken together these results show that the role of Dsor1 in the Wg pathway occurs after Dsh recruitment, but appears to be critical for the subsequent recruitment of Axin and the destruction complex.

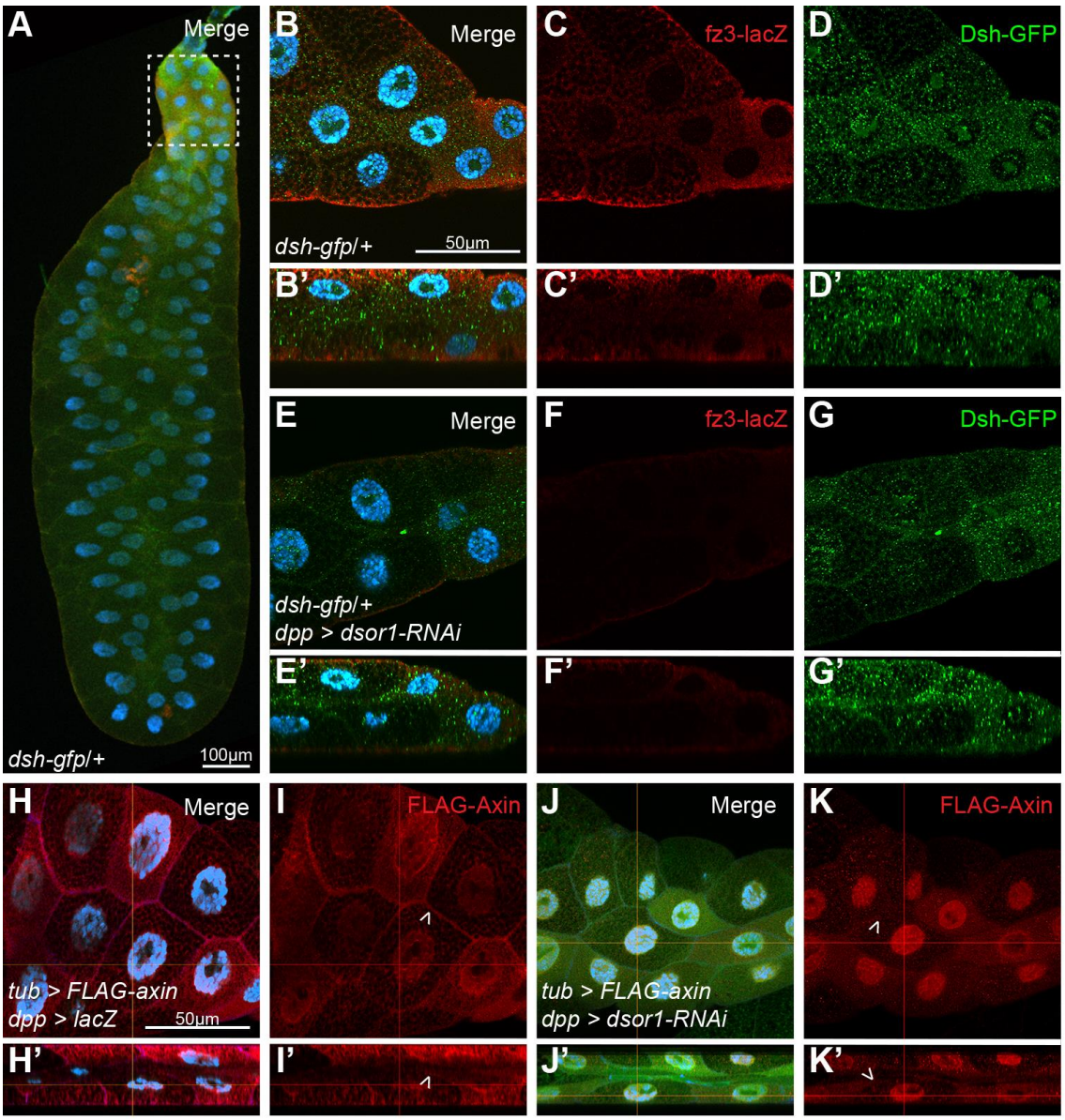

Figure 2.5 **Dsor1 acts within the Wg receiving cells after Dsh recruitment and appears to be required in recruitment of the destruction complex to the cell membrane.**

(A) Salivary gland stained with DAPI to mark cell nuclei, and anti-GFP and anti-Wg antibodies. White outlined box indicates proximal cells, with anterior to the right in all subsequent panels. (B-K') Zoomed in proximal cells of the salivary gland, nuclei marked with DAPI. (B-D') Wg target gene, *fz3,* has high expression in proximal cells (B-C'). Dsh-GFP is located mainly in the cytoplasm, with low nuclear levels. Dsh-GFP puncta are found in both cytoplasm and near the cell membrane (B, B', D, D'). (E-G') Expression of *dsor1-RNAi* resulted in a loss of *fz3* transcription (E-F'), and no change in Dsh-GFP localization (E, E', G, G'). (H-I') The fly strain, *tub>FLAG-axin/UAS-lacZ; dpp-GAL4, UAS-gfp/axin*^{null} expressed FLAG-tagged Axin throughout the proximal cells, with the highest levels seen at cell membranes (arrow heads). (J-K') Expression of *dsor1-RNAi* in *tub>FLAG-axin/UAS- dsor1-RNAi; dpp-GAL4, UAS-gfp/axin*^{null} flies caused a loss of

membrane-associated FLAG-Axin (arrow heads), and a large fraction appears to shuttle to the nucleus (K-K').

2.3.5. Rolled does not affect Wg signaling

Having determined that Dsor1 interacted with the Wg pathway at the level of recruitment of the destruction complex, it became imperative to confirm that loss of Wg signaling was directly due to loss of Dsor1, and not simply the failure to activate the downstream MAPK Rolled (Rl). An interaction between Wnt components and the Rl ortholog ERK has been identified in several cases (Červenka et al., 2011; Ding et al., 2005; Krejci et al., 2012), including in *Drosophila* (Freeman and Bienz, 2001). Knock down of *rl* by RNAi showed no effect on *Dll* expression and did not induce cell death in the wing disc (Fig. 2.6A-A'', B, B"), but was able to disrupt patterning and expression of the EGFR target gene *argos* (Fig. 2.6B, B', G). In addition *rl-RNAi* expressed along the anterior-posterior section of the wing resulted in a loss of vein tissue (Fig. 2.6D, arrow head), a hallmark of reduced Rl activity (Brunneret al., 1994), demonstrating the effectiveness of *rl-RNAi.*

To address the possibility that *rl-RNAi* was unable to reduce Rl levels enough to directly affect Wg targets, we used mutant alleles of *rl*, namely the *rl* hypomorphic allele rl^{1}, and the strong hypermorphic allele $rl^{sevenmaker\ (sem)}$(Brunneret al., 1994). Homozygous rl^{1} adult wings were smaller, creased and droopy (Fig. 2.7D) compared to wild type (Fig. 2.7A-B), indicative of reduced *rl* activity (Brunner et al., 1994), yet discs displayed normal Sens and stabilized Arm expression (Fig. 2.7C-C''). Heterozygous rl^{sem} adult wings contained excess vein material indicative of hyper-activated EGFR and Rl activity (Fig. 2.7F)(Brunner et al., 1994). Analysis of rl^{sem}/+ wing discs revealed undisrupted Sens and Arm expression compared to wild type (Fig. 2.7A-A'', E-E'').

To further confirm a Dsor1-specific role in the Wg pathway and rule out the predominant target of Dsor1 (i.e. the MAPK Rl), as an effector in this role, we expressed *dsor1-RNAi* in the posterior domain of the wing disc in an activated Rl genetic background (rl^{sem}/+). Adult wings exhibited a mix of ectopic and lost vein tissue in the posterior domain (Fig. 2.7H, asterisk), indicating that hyperactive Rl was still partially functional in the tissue even with reduced Dsor1. Additionally wings did not show creases, or the 'droopy' phenotype, suggesting that Rl activity was not reduced as a result of Dsor1 reduction. The wings also exhibited a notched wing phenotype, a hallmark of reduced Wg signaling (Fig. 2.7H). Staining of the imaginal disc revealed a complete loss of Sens and reduced Arm levels within the posterior domain, indicating

that this is a Dsor1-specific effect (Fig. 2.7G-G''). We also examined interactions between *UAS-Rl*^{sem} and Dsor1.The co-expression of *Rl*^{sem} and *dsor1-RNAi* still caused reduced Sens and a loss of stabilized Arm in the wing disc (Fig 2.6E-E''). Taken together, these results support the model that Dsor1 is acting in a Rl-independent manner to modulate Wg signaling.

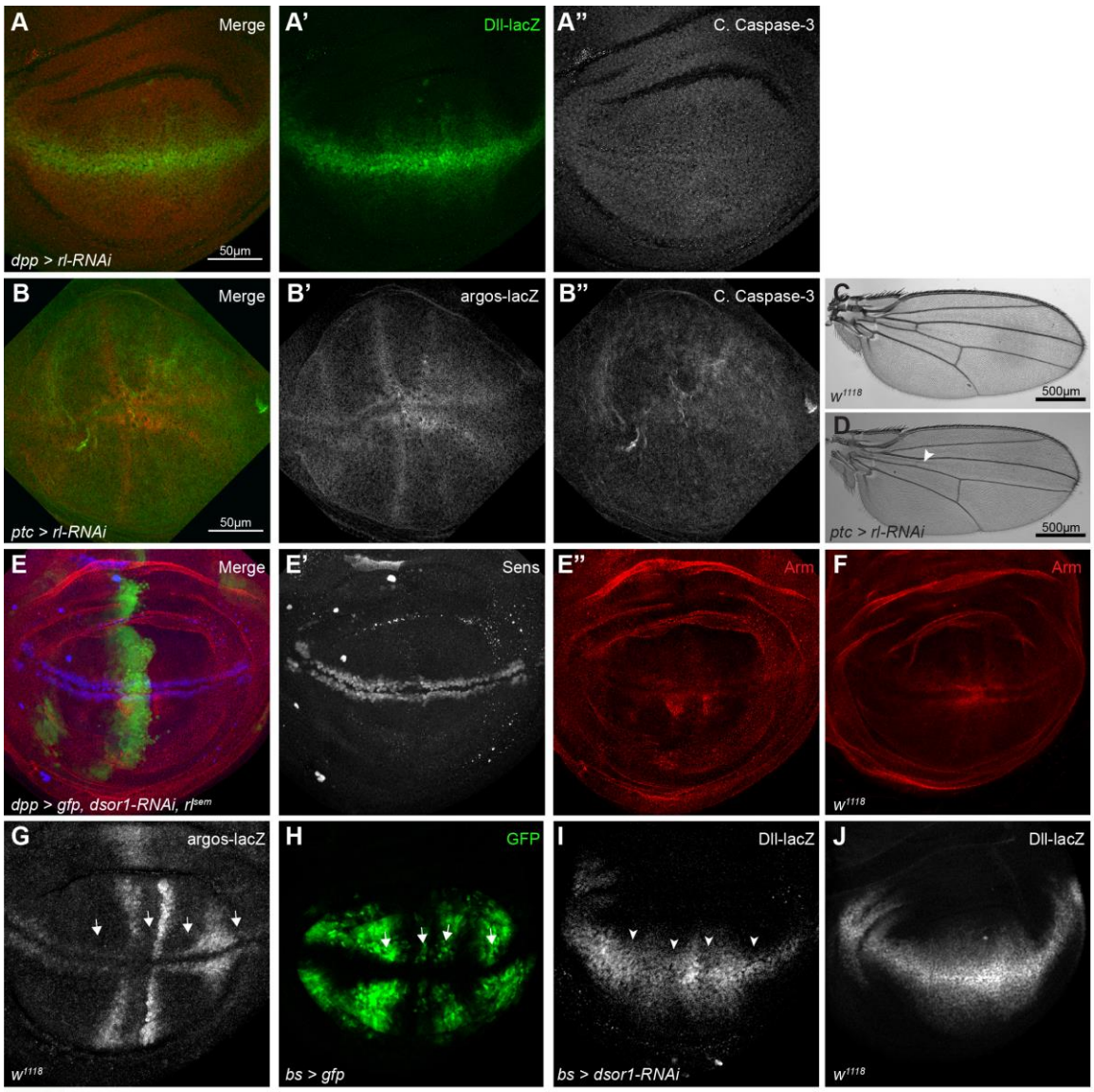

Figure 2.6 Dsor1 influence on Wg signaling is independent of Rl and active EGFR signaling in the developing wing disc

(A-A'') Expression of *rl-RNAi* had no effect of *Dll* transcription (A, A'), or cleaved caspase-3 levels (A'', B"). (B-D") Expression of *rl-RNAi* along the anterior/posterior section of the imaginal and adult wing reduces expression and patterning of *argos-lacZ*, and induces loss of vein tissue. (E-E") Co-expression of activated *rl* (rl^{sem}) with *dsor1-RNAi* resulted in a reduction of Sens (E') and Arm (E'') within the *dpp* expression domain marked by GFP (E). (F) Wild type Arm protein stabilization. (G-J) Active EGFR signaling, marked by target gene *argos-lacZ* expression, is expressed along the future wing margin and veins (G). *bs-Gal4* is expressed in the inter-vein tissue, marked by GFP (H) [inverse to active EGFR marked in (G)]. Expression of *dsor1-RNAi* results in a marked reduction in *Dll-lacZ* expression within the *bs* domain (I, arrow heads), compared to wild type (J).

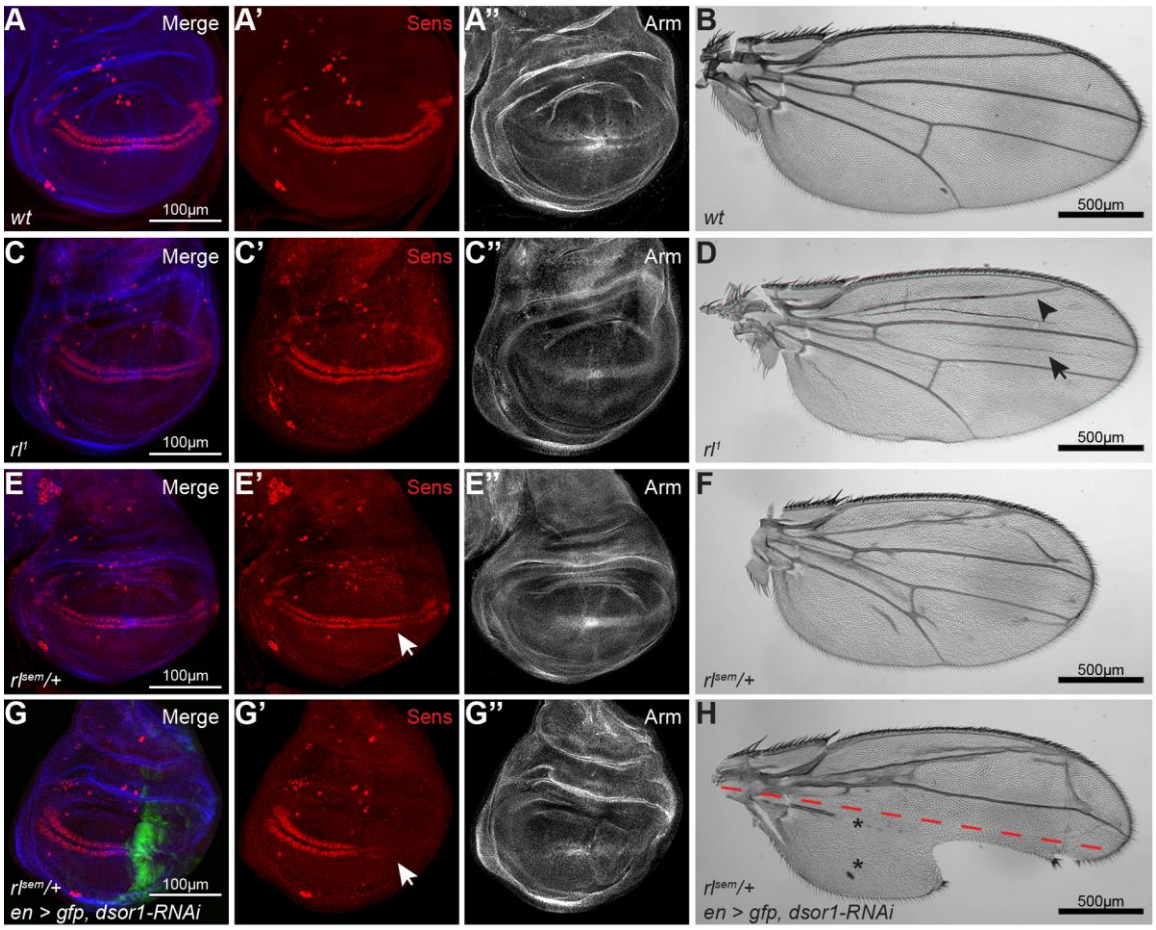

Figure 2.7 Rl does not affect Wg signaling

(A-B) Wild type expression of Sens (A'), Arm (A''), and an image of a wild-type adult wing (B). (C-D) Discs homozygous for the hypomorphic rl^{1} allele, displayed no change in Sens (C'), or Arm (C''), whereas the adult wing showed reduced size, wing creases (D arrow), and thinner veins (arrow head D). (E-F) Discs heterozygous for the hypermorphic rl^{sem} allele, displayed no change in Sens (E' arrow), or Arm (E''). Adult wings displayed excess vein material (F). (G-H) Expression of *dsor1-RNAi* in the posterior domain (marked with GFP; G) in a heterozygous rl^{sem} genetic background induced a loss of Sens (G' arrow), and stabilized Arm (G''). *dsor1-RNAi* induced notched wing margins, with a mix of loss and ectopic veins (asterisks; H).

2.3.6. Ras-activated Dsor1 signaling is independent of EGFR activation

As part of the MAPK signaling cascade, Dsor1 activation requires phosphorylation by upstream components (Gardner et al., 1994). It is essentially inert without upstream activation, as seen by the observation that overexpression of Dsor1 alone results in a completely wild type phenotype (Fig. 2.2E, I, Fig. 2.4L-L'"). This is supported by Fujioka et al., 2006, who found that Raf is the rate-limiting protein in the MAPK activation cascade, and MEK family proteins (the Dsor1 equivalent) are of highest concentration, with only a subset of them activated at any time.

In the developing larva, the most prominent activator of the MAPK cascade in the imaginal discs is EGFR (Shilo, 2003). EGFR has been shown to interact with Engrailed in early wing disc development to restrict *wg* expression to the wing pouch (Baonzaet al., 2000), before its final well-known role in patterning the wing veins in late third-instar larvae (Sturtevant et al., 1993). To avoid complications from possibly disrupting early patterning in the wing disc, we focused on the leg imaginal disc, which has simpler gene expression patterns. In the developing leg *wg* is expressed in the ventral domain (Fig. 2.8A''), and Decapentaplegic (Dpp) signaling in the dorsal, which together initiate patterning of the leg through distinct wedge domains. Wg and Dpp activate *dachshund* (*dac*) in the medial cells, followed by EGFR signaling in the distal cells in the early third instar, through inducing expression of the EGFR ligand *vein* and the protease *rhomboid* (Campbell, 2002; Galindo et al., 2002). The EGFR target gene *Bar,* in turn, represses *dac* expression in the distal cells (Giorgianni and Mann, 2011), resulting in refinement of Dac to a distinct domain of medial cells and its absence in the active distal EGFR domain (Fig. 2.8A''', arrow). We utilized the Wg-specific reporter, Fz3-dsRed (which is expressed in a wider wedge domain than Wg in the dorsal domain; Fig. 2.8A'), to monitor Dsor1's effect on Wg signaling. Using *wg-Gal4* to express *dsor1-RNAi* (marked by GFP; Fig. 2.8B''), we observed a strong reduction in Fz3-dsRed within the *wg* expression domain, yet surrounding Wg-receiving cells still expressed Fz3-dsRed (Fig. 2.8B, B'). This cell autonomous effect bolstered previous results showing that Dsor1 acts in the Wg-receiving cells and does not affect its secretion or processing. In addition, this loss of Fz3-dsRed was found in the Dac domain, which is outside of the zone of EGFR activity (Fig. 2.8B'''). This demonstrated that the effect of Dsor1 on Wg signaling is independent of endogenous EGFR signaling.

To extend these results we further examined the interaction between Wg and EGFR in the wing disc. In the late third-instar stage active EGFR signaling is refined to the primordial wing veins (Martín-Blanco et al., 1999), as seen by transcription of the target gene and pathway inhibitor *argos* (Fig.2.6G). *Blistered* (*bs)* expression is initiated in the inter-vein cells of the wing disc in third-instar larvae, in a pattern complementary to the domain of active EGFR signaling (Fig. 2.6G,H, arrows) (Fristrom et al., 1994; Grenier and Carroll, 2000). The use of *bs-GAL4* to drive *dsor1-RNAi* resulted in a notable reduction in *Dll* transcription in the inter-vein domain (marked by arrowheads) compared to wild type (Fig. 2.6I, J). This is significant because we can disrupt Wg signaling in cells where EGFR is not actively signaling. Furthermore a role for Dsor1 that is independent of EGFR was seen in the salivary glands. Dsor1 knockdown in the polyploid cells reduced Wg signaling, and EGFR signaling is not active in that cell type (Kuo et al., 1996). While we found that dominant negative EGFR can suppress Wg activity (data not shown), we showed that endogenous Dsor1 affected Wg signaling in cells that did not contain active EGFR activity. Taken together these results still show that in multiple contexts Dsor1 is required for Wg signaling, independent of upstream EGFR activation.

Having ruled out the EGFR as the mechanism for Dsor1 activation, we wanted to determine if traditional components of the MAPK cascade downstream of the receptor, like Ras, were still required for Dsor1 activation and affected the Wg pathway. Using a dominant negative variant of Ras*, ras^{N17}* (Feig and Cooper, 1988), we generated GFP-positive mitotic flip-out clones expressing *ras^{N17}* (Fig. 2.8C’’). Cells expressing *ras^{N17}* displayed a loss of stabilized Arm and a strong reduction of Sens, phenocopying Dsor1 loss (Fig. 2.8C’, C’’’). These experiments show that Dsor1 activity in Wg signaling is independent of EGFR, but appears to still require Ras-mediated activation of the MAPK cascade.

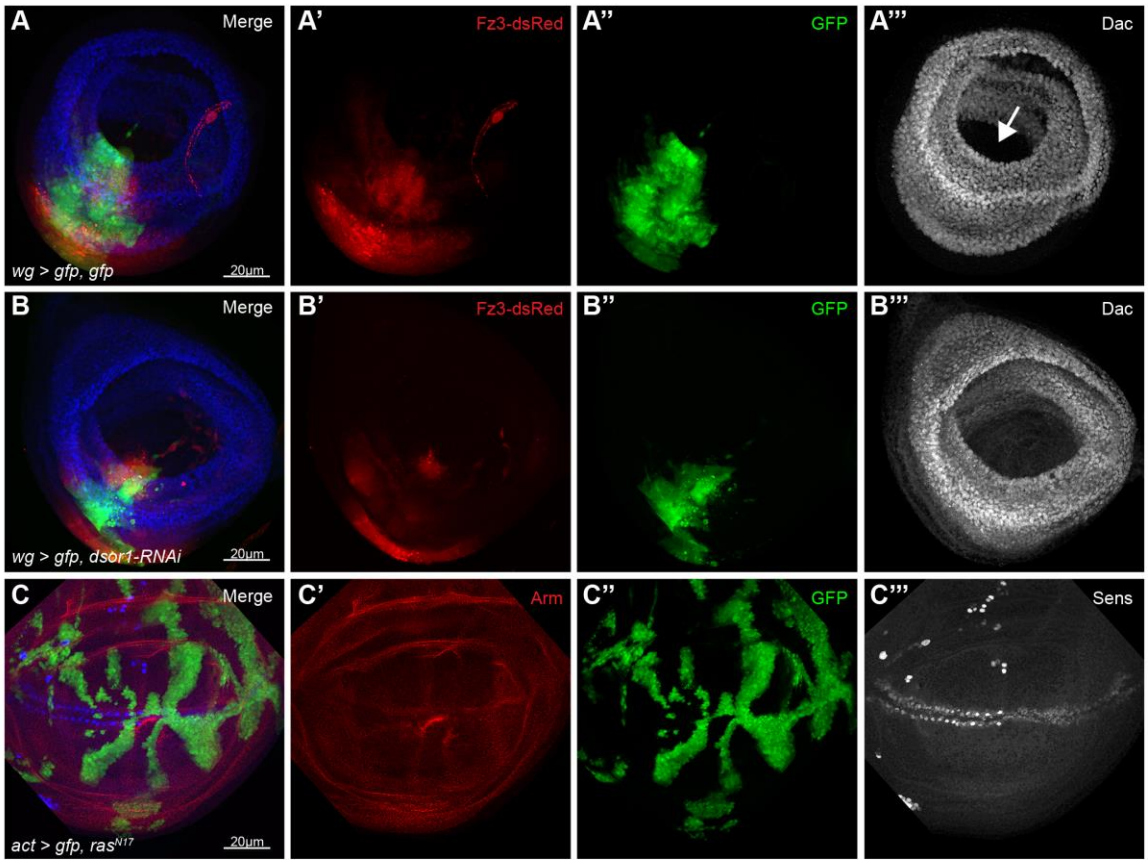

Figure 2.8 Dsor1 requires Ras activation, but is independent of EGFR signaling.

(A-B''') A third-instar leg imaginal disc, oriented with anterior leftwards and dorsal up. *wg* expression domain is marked by GFP using wg^{ND382}-*Gal4* (A''). Fz3-dsRed is expressed in a wider wedge, based around the *wg* expression domain (A'). Dac is present in cells bound for the medial leg tissue fate, and repressed in the most distal cells where EGFR is eventually activated (A''', arrow). Expression of *dsor1-RNAi* in the Wg-producing cells (B''), causes a reduction in Fz3-dsRed (B') within the Dac domain (B'''). (C-C''') GFP-marked actin flip-out clones driving expression of ras^{N17} (C'') phenocopy *dsor1-RNAi* phenotypes, with loss of stabilized Arm (C'), and reduced Sens (C''').

2.3.7. Insulin-like growth factor receptor promotes Wg signaling

Given that Dsor1 activity was independent of EGFR activation, but still appeared to require Ras, we wanted to identify the Ras activating source. Ras-MAPK signaling can be initiated by a myriad of sources in development, including other RTKs, G-protein coupled receptors (GPCR), and integrins (Chen et al., 2011; Crampton et al., 2009; Sopko and Perrimon, 2013). To refine our search, we focused on proteins that were expressed ubiquitously during development and could therefore serve as activators of Dsor1 in multiple contexts. We screened for potential activators of Ras-Dsor1-Wg pathway using transgenic RNAi and dominant negative (DN) variants to knockdown or inhibit different receptors, while monitoring *Dll* expression in the wing disc. RNAi and DN expression of the *Drosophila* insulin-like growth factor receptor (InR^{DN}) resulted in a strong reduction in *Dll* expression (Fig. 2.9A). InR has been identified to activate Ras-MAPK signaling to induce proliferation during *Drosophila* development, making it a strong candidate for the signal source (Oldham et al., 2002; Yenush and White, 1997). InR^{DN} did not affect total Wg levels, but did cause a reduction of stabilized Arm within the disc (Fig. 2.9B-C'). In addition, the reduction in active Wg signaling was not accompanied by any elevated levels of apoptosis, as seen with cleaved caspase-3 expression (Fig. 2.9C''). These results phenocopy what is seen in tissue with a reduction of active Dsor1.

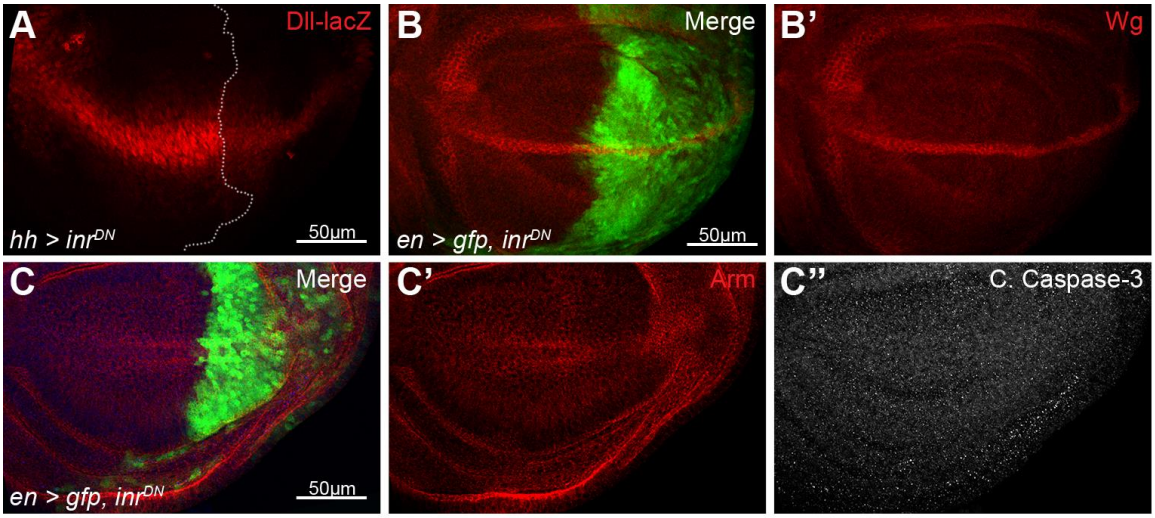

Figure 2.9 The InR might initiate Ras and Dsor1 activity to promote Wg signaling.

Expression of inr^{K1409A} (inr^{DN}) in the posterior domain (using *hh-Gal4*) of the wing imaginal disc induced a strong reduction in *Dll* expression (A), but failed to affect Wg protein levels (B, B'). InR^{DN} also phenocopied loss of Dsor1, with a reduction of stabilized Arm (C, C'), and did not lead to an increase in caspase-3 (C. Caspase-3) (C'').

2.3.8. Dsor1 interacts with Arm at the cell surface

To understand how Dsor1 might be required for the recruitment of Axin to the cell membrane, we focused on Dsor1 interactions with destruction complex components and the Wg receptors, Fz and Arrow. We utilized proximity ligation assays (PLA) to determine whether Dsor1 interacts with Wg components *in vivo*. In the PLA assay, probe fluorescence will only occur if two proteins of interest are <40 nm apart, only a slightly larger distance than with FRET (<10 nm), inferring strong evidence of protein interaction within cells, while examining whole tissue. As there is currently no anti-Dsor1 antibody available for immunofluorescence, *en-Gal4* was utilized to express a HA-tagged Dsor1 protein. To validate that ectopically expressed Dsor1 did not interact with non-specific proteins due to cellular saturation, GFP was co-expressed and probed for interaction. PLA against HA-tagged Dsor1 and GFP failed to produce any signal over background control tissue (Fig. 2.10A, A'). We next confirmed that Dsor1-HA could interact with a known target protein. PLA against Dsor1-HA and endogenous Rl (using an ERK1/2 antibody) produced a strong signal, exclusively in cells expressing Dsor1-HA, confirming that Dsor1-HA was capable of binding with endogenous proteins (Fig. 2.10B, B').

With validation of our assay conditions, we next tested Dsor1-HA for interactions with Wg pathway components. Dsor1-HA did not produce significant signal with Axin, Arrow, or Dsh (Fig. 2.10C-E). Surprisingly, Dsor1-HA and endogenous Arm gave a strong signal, indicating an interaction (Fig. 2.11A). Lateral view analysis revealed that the Dsor1-Arm interaction occurred solely at the apical and basal surfaces of the wing disc (Fig. 2.11C'). The wing disc consists of two layers of cells. DAPI-stained nuclei can be used to mark the tightly packed columnar cells, where Wg signaling occurs, and the thin layer of squamous peripodial cells above the apical surface (Fig. 2.11B, B'). The majority of Arm found within the columnar cells of the wing disc is located near the apical surface at the adherens junctions, and is not involved in Wg signaling (reviewed in Valenta et al., 2012). It is difficult to distinguish whether the Dsor1-Arm PLA signal at the apical surface is occurring in the peripodial cells, at the adherens junction, or near the Wg receptors on the apical surface. However, signal at the basal surface, which lacks adherens junctions, gives strong support that Dsor1 and Arm are in close contact with one another due to membrane recruitment of the destruction complex mediated by Wg signaling.

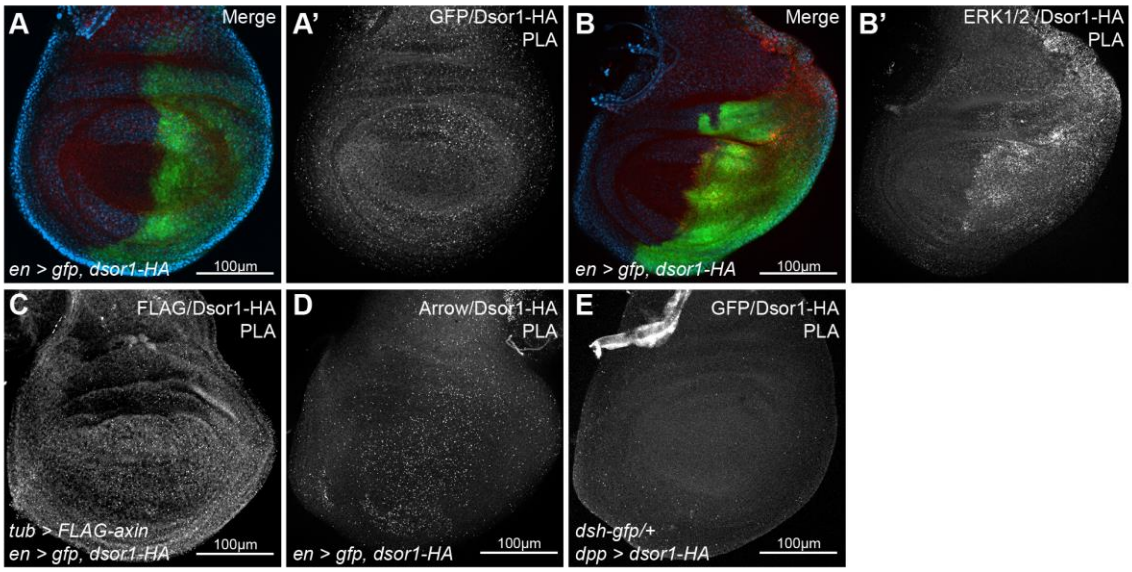

Figure 2.10 Proximity ligation assay validation.

PLA between HA tagged Dsor1 and GFP expressed in the posterior domain of the wing imaginal disc gave no signal (A, A'). PLA against HA tagged Dsor1 and endogenous ERK1/2 gave a strong signal in the posterior domain where *dsor1-HA* was expressed (B,B'). PLA revealed no close interaction signal between Dsor1-HA and ubiquitous FLAG-Axin (C), Arrow/Dsor1-HA (D), or Dsh-GFP/Dsor1-HA in the wing imaginal disc (E).

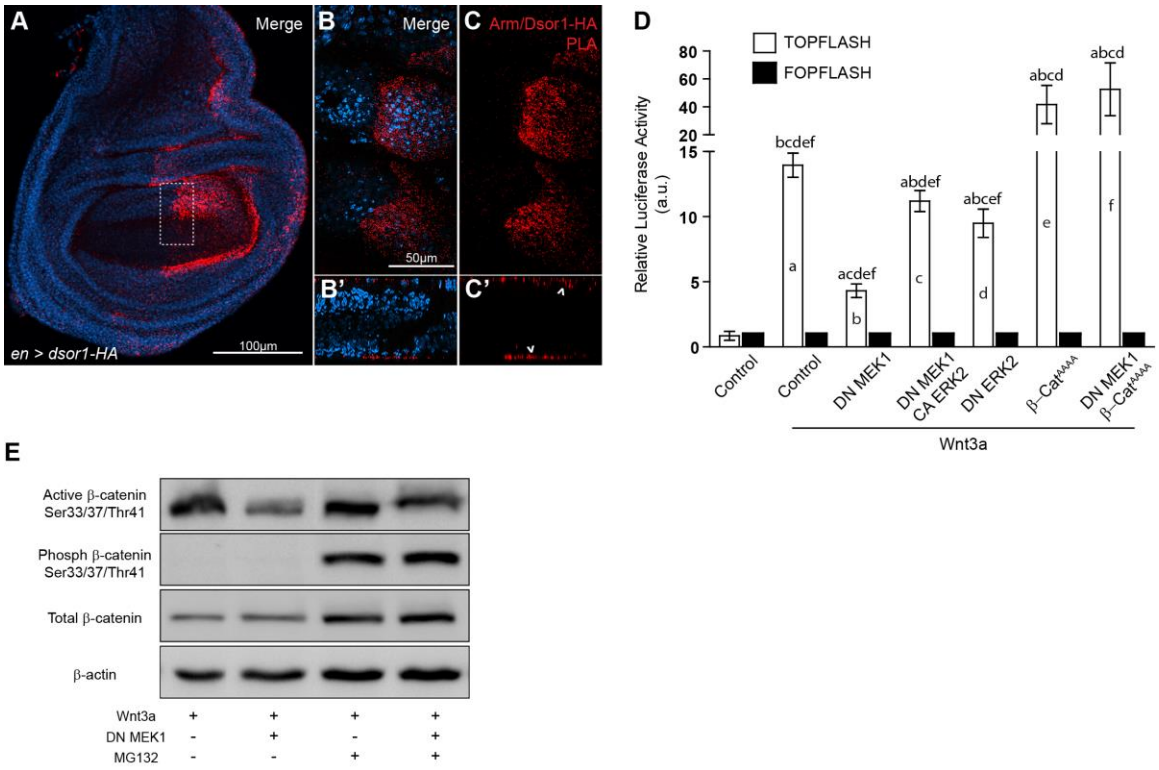

Figure 2.11 Dsor1 interacts with Arm at the cell surface and its role in Wnt signaling is conserved in the mammalian ortholog MEK.

(A-C') Proximity ligation assays (PLA) revealed a close interaction between HA-tagged Dsor1 expressed in the posterior domain of the wing imaginal disc and Arm. Cell nuclei marked with DAPI (A-B') were used to determine apical/basal orientation and differentiate between columnar and peripodial cells (B'). Cross-sections of the wing disc revealed Dsor1/Arm signal occurred at the apical and basal surface of the columnar cells (C'). (D) HEK-293 cells were transfected with the Wnt-responsive luciferase construct (TOPFLASH and negative control FOPFLASH) to determine the effects of MEK and ERK on TCF/LEF reporter activity during active Wnt signaling. Expression of dominant negative (DN) MEK1 led to a significant reduction in reporter activity (column 3). Expression of DN MEK1 with constitutively active (CA) ERK2 did provide a partial rescue of activity (column 4), but was unable to restore normal reporter activity (column 2). DN ERK2 only induced a partial reduction in reporter activity (column 5) compared to DN MEK1. Expression of stabilized β-catenin induced a strong increase in reporter activity (column 6). DN MEK1 does not influence this response (column 7). Data are presented as means ± S.D. with letters above representing significance from corresponding column, $p < 0.01$. (E) HEK-293 cell lysates transfected with or without DN MEK1 were analysed by western blotting. Cells were also treated with MG132 to inhibit proteasomal degradation prior to lysate collection. DN MEK1 did not substantially affect β-catenin phosphorylation, or its total protein levels, but did reduce its stable, active levels. β-actin was used as a loading control.

2.3.9. Catalytically active MEK directly promotes Wnt activity in mammalian cells

To determine whether the promotion of Wg signaling by Dsor1 is conserved, we examined the effects of MAPK components on Wnt signaling in HEK-293 cells. Wnt pathway activity was stimulated by Wnt3a and the cellular response was measured by using a TCF-responsive TOPFLASH transcriptional reporter (Korinek et al., 1997) (Fig. 2.11D, columns 1, 2). Transfection of validated catalytically inactive dominant-negative MEK1 (Mansour et al., 1994) (a Dsor1 homolog) resulted in a greater than 3 fold reduction in transcriptional activity (Fig. 2.11D, column 3). Although our studies thus far have indicated that the effect of Dsor1 in flies was not transduced through the MAPK Rl, we tested whether a validated constitutively active ERK2 (Emrick et al., 2001) (a Rl homolog) could rescue the transcriptional repression by dominant-negative MEK1, given that vertebrate ERK proteins have been previously identified as having a role in promoting Wnt signaling (Červenka et al., 2011; Ding et al., 2005; Krejci et al., 2012). Co-transfection of dominant-negative MEK1 and constitutively active ERK2 provided only a partial rescue (Fig. 2.11D, columns 2, 3, 4), suggesting that MEK proteins provide a direct role for Wnt signaling independently of activation of ERK. This was further supported by expression of dominant-negative ERK2 (Emrick et al., 2006), as it caused a reduced TCF-mediated response, but only roughly half that seen with dominant-negative MEK1 (Fig. 2.11D, columns 2, 3, 5). Taken together these results demonstrate the conservation of a MEK-specific role for Wnt target gene activation.

Next, epistasis were performed to determine if MEK functions similarly in Wnt signaling in mammalian cells as Dsor1 does in *Drosophila*. Transfection of a stabilized β-catenin, with its GSK3β and CK1α phosphorylation sites mutated to alanine (S33A, S37A, T41A and S45A) (β-catenin^{AAAA}), and which is therefore resistant to proteasomal degradation, induced much stronger TCF-transcriptional activity than Wnt3a alone (Fig 2.11D, columns 2, 6). Upon co-transfection of DN MEK1 with β-catenin^{AAAA}, there was no significant change in reporter activity (Fig 2.11D, column 7). This indicates that, like Dsor1, the role of MEK within the Wnt pathway does not occur after β-catenin stabilization.

Because the promotion of the Wnt pathway mediated by MEK is conserved in HEK-293 cells, we further examined whether MEK could also regulate β-catenin. HEK-

293 cells were transfected with dominant-negative MEK1, and the levels of β-catenin were assessed. First, using an antibody that recognizes active non-phosphorylated β-catenin (i.e. no phosphorylation on Ser33, Ser37 or Thr41) (active β-catenin), we observed dramatically reduced protein levels following expression of dominant-negative MEK1 (Fig. 2.11E). We next blocked proteasomal degradation using MG132 and examined active β-catenin, GSK3-phosphorylated β-catenin and total β-catenin. Western blotting of lysates showed no change in the levels of GSK3-mediated phospho-β-catenin (Ser33, Ser37 and Thr41). These phospho-sites serve to target β-catenin for proteasomal digestion, which suggests that the destruction complex, including GSK3, is functional in the absence of MEK1 (Fig. 2.11E). In addition, total β-catenin levels were not significantly disrupted (Fig. 2.11E). Protein levels of active β-catenin were dramatically reduced in the presence of dominant-negative MEK1, further suggesting a role for Wnt propagation by promoting β-catenin stability (Fig. 2.11E).

2.4. Discussion

In this study, we have demonstrated that Dsor1 and MEK are new regulators of Wg/Wnt signaling. We have shown that Dsor1 and the mammalian ortholog MEK are required for full activation of Wg/Wnt signal transduction. We have also demonstrated that their role in Wg/Wnt signaling is likely to be independent of MAPK phosphorylation, challenging the current dogma of the MAPK signaling cascade. Our study has also identified that the currently known activator of the Ras–Dsor1 pathway in imaginal discs, EGFR, is non-essential for a role in Wg signal propagation. Activation of this new crosstalk mechanism might be initiated through insulin-like growth factors (IGFs) or Drosophila insulin-like peptides (DILPs) and the InR (Fig. 2.12).

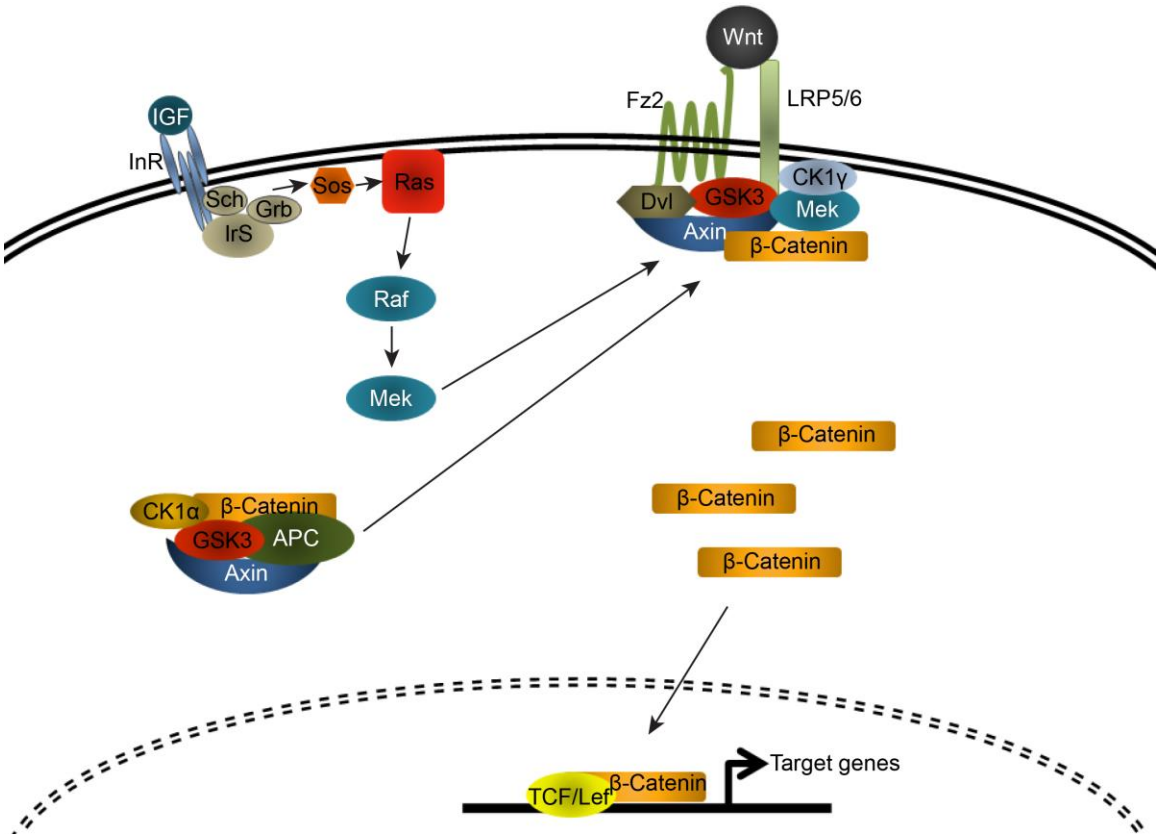

Figure 2.12 MEK/Dsor1 is required for the recruitment to the cell membrane and subsequent disruption of the destruction complex.

Activated InR induces the activation of the Ras/Raf/MEK cascade. Upon Wnt binding to co receptors Fz and LRP5/6, MEK is required to recruit the destruction complex to the membrane surface. This allows the accumulation of newly synthesized β-catenin to enter the nucleus and interact with TCF/Lef and other cofactors to initiate gene transcription.

2.4.1. Dsor1 and MEK is a novel kinase regulating Wg/Wnt signaling

Our findings have highlighted a new function for components of the MAPK signaling cascade in Wnt activation. These two crucial signaling pathways have been found to influence each other in many carcinomas (Zeller et al., 2013), yet their interaction has not been well established in normal developmental contexts. Our results uncover a role of Dsor1 in Wg signaling in the developing larval imaginal discs and salivary glands. Epistasis experiments have identified that Dsor1 acts upon the Wg pathway in the receiving cells after Dsh recruitment to the co-receptors Fz and Arrow, and its presence is needed for the recruitment of the destruction complex components to the membrane surface. As Dsor1 showed a close physical interaction with Arm itself at both the apical and basal cell surface, it suggests that Dsor1 acts to promote and retain the destruction complex near the receptor complex. Future experiments will need to clarify whether Dsor1 is utilized as a linker to promote destruction complex retention, or if its ability to phosphorylate specific target proteins within the complex is key. However, the utilization of catalytically inactive MEK1 resulted in reduced TCF reporter activity and significantly reduced active β-catenin, suggesting the phosphorylation activity of MEK is crucial for Wnt signaling in mammalian cells.

2.4.2. Dsor1 and MEK promotion of Wg/Wnt is independent of Rl or ERK

Quite surprisingly our results identified that Dsor1 and MEK activity was independent of its well-known function in Rl and ERK activation. The MAPK signaling cascade is one of the best characterized and understood phosphorylation pathways to date. Its central dogma has revolved around its simple and exclusively linear signaling series for the activation of Rl/ERK. A small number of previous studies have questioned this model, demonstrating that MEK is capable of phosphorylating other targets (Jo et al., 2011; Tang et al., 2015), even GSK3 (Takahashi-Yanaga et al., 2004). Our results are consistent with this alternative “MEK multiple substrate model”. We demonstrated, through RNAi knockdown, ectopic expression, and genetic interaction studies, that Rl does not influence Wg activity, and that the effect we observe is specific to Dsor1. Our mammalian cell culture experiment does support the previous findings that vertebrate ERK can promote Wnt activity (Červenka et al., 2011; Ding et al., 2005; Hoschuetzky et al., 1994; Krejci et al., 2012), suggesting the mechanism might diverge slightly between

flies and vertebrates. Moreover, we demonstrate a novel new MEK function for direct promotion of Wnt signaling.

2.4.3. Dsor1 activation may require InR signaling

Our findings reveal that the predominant larval MAPK signaling cascade initiated by EGF is not required for the activation of this new Ras-Dsor1-Wg interaction. Endogenous EGFR signaling is the only identified activator of di-phospho-Rolled in the developing wing (Martín-Blanco et al., 1999). Our results do not contradict the current understanding of MAPK activity in the developing wing, but reveal a new pathway using a subset of MAPK cascade components. It was surprising to identify that inhibition of the InR resulted in a striking phenocopy of Dsor1 disruption, suggesting that InR might be the upstream activator of the Ras-Dsor1 pathway. InR activation of Ras-MAPK signaling for a proliferation response has been previously identified (Oldham et al., 2002). Our results suggest that DILPs might also play a role in patterning through Wg signaling. It has been identified that insulin and IGF1 can promote Wnt activity by increasing β-catenin stability and nuclear accumulation, as well as by upregulating other pathway components through multiple distinct mechanisms (Sun and Jin, 2008; Sun et al., 2009, 2010). In future studies it will be interesting to identify if InR-Ras-MEK-Wnt crosstalk can also be elucidated in mammalian cells, as well as trying to distinguish whether IGF or DILPs promote Dsor1 activity for Wg signaling.

Chapter 3. The protein phosphatase 4 complex promotes the Notch pathway and wingless transcription

This chapter is based off published work from:

Hall E. T.*, Pradhan-Sundd T.*, Samnani F. and Verheyen E. M. (2017). The Protein Phosphatase 4 complex promotes the Notch pathway and *wingless* transcription. Biology Open vol: 6 (8) pp: 1165-1173. doi: 10.1242/bio.025221. * Joint first authors

3.1. Contributions to the chapter:

This project was initiated by Tirthadipa Pradhann-Sundd, who conceptualized the initial experiments and manuscript, and performed imaging for Fig 3.3 A, B, D-G, I. After Tirthadipa Pradhann-Sundd graduated, I conceptualized and performed the remainder of the work and analysis included in this thesis, and we serve as joint first authors on the paper.

Faaria Samnani assisted with experiments and contributed to data analysis.

Esther M. Verheyen assisted with experiments, edited the manuscripts, and provided guidance.

3.2. Abstract:

The Wnt/Wingless (Wg) pathway controls cell fate specification, tissue differentiation and organ development across organisms. Using an *in vivo* RNAi screen to identify novel kinase and phosphatase regulators of the Wg pathway, we identified subunits of the serine threonine phosphatase Protein Phosphatase 4 (PP4). Knockdown of the catalytic and the regulatory subunits of PP4 cause reductions in the Wg pathway targets Senseless and Distal-less. We find that PP4 regulates the Wg pathway by controlling Notch-driven *wg* transcription. Genetic interaction experiments identified that PP4 likely promotes Notch signaling within the nucleus of the Notch-receiving cell. Although the PP4 complex is implicated in various cellular processes, its role in the regulation of Wg and Notch pathways was previously uncharacterized. Our study identifies a novel role of PP4 in regulating Notch pathway, resulting in aberrations in Notch-mediated transcriptional regulation of the Wingless ligand. Furthermore, we show that PP4 regulates proliferation independent of its interaction with Notch.

3.3. Introduction

The progression from a fertilized egg into a multicellular organism is a complex process, requiring proliferation and intricate cell-cell communication between individual cells for the eventual formation of tissues and organs. Only a handful of evolutionarily conserved signal transduction pathways are used reiteratively, both spatially and temporally to control development. In metazoans, the Wnt signaling [Wingless (Wg) in *Drosophila*] pathway regulates growth and proliferation, cell-fate differentiation, stem-cell renewal and homeostasis (Clevers and Nusse, 2012; Swarup and Verheyen, 2012). Wnt signaling alone does not control all these processes; its activity is extensively regulated by other signaling pathways and cellular mechanisms (Collu et al., 2014; Itasaki and Hoppler, 2010; Kim and Jho, 2014; Zeller et al., 2013). Determining how these interactions occur is critical for understanding basic cellular function and disease progression, as the disruption of the Wnt pathway has been implicated in a variety of developmental disorders and cancer (Clevers and Nusse, 2012).

The *Drosophila* wing imaginal disc is a powerful tool for studying Wg signaling (Swarup and Verheyen, 2012). In the developing wing disc the Wg ligand is expressed throughout different stages of disc development. At the end of the larval third instar

stage, Wg expression is confined to the presumptive wing margin along the dorsal/ventral (D/V) boundary, which controls patterning and fate specification (Couso et al., 1994; Williams et al., 1993). Wg produced in this narrow band of cells induces the nested expression of target genes including Senseless (Sens) and Distal-less (Dll), in the flanking non-boundary cells (Neumann and Cohen, 1997; Zecca et al., 1996).

The directed expression of Wg at the D/V boundary requires the transmembrane receptor Notch in these boundary cells. The Notch ligands Delta (Dl) and Serrate (Ser) signal from the flanking non-boundary cells, inducing proteolytic cleavages of Notch to generate a free Notch intracellular domain (N^{ICD}) (Bray, 2016; Fortini, 2009). N^{ICD} translocates to the nucleus where it binds transcriptional co-activators and DNA binding proteins to initiate target gene transcription, including *wg* and *cut* (de Celis et al., 1996; Rulifson and Blair, 1995). The absence of Notch results in reduced *wg* transcription and therefore reduced Wnt pathway activation (Rulifson and Blair, 1995).

Both Notch and Wg signaling act to regulate common developmental processes such as tissue patterning, fate specification and growth of different *Drosophila* appendages (Hing et al., 1994). These two pathways share a number of common regulators which affect the activity of their signaling outcome. In an *in vivo* RNAi screen to identify novel kinase and phosphatase modulators of the Wg pathway, we found that the components of the Protein Phosphatase 4 (PP4) complex appeared to promote Wg signaling (Swarup et al., 2015). The serine threonine phosphatase PP4 belongs to the Protein Phosphatase 2A (PP2A) group of phosphatases (Cohen et al., 2005). Similar to what is found with PP2A, PP4 forms a heterotrimeric complex, which in *Drosophila* consists of a catalytic subunit, Protein Phosphatase 4-19C (PP4-19C), and two regulatory subunits called Protein Phosphatase 4 Regulatory subunit 2-related protein (PPP4R2r) and PP4R3/Falafel (Flfl) (Cohen et al., 2005; Gingras et al., 2005).

PP4 is a highly conserved phosphatase seen across metazoans, and has been implicated in a wide range of cellular processes, including chemotaxis in slime molds (Mendoza et al., 2007), developmental signaling pathways such as Hedgehog (Jia et al., 2009), JNK (Huang and Xue, 2015; Zhou et al., 2002), Insulin-like growth factor (Mihindukulasuriya et al., 2004), as well as TOR (Raught et al., 2001). The major functional role of PP4 is as a key regulator in cell cycle progression and regulation of cell

division (Helps et al., 1998; Huang et al., 2016). No previous studies have implicated PP4 in Notch or Wnt/Wg signaling.

In this study we demonstrate that our previous observations of reduced Wg signaling due to knockdown of PP4 components are caused by effects on *wg* transcriptional regulation by Notch. Using genetic interaction studies and expression of mutant Flfl, we determine that PP4 promotes the activity of nuclear Notch. We further elucidated that the function of PP4 in promoting Notch signaling was independent of its previously described role in cell cycle progression and proliferation. Taken together we have identified a novel role for PP4 in promoting Notch signaling and expression of *wg* during *Drosophila* development.

3.4. Results

3.4.1. PP4 promotes Wg signaling in the Drosophila wing imaginal disc

In a screen for modifiers of Wg signaling in the *Drosophila* wing imaginal disc, three components of PP4 were found to reduce Wg target genes following their knockdown through RNAi (Swarup et al., 2015). An involvement of PP4 in Wg signaling has not been previously identified, so we were curious to determine mechanistically how PP4 may be involved in regulating the output of the Wg pathway. In the developing wing imaginal disc the Wg target gene *Dll is* expressed in a distinct nested pattern along the dorsoventral (D/V) boundary (Fig. 3.1A, A'). We utilized *hedgehog* (*hh*)-*Gal4* expressed in the posterior compartment of the wing disc (marked by GFP; Fig. 3.1A) to express RNAi constructs to knockdown expression of the individual PP4 components. The knockdown of the catalytic subunit *Pp4-19C* caused a strong reduction in *Dll-lacZ* expression (Fig. 3.1C, C'). Reduction of the PP4 targeting subunits *ppp4R2* or *flfl* via RNAi caused a mild to moderate reduction in *Dll* expression levels (Fig. 3.1E', G'). We also used *dpp-Gal4*, which is expressed along the anterior-posterior boundary of the wing disc (Fig. 3.2B'), to knock down *Pp4-19C* (Fig. 3.2C)*, ppp4R2* (Fig. 3.2E) and *flfl* (Fig. 3.2G) and observed variable reductions in the levels of the Wg targets Senseless (Sens) (Fig. 3.2C, E, G) and Dll (Fig. 3.2C', E', G').

Reduction of PP4 components has previously been shown to affect cell viability by promoting JNK-dependent cell death (Huang and Xue, 2015). To determine if the reduction in Wg target gene expression was due to cell death, discs were stained for the apoptotic marker, cleaved caspase-3 (C. Casp-3). Compared to control cells expressing GFP (Fig. 3.1A), reduction of any individual PP4 component did not noticeably increase levels of apoptosis within the *hh* domain of the imaginal disc (Fig. 3.1C'', E'', G''). Similarly, we did not observe any increase in cleaved caspase-3 when *dpp-Gal4* was used to knock down the three PP4 subunits (Fig. 3.2D, F, H).

Following Wg pathway activation, the key effector protein Arm is stabilized at the highest concentration in two bands of cells flanking the Wg-producing cells of the D/V boundary (Fig. 3.1B, arrow) (Peifer et al., 1991). Expression of PP4 components RNAi in the posterior domain of the wing imaginal disc, caused a reduction of stabilized Arm (Fig. 3.1D, F, H). In subsequent experiments, we utilized *flfl-RNAi* to reduce PP4 activity, as it has been previously confirmed as a functional indicator of the entire complex (Sousa-Nunes et al., 2009). Together, these data suggest PP4 is required for promoting Wg pathway activation.

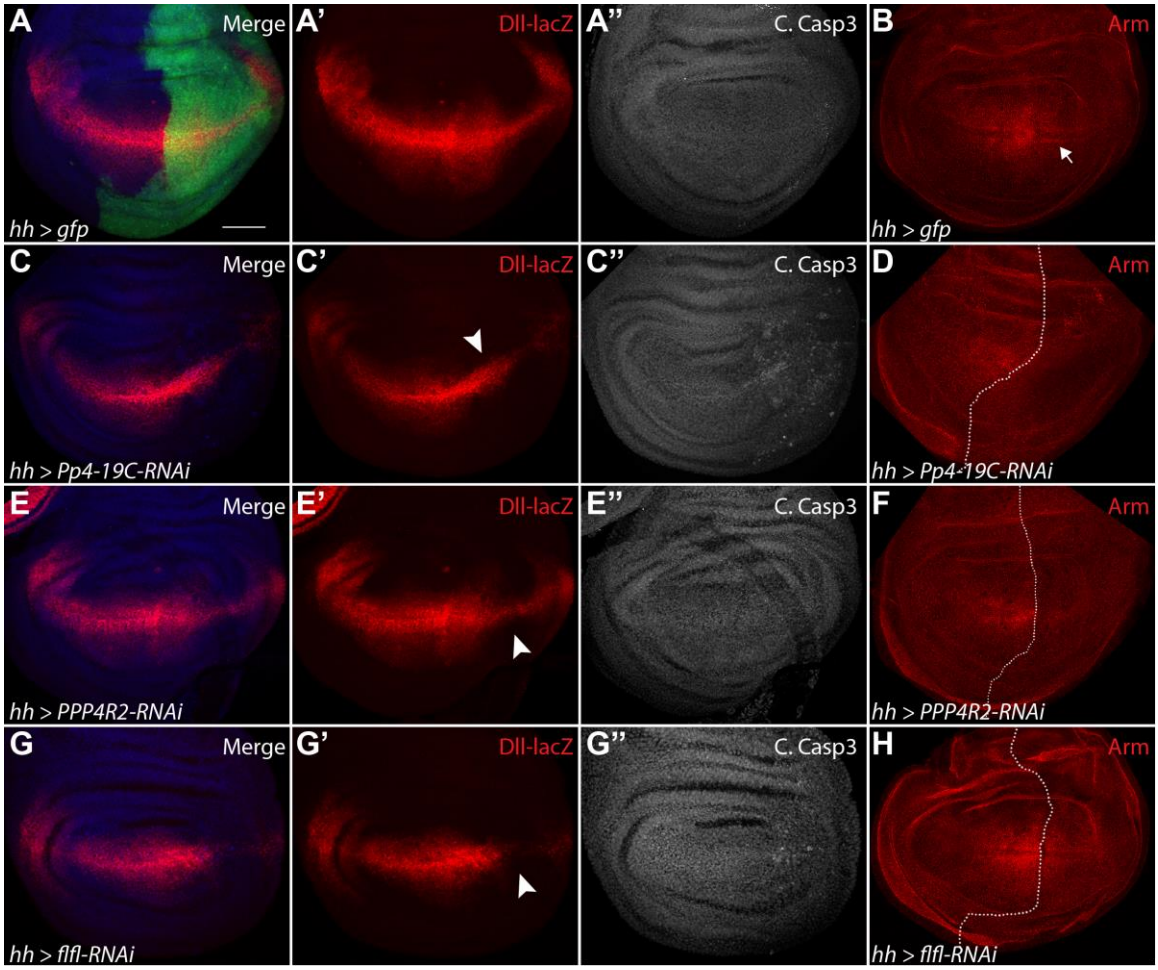

Figure 3.1 Reduction of PP4 subunits inhibits Wg pathway activation without inducing cell death.

(A, B) Normal expression pattern of *hh-Gal4* (A) in the posterior domain of the developing wing disc, shown with wild-type expression of Wg target gene *Dll-lacZ* (A'), as well as cleaved caspase 3 (A'') and stabilized Arm in bands flanking the D/V boundary (B, arrow). (C-D) The knockdown of PP4-19C with RNAi in the posterior domain causes a reduction in *Dll* expression (C, C', arrow head), but did not significantly increase C. Casp3 levels (C''), while inducing a marked reduction in stabilized Arm (D). (E-F) Knockdown of PPP4R2 caused a minor reduction in *Dll-lacZ* (E', arrow head) and Arm (F), but did not affect C. Casp3 levels (E''). (G-H) Flfl knockdown reduced *Dll* expression (G, G', arrow head) without increasing C. Casp3 activity (G''), and caused a reduction in stabilized Arm (H). Scale bar: 50 μm.

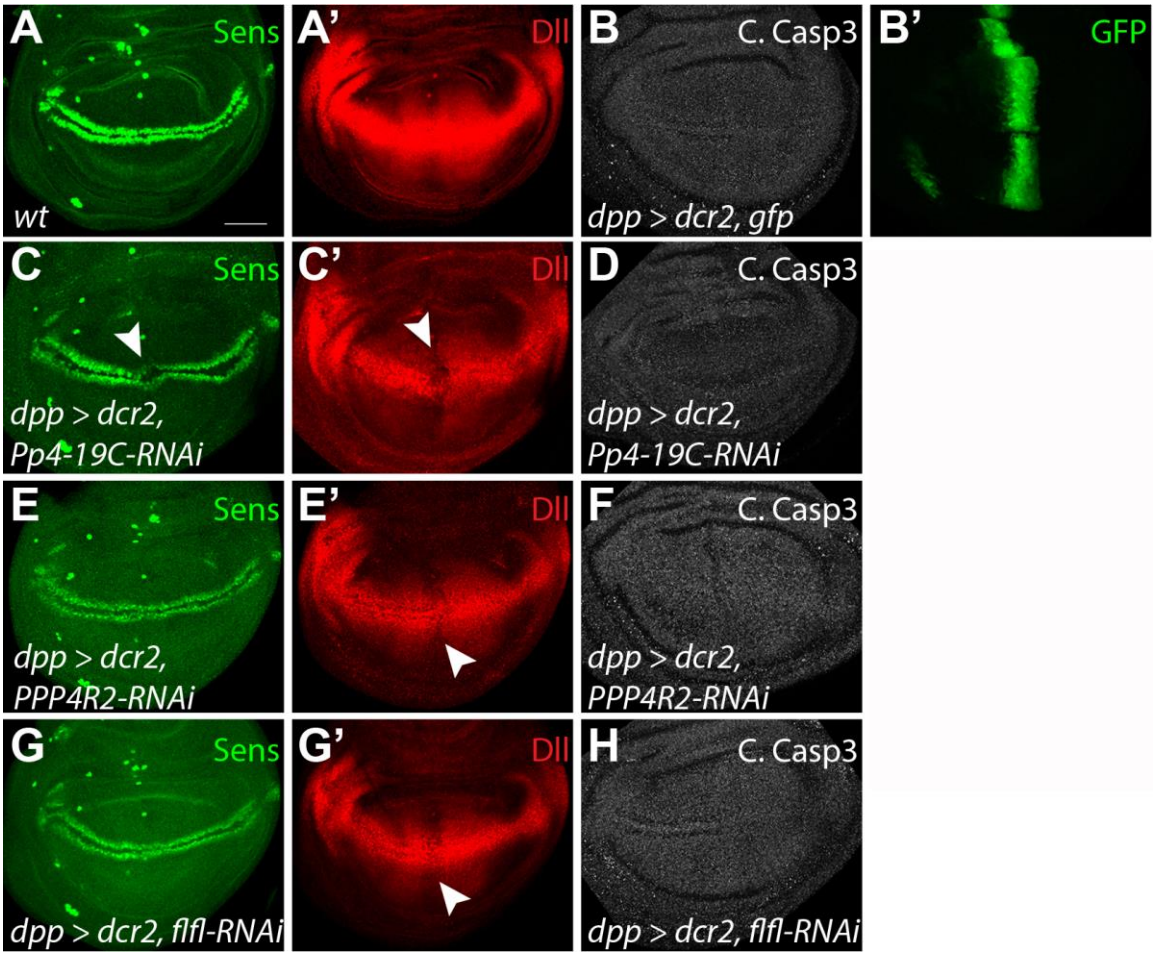

Figure 3.2 Reduction of PP4 subunits inhibits Wg pathway activation without inducing cell death.

(A-B') Wild-type expression pattern of Wg target genes Sens (A), and Dll (A'), as well as cleaved caspase 3 (B) with normal expression pattern of *dpp-Gal4* (B') along the anterior/posterior boundary in the developing wing disc. (C-D) The knockdown of PP4-19C with RNAi along the anterior/posterior boundary causes a loss of Sens (C, arrow head) and Dll (C', arrow head), but does not elevate C. Caspase 3 activity (D). (E-F) Knockdown of PPP4R2 was able to effectively reduce Dll (E', arrow head), but did not affect Sens (E) or C. Casp3 (F). (G-H) Flfl knockdown did not affect Sens (G) or C. Casp3 levels (H), but did reduces Dll (G', arrow head).

3.4.2. PP4 promotes Wg signaling through Notch pathway activation

As the reduction of Wg target genes and Arm was apparent upon knockdown of PP4 components, we next wanted to look at the Wg ligand and its transcription. In third instar wing imaginal discs, *wg* is transcribed, translated, and undergoes post-translational modification, which can affect its stability, before being secreted to activate the Wg pathway in neighbouring cells (Franch-Marro et al., 2008; Tanaka et al., 2002). We used Wg antibodies, and the *wg* transcriptional reporter *wg-lacZ*, to identify any defects in the ligand's transcription, processing, or stability. In a wild-type wing imaginal disc, Wg and *wg-lacZ* expression are refined along the D/V boundary in a narrow band two to three cells wide (Fig. 3.3A, D). Expression of *flfl-RNAi* in the posterior domain of the wing disc, using *hedgehog* (*hh*)-*Gal4*, resulted in a reduction of both total Wg protein levels and transcription (Fig. 3.3B, E), suggesting that PP4 is involved in regulation of *wg* transcription. We confirmed that this effect was specific to *flfl* knockdown by generating somatic loss of function clones with the hypomorphic $flfl^{795}$ allele in the posterior domain of the wing disc with *en-Gal4* driving *UAS-Flp* enzyme. Consistent with the *flfl-RNAi* result, reduction of *flfl* led to decreased Wg protein in the posterior domain (Fig. 3.3C, C').

wg transcription is controlled along the D/V boundary of the wing disc by Notch signaling (Rulifson and Blair, 1995). We next wished to determine if PP4 regulation of *wg* transcription is mediated through the involvement of the Notch signaling pathway. *cut*, another Notch target gene (de Celis et al., 1996), is expressed in a similar pattern to Wg along the D/V boundary (Fig. 3.3F). The reduction of *flfl* in the posterior domain of the wing disc via RNAi resulted in a strong loss of Cut expression, indicating an overall reduction in Notch signaling (Fig. 3.3G). Looking at the Notch ligand Delta (Dl), which is enriched in the cells adjacent to the D/V boundary (Fig. 3.3H), it was apparent that *flfl-RNAi* expressed in the posterior domain of the disc, resulted in reduced Dl and a failure of its refinement (Fig. 3.3I). We could not discern if this effect on Dl is from upstream regulation of *Dl* expression, or on Notch activation itself, as the refinement of Dl involves a cis/trans feedback mechanism with N for pattern refinement, through lateral inhibition of each gene (Axelrod, 2010). Together, these results demonstrate that PP4 normally appears to influence Notch signaling to promote multiple pathway targets including *wg*.

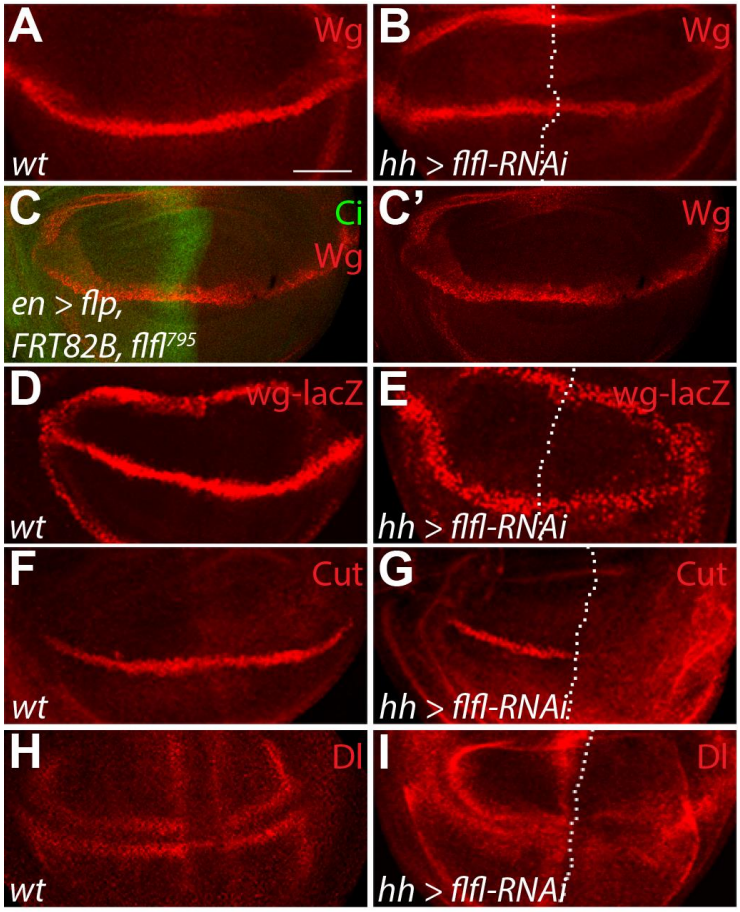

Figure 3.3 PP4 promotes Wg signaling through Notch pathway activation.

(A) Wild-type pattern of Wg protein. (B) Using *hh-Gal4*, expressed in the posterior domain of the wing disc (right of the dotted line), to express *flfl-RNAi*, caused a reduction in total Wg protein levels. (C, C') Somatic clones of the hypomorphic *flfl*^{795} allele in the posterior domain (marked by the absence of Ci) also showed reduced Wg protein. (D-I) Wild-type pattern of *wg* transcription (D), Cut protein (F), and Dl protein (H). Expression of *flfl-RNAi* in cells in the posterior domain (right of dotted line), caused a reduction in *wg* transcription (E), loss of Cut (G), and Dl (I) in the developing wing disc. Scale bar: 50 µm.

3.4.3. PP4 promotes Notch signaling in the Notch signal receiving cells.

Having identified that Flfl, and by extension PP4, is involved in promoting Notch signaling we sought to further elucidate how. During wing imaginal disc development Notch and its ligands Dl and Serrate (Ser) undergo refinement through lateral inhibition, resulting in high levels of active Notch (N^{ICD}) being expressed along the D/V boundary and suppressed in the flanking cells (Fig. 3.4D, arrow head), which conversely have high levels of Dl (Fig. 3.3H) and Ser (de Celis et al., 1996). This feed forward loop of lateral inhibition creates Notch signal-sending cells (cells flanking the D/V boundary), and signal-receiving cells (D/V boundary cells) with active Notch signaling (Axelrod, 2010).

To further analyze the role of the PP4 complex in the complementary ligand-expressing and Notch-expressing cells, we used *C5-Gal4* and *wg-Gal4,* respectively, to express *flfl-RNAi* in the wing imaginal disc. *C5-Gal4* is expressed in N ligand expressing cells flanking the D/V boundary (Fig. 3.4E), while *wg-Gal4* is expressed along the D/V boundary, in the active N signal receiving cells as well as the ring domain (Fig. 3.4J). By looking at Wg and Notch target genes, we could determine in which cells Flfl, and by extension PP4, is working to affect the Notch pathway. *C5>flfl-RNAi* appeared to have no affect on *Dll* expression (Fig. 3.4A, F), Wg (Fig. 3.4B, G), or Cut (Fig. 3.4C, H). The enrichment of the N^{ICD} along the D/V boundary also appeared to be unaffected (Fig. 3.4D, I, arrowheads). *wg>flfl-RNAi* gave very contrasting results. Knockdown of *flfl* in the Notch receptor expressing cells resulted in a complete loss of *Dll-lacZ (*Fig. 3.4K), strong reduction of Wg (Fig. 3.4L), loss of Cut (Fig. 3.4M), and a failure of enrichment of N^{ICD} (Fig. 3.4N, arrow). Knockdown of the other components of PP4 using *wg-Gal4*, but not *C5-gal4*, also caused loss of Wg expression (Fig. 3.5A-D). Taken together, these results suggest that PP4 functions within the Notch-expressing cell to promote full pathway activation and target gene expression. We also observed reduction in Wg expression within the hinge domain, which is controlled by a number of factors (Rodríguez et al., 2002). This may reveal another novel role for PP4 components in the presumptive hinge region.

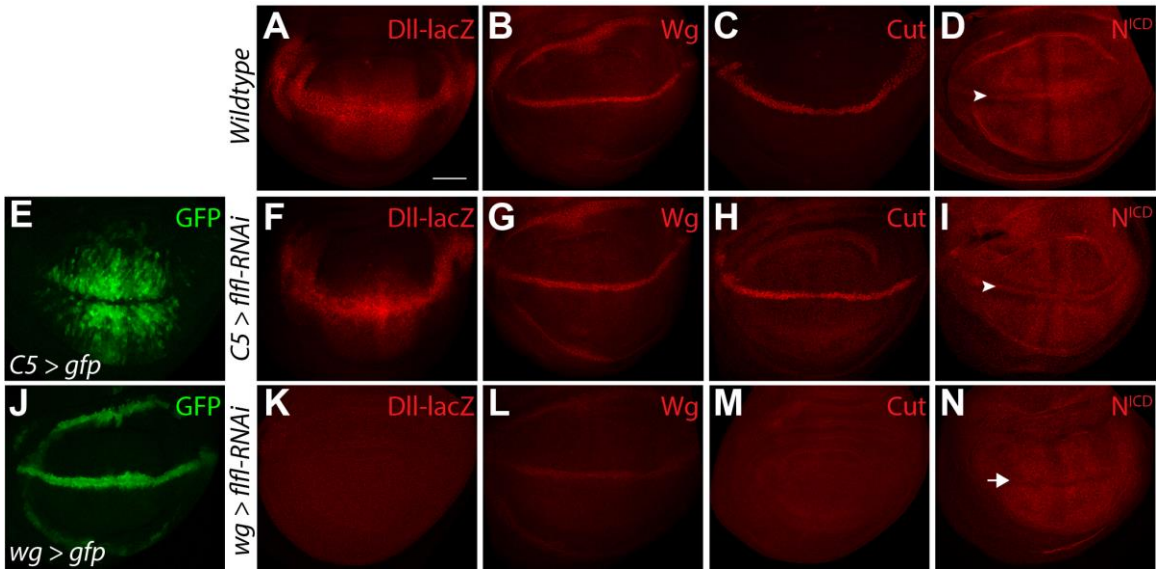

Figure 3.4 PP4 promotes Notch signaling in the Notch-signal receiving cells.

(A-D) Wild-type expression pattern of *Dll-lacZ* (A), Wg (B), Cut (C), and N^{ICD} (D) in the developing wing disc. N^{ICD} is enriched along the dorsal/ventral (D/V) boundary (D, arrowhead) and suppressed in the adjacent cells. (E) Expression pattern of *C5-Gal4* driving GFP in the D/V boundary flanking cells of the wing pouch. (F-I) The knockdown of *flfl* with RNAi in the D/V boundary flanking cells does not affect *Dll-lacZ* (F), Wg (G), Cut (H), or N^{ICD} (I). (J) Expression pattern of *wg-Gal4* driving GFP along the D/V boundary. (K-N) Knockdown of *flfl* in the D/V boundary cells causes a loss of *Dll-lacZ* (K), strong reduction of Wg (L), loss of Cut (M), and a failure of N^{ICD} enrichment along the D/V boundary (N, arrow). Scale bar: 50 μm.

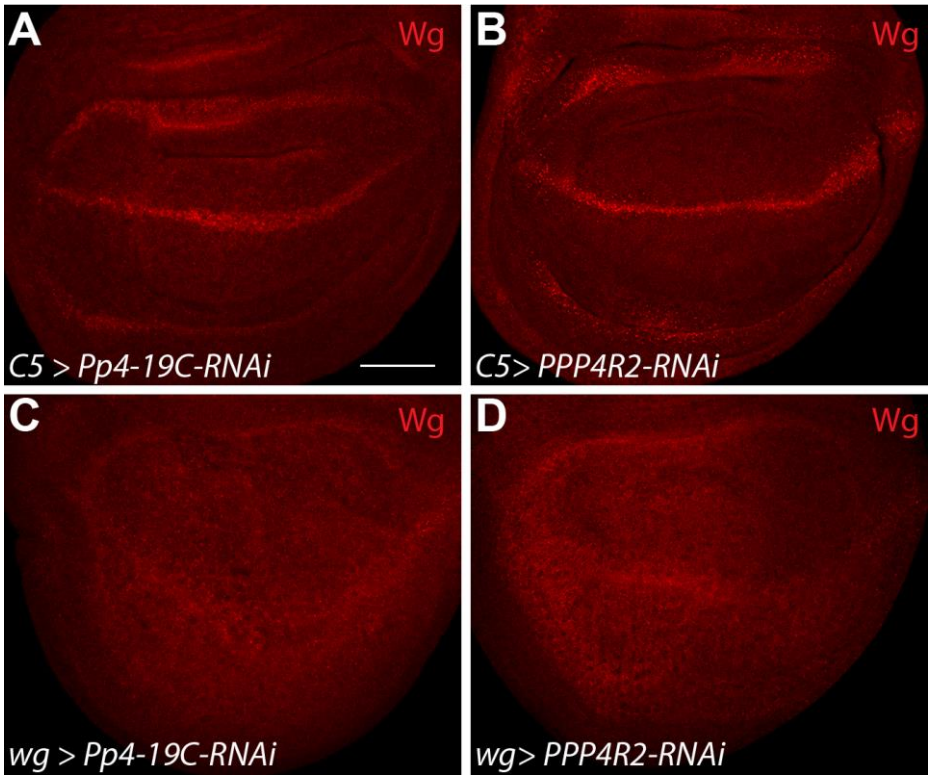

Figure 3.5 PP4 subunits promote Notch signaling in the Notch receiving cells.

(A, B) *C5-Gal4* expressing *Pp4-19C-RNAi* or *PPP4R2-RNAi* along the D/V boundary flanking cells of the wing pouch did not affect Wg protein levels or patterning. (C, D) *wg-Gal4* expression of *Pp4-19C-RNAi* or *PPP4R2-RNAi* resulted in strong reduction of Wg in the wing disc. Scale bar: 50 μm.

3.4.4. PP4 functions within the nucleus to promote Notch signaling.

To further refine where PP4 functions within the Notch signal receiving cell, we utilized mutant transgenes of Flfl and N in the adult *Drosophila* wing. During pupal wing metamorphosis, the activation and refinement of Dl and N are required to refine adult vein formation (Huppert et al., 1997). Notch signaling is also critical for the development of sensory bristles along the adult wing margin (reviewed in Posakony, 1994). Any developmental defects from expression of the various Flfl transgenes in adult wings could provide insight into the role of PP4 in the Notch pathway. Using *MS1096-Gal4*, which is expressed across the entire developing wing pouch, to ectopically express wild type Flfl or a cytoplasmic form, Flfl$^{\Delta 3NLS+2NES}$ (Flfl-cyto), had no effect on the adult wing compared to wild-type (Fig. 3.6A-C). Endogenous Flfl is a predominantly nuclear protein and the wild-type Flfl transgene has been shown to function similarly (Sousa-Nunes et al., 2009). Knockdown of *flfl* via RNAi induced ectopic and thicker veins in the adult wing (Fig. 3.6D), a hallmark of reduced Notch activity (Huppert et al., 1997). This phenotype could be suppressed by reintroduction of the wild-type *flfl* transgene (Fig. 3.6E), but not with expression of *flfl-cyto* (Fig. 3.6F). This suggests that Flfl functions within the nucleus, rather than the cytoplasm, to promote Notch.

To confirm the hypothesis that Flfl likely acts in nuclear Notch signaling, we expressed a construct encoding the intracellular domain of Notch that localizes to the nucleus (N^{nucl})(Rebay et al., 1993). This activated nuclear Notch suppressed wing vein formation and the formation of sensory bristles (Fig. 3.6G, G') compared to wild type (Fig. 3.6A). Notch-dependent activation of *wg* expression is essential for Wg signaling to induce expression of proneural genes, such as *Sens* for the specification of sensory organ precursor (SOP) cells (Nolo et al., 2000). SOPs then divide and differentiate, giving rise to the sensory bristles in the adult fly via Notch signaling (Guo et al., 1996; Hartenstein and Posakony, 1990). Although ectopic Notch signaling increases the number of SOPs in the wing disc via Wg, they do not differentiate correctly, resulting in double-socket cells, and loss of bristle cells (Guo et al., 1996). Knockdown of *flfl* in the N^{nucl}-expressing cells was able to partially recover vein loss, but did not significantly rescue the bristle defect (Fig. 3.6H, H'). Conversely, the expression of Flfl or Flfl-cyto had no effect on the N^{nucl} phenotype (Fig. 3.6I-J'). We interpret the inability to specifically rescue the bristle defect as being due to the combination of the strength of N^{nucl} as well as an incomplete knockdown of *flfl* via RNAi. To confirm that this phenotype could be

rescued in our assay, we tested whether loss of *wg* could rescue the effect since up-regulated target genes expression causes the N^{nucl} phenotype. Expression of a weak *wg-RNAi* transgene was able to induce sporadic sensory bristle loss (Fig. 3.6K, K', arrow), due to reduced SOPs (Nolo et al., 2000; Parker et al., 2002). When combined with N^{nucl}, *wg-RNAi* can partially suppress the overactive Notch phenotype of inhibited bristle formation and wing vein defects (Fig. 3.6L, L', arrowhead).

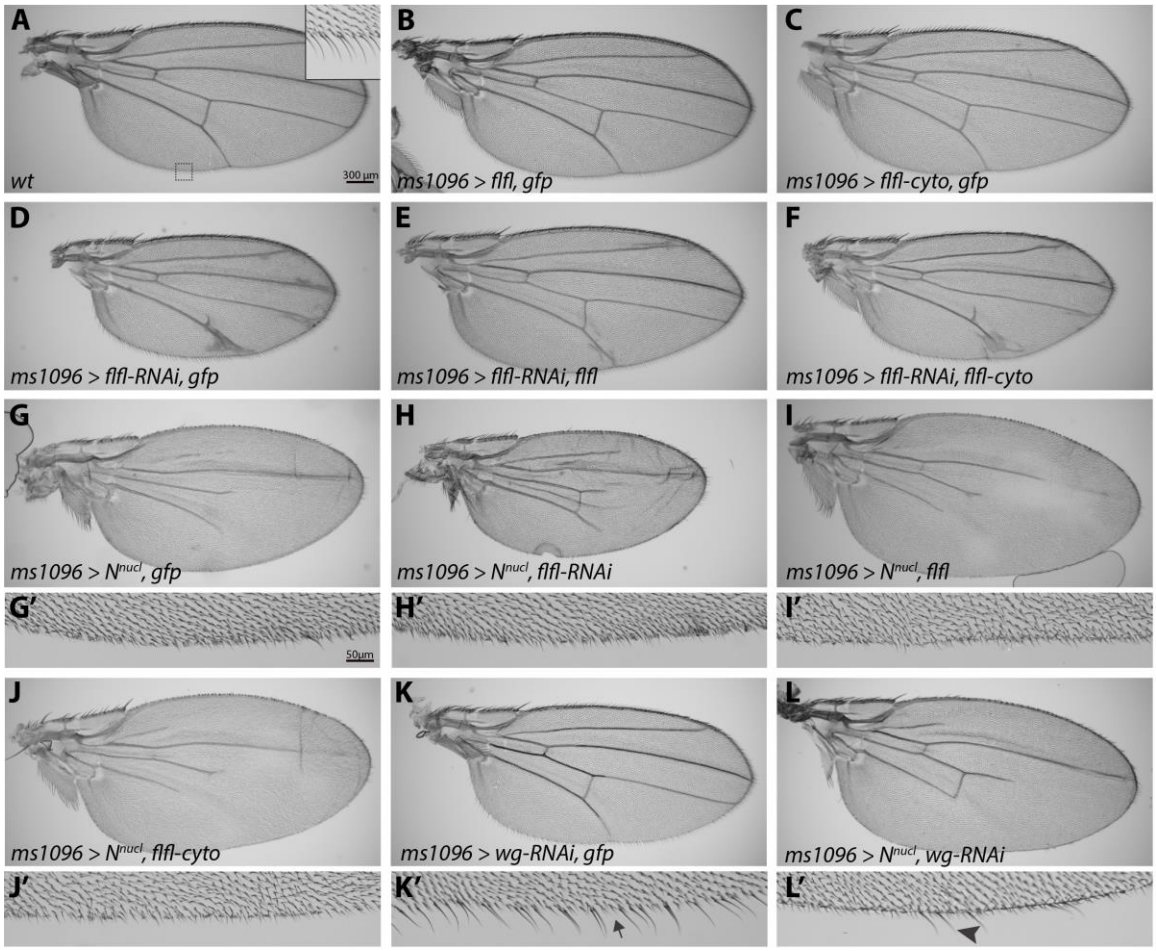

Figure 3.6 PP4 likely functions within the nucleus to promote Notch.

(A-C) Adult wild-type wing and margin (A, inset). Over expression of Flfl (B), or Flfl-cyto(C) throughout the entire wing does not induce any noticeable phenotype. (D-F) Knockdown of Flfl induces ectopic veins and thickening of veins, as well as a reduced wing size (D). This effect can be primarily rescued by reintroduction of a full length Flfl transgene (E), but not by Flfl-cyto (F). (G-L') Over-expression of N^{nucl} induces a loss of wing veins (G) and wing margin bristles (G'). Knockdown of *flfl* induces a mild rescue of the N^{nucl} loss of vein phenotype, and still reduces the overall wing size (H, H'). The over expression of Flfl (I, I'), or Flfl-cyto (J, J') did not disrupt the N^{nucl} phenotype. (K-L') Expression of *wg-RNAi* in the wing induced sporadic loss of margin bristles (K, K', arrow). N^{nucl} with *wg-RNAi* is able to maintain several margin bristles (L, L', arrowhead).

3.4.5. Flfl is required for proliferation and maintenance of overall tissue size independent of Notch signaling.

Adult flies with reduced *flfl* expression displayed smaller wing blades compared to control flies (Fig. 3.6A, D). This was expected given the known role of PP4 in cell cycle progression and growth (Helps et al., 1998; Huang et al., 2016; Martin-Granados et al., 2008; Zhuang et al., 2014). Notch has been implicated in cell proliferation in the wing imaginal disc, but a direct mechanism for its involvement is not fully understood (Baonza and Garcia-Bellido, 2000; Giraldez and Cohen, 2003; Go et al., 1998). We quantified the area of the adult wings of the different genotypes, in order to determine if the role of PP4/Flfl in growth is mediated through Notch signaling. Overexpression of Flfl and Flfl-cyto had no significant effect on wing size compared to wild type (Fig. 3.7A, box plots a,b,c). Knockdown of *flfl* resulted in a ~28% reduction in wing size, and could be fully rescued by the wild-type *flfl* transgene (Fig. 3.7A, box plots d,e). Flfl-cyto was able to slightly rescue the growth defect from *flfl-RNAi*, but not to a significant level (Fig. 3.7A, box plot f). The ability to rescue partially may be due to the role of PP4 in mitotic progression after nuclear envelope break down at prometaphase, allowing for Flfl-cyto to perform its function at this step in mitosis (Huang et al., 2016). Wings expressing N^{nucl} did not have a significantly smaller area than wild type wings, and were unable to rescue the growth defect from *flfl-RNAi* (Fig. 3.7A, box plots g,h). As N^{nucl} is unable to rescue the growth defect from reduced Flfl levels, it indicates that the role of PP4/Flfl in regulating growth is likely independent of its function in propagating Notch signaling. An alternative interpretation could be that Flfl acts downstream of N^{nucl} or that Flfl is required for proper Notch function in proliferation.

To determine if the growth defects from loss of PP4 were due to decreased cell proliferation or overall cell size, we looked at the developing wing imaginal disc. We utilized *en-Gal4* driving GFP to mark the posterior portion of the wing disc, representing ~50% of the overall tissue (Fig. 3.7B). We compared the size of the GFP-positive region to the control anterior side of the disc in different genotypes to determine the effects that changes in the levels of Flfl have on tissue growth. In control discs expressing *UAS-lacZ*, the ratio between the internal control area of the anterior, to the GFP positive posterior was equal (Fig. 3.7B, E). Overexpression of Flfl in the posterior domain did not affect the posterior/anterior area ratio (Fig. 3.7C, E). However, reduction of *flfl* via RNAi resulted in a significant decrease in size of the posterior domain (Fig. 3.7D, E).

We next looked at the number of mitotic cells in these genotypes using a phospho-Histone H3 (Ser10) (PH3) antibody. This experiment would reveal the rate of proliferation, as this specific phosphorylation of histones occurs during mitosis. There was no significant difference between our control discs and those overexpressing of Flfl (Fig. 3.7B', C', F). Surprisingly, we found that *flfl-RNAi* tissue had significantly elevated levels of PH3-positive cells (Fig. 3.7D', F). This result was perplexing considering the decreased tissue size, yet apparent increase in proliferation rate. As PH3 marks condensed chromatin prior to chromosomal segregation in cells along the G2/M transition (Hendzel et al., 1997), it is possible that *flfl-RNAi* cells were arrested during early mitosis, and had not undergone mitotic exit. Previously, Sousa-Nunes et al. (2009) identified a similar effect. *Drosophila flfl/+* brains exhibited much lower rates of Bromodeoxyuridine (BrdU) incorporation and reduced proliferation, yet exhibited elevated levels of PH3 positive cells, demonstrating that *flfl* is important for mitotic progression. Similar results have been found in multiple cases (Huang et al., 2016; Martin-Granados et al., 2008). Our results suggest a similar function for PP4/Flfl in the wing disc, where PP4 is critical for cell cycle progression and mitosis, affecting proliferation rates and overall tissue size, yet this function is independent of its role in promoting Notch signaling.

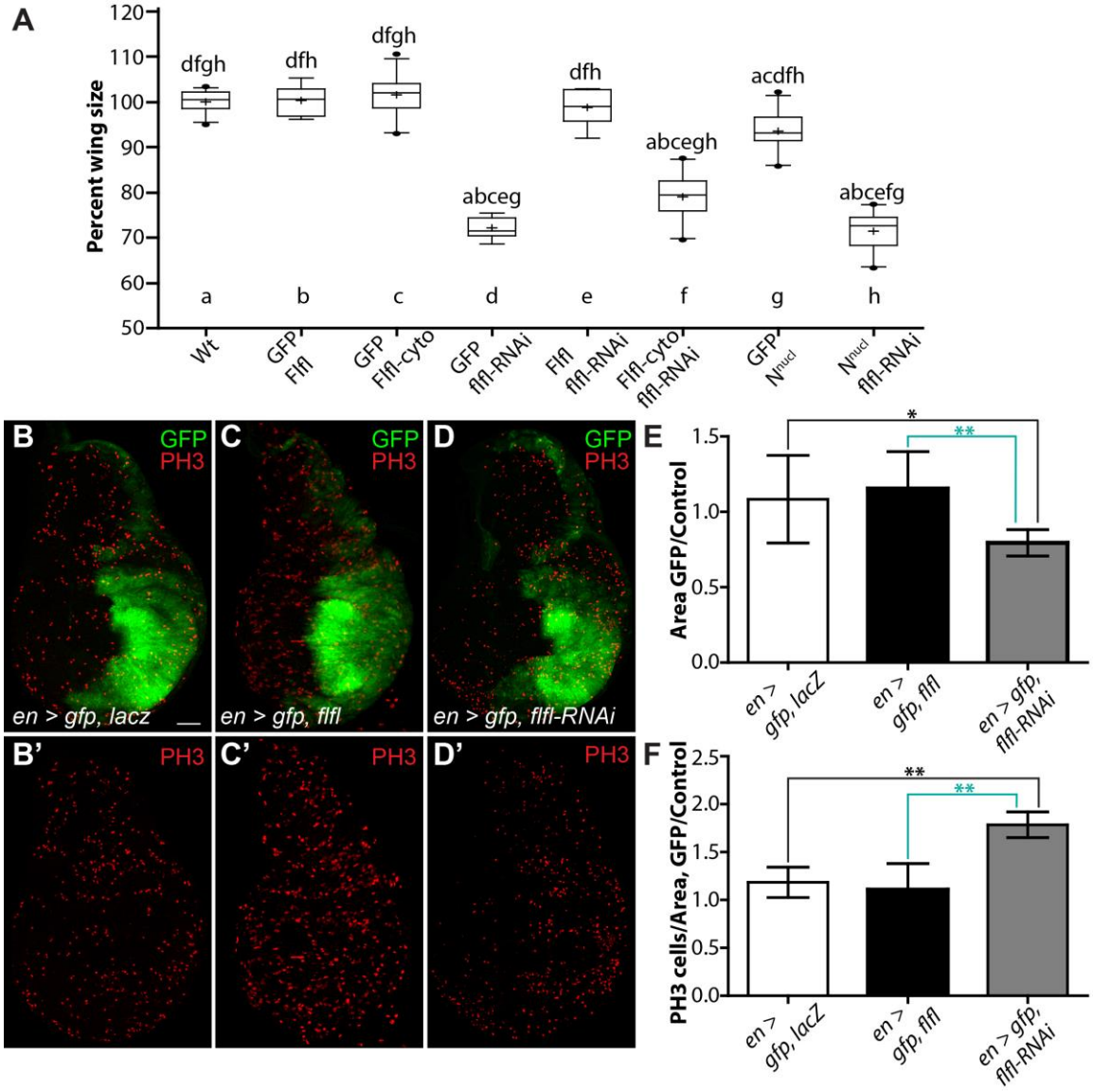

Figure 3.7 Flfl is required for proliferation and overall tissue size independent of Notch signaling.

(A) Box plots representing total wing area of the genotypes shown in Fig. 3.6 (n = 8-13). Over expression of Flfl (b) or Flfl-cyto (c) did not affect wing size compared to wild-type (a). *flfl-RNAi* caused a significant reduction in wing size (d). The *flfl-RNAi* size defect could be fully rescued by reintroduction of full length Flfl (e), but no effect was seen with Flfl-cyto (f). Wings expressing N^{nucl} (g) are slightly smaller than wild-type wings. N^{nucl} and *flfl-RNAi* wings (h) have a significant size reduction compared to wild-type (a), equivalent to that of *flfl-RNAi* alone (d). Data are presented as box plot 25-75 percentile, whiskers 10-90 percentile, (—) median, (+) mean and (•) outliers, with letters above representing significance from corresponding genotypes, (*P<0.01*) generated from one-way ANOVA. (B-F) The normal expression pattern of *en-Gal4* marked by GFP (B) in the posterior domain of the developing wing disc, shown with mitotic cell marker PH3 (B') and represented as a ratio of posterior domain vs. the anterior control (n = 8)(E, F). Over expression of Flfl in the posterior domain had no effect on area (C, E) or

proliferation rate (n = 7)(C’ F). The knockdown of Flfl with RNAi in the posterior domain induced a significant reduction in area (D, E), and exhibited a significantly higher number of PH3 positively marked cells (n=9)(D’ F). Data are presented as means ± s.d.;
(*) $P<0.05$, (**) $P<0.01$ generated from one-way ANOVA. Scale bar: 50 µm.

3.4.6. aPKC is not involved with PP4 and Notch signaling in the Drosophila wing imaginal disc

We examined whether PP4 mechanistically interacted with other known modulators of the Notch pathway. One well-characterized regulator is atypical protein kinase C (aPKC). aPKC is a protein kinase widely studied for its role in developmental processes, including asymmetric cell division (ACD). The regulators of ACD (including aPKC, Bazooka, and Crumbs) act upstream of Notch signaling and determine the identity of the Notch signal sending and signal receiving cells (reviewed in Knoblich, 2008). aPKC also promotes the Notch pathway by inhibiting Numb-mediated endocytosis of the Notch pathway components (Frise et al., 1996; Smith et al., 2007; Wang et al., 2006b). Previous studies have shown a role for PP4/Flfl in the localization of the Miranda complex to promote neuroblast ACD in *Drosophila* by acting downstream or parallel to aPKC (Sousa-Nunes et al., 2009). Since such a role has not been identified in a proliferating epithelium such as the wing disc, we sought to investigate if this mechanism was conserved during the development of the wing disc.

Using *MS1096-Gal4* to express *aPKC-RNAi* in the wing disc resulted in small, crumpled adult wings, with only sporadic sensory bristles (Fig. 3.8B), indicating disrupted patterning and growth. Overexpression of an aPKC transgene did not induce any visible phenotype (Fig. 3.8C), and was able to rescue the *aPKC-RNAi* phenotype, confirming the phenotype seen from the RNAi was directly a result of loss of *aPKC* (Fig. 3.8D). The knockdown of *flfl* via RNAi or over expression of the wild type *flfl* transgene had no effect on the *aPKC-RNAi* phenotype (Fig. 3.8E, F). Importantly, expression of N^{nucl} was unable to rescue the crumpled wing from *aPKC* knockdown, indicating that aPKC is most likely not a direct upstream regulator of Notch in the wing imaginal disc (Fig. 3.8G). In addition to this, overexpression of *aPKC* had no effect on the *flfl-RNAi* vein thickening compared to *flfl-RNAi* alone (Fig. 3.6D, 3.8H). Although aPKC is involved with PP4 and Notch signaling in ACD (Sousa-Nunes et al., 2009; Zhang et al., 2016), it does not appear to be directly involved in Notch signaling and pattering in the developing wing imaginal disc.

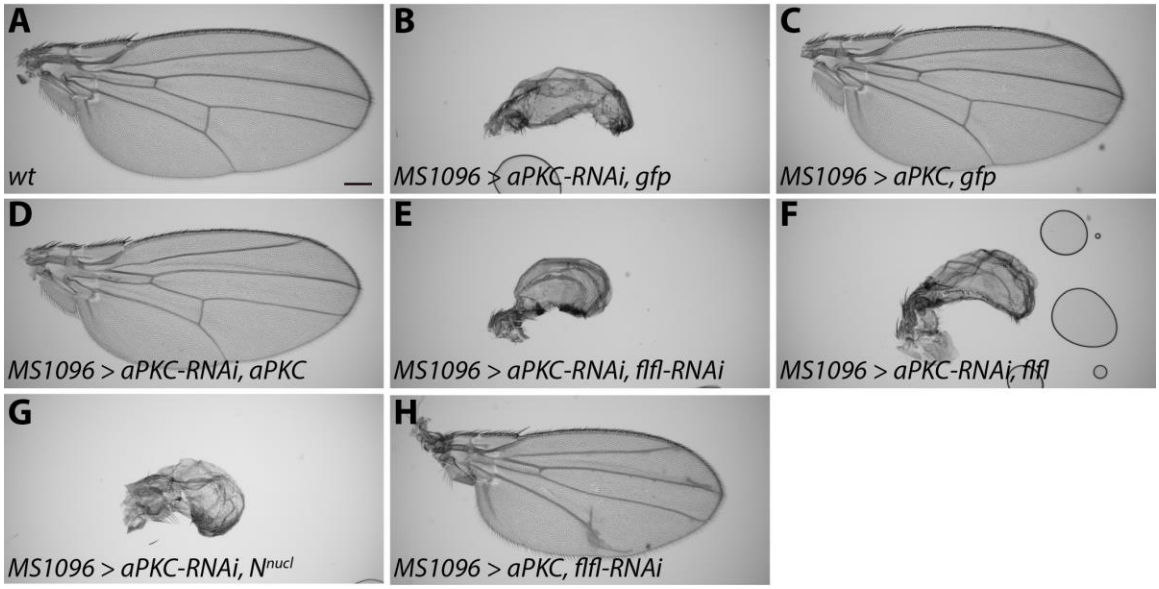

Figure 3.8 aPKC does not promote Notch signaling in the Drosophila wing.

(A) Adult wild-type wing. (B) Knockdown of aPKC with RNAi throughout the entire wing induces small crumpled, blistered, and malformed wings. (C-D) Over expression of an aPKC transgene induces no visible phenotype (C), but can fully rescue the effects of *aPKC-RNAi* (D). (E-G) The knockdown of Flfl (E), or its over expression (F) had no effect on the *aPKC-RNAi* phenotype. N^{nucl} was also unable to rescue the *aPKC-RNAi* phenotype (G). (H) Over expression aPKC does not affect the *flfl-RNAi* phenotype. Scale bar: 300 µm.

3.5. Discussion

An *in vivo* RNAi screen initially identified three components of the PP4 enzyme complex as modulators of endogenous Wg signaling during wing development (Swarup et al., 2015). The PP4 complex in *Drosophila melanogaster* has been implicated in many signaling pathways, cellular functions and developmental processes, yet its role in regulating Wg signaling was previously uncharacterized. In this study, we revealed that the effect on Wg pathway was at the level of expression of the Wg ligand, by promotion of Notch signaling. Notch signaling regulates the precise expression of Wg in the cells of the D/V boundary of the wing imaginal disc. This expression is required for specification of the wing margin and bristle structures (de Celis et al., 1996; Couso et al., 1994; Neumann and Cohen, 1996).

A partial knockdown of Flfl, PP4-19C and PPP4R2 by RNAi in the posterior domain of the wing imaginal discs was able to effectively reduce Wg target genes, yet did not induce elevated levels of JNK-mediated cell death as previously reported (Huang and Xue, 2015). Cell death was inducible upon stronger expression of the RNAi using *act-Gal4* with heat-shock inducible flip-out clones (data not shown). The knockdown of Flfl was further found to reduce expression of the Wg ligand as well as other Notch pathway target genes, implicating PP4 in the Notch pathway. Reduction of PP4 proteins in the D/V boundary all resulted in reduced Wg expression, while their knockdown in neighbouring Dl- and Ser-expressing cells had no effect. This result highlights that the PP4 complex acts in boundary cells to regulate Notch-dependent gene expression.

Previously, PP4 has been indirectly associated with Notch signaling in *Drosophila* for its involvement in asymmetrical cell division (ACD) of the developing neuroblasts (Sousa-Nunes et al., 2009; Zhang et al., 2016). While PP4 acts in concert with aPKC and Notch signaling to drive proper ACD, we were unable to identify a role for aPKC in Notch signaling in the epithelial cells of the wing imaginal disc. However, further genetic interaction experiments also identified that PP4's involvement in Notch signaling in the wing imaginal disc appears to be independent of its role in cell cycle progression and tissue growth. These results demonstrated that although both PP4 and Notch are required for cell cycle (Giraldez and Cohen, 2003; Go et al., 1998; Huang et al., 2016), in the wing imaginal disc, it is likely not through the same mechanism.

Subsequent genetic interaction studies revealed that most likely Flfl acts to promote Notch through its role in the nucleus. A cytoplasmic form of Flfl could not recue the phenotypes generated by *flfl-RNAi* in the adult wing, while expression of a wildtype transgene could. The required function of Flfl in the nucleus was further bolstered by the fact that the wing phenotype induced by activated nuclear N was partially suppressed by *flfl-RNAi*. As the N^{ICD} enters the nucleus and binds to Suppressor of Hairless and Mastermind to initiate target gene transcription, a multitude of cofactors must be recruited, while others must be removed, from the transcriptional initiation site (reviewed in Bray, 2016). This includes the inhibition of histone deacetylase (HDAC) co-repressor complexes (Kao et al., 1998). PP4 has been previously identified to dephosphorylate and inhibit HDAC activity, while its depletion stimulates HDACs (Zhang et al., 2005). Taken together a possible mechanism for PP4 to promote Notch signaling is through the dephosphorylation of HDACs. This could allow for increased chromatin remodelling, which is needed for the binding of other transcriptional co-factors to ensure full transcriptional initiation of target genes (reviewed Bray, 2016). This is just one possibility, as PP4 may be responsible for the dephosphorylation and modulation of any number of components that cooperate with transcription factors, or regulate the activity of N^{ICD} leading to appropriate target gene expression. Future studies will hopefully address the exact mechanism PP4 plays in promoting nuclear Notch signaling for full expression of target genes like *wg*.

Chapter 4. Actomyosin contractility modulates Wnt signaling through adherens junction stability.

This chapter is based off work submitted and currently under review from:

Hall E. T., Hoesing E., Sinkovics E., and Verheyen E. M. (2017). Actomyosin contractility modulates Wnt signaling through adherens junction stability. Developmental cell. Under review.

4.1. Contributions to the chapter:

This project was initiated by me, I conceptualized and performed the experiments, and wrote the manuscript.

Elizabeth Hoesing performed experiments and imaging for Fig 4.5 C-C''.

Endre Sinkovics assisted with experiments and contributed to data analysis.

Esther M. Verheyen assisted with editing the manuscript, and provided guidance.

4.2. Abstract

Mechanical forces can influence the canonical Wnt signaling pathway in processes like mesoderm differentiation and tissue stiffness during tumorigenesis, but a molecular mechanism involving both in a developing epithelium and its homeostasis is lacking. We identified that increased non-muscle myosin II activation and cellular contraction inhibited Wnt target gene transcription in developing *Drosophila*. Genetic interactions studies identified this effect was due to myosin-induced accumulation of cortical F-actin resulting in clustering and accumulation of E-cadherin to the adherens junctions. E-cadherin titrates any available β-catenin, the Wnt pathway transcriptional co-activator, to the adherens junctions in order to maintain cell-cell adhesion under contraction. We show that decreased levels of cytoplasmic β-catenin result in insufficient nuclear translocation for full Wnt target gene transcription. Our work elucidates a mechanism in which the dynamic activation of actomyosin contractility refines patterning

of Wnt transcription during development and maintenance of epithelial tissue in organisms.

4.3. Introduction

The Wnt signaling pathway [Wingless (Wg) in *Drosophila*], is highly conserved across metazoans and essential during development and tissue homeostasis for the regulation of proliferation and patterning (Clevers and Nusse, 2012). Wnt signaling achieves proper biological outcomes through extensive crosstalk with other signaling pathways. Recent studies have begun to elucidate how mechanical forces may also play critical roles in regulating signaling pathways during development (Farge, 2011). Here, we identified a molecular mechanism in which actomyosin activation and the resulting contractile forces within a cell can regulate Wnt signaling.

The canonical Wnt/Wg pathway centers on the stabilization and localization of the key effector protein, β-catenin (β-cat) [Armadillo (Arm) in *Drosophila*]. β-cat is continuously produced in most cells for its roles in both the formation and maintenance of adherens junctions (AJs) and as a transcriptional activator for Wnt signaling (Valenta et al., 2012). AJs are major epithelial cell-cell adhesion complexes that maintain tissue integrity in response to external forces like morphogenesis (Harris and Tepass, 2010). AJs mainly form an apical-lateral belt-like structure around cells, holding neighbouring cells together through the homophilic binding of the transmembrane protein E-cadherin (E-cad). β-cat binds to the cytoplasmic tail of E-cad and to α-catenin, which interacts with the actin cytoskeleton. Thus AJs act as mechanical force integration sites across cells and at a tissue level (Lecuit and Yap, 2015).

In the absence of a Wnt ligand, cytoplasmic β-cat is targeted for degradation by a multi-protein destruction complex which assembles on the scaffolding protein Axin and includes kinases that phosphorylate β-cat, targeting it for ubiquitination and subsequent proteasomal digestion. Upon Wnt/Wg binding to its coreceptors Frizzled (Fz) and LRP/Arrow, Dishevelled (Dvl/Dsh) is recruited to Fz and triggers the recruitment of the destruction complex to the membrane. This event disrupts the destruction complex, allowing β-cat to accumulate and translocate to the nucleus, where it acts with T-cell factor (TCF)/lymphoid enhancer factor (LEF) transcription factors to initiate target gene expression (Daniels and Weis, 2005). Disruptions of the core components or regulatory

proteins have been found in numerous cancers and developmental disorders (Clevers and Nusse, 2012).

Recent studies suggest that canonical Wnt signaling and mechanical forces are integrated in regulation of development and homeostasis. Wnt activation can drive mechanical strain-induced cell proliferation (Benham-Pyle et al., 2015) as well as activation of non-muscle myosin II (NMII) leading to morphogenesis (Zimmerman et al., 2010). Conversely, force induction and subsequent cytoskeletal rearrangements can regulate Wnt signaling, but these studies have typically focussed on extracellular matrix (ECM) stiffness in stem cells or on tumorigenic situations (Fernández-Sánchez et al., 2015; Przybyla et al., 2016; Samuel et al., 2011; Schlessinger et al., 2009). Insight is lacking on the role of force induction and its regulation of Wnt activation in normal developing epithelial tissues. Recently multiple components of myosin phosphatase were identified in a kinome and phosphatome RNA interference (RNAi) screen to identify novel phospho-regulators of Wnt signaling in developing *Drosophila* larvae (Swarup et al., 2015).

Myosin phosphatase is the major inhibitor of NMII in cells. It consists of two major proteins, either one of two targeting subunits, the myosin phosphatase targeting protein MYPT1/2 (Myosin binding subunit (MBS) in *Drosophila*) or MYPT3 (*Drosophila* Mypt-75D) and the catalytic protein phosphatase type 1β (PP1β) subunit (encoded by *flapwing (flw)* in *Drosophila*) (Vereshchagina et al., 2004). Myosin phosphatase inactivates NMII by dephosphorylating Thr-18 and Ser-19 (*Drosophila* Thr-20 and Ser-21), the two critical activation residues of the regulatory light chain (encoded by *spaghetti squash* (*sqh*) in *Drosophila*) of NMII (Hirata et al., 2009; Karess et al., 1991).

NMII is the major actin-binding motor protein that drives actomyosin cytoskeletal contraction. Its activation controls a diverse range of mechanisms included cell shape, adhesion, migration, cell cycle and cell division (Vicente-Manzanares et al., 2009). NMII regulatory light chain phosphorylation and the resulting contractile force activity can be induced by numerous kinases, some of which also phosphorylate and inhibit myosin phosphatase (Vicente-Manzanares et al., 2009). Several upstream Rho GTPases that activate myosin kinases and thus stimulate NMII can inhibit Wg activity in *Drosophila*, but a fully defined mechanism is not known (Greer et al., 2013). Here we show that actomyosin-based force generated by NMII stimulation within and across cells in an

epithelium can modulate Wnt signaling and tissue patterning by preferentially stabilizing cell-cell adhesion at the AJs to maintain tissue integrity at the expense of transcription and patterning.

4.4. Results

4.4.1. Myosin Phosphatase promotes activation of Wg signaling

Components of myosin phosphatase were identified in an RNAi screen due to their ability to modulate Wg target gene expression in the wing imaginal disc (Swarup et al., 2015). The Wg target gene *Distal-less (Dll)* is expressed in a broad domain within the wing pouch (Fig. 4.1A) (Zecca et al., 1996). Expression of *mypt-75D-RNAi* or *flw-RNAi* in the posterior domain of the wing imaginal disc using *hedgehog (hh)-Gal4* (referred to as *hh>mypt-RNAi*) caused a strong reduction in *Dll* transcription (Figs. 4.1A', 4.2A). Adult flies had a dramatic size reduction in the posterior of the wing blade as well as notches and loss of wing bristles, hallmarks of reduced Wg signaling (Fig. 4.1E). The Wg ligand is expressed in a band 2-3 cells wide along the dorsoventral (D/V) boundary (Fig. 4.1B), which was unaffected in GFP-marked actin flip-out clones expressing *mypt-75D-RNAi* or *flw-RNAi* (Figs. 4.1B', 4.2B), indicating that reduced myosin phosphatase was not disrupting ligand production to inhibit Wg signaling.

We next examined the stability of the key effector, Arm, which is highest in the cytoplasm and nucleus in two bands of cells flanking the Wg-producing cells (Fig. 4.1C) (Marygold and Vincent, 2003). Flip-out clones expressing *flw-RNAi* (Fig. 4.1C') or *hh-Gal4>mypt-75D-RNAi* (Fig. 4.2C) both caused reduced stabilized Arm.

To confirm that the reduction of Arm was not due to cell death we stained for the apoptotic marker cleaved caspase-3 (C.Casp-3) following knockdown of *flw* or *mypt-75D* (Fig. 4.2B, C). Knockdown of the other targeting subunit, MBS, gave similar results to *flw-RNAi* or *mypt-RNAi*, but could induce cell death, and was therefore not used in further experiments (Fig. 4.3). This may be due to the increased effectiveness of the *mbs-RNAi*, or that MYPT-75D acts only upon cortical NMII, while MBS is cytoplasmic and may affect other functions of NMII. Taken together these results demonstrate a previously uncharacterized role for myosin phosphatase in the promotion of Wg signaling in *Drosophila*.

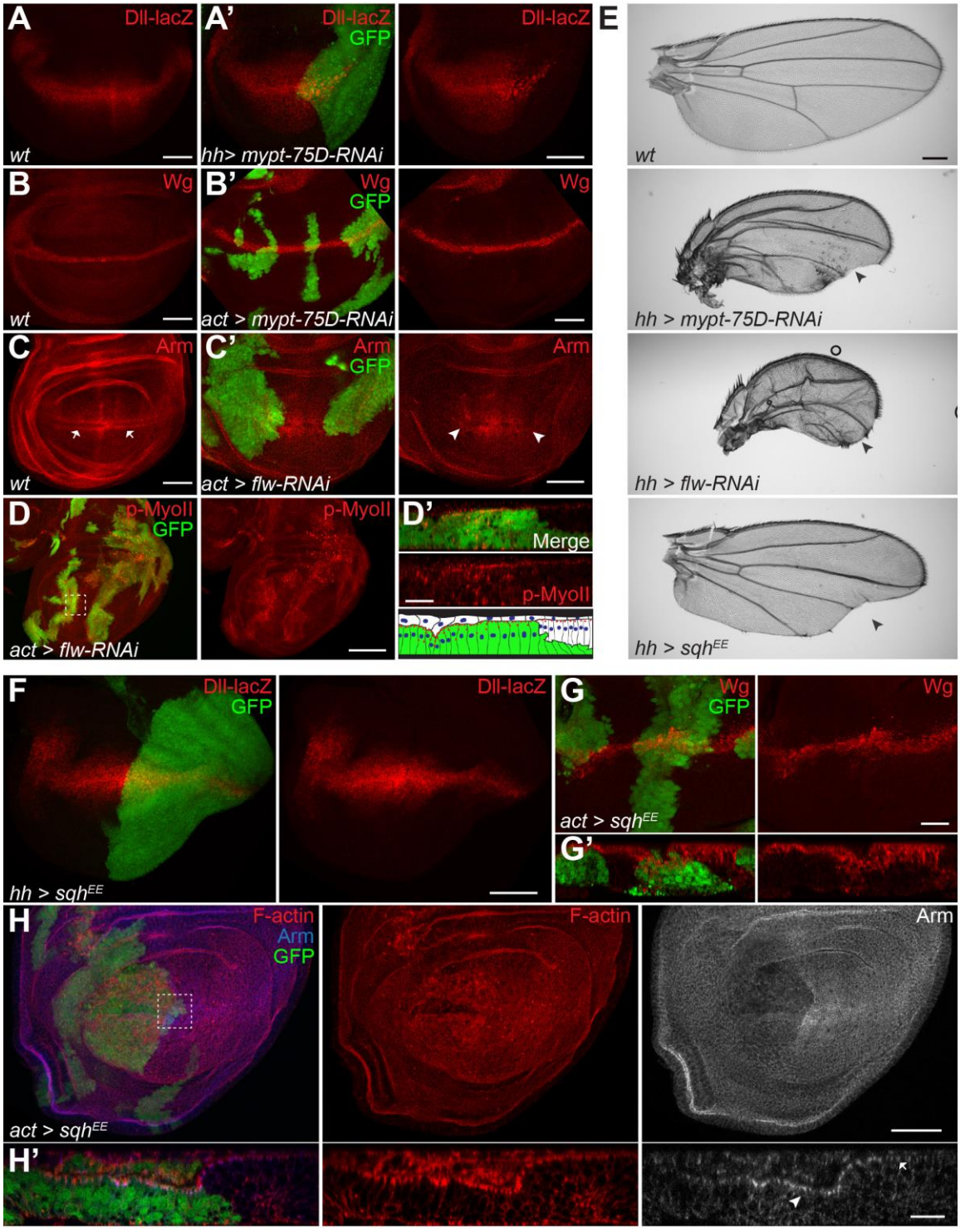

Figure 4.1 Myosin phosphatase and NMII regulate Wg activity during wing development.

(A,A') *Dll-lacZ* expression in wild type (A) and *hh-Gal4* driving *gfp* and *mypt-75D-RNAi* (A') third-instar wing imaginal discs. (B,B') Wg protein expression in wild

type (B) and GFP-marked actin flip-out clones driving *mypt-75D-RNAi* (B'). (C,C') Arm stabilization pattern in wild type (C, arrows) and in flip-out clones driving *flw-RNAi* (C', arrowheads). (D,D') p-MyoII stained in *flw-RNAi* flip-out clones. Z-sections seen in (D') is the magnified slice through the dashed line area of (D). (E) Adult wings of wild type, and *hh-Gal4* driving *mypt-75D-RNAi*, *flw-RNAi*, or sqh^{EE} (arrowheads mark loss of bristles and wing margins). (F) *hh>*sqh^{EE}*, gfp* stained for *Dll-lacZ* expression. (G, G') Total Wg in sqh^{EE} flip-out clones, and cross section showing cell constriction. (H,H') GFP flip-out clones driving sqh^{EE} stained for F-actin and Arm. (H') Cross section (magnified dashed line area of (H)) shows apical F-actin and Arm (H' arrowhead vs. arrow). Scale bars: (A-C,F,H) 50 µm, (D) 100 µm, (D',G,G',H') 20 µm, (E) 300 µm.

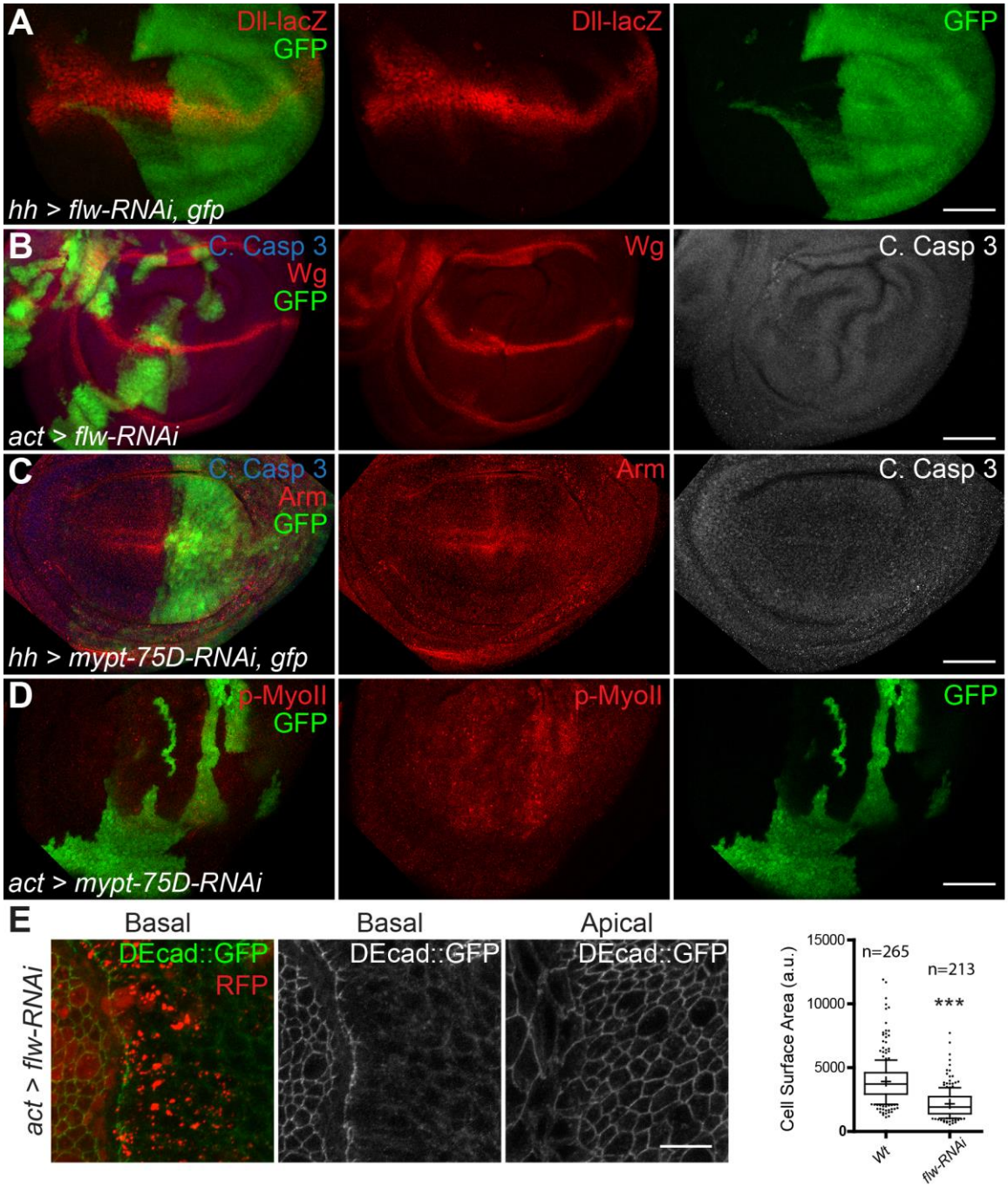

Figure 4.2 Knockdown of myosin phosphatase inhibits Wg activity, and promotes NMII activity during wing development.

(A) Wing discs in which *hh-Gal4* drives GFP and *flw-RNAi* in the posterior compartment, stained for *Dll-lacZ*. (B) GFP-marked actin flip-out clones expressing *flw-RNAi*, stained for Cleaved Caspase 3 (C. Casp3) and Wg. (C) Arm and C. Casp3 staining in discs with *hh-Gal4* driven *mypt-75D-RNAi* and *GFP*. (D) GFP-marked actin flip-out clones expressing *mypt-75D-RNAi,* stained for phospho-Myosin II (p-MyoII). (E) Cell surface areas of apical and basal sections of cells ubiquitously expressing DEcad::GFP fusion proteins to mark cell boundaries, with RFP-marked actin flip-out clones expressing *flw-*

RNAi. Cell surface area data represented as box plots 25-75 percentile, whiskers 10-90 percentile, (–) median, (+) mean and (·) outliers. Wild-type (n=265) and *flw-RNAi (n=213)* cells, *** = *P*< 0.001.

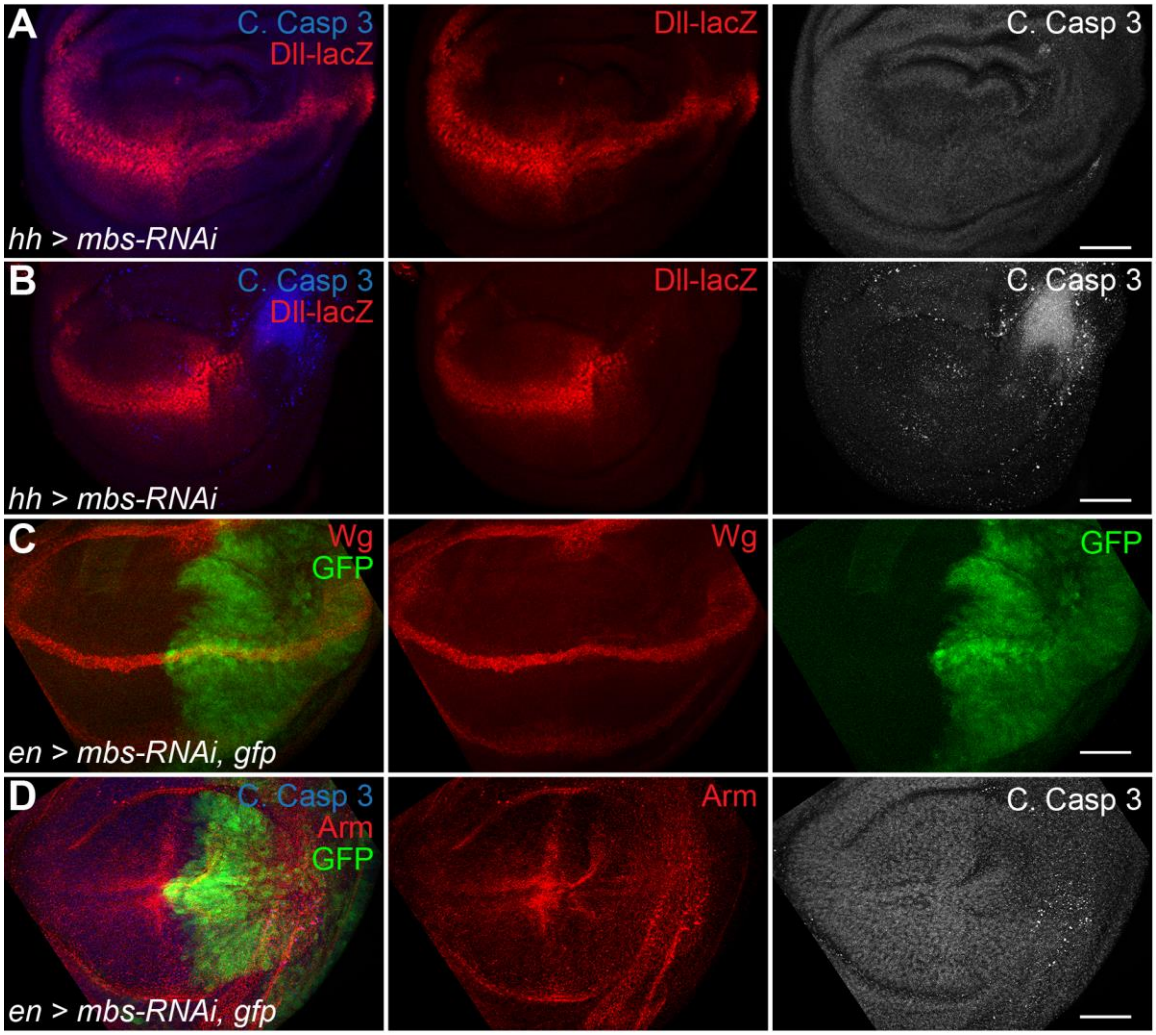

Figure 4.3 Knockdown of Myosin Binding Subunit, inhibits Wg activity but can induce cell death.

(A,B) *hh-Gal4* expressing *mbs-RNAi* in the posterior domain of the wing imaginal disc, reduces *Dll-lacZ* expression and can induce C. Casp 3 sporadically. (C) *en-Gal4* expressing GFP and *mbs-RNAi* in the posterior domain, does not affect Wg. (D) *en-Gal4* expressing GFP and *mbs-RNAi*, reduces stabilized Arm, without activating C. Casp 3. Scale bars: 50 µm.

4.4.2. Increased NMII activity inhibits Wg signal activation

The key role of myosin phosphatase is to dephosphorylate and inactivate NMII. We confirmed that knockdown of *flw* or *mypt-75D* lead to hyperactive phospho-NMII. RNAi clones of either *flw* or *mypt-75D* had increased phosphorylated Sqh (p-MyoII) (Figs. 4.1D, 4.2D). Cross sections showed other phenotypes associated with elevated NMII activation (Fig. 4.1D'). The wing imaginal disc consists of tightly packed columnar epithelial cells where Wg signaling occurs, and a thin layer of squamous peripodial epithelium above its apical surface (Fig. 4.1D' cartoon) (Widmann and Dahmann, 2009). *flw-RNAi* cells had elevated levels of p-MyoII, were constricted and formed clefts (Fig. 4.1D') and had reduced apical surface area, indicated by E-cad::GFP (Fig. 4.2E), another sign of increased NMII activity, and a proxy to force generation (Xie and Martin, 2015).

We next asked if directly activating NMII could phenocopy the loss of Wg signaling seen with myosin phosphatase knockdown. An activated phosphomimetic NMII regulatory light chain (Sqh^{EE}) could inhibit Wg target gene expression and induce notched wings in adults (Fig. 4.1E, F). Like myosin phosphatase knockdown, Sqh^{EE} could induce tissue constriction (Fig. 4.1G', H'), but did not affect Wg protein levels (Fig. 4.1G). Cells with increased NMII activity also had elevated levels of F-actin (Fig. 4.1H, H'). Activated NMII binds actin and stabilizes filaments as it pulls them together, reducing their turnover rate and causing an overall increase in F-actin in the cell (Murthy et al., 2005). Like reduced myosin phosphatase, Sqh^{EE} could reduce levels of stabilized cytoplasmic and nuclear Arm (Fig. 4.1H), but cross sections showed increased levels of AJ Arm at the apical surface of constricting cells (Fig. 4.1H'). This suggested that a defect in Arm distribution within cells having increased NMII activity may underlie the reduction in Wg targets. Moreover, we found that directly increasing myosin activation can modulate Wg activation.

4.4.3. Myosin phosphatase mediates Wg signaling through NMII activation

Myosin phosphatase seems to affect Wg signaling though regulation of NMII activation, given the similar effects upon reducing myosin phosphatase or activating NMII. However these results to not exclude a possible role for myosin phosphatase in

directly regulating Wg, in addition to indirectly through NMII. To test this model we performed a series of genetic interaction experiments. Knockdown of total NMII (*hh>sqh-RNAi)* predominantly induced widespread cell death and was non-viable (data not shown), wing disc that survived exhibited a dramatic reduction in total area of the posterior domain of the wing disc and a complete loss of *Dll* expression (marked by the dotted line, Fig. 4.4B). Knockdown of myosin phosphatase components in this background could partially restore *Dll* expression and some of the growth defects (Fig. 4.4D, F), suggesting that low levels of NMII can inhibit Wg activity, but activating the remaining NMII complexes (by removal of myosin phosphatase) can partially restore Wg activity, or more likely, is able to restore cellular viability and therefore Wg. These results were supported by the inverse experiment. Overexpression of Mypt-75D (inactivating NMII) also caused a complete loss of *Dll* expression (Fig. 4.4H). Co-expression of activated Sqh^{EE} could partially restore *Dll* expression (Fig. 4.4I). Taken together these results indicate myosin phosphatase affects Wg signaling through inactivation of NMII (Fig. 4.4J). Therefore, in subsequent experiments knockdown of myosin phosphatase is analogous to specifically stimulating NMII. Additionally these results show that a reduction of NMII activity in the developing tissue can reduce Wg activity. However, this tissue frequently becomes apoptotic and becomes extruded from the surrounding epithelium, making it exceedingly difficult to analyze. Although this may be a distinct mechanism for possibly regulating Wg activity, the widespread induction of cell death and extrusion due to loss of NMII should be examined in the future.

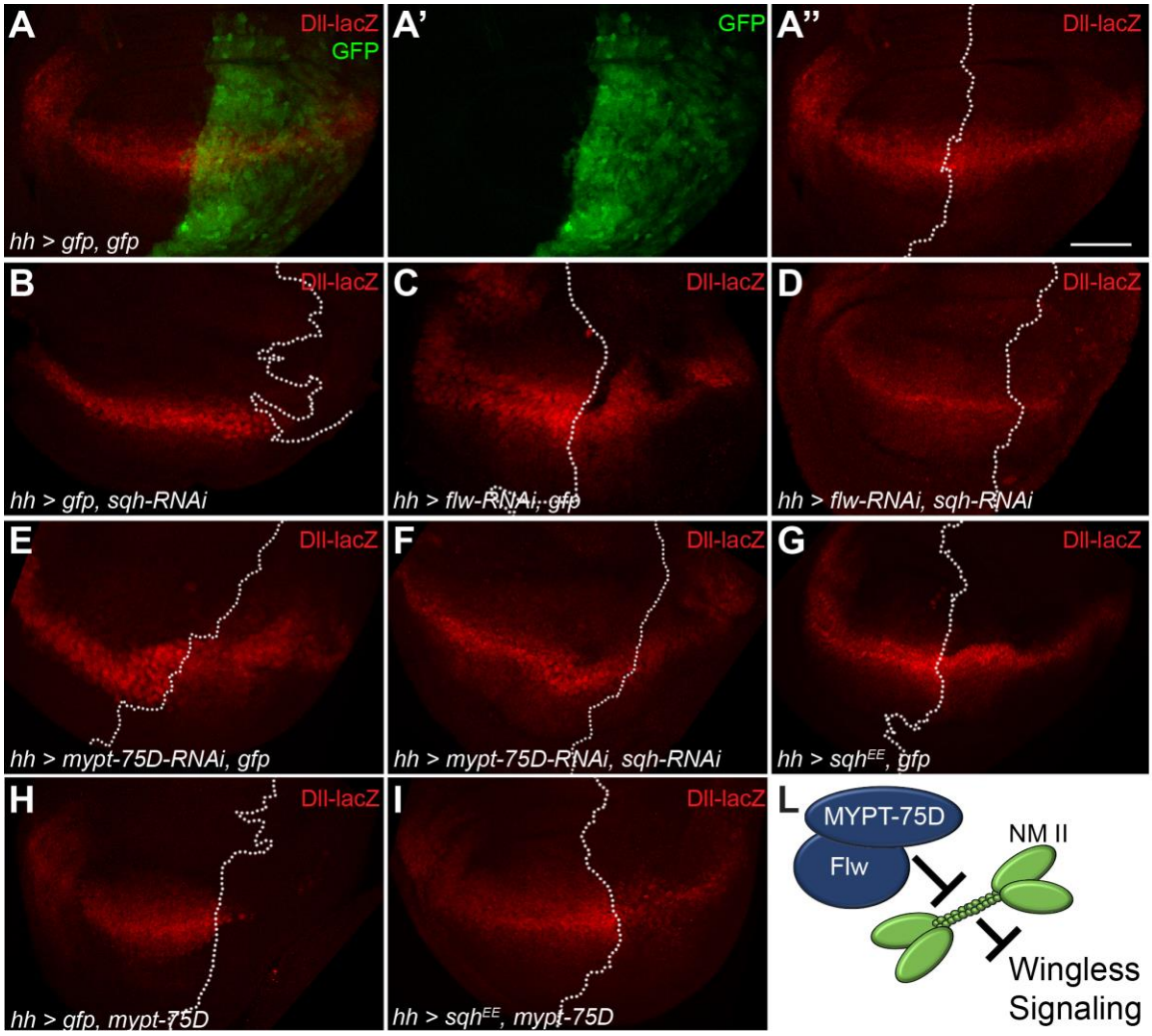

Figure 4.4 Myosin phosphatase mediates Wg activity through NMII activation.

(A-K) Genetic interactions between myosin phosphatase components and Sqh utilizing *hh-Gal4* expressed in the posterior domain of the wing disc, stained for expression of *Dll-lacZ*. (A-A") Control disc expressing GFP, (B) GFP and *sqh-RNAi*, (C) *flw-RNAi* and GFP, (D) *flw-RNAi* and *sqh-RNAi*, (E) *mypt-75D-RNAi* and GFP, (F) *mypt-75D-RNAi* and *sqh-RNAi*, (G) Sqh^{EE} and GFP, (H) GFP and MYPT-75D, (I) Sqh^{EE} and MYPT-75D. (J) Model for regulation of Wg signaling, myosin phosphatase regulates Wg activity through inhibition of NMII. Scale bar: 50 µm.

4.4.4. NMII activation reduces nuclear Arm independently of the destruction complex

Since increased NMII activity led to reduced stabilized Arm and a loss of Wg target gene expression, we next asked if NMII could affect destruction complex proteins in *Drosophila* salivary gland cells, as their large cells are ideal for studying protein localization *in vivo,* and glands have been characterized with respect to Wg signaling (Hall and Verheyen, 2015).

Knockdown of *flw* using *dpp-Gal4* resulted in a loss of the Wg target gene *fz3* (Fig. 4.5A), indicating that activated NMII can also inhibit Wg signaling in the salivary gland. After Wg binds to its receptors in the proximal cells of the salivary gland, Dsh, Axin and other the components of the destruction complex are recruited to Fz (Fig. 4.5B), causing inactivation of the complex (Bilic et al., 2007). *flw-RNAi* had no effect on the cell surface distribution of Dsh-GFP or FLAG-Axin (Fig. 4.5B), indicating that Wg's regulation of the destruction complex still occurs in cells with elevated NMII activity. These results suggest that increased NMII activity affects Wg signaling downstream of the receptor mediated recruitment of the destruction complex.

To determine where NMII acts within the pathway, we induced ectopic Wg signaling at different points within the signaling cascade and asked if NMII could suppress ectopic target gene activation. An activated Fz-Arrow fusion protein induced ectopic *Dll* expression, which could be suppressed by *flw-RNAi* (Fig. 4.5C), confirming that increased NMII inhibits Wg activity below the level of the receptors. To determine if NMII affects the destruction complex itself we generated $axin^{null}$ MARCM clones, as Axin is the scaffolding protein on which the destruction complex assembles (Zeng et al., 1997). Clones lacking Axin had high levels of ectopic *Dll* and were large due to increased proliferation (Fig. 4.5C'). Expression of *flw-RNAi* in $axin^{null}$ MARCM clones could not suppress ectopic *Dll*, but clones were generally smaller and did not show the smoothed edges seen in the $axin^{null}$ clones (Fig 4.5C'), suggesting that NMII can affect aspects of the $axin^{null}$ phenotype. We next tested degradation resistant Arm^{S10} (Pai et al., 1997). *flw-RNAi* suppressed ectopic and even some endogenous *Dll* expression in clones with Arm^{S10} (Fig. 4.5C").

Cells with increased NMII activity had decreased levels of cytoplasmic and nuclear Arm, but increased Arm at the apical surface (Fig. 4.1H, H'), suggesting that NMII could suppress Arm^{S10} activity by inhibiting its ability to enter the nucleus. To confirm this we looked at the relative distribution of Arm in *axin*^{null} tissue, to eliminate any variables NMII may have on destruction complex effectiveness and Arm turnover rates. Using F-actin to mark the edges of individual cells and DAPI to stain nuclei, intensity plots were drawn across individual cells to look at the distribution of Arm (Fig. 4.5D dotted line). *axin*^{null} cells had roughly double the amount of Arm in the nucleus as wild type (Fig. 4.5D'). Introduction of *flw-RNAi* resulted in a significant decrease in nuclear Arm in an *axin*^{null} background, but which was still higher than in wild type cells (Fig. 4.5D'). These results are consistent with the level of Wg activity and maintained ectopic *Dll* seen in *axin*^{null} cells with *flw-RNAi* (Fig. 4.5C'). These findings suggest that increased NMII activity results in reduced entry or retention of Arm in the nucleus to initiate target gene transcription.

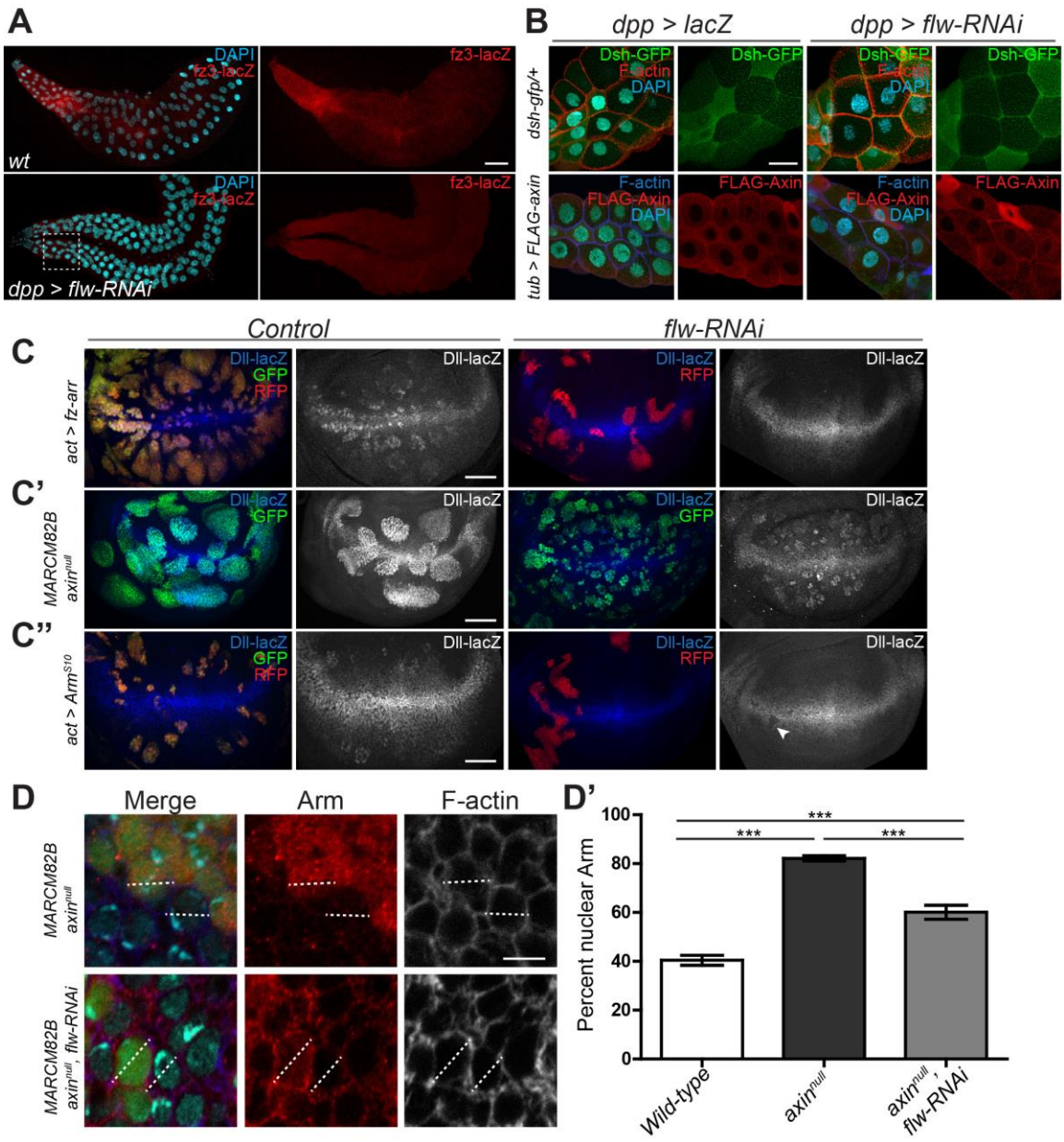

Figure 4.5 NMII activity inhibits Wg activation by reducing nuclear Arm independently of the destruction complex.

(A) Salivary glands from control or *dpp>flw-RNAi* stained for *fz3* expression. (B) Localization of Dsh-GFP and FLAG-Axin in the proximal cells of the salivary gland, identified in the dashed line area of (A), (C-C") Effects of *flw-RNAi* on ectopic *Dll-lacZ* in wing imaginal discs: (C) RFP marked flip-out clones expressing Fz-Arr and GFP or *flw-RNAi* (C') GFP-positive *axin*^{null} MARCM clones and *flw-RNAi* in *axin*^{null} MARCM clones. (C") Arm^{S10} flip out clones with GFP or *flw-RNAi.* (D,D') Effects of *flw-RNAi* on Arm distribution in GFP-marked *axin*^{null} cells. (D) DAPI was used to identify nuclei, and F-actin to mark the edges of the cell. (D') Percent of nuclear Arm in cells was measured as an intensity plot (dotted line D) in wild type (n = 16), *axin*^{null} (n = 20), and *axin*^{null}, *flw-RNAi* cells (n = 15). Data presented as mean ± SEM; ***P< 0.001. Scale bars: (A) 100 µm, (B-C") 50 µm, (D) 5 µm.

4.4.5. NMII activation increases retention of adherens junction proteins

The regulation of Arm localization by NMII could be mediated by any one of the processes that NMII normally influences, including other downstream signaling pathways. We systematically examined key cellular functions of NMII to determine how NMII can modulate Wg signaling.

Loss of myosin phosphatase and increased NMII activity can stimulate JNK [*Drosophila* Basket (Bsk)] activity in the developing wing disc (Kirchner et al., 2007), and JNK has been shown to promote Wnt signaling (Wu et al., 2008). Using *dpp-Gal4* expressed along the anterior/posterior (A/P) boundary of the wing disc (Fig. 4.6A, E) to express *flw-RNAi* reduced *Dll* expression, but in this context did not cause elevated JNK activity, seen by expression of JNK target gene *puc* (Martín-Blanco et al., 1998)(Fig. 4.6A, A', C, E, E', G). Expression of a dominant negative Bsk^{DN}, inhibiting JNK, did not affect *Dll* or *puc* in the wing pouch (Fig. 4.6B, F). Importantly when co-expressed with *flw-RNAi*, *Dll* was still reduced and *puc* was unaltered (Fig. 4.6D, H), indicating that NMII's ability to suppress Wg signaling is not mediated through JNK. We next investigated NMII's role in controlling integrin clustering for the formation of focal adhesion and ECM attachment (Vicente-Manzanares et al., 2009). Loss of function clones for the sole *Drosophila* β_{PS} integrin subunit (Brown, 1993) had no effect on expression of the Wg target Sens (Fig. 4.6I).

Engl et al. (2014) studied the dynamics of NMII in suspension cell doublets. Following NMII activation, cells begin to constrict and pull away from one another, causing an influx and retention of E-cad to the AJ along with other proteins, including β-cat/Arm, to maintain and reinforce cell-cell adhesion. The increased apical Arm in cells with elevated NMII activity suggested that Wg signaling may be modulated by NMII's ability to control E-cad clustering and retention during cell constriction. In clones expressing activated NMII (Sqh^{EE}), constricting cells had increased *Drosophila* E-cad (DE-cad) and Arm along the apical surface at the AJ (Fig 4.7A, arrowheads). Activated myosin did not affect transcription of these genes, as seen by lacZ reporters (Fig. 4.7B), suggesting that Arm and DE-cad were accumulating at the AJ in cells with increased NMII activity. Such an effect was previously shown, although no link to Wg signaling was tested (Hong et al., 2013; Wu et al., 2014). We performed Fluorescence Recovery After

Photobleaching (FRAP) analysis to measure the turnover of DE-cad and Arm at the AJ. FRAP of ubiquitously expressed DE-cad::GFP or Arm::GFP was measured along cell interfaces in wild type cells (Fig. 4.7C, D, green box), cells expressing elevated NMII via *flw-RNAi* (Fig. 4.7C, D, red box) and at the interface of wild-type*/flw-RNAi* cells (Fig. 4.7C,D, blue box). FRAP revealed DE-cad recovery rates are significantly reduced at any *flw-RNAi* cell interfaces (Fig. 4.7C') and contained a significantly higher immobile fraction (Fig. 4.7C"), while Arm was unaltered (Fig. 4.7D', D"). The altered DE-cad recovery and immobile fraction rate, unaltered transcription yet protein accumulation is likely due to the increased force generated by NMII which can stabilizes cortical F-actin, which in turn stabilizes DE-cad at the AJ (Engl et al., 2014; Goldenberg et al., 2013; Hong et al., 2013; Wu et al., 2014). Accumulation of DE-cad at the AJ can subsequently bind and accumulate Arm.

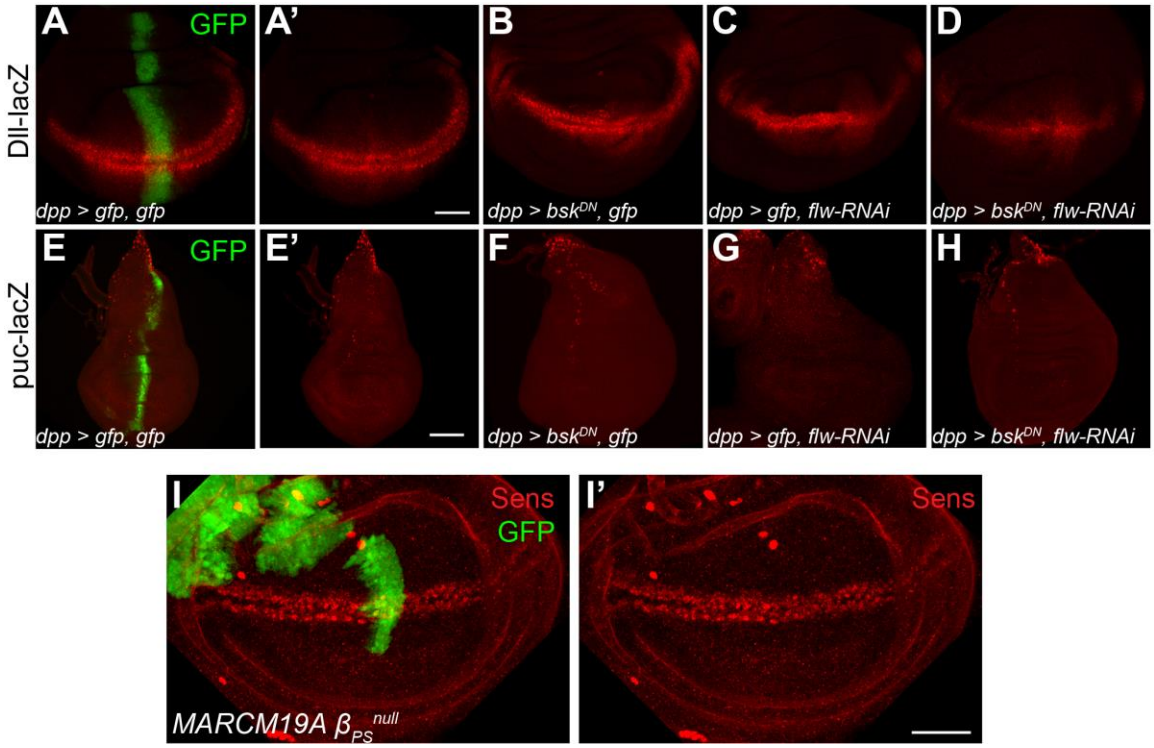

Figure 4.6 NMII does not regulate Wnt through JNK or integrin signaling in wing imaginal discs.

(A-D) *dpp-Gal4* expressing (A,A') GFP, (B) Bsk^{DN} and GFP, (C) GFP and *flw-RNAi*, (D) Bsk^{DN} and *flw-RNAi*, stained for expression of *Dll-lacZ*. (E-H) *dpp-Gal4* expressing (E,E') GFP, (F) Bsk^{DN} and GFP, (G) GFP and *flw-RNAi*, (H) Bsk^{DN} and *flw-RNAi*, stained for expression of *Dll-lacZ*. (I,I') GFP-marked β_{PS}^{null} MARCM clones, stained for Sens. Scale bars: (A-D,I,I') 50 μm, (E-H) 100 μm.

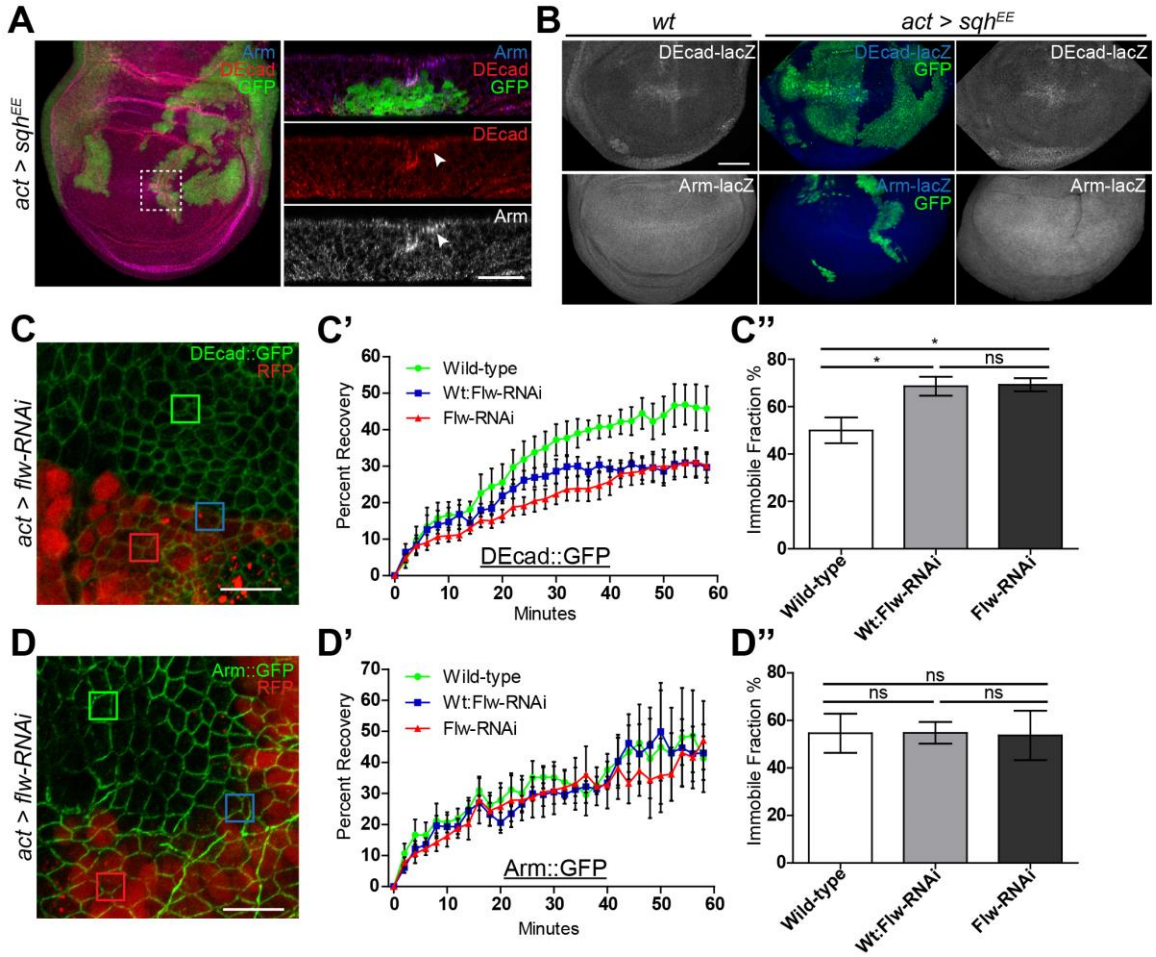

Figure 4.7 NMII activation increases retention of adherens junction proteins.

(A-B) GFP-marked actin flip-out clones driving *sqh*^{EE} stained for (A) DE-cad and Arm (arrowheads identify apical increases),(B) expression of *DE-cad* or *arm*. (C-D") FRAP analysis of DE-cad::GFP and Arm::GFP in wing imaginal discs with RFP-marked *flw-RNAi* expressing flip-out clones. (C,D) DE-cad::GFP and Arm::GFP wing imaginal disc with squares indicating bleached regions of the wing disc. Green squares represents wild type cell interfaces, Blue for *wt:flw-RNAi* cell interface, and Red for *flw-RNAi* cell interfaces. (C') AJ DE-cad::GFP (n = 6) recovery curves of FRAP analyses show cells adjacent to or expressing *flw-RNAi* have significantly slower recovery rates than wild type ($P = 0.0029$), (C") and greater immobile protein fractions, $^*P < 0.05$. (D') *flw-RNAi* had no effect on AJ Arm::GFP (n = 6) recovery curves from FRAP analyses ($P = 0.4794$), (D") or immobile protein fractions. Data presented as mean and mean curve ± SEM. Scale bars: (A) 20 µm, (B) 50 µm, (C,D) 10 µm.

4.4.6. NMII mediates DE-cad accumulation and sequesters Arm to the AJs, inhibiting Wg signaling

To further study the role of DE-cad in regulation of Arm, we expressed full length and a truncated version of DE-cad lacking the Arm binding domain (DEcadΔβ). Ectopic wild-type DE-cad was uniformly enriched along the cell periphery at the AJs, while DEcadΔβ expression was also seen in puncta (Fig. 4.8A), since DE-cad unable to bind Arm is endocytosed and accumulates in vesicles (Langevin et al., 2005). Expressing either transgene had no effect on levels or distribution of F-actin (Fig. 4.8B). However, ectopic DE-cad dramatically increased Arm at the AJ (Fig. 4.8B), and could strongly suppress *Dll* expression (Fig. 4.8C). DE-cad's ability to suppress Wg signaling has been previously reported (Sanson et al., 1996), and is likely due to the higher binding affinity of Arm to DE-cad over TCF binding for transcriptional activation (Torres et al., 2007). Any cells exhibiting increased levels of DE-cad will titrate freely available Arm to the AJ, stabilizing DE-cad and increasing cellular adhesion. This is supported by the fact that expression of DEcadΔβ resulted in decreased levels of AJ Arm and did not suppress *Dll* expression (Fig. 4.8B, C).

We next examined the effects of reduction of overall DE-cad on Wg. RNAi against *shotgun* (*shg*), which encodes DE-cad, could induce cell death, but had no apparent effect on *Dll* (Fig. 4.8D). Activated NMII (Sqh^{EE}), caused a strong suppression of *Dll*, which was rescued by co-expression of *shg-RNAi* (Fig. 4.8D), and *shg-RNAi* with Sqh^{EE} did not induce widespread cell death. Finally, *hh>mypt-75D-RNAi* adult flies had a much lower than expected viability and eclosion rate, which was rescued by heterozygosity for the shg^{R69} null allele (Godt and Tepass, 1998)(Fig. 4.8E). These results suggest that elevated NMII can inhibit Wg activity through the accumulation of DE-cad, resulting in the titration of Arm to the AJ.

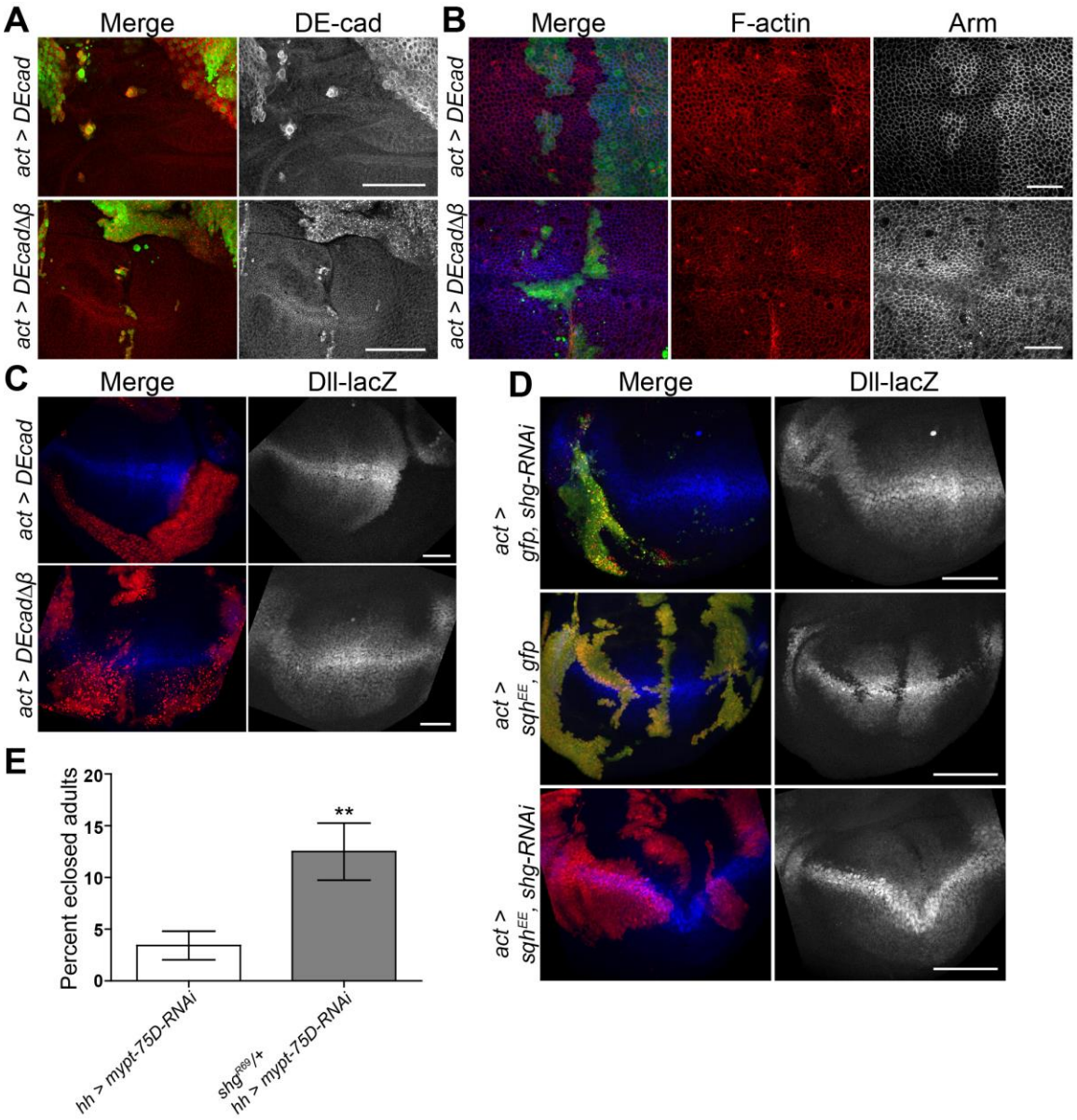

Figure 4.8 NMII activation inhibits Wg signaling through DE-cad.

(A,B) GFP-marked actin flip-out clones expressing *DE-cad* or *DE-cadΔβ,* stained for (A) DE-cad, or (B) F-actin and Arm. (C) RFP-marked actin flip-out clones expressing *DE-cad* or *DE-cadΔβ,* stained for *Dll* expression. (D) *Dll-lacZ* expression in RFP-marked clones of the indicated genotypes. (E) Eclosion percentage of *hh>mypt-75D-RNAi* and *hh>mypt-75D-RNAi* heterozygous for *shg Drosophila*. Data presented as mean ± SEM; ***P* = 0.0022; n ≥145. Scale bars: (A,C,D) 50 μm, (B) 20 μm.

4.4.7. NMII's effect on the Wg pathway is mediated through F-actin stability

Engl et al. (2014) demonstrated that increased NMII activity results in decreased F-actin turnover, which can guide E-cad clustering and retention (Hong et al., 2013). To confirm if F-actin levels in a developing tissue could also affect Wg activation we used the formin protein Diaphanous (Dia) which promotes the polymerization of filamentous actin (Afshar et al., 2000). Mitotic clones expressing a constitutively active Dia protein lacking its autoinhibitory domain (DiaΔDAD) had dramatic increases in levels of F-actin (Fig. 4.9A-A"), and phenocopied the effects of increased NMII activation. Clones had decreased levels of *Dll* (Fig. 4.9A, arrowhead), increased Arm and DE-cad along the apical surface of the cells (Fig. 4.9A' arrow, A", open arrowhead), and cells in larger clones began to constrict (Fig. 4,9A", open arrowhead). To confirm if the effect of NMII on Wg is directly mediated through F-actin stability, we tested if reduced F-actin could alleviate NMII's suppression of Wg signaling, using *dia-RNAi*. Cell with low levels of Dia had lower levels of F-actin, as well as increased apical cell surfaces, marked by Arm (Fig. 4.9B). Reduction of F-actin via *dia-RNAi* had no major effect on endogenous Wg signaling, as seen by wild type *Dll* expression (Fig. 4.9C). However, in an activated myosin background (Sqh^{EE}), which strongly inhibits *Dll*, the co-expression of *dia-RNAi* could restore wild type *Dll* expression (Fig. 4.9C). These results confirm that NMII can influence Wg pathway activity through its function to bind and stabilize actin leading to accumulation of filamentous actin.

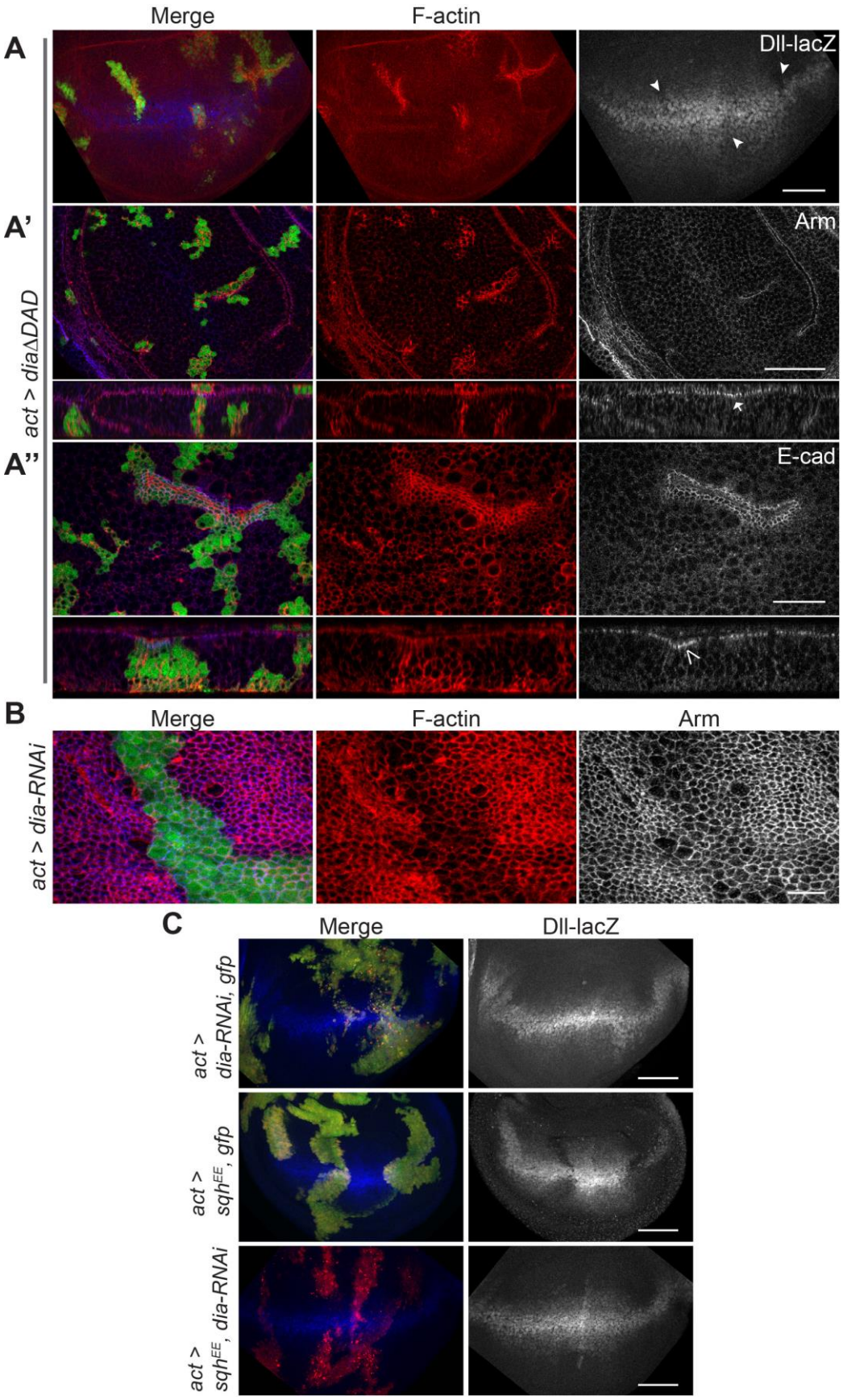
Merge
F-actin
A
Dll-lacZ
A'
act > diaΔDAD
Arm
A''
E-cad
B
act > dia-RNAi
Merge
F-actin
Arm
C
Merge
Dll-lacZ
act > dia-RNAi, gfp
act > sqh^EE, gfp
act > sqh^EE, dia-RNAi

Figure 4.9 NMII inhibits Wg signaling by increased F-actin.

(A-A") GFP-marked actin flip-out clones expressing *dia*Δ*DAD* stained to detect (A) F-actin and *Dll-lacZ* (arrowheads indicate loss), (A') F-actin and Arm and (A'') F-actin and DE-cad. *dia*Δ*DAD* induces increased apical AJ Arm (A' arrow) and DE-cad (A" open arrowhead), and cell contractions (A" open arrow head). (B) GFP-marked actin flip-out clones expressing *dia-RNAi* stained for F-actin and Arm. (C) GFP-marked actin flip-out clones of indicated genotypes stained to detect *Dll-lacZ*. Scale bars: (A,A',C) 50 µm, (A") 20 µm, (B) 10 µm.

4.4.8. NMII regulates Wnt in mammalian cells by sequestering β-cat to the AJs

We next examined the effects of increased NMII activation on Wnt signaling in human cell lines. Wnt pathway activity was induced in MCF7 and RKO cells by transfection of Wnt3A, and the response was measured using a TCF-responsive TOPFLASH transcriptional reporter (Korinek et al., 1997). MCF7 cells are epithelial, polarized and have well defined adherens junctions (de Beco et al., 2009), while RKO cells are mutant for E-cad and completely lack adherens junctions (Fig. 4.10C). The only β-cat present in RKO cells is solely for the regulation of Wnt activation (Gagliardi et al., 2008). Transfection of Wnt3A resulted in a significant increase in reporter activity in both cell lines, although RKO cells had a more robust response (Fig. 4.10A, B). To increase NMII activation within these cell lines we transfected in siRNA against individual myosin phosphatase components. siPP1β could reduce total PP1β by ~70% (Fig. 4.10C), while siMYPT3 reduced MYPT3 (the ortholog of Mypt-75D) by ~60% (Fig. 4.10C). Knockdown of these components reduced the amount of the other myosin phosphatase protein, suggesting complex formation is essential for stability (Fig. 4.10C). In MCF7 cells, knockdown of PP1β or MYPT3 could reduce Wnt activation significantly, and cotransfection of siPP1β and siMYPT3 reduced transcriptional activity back to baseline levels similar to cells with no Wnt3A (Fig. 4.10A). In RKO cells there was no significant change, in fact there was a slight increase in Wnt transcriptional activation (Fig. 4.10B). These results indicate that increased NMII activation from reduction of myosin phosphatase components can inhibit Wnt activity in mammalian cells as well, but only in cells that contain adherens junctions.

Although reduction of PP1β or MYPT3 was able to inhibit Wnt signaling in MCF7 cells there was no dramatic change in overall β-cat levels (Fig. 4.10C), suggesting that there may be a localization defect as seen in *Drosophila*. Transfection of Wnt3A induced a significant increase of cytoplasmic and chromatin-bound (transcriptionally active) β-cat, while membrane associated (AJ) β-cat slightly decreased (Fig. 4.10D, E). The decrease in membranous β-cat is likely due to the fact that Wnt can induce mild EMT effects in MCF7 and other epithelial cancer lines (Green et al., 2013). Similar effects were seen with E-cad (Fig. 4.11). Whole cell extracts only showed a minor increase in total β-cat

(Fig. 4.10D, E). A striking inverse in distribution was seen after increasing NMII activation via siPP1β and siMYPT3 transfection. Cytoplasmic levels of β-cat decreased, and there was a significant reduction in chromatin-bound levels back to baseline, matching results seen in TOPFLASH assays (Fig. 4.10A, D, E). Cells with activated NMII had a significant increase in membrane associated β-cat levels, as well as increased total β-cat (Fig. 4.10D, E). Considering the increase in total β-cat, yet lack of transcriptional activation, and redistribution of the protein within the cell, we propose that in mammalian cells that have elevated NMII activity, titrate freely available β-cat to the adherens junctions to enforce cell-cell adhesion at the cost of transcriptional activation of Wnt targets.

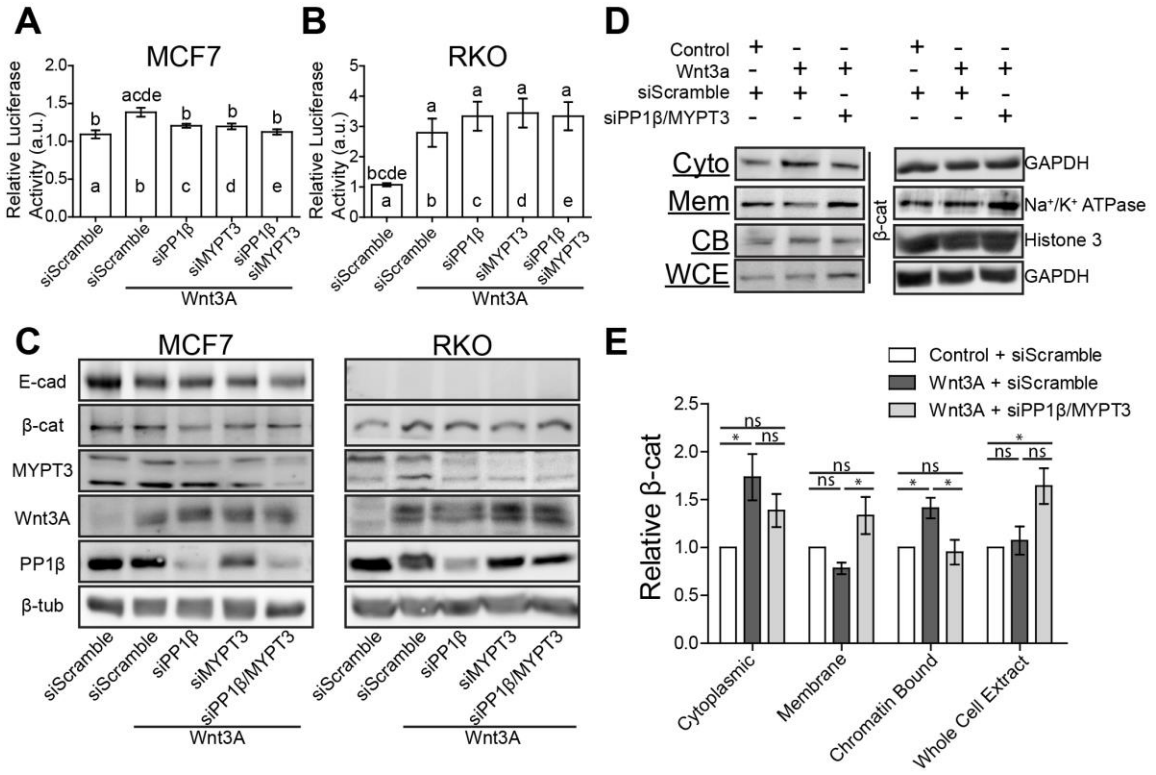

Figure 4.10 NMII activation recruits β-cat to cell membranes inhibiting Wnt signaling.

(A,B) Wnt-responsive luciferase TOPFLASH assay measuring TCF/LEF reporter activity in (A) MCF7 and (B) RKO cells following Wnt3A transfection and siPP1β and siMYPT3 transfection. Data are presented as mean ± SEM with letters above representing significant difference from corresponding column, (*P*<0.01). (C) Western blot analysis of total cellular levels of E-cad, β-cat, MYPT3, Wnt3A and PP1β. β-tub was used as a loading control. (D) Western blot analysis of β-cat in cytoplasmic (Cyto), membranous (Mem), chromatin-bound (CB), and whole cell extract (WCE) fractions in MCF7 cells. GAPDH, Na^+/K^+ ATPase, and Histone 3 were used as loading controls for corresponding fractions. Complete fraction, see Fig. 4.11. (E) Quantification of relative levels of β-cat from each fraction taken from (D), normalized to Control + siScramble conditions. Data shown as mean ± SEM (n = 4 biological replicates), ns = not significant, **P*<0.05.

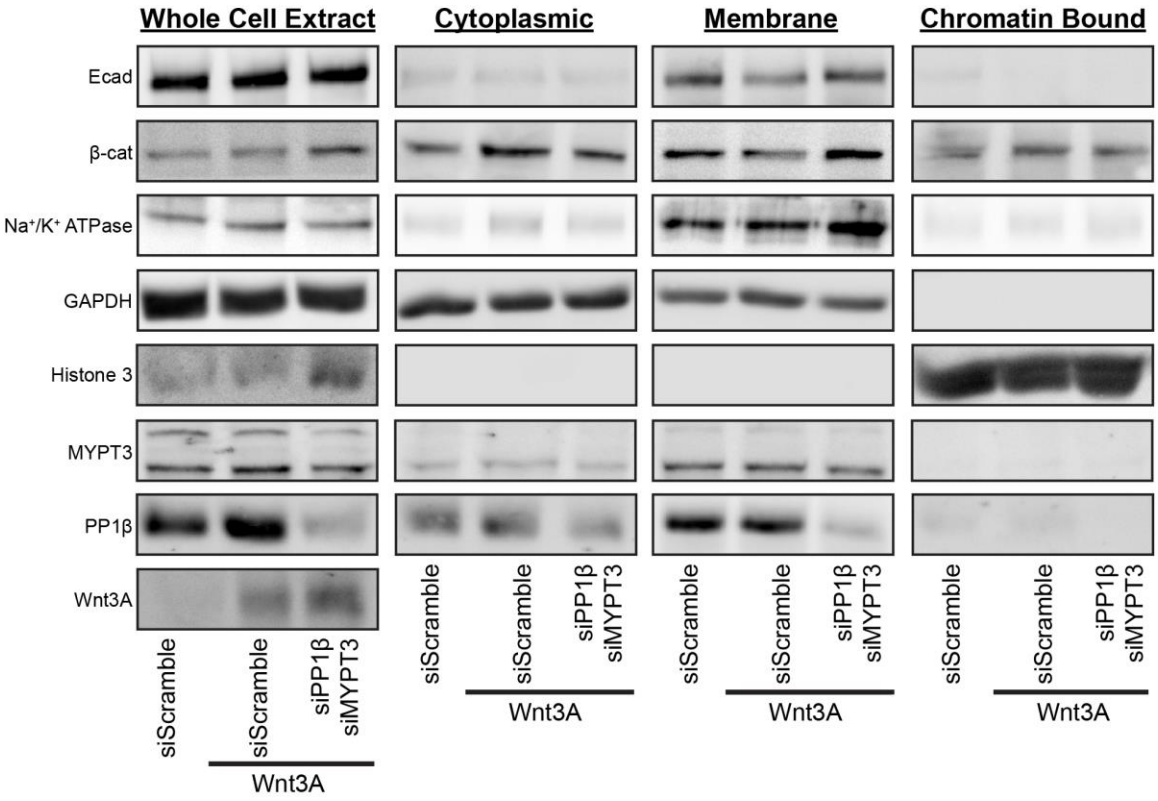

Figure 4.11 Complete fractionation of MCF7.

MCF7 cells transfected with or without Wnt3A, siPP1β and siMYPT3. Whole cell extracts and cell fractions were analyzed by western blots, probed for E-cad, β-cat, MYPT3, PP1β, and Wnt3A. GAPDH (whole cell extracts, and cytoplasmic), Na^+/K^+ ATPase (Membrane), and Histone 3 (Chromatin Bound) were used as loading controls for individual fractions. Blots shown represent one of 4 biological replicates.

4.4.9. NMII activation modulates Wnt signaling during development and homeostasis to maintain cell-cell adhesion

We next tested this model in *Drosophila*. We generated mitotic recombinant clones that can form and maintain AJs without the need for Arm using functionally validated fusion proteins in which DE-cad is fused to α-cat (DEcad::αCat), as well as a truncated fusion of the proteins lacking their Arm binding domains (DEcadΔβ::αCatΔVH1) (Desai et al., 2013). Actin flip-out clones expressing either transgene led to increased levels of DE-cad and did not affect levels of F-actin (Fig. 4.12A-D). DEcad::αCat could still bind Arm, forming puncta within the cells, and resulting in a suppression of *Dll* expression (Fig. 4.12A, C). DEcadΔβ::αCatΔVH1 did not affect Arm distribution or *Dll* expression (Fig. 4.12B, D), so we utilized this transgene for further experiments.

Mitotic clones of the shg^{R69} null allele are non-viable and were quickly extruded from wing disc (data not shown). When DEcadΔβ::αCatΔVH1 was expressed in these cells, clones could divide and grow (Fig. 4.13A), confirming that DEcadΔβ::αCatΔVH1 could form AJs without binding Arm. Clonal tissue had normal Dll protein levels and F-actin (Fig. 4.13A). The expression of *mypt-75D-RNAi* in *shg* clones had no effect on Dll, but did induce minor accumulations in F-actin (Fig. 4.13A' arrowheads). These results were mimicked when DEcadΔβ::αCatΔVH1 was co-expressed with Sqh^{EE}, namely clonal tissue still constricted and had elevated F-actin, but the reduced *Dll* expression was significantly rescued (Fig. 4.12E, Fig. 4.8D). These results indicate that NMII activation can only suppress Wg signaling in this epithelium when DE-cad binds to Arm.

We wanted to determine what physiological role this regulation may have during development and homeostasis of an epithelial tissue. In the wing disc, mechanical forces are the highest along the D/V and A/P compartment boundaries, culminating in the center of the wing pouch (Aliee et al., 2012; Landsberg et al., 2009; LeGoff et al., 2013). To determine if the variable contractile forces across the wing disc normally play a role in regulating the patterning of Wg target gene expression, *Dll-lacZ* was examined in clones co-expressing activated Arm^{S10} with either GFP or *flw-RNAi* to induce increased actomyosin contractility. Clones were scored as either increased, no change, or decreased *Dll* expression in the medial (high constriction), or peripheral (lower constriction) zones of the wing pouch (marked by RFP, Fig. 4.13B, B'). In the

presumptive notum region, Arm^{S10}, GFP clones generally were large and could induce ectopic *Dll* expression frequently resulting in axis duplications, while Arm^{S10}, *flw-RNAi* clones did not (Fig. 4.13B, B'). In the medial section of the wing disc, clones of both genotypes induced ectopic Dll at similar rates (Fig. 4.13C). However, in the peripheral zone Arm^{S10} was significantly less able to induce ectopic Dll in the presence of *flw-RNAi* (p =0.0139). Furthermore, the co-expression of *flw-RNAi* could suppress endogenous *Dll* (Fig. 4.13C). These results indicate that cells in the periphery of the wing disc, which are normally under less contractile forces are much more sensitive to increases in NMII activity. Together these results suggest that the dynamic distribution of actomyosin contractility across the wing imaginal disc can directly affect, and is required for, the patterning and refinement of Wg signaling during development.

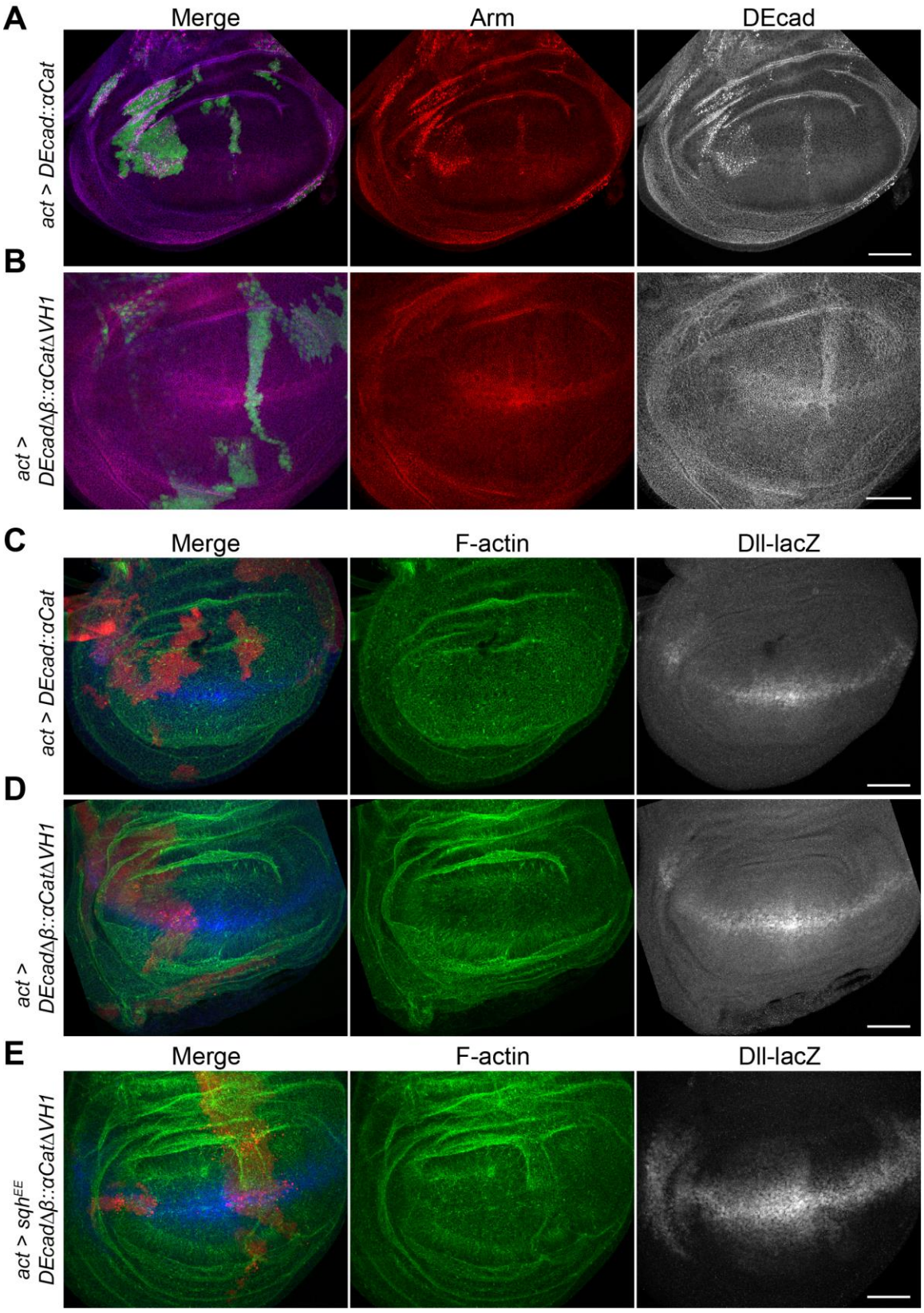

Figure 4.12 **Full length and truncated DE-cad::α-cat fusion proteins effects on the wing imaginal disc.**

(A,B) GFP-marked actin flip-out clones expressing (A) *DE-cad::α-cat* and (B) *DE-cadΔβ::α-catΔVH1*, stained for Arm and DE-cad. (C-E) RFP-marked actin flip-out clones expressing (C) *DE-cad::α-cat* and (D) *DE-cadΔβ::α-catΔVH1*, and (E) sqh^{EE} with *DE-cadΔβ::α-catΔVH1,* stained for F-actin and *Dll-lacZ* expression. Scale bars: 50 μm.

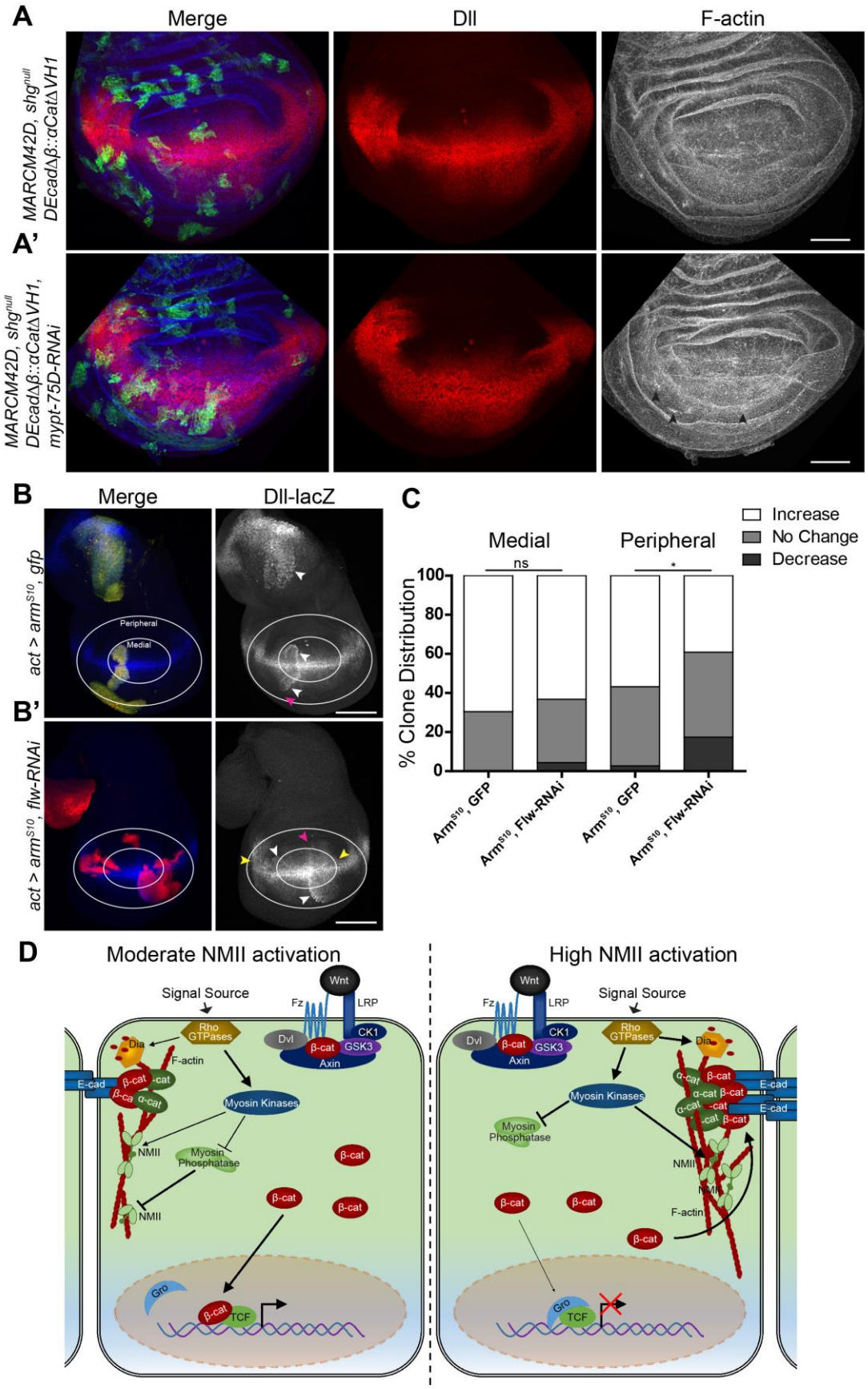
A
Merge
Dll
F-actin
MARCM42D, shg^null DEcadΔβ::αCatΔVH1
A'
MARCM42D, shg^null DEcadΔβ::αCatΔVH1, mypt-75D-RNAi
B
Merge
Dll-lacZ
act > arm^S10, gfp
Peripheral
Medial
B'
act > arm^S10, flw-RNAi
C
Increase
No Change
Decrease
Medial
Peripheral
ns
*
% Clone Distribution
100
80
60
40
20
0
Arm^S10, GFP
Arm^S10, Flw-RNAi
Arm^S10, GFP
Arm^S10, Flw-RNAi
D
Moderate NMII activation
High NMII activation
Signal Source
Wnt
Fz
LRP
Dvl
CK1
β-cat
GSK3
Axin
Rho GTPases
Dia
F-actin
E-cad
α-cat
Myosin Kinases
Myosin Phosphatase
NMII
Gro
TCF

Figure 4.13 NMII activation inhibits Wnt signaling in a dynamic fashion across developing tissue by Arm titration to AJs.

(A,A') GFP-marked *shg*^{null} MARCM clones expressing (A) *DE-cadΔβ::α-catΔVH1* and (A') *DE-cadΔβ::α-catΔVH1* with *mypt-75D-RNAi*, stained for Dll and F-actin (arrowheads show F-actin accumulation). (B,B') Highlighted peripheral and medial zones of the wing pouches in third-instar larva with RFP-marked actin flip-out clones driving *arm*^{S10} with (B) *GFP* or (B') *flw-RNAi*, stained for *Dll* expression. White arrowheads = increased *Dll*, magenta = no change, yellow = decreased *Dll*. (C) Quantification of clonal distribution in GFP control (n = 23 medial, 37 peripheral) and *flw-RNAi* (n = 68 medial, and 115 proximal) clones (B,B'), in medial and peripheral zones. ns = not significant, **P*<0.05. (D) Model for regulation of Wnt signaling by activation of NMII resulting in AJ accumulation and stabilization in response to contractile forces; see text for details. Scale bars: (A,A') 50 μm, (B,B') 100 μm.

4.5. Discussion

The link between mechanical forces and canonical Wnt signaling has been extensively studied in contexts such as mesoderm differentiation during cardiomyogenesis (Happe and Engler, 2016) and in tissue stiffness of the ECM in stem cell behavior or carcinogenesis (Benham-Pyle et al., 2015; Przybyla et al., 2016). Less research has focused on how mechanical forces may directly influence Wnt activation in normal developing epithelia. Our work shows that increased NMII activation in epithelial cells induces contraction and accumulation of cortical F-actin, and as a result E-cad accumulates and titrates freely available Arm/β-cat to the AJs in order to maintain cell-cell adhesion. The resulting decreased levels of cytoplasmic Arm/β-cat causes insufficient nuclear translocation and reduced Wnt target gene transcription (Fig. 4.13D).

We show that NMII activation can inhibit the nuclear accumulation of Arm causing a suppression of overall transcriptional initiation, even in genotypes lacking Arm degradation machinery or expressing Arm resistant to degradation. These results were complementary to those of Greer et al. (2013), who identified that RhoGEF and GTPase activity (upstream activators of NMII) could suppress Arm localization or activation in developing *Drosophila*. We further excluded the possibility that NMII suppresses Wnt through several known interaction mechanisms, like JNK and ECM/Integrin signaling (Przybyla et al., 2016; Wu et al., 2008).

Cells with elevated NMII activity and nearby adjacent cells that were under increased contraction exhibited elevated Arm and DE-cad at AJ, while transcription rates of the genes encoding these proteins appeared normal. DE-cad (*shg*) was previously identified as a Wnt target gene in wing discs (Widmann and Dahmann, 2009). Its maintained transcription in *flw-RNAi* cells may be due to compensation by another transcriptional mechanism. Furthermore, the recovery rate of DE-cad to the AJ was reduced, and contained a higher immobile fraction of DE-cad, indicating accumulation and retention. Although we did not detect any significant changes in Arm recovery rates or immobile fraction at the AJs, this may be due to positional effect of our measurements across the wing disc. Total Arm, and its distribution within a cell vary dramatically across the wing disc. In order to maintain healthy tissue to generate accurate measurements, our *flw-RNAi* clonal induction at random positions may explain the high variance. As FRAP experiments encompassed the entire AJ and membrane, the recovery rates are

likely an indirect measure of vesicle trafficking of Arm and DE-cad (Goldenberg et al., 2013). This is bolstered by the fact that decreased actomyosin levels have been shown to increase AJ endocytosis in developing *Drosophila* (Goldenberg et al., 2013). The accumulation of E-cad is likely an active mechano-sensitive mechanism to bolster cell-cell adhesion, potentially through plasma membrane clustering and vesicle-based redistribution (Engl et al., 2014; Hong et al., 2013; Lecuit and Yap, 2015).

Elevated E-cad has been previously shown to suppress Wg signaling (Sanson et al., 1996), but no defined mechanism was identified. We propose this effect is likely due to the higher binding affinity of Arm/β-cat to E-cad over TCF for transcriptional activation (Torres et al., 2007). We validated this model by expressing wild type DE-cad or mutant DE-cad, lacking the Arm binding sequences. Our results demonstrated that ectopic DE-cad caused high levels of Arm to be enriched along the AJ, and strongly suppressed Wg target gene expression, while mutant DE-cad led to reduced AJ Arm and did not affect Wg targets. Importantly neither of these transgenes had any effect on F-actin, showing that E-cad acts downstream of F-actin in this NMII activation pathway to suppress Wnt signaling. In addition the reduction of DE-cad in wing disc tissue was able to rescue Wg activity defects and viability of flies expressing activated NMII.

In our *in vivo* work, we were able to confirm the model by Engl et al. (2014) and Hong et al. (2013) that NMII activation recruits and stabilizes DE-cad, Arm, and other AJ core proteins in developing tissue by stabilization and accumulation of F-actin, and in our context resulting in a suppression of Wg activation. The expression of a constitutively active Formin protein phenocopied the ability of activated NMII to inhibit Wg target gene expression, and the reduction of F-actin was able rescue the effect of increased NMII activity on Wg target gene expression.

Building on our *Drosophila* work, we were able to confirm that NMII has similar effects on Wnt in human cells that contain AJs. Stimulation of NMII was able to suppress Wnt transcriptional activation in polarized MCF7 cells containing AJ, but had no effect in RKO cells lacking E-cad. Importantly, increased NMII activity following knockdown of myosin phosphatase induced a significant redistribution of β-cat out of the chromatin-bound fraction to the membrane, and increased overall β-cat protein levels within the cells. Although these cells had significantly higher levels of β-cat, their inability to initiate Wnt target gene transcription indicates that β-cat is being sequestered to the AJ. We

validated this model by generating clonal tissue in which we replaced endogenous E-cad with a fusion protein that does not require Arm/β-cat for the formation of complete AJ. In these cells, when NMII activity was stimulated there was no suppression of Wnt target gene transcription, confirming NMII inhibits Wnt by titrating Arm/β-cat to the adherens junctions.

This may be a physiological regulatory mechanism in developing tissue for proliferation, patterning, and morphogenesis, and later in the homeostasis of epithelia. As tissues proliferate, change shape, and respond to physical cues, the cells respond to all these factors and induce variable levels of NMII activation. In order to maintain overall tissue integrity as cells change their shape, cell-cell adhesion must be increased. This results in the sequestration of Arm/β-cat to increase AJ adhesion and inhibit canonical Wnt's ability to promote patterning. In essence the preservation of tissue integrity overrides Wnt-inducible gene expression in epithelia. Recently there have been comparable instances of this in other developmental signaling pathways, through distinct mechanisms. Increased NMII activation and cytoskeleton tension have been widely identified to inhibit Hippo signaling, while stimulating JNK activation in epithelia (Khoo et al., 2013; Kirchner et al., 2007; Rauskolb et al., 2014). With this study, we demonstrate that canonical Wnt signaling is another key developmental pathway that is regulated by NMII.

We found that the ability of NMII to regulate the extent of Wnt activation in developing tissue has a direct physiological effect on the refinement of tissue patterning within the developing wing. In the medial section of the wing pouch, which has the highest endogenous level of NMII activation (Aliee et al., 2012; Landsberg et al., 2009; LeGoff et al., 2013), Wg signaling was generally insensitive to increased NMII. In contrast, peripheral cells with lower overall NMII activity, when exposed to activated NMII showed decreased Wnt target gene expression. These results indicate that cells at the periphery of the disc are much more sensitive to contractile forces, and that the dynamic activity of NMII across the developing tissue plays an important role in the refinement of Wnt target gene expression. It will be interesting to determine if these dynamic contractile forces exerted upon developing tissue are also critical for the maintenance of stem cell niches. For instance in intestinal crypts, Wnt activity is refined to the very basal cells of the crypt for the maintenance of stem cells, where cells are apically constricted to form the concave base of the crypt (Buske et al., 2012).

Monitoring Wnt activity in crypt cells as well as proliferation and differentiation rates when exposed to increased or decreased levels of NMII activity, or even removing the tissue to grow on a flat surface, may provide insights into the relevance of why and how tissue structures arise due to the forces that are exerted on cells across a tissue in order to regulate homeostasis. The modelling of stem cell niche formation in crypts has suggested that the loss of curvature regulation can result in tissue consisting of Paneth cells of the crypt and undifferentiated cells, which is seen in some cases of intestinal adenoma and carcinoma (Buske et al., 2012). Our results here have provided new and supportive evidence that the interactions between biochemical signaling, Wnt in this case, and mechanical forces are critical for the normal development and maintenance of healthy epithelial tissue in an organism.

Chapter 5. Conclusion

Since the discovery of the *Wnt-1* gene 35 years ago (Nusse and Varmus, 1982), our comprehension of the Wnt signaling pathway and its involvement in metazoan biology has exploded. From this single gene, genomic, genetic, and functional biology studies have found 13 Wnt subfamilies, a subset of which are found in all metazoans ranging from simple sponges, to fruit flies, worms, fish and humans (Janssen et al., 2010). As Wnt signaling has been implicated in a myriad of different biological functions, when it becomes dysregulated it can lead to a wide range of developmental defects and disorders. The combined roles of wide spread influence on cell functions and implication in human diseases has cemented the study of Wnt signaling as a continual exciting area of research in cell biology and medicine.

The precise regulation of Wnt signaling has been identified to be predominantly controlled by the dynamic phosphorylation of core pathway proteins, at one or more sites (Verheyen and Gottardi, 2010). This regulation involves the use of many distinct identified kinases and phosphatases, but due to the complexity of phospho-regulation of Wnt, it is thought that there are many more unidentified phospho-regulators influencing pathway activity. A genome-wide *in vivo* RNAi screen of Drosophila kinases and phosphatases previously performed in our lab, identified 54 proteins capable of modulating Wnt activity, twenty two of which had not been previously implicated in Wnt signalling (Swarup et al., 2015). From this group of modifiers, I performed subsequent analysis on three of the potential novel regulators of Wnt signaling, and determined how they were involved in controlling overall Wnt activity in Drosophila development and human cells. Identifying the function of these proteins in the Wnt pathway was then followed by trying to determine how they are regulated by upstream signaling cues and cellular mechanisms. My work attempts to build towards a better understanding of the integrated signaling networks that occur within a cell to guide the Wnt pathway and normal biological outcomes.

5.1. Cross activation between Ras-MAPK signaling and Wnt: serious implication in health and medicine

The interactions between Ras-MAPK and Wnt signaling have been characterized multiple times through several distinct mechanisms, and frequently synergize in tumor progression (Zeller et al., 2013). These interactions frequently occur through ERK, phosphorylating and promoting activity of different Wnt proteins. My work demonstrates that the upstream activator of ERK, MEK/Dsor1, also plays a distinct and crucial role in the promotion of Wnt signaling in cells. Importantly, my experiments in developing Drosophila show Dsor1 can promote Wnt signaling independently of any activation of ERK. This is surprising as the core MAPK cascade is thought to a very linear and non-divergent pathway, where MAPK kinases (MAPKK, i.e. MEK/Dsor1) solely target and phosphorylate MAPKs. The apparent requirement that Dsor1 still needs upstream activation by Ras, yet does not subsequently lead to the activation of ERK, suggests that MAPKKs may be more promiscuous than previously thought.

The Ras-MAPK cascade is a commonly targeted pathway for drug based inhibitors for the treatment of various cancers (Sebolt-Leopold, 2008). There are currently several MEK specific small molecule inhibitors that are thought to be excellent drugs for MAPK inhibition, because of the specificity of MEK to ERK (Sebolt-Leopold, 2008). This may be true, but the direct inhibition of Wnt signaling may now also be taken into consideration when choosing treatment. Side effects of these MEK inhibitors may be contributing to decreased Wnt activity in some cases. Additionally in many tumors both Ras-MAPK and Wnt signaling may become over activated (Zeller et al., 2013). MEK inhibitors may provide an effective way of simultaneously inhibiting both pathways and inhibiting growth.

My work also highlights a potential mechanism of action between two diseases that are often correlated, type 2 diabetes mellitus and colorectal cancer. Colorectal cancers are almost always attributed to overactive Wnt signaling (Basu et al., 2016; Najdi et al., 2011; Schatoff et al., 2017), and people with type 2 diabetes are put at a dramatically increased rate of developing colorectal cancers (Berster and Göke, 2008). It is thought that the hyperinsulinemia-like conditions that patients experience, when treated with sulphonylureas or insulin, actually can drive transformation in colon cells (Berster and Göke, 2008). The proposed signaling pathway that I identified in Drosophila

strongly supports this idea, and may shed light on the cellular mechanism driving colorectal cancer in patients with type 2 diabetes. Considering inhibition of the insulin-like receptor phenocopied the effects on the Wnt pathway the same as Dsor1 and Ras, and Dsor1 activation was independent of EGFR, suggests that in Drosophila secreted insulin like peptides likely drive Ras-Dsor1 activity to allow propagation of Wnt signaling (Fig. 2.12). If this is true, high levels of free insulin and IGF-1 may be driving overactive Wnt signaling through MEK in colon cells, driving over proliferation and eventual transformation. This novel interaction between Ras and Wnt signaling may have serious implications in understanding disease progression and therapeutic application.

5.2. Protein phosphatase 4 and Notch signaling

The identification of the role of PP4 in promoting Notch and subsequent initiation of *wg* transcription in the developing wing imaginal disc, is just the first hurdle in understanding how the PP4 phosphatase complex promotes this signaling cascade, and possibly more. Additional work is needed to answer several critical remaining questions. The first, is to determine the exact mechanism PP4 plays in promoting Notch signaling. Our results suggest that PP4 mediates Notch signaling in the nucleus of the receiving cell. To gain more insight into how this may be occurring, due to the complexity of events that guide transcriptional initiation, such as PTM of chromatin remodelling proteins, transcription factors, and other cofactors within a cell, a series of experiments should attempt to identify PP4 targets within the nucleus. An example would be to perform a BioID screen (Roux et al., 2013), fusing a biotin ligase to the PP4 regulatory subunits, Flfl and PPP4R2r, to attempt to identify interaction with any putative targets. Although, PP4 has been widely identified to interact with nuclear proteins in cell cycle progression (Helps et al., 1998; Huang et al., 2016), identifying all biotinylated proteins from this screen may identify some Notch specific regulators. Molecular and genetic interaction experiments may then be performed to identify the target/s of PP4 in regulating Notch.

The second major question remaining is if the role PP4 has in regulating Notch in the wing imaginal disc is a general component in promoting Notch in Drosophila, and is this function also conserved in other species? These questions can be addressed in a very straightforward manner. Looking at Notch signaling in other developing tissues, we can determine what affects the loss of PP4 components may have on target gene expression. This same process can be applied to human cell lines, utilizing RNAi to

knockdown the human homologs of PP4, and looking at transcriptional activity with Notch transcriptional reporter assays.

This work highlights and adds to the complexity of signaling networks that control developmental outcomes, and shed light on how regulation of other signaling pathways can have dramatic downstream effects affecting Wnt activity.

5.3. Mechanotransduction and refinement of Wnt signaling

The field of mechanotransduction has dramatically expanded in the past few years, as new technologies are now allowing researchers to measure, visualize and record the endogenous minuscule forces individual cells are continuously being exposed to and exert on one another. Considerable research has focused on how the ECM develops a cell's microenvironment and guides differentiation cues and the resulting propagation of intracellular signals to affect transcription and the cells cytoskeleton (Sheehy and Parker, 2011). Much of our current knowledge on mechanotransduction has been gleaned from mesoderm differentiation, particularly in cardiomyogenesis and osteo vs chondrogenesis (Happe and Engler, 2016; Sun et al., 2012). Wnt signaling is also critical in these processes, and subsequent research has revealed the role of ECM/integrin signaling in regulating Wnt activity in these processes, through distinct and sometimes conflicting mechanisms (Crampton et al., 2009; Oloumi et al., 2006; Przybyla et al., 2016). Much less research has focused on the mechanical stimuli one cell may induce on another through adherens junctions.

NMII induction of cortical tension in a single cell is able to transduce force on a supra-cellular tissue level through AJs. This cell-cell adhesion complex's ability to transduce and respond to mechanical cues across a tissue and simultaneously affect individual cytoskeletal responses and signal transduction is just starting to come to light (Lecuit and Yap, 2015). Two signaling pathways, Hippo and JNK, have been the first well characterized developmental signaling cascades to be affected by cell density, pulling forces, and actomyosin activity mediated through AJs (Codelia et al., 2014; Gumbiner and Kim, 2014; Khoo et al., 2013). The integration of Wnt signaling with both of these pathways has also recently been identified in strain induced proliferation and cell survival, but a clear mechanism for this has not been fully elucidated (Benham-Pyle et al., 2015; Greer et al., 2013; Wu et al., 2008).

The interplay between cell-cell adhesion and Wnt signaling has been debated for decades. Since the finding that β-cat plays a critical function in both processes, it would suggest that the two are interwoven, yet there has been a striking absence of evidence for this *in vivo* through any clear mechanism. Early work suggested that cadherins were capable of supressing Wnt through their higher binding affinity for β-cat, than that of TCF/LEF, titrating β-cat out of nucleus (Fagotto et al., 1996, 1998; Sanson et al., 1996). However, later work put forth a different model where increased cell-cell adhesion supressed Wnt signaling by recruiting and promoting destruction complex activity (Maher et al., 2009), as well as by affecting LRP5/6 phosphorylation and endocytosis of the signalosome (Bilic et al., 2007; Blitzer and Nusse, 2006; Haÿ et al., 2009). Since this time, a defined mechanism of actomyosin induced E-cadherin clustering and retention to promote cellular adhesion in cells has been identified (Engl et al., 2014; Hong et al., 2013). Building on this newly identified mechanism, my work lends credence to the early models of binding affinity and the sequestration of β-cat to the AJs to inhibit Wnt, and demonstrates this effect does occur, not only in tissue culture, but in developing organisms as well. In addition, even in the absence of a destruction complex, increased contractile forces were able to supress Wnt activation. This contradicts the model of increased cadherin levels promoting recruitment and destruction complex activity. It should be noted that my titration mechanism does not detract from, but also supports the fact that increased cell-cell adhesion likely restricts Wnt by decreased endocytosis. My work provides for the first time a clear mechanism of how cell-cell force induction mediated across cells, and the resulting adhesive changes that occur at a tissue level, aid in the refinement and patterning of Wnt signaling.

The ability of mechanical forces to restrict developmental signaling pathways through this general cell adhesion mechanism is not unique. Cytoskeletal tension has been well documented to inhibit Hippo signal in a similar manner (Rauskolb et al., 2014), while Notch signaling can be inhibited in cells with increased cytoskeletal tension and cell-cell adhesion by restricting proper endocytosis of receptors and ligands (Goldenberg et al., 2013; Kandachar and Roegiers, 2012). It is likely that mechanotransduction plays a significant role in refining all signaling pathways in one aspect or another. The ability for physical forces to affect cellular adhesion, endocytosis, cytoskeletal shape, and overall general physiology of an individual cell to entire tissue, makes it almost certain that force modulates and refines all cell signal transduction pathways in development

and homeostasis. The integration of force and biochemical signaling is there; we are just now starting to look for it.

5.4. Concluding remarks

I hope this thesis has made it clear and emphasized that phospho-regulation of Wnt signaling is incredibly dynamic, and affects the pathway at every stage of progression. Kinases and phosphatases guide in the transcription of *wg*, in pathway protein localization and in activity, as well as affecting overall initiation of target gene expression. Cells utilize and integrate a range of diverse mechanisms in order to control the use of these phospho-regulators. The identification of novel pathway components and how they are regulated is crucial for our understanding of cellular biology, and hopefully aids in the understanding of the mechanism of disease progression and applications in medicine.

Chapter 6. Materials and Methods

6.1. Drosophila strains, husbandry, crosses and clone generation

6.1.1. Chapter 2: Ras-activated MEK1/Dsor1 promotes Wnt signaling

Flies and crosses were raised on standard media at 25°C unless stated otherwise. w^{1118} was used as wild type. The following fly strains were used in this study: *UAS-GFP*, *UAS-lacZ/TM6B,UAS-rl-RNAi* (BL34855), rl^{1}(BL386), rl^{sem}*/CyO* (BL108365), *UAS-p35* (BL5072, 5073), *dpp-Gal4* (BL1553), *ptc-Gal4* (BL56807), bs^{1348}*-Gal4/CyO* (also referred as *1348-gal;* BL25753), *UAS-*ras^{N17}(BL4845), *UAS-*inr^{K1409A} (InR^{DN}, BL8252/8253), *Dll-lacZ* (BL10981), [obtained from the Bloomington Drosophila Stock Center], *dpp-Gal4,UAS-gfp,dpp-Gal4,UAS-dsor1-HA, UAS-dsor1-RNAi* (VDRC 107276, 40026) [obtained from the Vienna Drosophila Resource Center, (Dietzl et al., 2007)], *yw,dsor1*^{K8C13}*,FRT19A/FM7i* (a gift from JessicaTreisman, utilized as the $dsor1^{LOF}$ allele), *UAS-dsor1/TM3,Sb*, *UAS-dsor1-HA*, *hh-Gal4/TM6B* (Port et al., 2011),*wg-Gal4(ND382)* and *en-Gal4,UAS-gfp* (gifts from Konrad Basler), *axin*^{S044230}*,FRT82/TM3, Sb* (a gift from Yashi Ahmed), MARCM82B and *hs-flp; Act>CD2>UAS-Gal4, UAS-gfp/SM6~TM6* (gifts from Bruce Edgar), *yw;tub>FLAG-axin/CyO;axin*^{S044230}*,FRT82* (a gift from Marcel Wehrli), MARCM19A (a gift from Ronwen Xi), *ci-GAL4,UAS-Dcr2* (gift from Ken Irvine), *dsh-gfp/CyO* (a gift from Jeffrey Axelrod), *wg-lacZ/CyO* (Kassis et al., 1992) , *fz3-lacZ/FM7a*, *fz3-dsRed/TM6B* (a gift from Ramanuj Dasgupta), *argos-lacZ/TM6B.*

UAS-dsor1-RNAi (VDRC 107276, 40026) strains target regions of *dsor1*s second exon. Specific targeting sequences for these two lines and additional information can be found on the Vienna Drosophila Resource Center website at; http://stockcenter.vdrc.at/control/product/~VIEW_INDEX=0/~VIEW_SIZE=100/~product_id=107276, and http://stockcenter.vdrc.at/control/product/~VIEW_INDEX=0/~VIEW_SIZE=100/~product_id=40026 respectively.

In assays examining interaction between two UAS transgenes, control crosses were performed with *UAS-GFP or UAS-lacZ*, to rule out suppressive effects due to titration of Gal4. Mosaic analysis with a repressible cell marker (MARCM) clones were generated by crossing *yw,hs-flp, tub-Gal4,UAS-GFP;; tub-Gal80, FRT82B* (MARCM82B) and *hs-flp^{122}, tub-Gal80, FRT19A; act-Gal4,UAS-GFP* (MARCM19A) to corresponding lines and heat-shocking first instar larvae at 37°C for 2 hours and incubating them at 29°C until dissection. Heat shock inducible flip-out clones were generated by crossing *hs-flp;;Act>CD2>UAS-GAL4,UAS-GFP/SM6~TM6* to corresponding lines and heat-shocking first instar larvae at 37°C for 15 min and incubating them at 29°C until dissection.

6.1.2. Chapter 3: The protein phosphatase 4 complex promotes the Notch pathway and wingless transcription

Fly strains and crosses were raised on standard medium at 25°C unless stated otherwise. *w^{1118}* was utilized as wild type. In assays examining genetic interactions between two UAS-driven transgenes, control crosses were performed with *UAS-lacZ* and *UAS-gfp* to eliminate effects caused by the titration of Gal4. The following fly strains were used: (1) *UAS-GFP*, (2) *UAS-lacZ/TM6B*, (3) *UAS-dicer*, (4) *dpp-Gal4*, (5) *Dll-lacZ*, (6) *MS1096-Gal4*, (7) *UAS-aPKC-GFP* (obtained from the Bloomington *Drosophila*Stock Center, Bloomington, USA), (8) *C5-Gal4* (Hugo Bellen, Baylor College of Medicine, Houston, USA) (9) *UAS-flflΔ3NLS+2NES* (*flfl-cyto*) (W. Gregory Somers, The University of Melbourne, Melbourne, Australia), (10) *UAS-flfl* (Zoltan Lipinski, Hungarian Academy of Sciences, Budapest, Hungary), (11) *wg-lacZ/CyO* and (12) *UAS-N[nucl]* (Spyros Artavanis-Tsakonas, Harvard Medical School, Boston, USA), (13) *UAS-flfl-RNAi* (VDRC 24143,103793), (14) *UAS-PP4-19C-RNAi* (VDRC 25317, 103317, 43250), (15) *UAS-PPP4R2R-RNAi* (VDRC 25445, 105399), (16) *UAS-aPKC-RNAi* (VDRC 2907, 105624) [obtained from the Vienna *Drosophila* Resource Center, Vienna, Austria (Dietzl et al., 2007)], (17) *hh-Gal4/TM6B*, (18) *UAS-wg-RNAi*, (19) *wg-Gal4* (ND382) and (20) *en-Gal4,UAS-GFP* (gifts from Konrad Basler, Institute of Molecular Life Sciences, University of Zurich, Zurich, Switzerland). For loss of function somatic clones, we crossed the *P{neoFRT}82B flfl^{795}/TM6B, Tb^{+}* [B#66535] hypomorphic allele to *en-GAL4, UAS-flp/CyO; FRT82B, ry/TM6B*.

Crosses involving *C5-Gal4* were performed at 29°C to induce maximal Gal4 expression in the developing wing disc.

6.1.3. Chapter 4: Actomyosin contractility modulates Wnt signaling through adherens junction stability

Fly strains and crosses were raised on standard medium at 25°C unless stated otherwise. w^{1118} was used as wild type. In assays examining the interactions between two or more UAS transgenes, control crosses were performed with *UAS-lacZ* or *UAS-GFP*, to rule out effects due to titration of Gal4. Heat-shock inducible actin flip-out clones were generated by crossing either RFP-marked flip-out or GFP-marked flip-out strains to corresponding lines, then larvae were heat-shocked at 37°C for 12.5 or 15 minutes respectively, 48-72 hours after egg laying (AEL) (depending on the assay), and incubated at 29°C until dissection. Mosaic analysis with a repressible cell marker (MARCM) clones were generated by crossing MARCM lines to corresponding lines and larvae were heat-shocked at 37°C for 1.5 hours, 48 (*MARCM82B*) or 72 (*MARCM42D*) hours AEL, and incubated at 29°C until dissection. RNAi strains have been previously published to knock down target gene of interest, or stated to have no predicted off-targets by the producer.

The following fly strains were used: (1) *Dll-lacZ* (BL10981), (2) *dpp-Gal4* (BL 1553),(3) y^1 *sc* v*^{1}*; P{TRiP.HMS00521}attP2 (mbs-RNAi*) (BL 32516), (4) *UAS-sqh-RNAi* (BL 31542, 38222, 32439, 33892), (5) *UAS-bsk*^{DN} (BL 6409), (6) y^1 w^{67c23}*; P{lacW}shg*^{k03401}*/CyO (shg-lacZ)* (BL 10377), (7) *w*; P{FRT(w*^{hs}*)}G13 shg*^{1}*/CyO; P{Ubi-p63E-shg.GFP} (ubi-shg-GFP)* (BL 58471), (8) *UAS-arm*^{S10} (BL 4782), (9) *arm-GFP* (BL 8555), (10) *UAS-dia∆DAD* (BL 56752), (11) y^1 v^1*; P{TRiP.HM05027}attP2 (UAS-dia-RNAi)* (BL 28541), (12) *mys*^{1}*,FRT19A/FM7c (*β_{PS}^{null}) (BL 23862) (obtained from the Bloomington Drosophila Stock Center), (13) *UAS-flw-RNAi*) (VDRC 104677, 29622), (14), *UAS-mypt-75D-RNAi* (VDRC 109909), (15) *UAS-mbs-RNAi* (VDRC 105762), (16) *UAS-shg-RNAi* (VDRC 27082), (obtained from the Vienna Drosophila Resource Center), (17) *;;puc*^{E69}*-lacZ* (Ring & Martinez Arias, 1993), (18*) fz3-lacZ/FM7a* (Sato et al., 1999), (19), *yw, arm-lacZ, FRT19A;; eyFLP/TM6B* (*arm-lacZ*) (Vincent et al., 1994), (20) *hh-GAL4* (Port et al.,2011), (21) *UAS-sqh*^{E20E21} (*UAS-sqh*^{EE}) (Winter et al., 2001), (22) UAS-DEcad::αcatΔVH1 (Desai et al., 2013), (23) *shg*^{R69}*, FRT42D/CyO* (*shg*^{null}) (Godt & Tepass, 1998), (24) *hsFLP;; Act>CD2>Gal4, UAS-GFP/SM6~TM6* (GFP-marked flip-

out) (Bruce Edgar, Zentrum für Molekulare Biologie der Universität Heidelberg, Germany), (25) *hsflp^{122}, tub-gal80, FRT19A; Act-Gal4, UAS-GFP*; (MARCM19A) (Rongwen Xi, NIBS, Beijing, China), (26) *y,w,hsflp,UAS-GFP,tub-Gal4;;FRT82B tubGal80* (MARCM82B) (Bruce Edgar, Zentrum für Molekulare Biologie der Universität Heidelberg, Germany), (27) *;;UAS-GFP,hsflp122,FRT42,tub-GAL80,tub-GAL4/TM6B* (MARCM42D) (Jessica Treisman, NYU School of Medicine, USA), (28) *UAS-DEcadΔβ::αcatΔVH1* (Ulrich Tepass, University of Toronto, Department of Cell & Systems Biology), (29*) Dsh-GFP/CyO* (Jeffrey Axelrod, Dept. of Pathology, Stanford University School of Medicine, USA), (30) *yw; tub>FLAG-axin/CyO* (Marcel Wehrli, Oregon Health & Science University, USA), (31) *UAS-fz-myc-arr*, (Marcel Wehrli, Oregon Health & Science University, USA), (32) *axin^{S044230},FRT82B/TM6B* (*axin^{null}*) (Marcel Wehrli, Oregon Health & Science University, USA), (33) *en-Gal4,UAS-gfp* (Konrad Basler, Institute of Molecular Life Science, University of Zurich, Switzerland), (34) *y,w,hsflp122; sp/CyO; Act>CD2>GAL4,UAS-RFP/TM6B* (RFP-marked flip-out), (35) *shg^{R69},FRT42D,mypt-75D-RNAi; UAS-DEcadΔβ::αcatΔVH1/SM6a~TM6B*.

6.2. Plasmid constructs

The following plasmids were used in this study: pMCL-HA-MAPKK1-8E (K97M) (Addgene plasmid # 40811) (DN MEK1) (Mansour et al., 1994), pCMV5-rat ERK2-L73P/S151D (Addgene plasmid # 40819) (CA ERK2) (Emrick et al., 2001), pCMV5-rat ERK2-K52R (DN ERK2) (Addgene plasmid # 40813) (Emrick et al., 2006), all a gift from Natalie Ahn, pCMV-Myc (empty vector) (Clontech), TOPFLASH (Korinek et al., 1997), FOPFLASH (Korinek et al., 1997), pRL-CMV (Renilla Luciferase) (Promega), pcDNA-Wnt3A and pcDNA-β-catenin^{AAAA} a gift from Cara Gottardi.

6.3. Cell culture

6.3.1. Chapter 2: Ras-activated MEK1/Dsor1 promotes Wnt signaling

HEK-293 cells were cultured in 6 well plates at 37°C in 5% $CO_2$with DMEM (Gibco) supplemented with 10% FBS (Invitrogen). Transient transfection was performed with 2µg total DNA with Polyfect transfection reagent (Qiagen) according to the manufacturer's instructions. When required, the final amount of DNA used for transfection was kept constant by the addition of empty vector DNA. All cells were harvested and lysed 36 hours post transfection with lysis buffer [20 mMTris-HCl (pH 7.5), 150 mMNaCl, 1 mM Na2EDTA, 1 mM EGTA, 1% Triton, 2.5 mM sodium pyrophosphate, 1 mM beta-glycerophosphate, 1 mM Na3VO4, 1 µg/ml leupeptin] (Cell Signaling Technology), supplemented with protease inhibitors (Roche). For analysis of degradation bound β-catenin (Phospho-β-catenin), MG132 (Calbiochem) was used to treat cells at a concentration of 25 µM for 6 h, prior to harvesting to prevent proteasomal digestion.

6.3.2. Chapter 4: Actomyosin contractility modulates Wnt signaling through adherens junction stability

Cells were cultured in six-well plates at 37°C in 5% CO2. RKO (CRL-2577; ATCC) cells were grown in Dulbecco's modified Eagle's medium (DMEM; Gibco) supplemented with 10% heat-inactivated fetal bovine serum (hi-FBS; Invitrogen). MCF7 (HTB-22; ATCC) cells were grown in DMEM:F-12 (Gibco) supplemented with 10% hi-FBS (Invitrogen). Reverse transfections of siRNA complexes was performed in cells seeded at 50% confluence with Lipofectamine RNAiMAX (ThermoFisher Scientific) in Opti-MEM (Gibco), according to manufacturer's instructions. 24 hours after seeding, transfections of plasmid DNA was performed with Lipofectamine 3000 and P3000 reagent (ThermoFisher Scientific), according to manufacturer's instructions. When required, the final amount of DNA used for transfection was kept constant by the addition of control vector DNA. All cells were harvested 48 hours after transient DNA plasmid transfection for subsequent assays.

6.4. Immunofluorescence, wing mounting and imaging

Third-instar larvae were dissected in phosphate-buffered saline (PBS). Wing imaginal discs and salivary glands were fixed in 4% paraformaldehyde at room temperature for 20 min followed by three washes in PBS for 5 minutes. Tissue was blocked [2% BSA diluted in PBS 0.1% Triton X-100 (PBST)] for 45 min at room temperature, followed by incubation with primary antibodies overnight at 4°C. Tissue was then washed three times for 5 minutes with PBST and incubated with secondary antibodies at room temperature for 1.5 hours. Phalloidin and DAPI were added at this point, if required. A final series of three PBST washes were performed, followed by mounting in 70% glycerol in PBS. A minimum of 20 discs or glands were mounted per slide for a given genotype. Adult wings were dissected in 95% ethanol and mounted in Aquatex (EMD Chemicals). A minimum of 12 wings were mounted per genotype for analysis. Microscopy images were taken with an A1R laser scanning confocal microscope (Nikon) and adult wings were imaged with a Zeiss Axioplan 2 microscope.

6.4.1. Chapter 2: Antibodies

The following primary antibodies were used in this study: mouse anti-Wg 4D4 (1:100, 1:500 SGs, DSHB), mouse anti-Arm (1:50, 1:200 SGs, DSHB), mouse anti-β-galactosidase (1:2000, Promega), rabbit anti-cleaved Casp3 (1:100, Cell Signaling), guinea pig anti-Sens (1:1000, a gift from Hugo Bellen), mouse anti-HA (1:500, Sigma), rabbit anti-HA (1:1600, Cell Signaling), rabbit anti-ERK1/2 (1:200, Cell Signaling), rabbit anti-FLAG (1:200, Sigma), mouse anti-GFP (1:500, Cell Signaling), mouse anti-Dac2-3 (1:75, DSHB), rabbit anti-Arrow (1:15000, a gift from Stephen DiNardo), mouse anti-Fz2 (1:50, DSHB). All secondary antibodies (Jackson Immuno Research) were used at a 1:200 dilution. Proximity Ligation Assays were performed using Duolink In Situ Red Starter Kit Mouse/Rabbit, following the manufacturer's protocol.

6.4.2. Chapter 3: Antibodies

The following primary antibodies and dilutions were used: mouse anti-β-galactosidase (1:2000 Promega), mouse anti-Wg (1:100 DSHB), mouse anti-Cut (1:50 DSHB), mouse anti-N^{ICD} (1:50 DSHB), rat anti-Ci (1:50 DSHB), mouse anti-Delta (1:50 DSHB), mouse anti-Arm (1:50 DSHB), rabbit anti-cleaved Caspase 3 (1:100 Cell

Signaling), rabbit anti-PH3 (1:200 Cell Signaling), guinea pig anti-Sens (1:500, a gift from Hugo Bellen, Dept. of Molecular and Human Genetics, Baylor College of Medicine, USA), mouse anti-Dll (1:300, a gift from Ian Duncan, Dept. of Biology, Washington University in St. Louis, USA). Secondary antibodies (Jackson ImmunoResearch) were used at a 1:200 dilution.

6.4.3. Chapter 4: Antibodies

The following primary antibodies and dilutions were used: mouse anti-β-galactosidase (1:2000 Promega), mouse anti-Wg (1:100 DSHB), mouse anti-Arm (1:50 DSHB), rabbit anti-cleaved Caspase 3 (1:100 Cell Signaling), guinea pig anti-Sens (1:500, a gift from Hugo Bellen, Dept. of Molecular and Human Genetics, Baylor College of Medicine, USA), mouse anti-Dll (1:300, a gift from Ian Duncan, Dept. of Biology, Washington University in St. Louis, USA), rabbit anti-Phospho-Myosin Light Chain 2 (Ser19) (p-MyoII) (1:25 Cell Signaling), mouse anti-GFP (1:500, Cell Signaling), rabbit anti-FLAG (1:200, Sigma), rat anti-DEcad (extracellular domain) (1:50 DSHB)Secondary antibodies (Jackson ImmunoResearch) were used at a 1:200 dilution.

6.5. Live imaging and FRAP

Third-instar wing imaginal discs were dissected and mounted in SFX-Insect serum-free insect cell culture medium (Hyclone) supplemented with methyl cellulose (Sigma-Aldrich) at a concentration of 4% wt/vol to increase viscosity to prevent disc drifting while imaging. FRAP assays were carried out on an A1R laser scanning confocal microscope (Nikon), with 60× objective, 5× artificial zoom. GFP within the region of interest (ROI) was photobleached with a 405 nm and 488 nm UV laser at 100% power for 15 seconds. GFP recovery specifically along the AJs was then recorded by time-lapse imaging over 60 minutes at 2-minute intervals. Focal planes were maintained by manual focus during time-lapse. Any samples that exhibited phototoxicity or additional photobleaching in control regions during the time-lapse were excluded. GFP recovery rates of individual ROI data were normalized with pre-FRAP equal to 100% and post-FRAP equal to 0%. AJ immobile fractions of proteins were calculated as pre-FRAP

fluorescence intensities, minus the end value of recovered fluorescence intensity of individual ROI.

6.6. Image processing, measurements, and statistical analysis

6.6.1. Chapter 3: The protein phosphatase 4 complex promotes the Notch pathway and wingless transcription

Following image acquisition, images were processed using NIS Elements (Nikon) and Adobe Photoshop CS6. Immunofluorescence images are presented as maximum intensity projections of Z-steps spanning the entire tissue.

Adult wings were imaged with an Axioplan 2 microscope. Adult wing and wing disc areas were quantified using ImageJ software. PH3 cell counts were performed using the ImageJ plugin, “Cell Counter”. To compare PH3 positive cell counts per genotype, counts were converted as a ratio of PH3 cells/area, then analysed as experimental condition over control tissue. Significance between groups was assessed by one-way analysis of variance (ANOVA), and $p<0.01$ was considered significant unless stated otherwise.

6.6.2. Chapter 4: Actomyosin contractility modulates Wnt signaling through adherens junction stability

Following image acquisition, images were processed using NIS Elements (Nikon) and Adobe Photoshop CS6. Immunofluorescence images are presented as maximum intensity projections of Z-steps spanning the entire tissue.

Distribution of Arm was determined by single line fluorescence intensity plot across individual cells with NIS Elements (Nikon). Cell edges were determined by peak F-actin fluorescence, and increased DAPI across the plot line marked the nucleus. Percentage of nuclear Arm, was determined as the value of Arm within the nuclear area over the total Arm across the intensity plot of the cell. Cell surface area was quantified

using ImageJ (NIH) software. All data quantifications were performed in Microsoft Excel or GraphPad Prism and figures were made using Adobe Illustrator CS6.

Statistical analyses were performed using GraphPad Prism. Significant differences between two genotypes was determined by two-tailed Student's t tests. One-way ANOVA was performed for multiple comparisons, with Tukey's multiple comparison as a post-test. All quantified data are presented as mean ± SEM, and $P< 0.05$ was considered statistically significant. Significance depicted as * = $P< 0.05$, ** = $P< 0.01$, *** = $P< 0.001$, ns = not significant.

6.7. Lysate collection and immunoblotting

6.7.1. Chapter 2: Ras-activated MEK1/Dsor1 promotes Wnt signaling

HEK-293 cells transfected with Wnt3A and empty vector, or Wnt3a and DN MEK1 were treated with lysis buffer. Lysates were then sonicated for several seconds on ice, followed by 16,300xG centrifugation for 10 minutes at 4°C. The supernatant was removed and boiled for 10 minutes with Laemmli buffer, then separated on 10% SDS-PAGE. Proteins were transferred to nitrocellulose membranes, and probed against the following primary antibodies: anti-Phospho-β-catenin (Ser33/37/Thr41) (1:1000, Cell Signaling), anti-β-catenin (1:1000, Cell Signaling), anti-Non-phospho (Active) β-catenin (Ser33/37/Thr41) (1:1000, Cell Signaling), anti-β-Actin (1:1000, ABM). Membranes were visualized using the Enhanced Chemiluminescence Western Blotting Substrate (Pierce) with a LAS4000 luminescent imager (Fujifilm). The protein levels were determined using ImageJ software to perform densitometry. Each sample was normalized to β-Actin levels. Transfections and Western blotting was performed in triplicate

6.7.2. Chapter 4: Actomyosin contractility modulates Wnt signaling through adherens junction stability.

Lysates of whole cell extract of MCF7 and RKO cells transfected with respective plasmids and siRNA were generated by collecting and treating the cells with cell lysis buffer (Cell Signaling Technology) supplemented with protease inhibitors (Roche). Lysates were then sonicated for several seconds on ice, followed by a 16,300 g

centrifugation for 10 min at 4°C. The supernatant was removed and protein concentrations were determined by bicinchoninic acid (BCA) assay (ThermoFisher Scientific). MCF7 cellular fraction lysates were generated by the Subcellular Protein Fractionation assay (ThermoFisher Scientific) according to manufacturer's instructions. Protein concentrations were equalized within individual fractions, as determined by BCA assay (ThermoFisher Scientific). Lysates were boiled for 10 min with Laemmli buffer, then separated on 8-12% SDS-PAGE gels. Proteins were transferred onto nitrocellulose membranes, and and probed against the following primary antibodies: rabbit anti-β-catenin (1:1000, Cell Signaling), rabbit anti-E-cadherin (1:1000, Cell Signaling), mouse anti-PPP1R16A (MYPT-3) (1:500, abcam), mouse anti-Protein Phosphatase 1 beta (PP1β) (1:1000, abcam), rabbit anti-Wnt3A (1:1000, Cell Signaling), mouse anti-β-tubulin (1:1000, ABM), rabbit anti-GAPDH (1:3000, Cell Signaling), mouse anti-Na^+/K^+ ATPase (1:50 DSHB), rabbit anti-Histone H3 (1:1000 Cell Signaling). Membranes were visualized using the enhanced chemiluminescence (ECL) western blotting substrate (Pierce) with a LAS4000 luminescent imager (Fujifilm). The protein levels were determined using ImageJ (NIH) software to perform densitometry. Transfections and western blotting was performed in triplicate.

6.8. Transcriptional reporter assay and statistical analysis

Luciferase assays were performed in HEK-293, MCF7 and RKO cells with the Dual-Luciferase Reporter Assay System (Promega) according to manufacturer's instructions. TOPFLASH or negative control FOPFLASH reporter gene plasmids, with the control reporter plasmid encoding Renilla luciferase (to normalize transfection efficiencies and for monitoring cell viability) were transfected with each expression vector as indicated, to determine overall Wnt pathway activity through TCF/LEF reporter activity. The values shown represent the mean ± SD of three biological replicate transfections, performed in triplicate for HEK-293 cells, and mean ± SEM from four biological replicate transfections, performed each time in triplicate. TOPFLASH values were normalized to the FOPFLASH reporter activity equal to 1 for each individual transfections series.

References

Aberle, H., Butz, S., Stappert, J., Weissig, H., Kemler, R., and Hoschuetzky, H. (1994). Assembly of the cadherin-catenin complex in vitro with recombinant proteins. J. Cell Sci. *107 (Pt 12)*, 3655–3663.

Aberle, H., Bauer, A., Stappert, J., Kispert, A., and Kemler, R. (1997). β-catenin is a target for the ubiquitin–proteasome pathway. EMBO J. *16*, 3797–3804.

Affolter, M., Pyrowolakis, G., Weiss, A., and Basler, K. (2008). Signal-Induced Repression: The Exception or the Rule in Developmental Signaling? Dev. Cell *15*, 11–22.

Afshar, K., Stuart, B., and Wasserman, S.A. (2000). Functional analysis of the Drosophila diaphanous FH protein in early embryonic development. Development *127*.

Ahumada, A., Slusarski, D.C., Liu, X., Moon, R.T., Malbon, C.C., and Wang, H. (2002). Signaling of Rat Frizzled-2 Through Phosphodiesterase and Cyclic GMP. Science (80-.). *298*, 2006–2010.

Akhurst, R.J., and Hata, A. (2012). Targeting the TGFβ signalling pathway in disease. Nat. Rev. Drug Discov. *11*, 790–811.

Aliee, M., Röper, J.-C., Landsberg, K.P., Pentzold, C., Widmann, T.J., Jülicher, F., and Dahmann, C. (2012). Physical Mechanisms Shaping the Drosophila Dorsoventral Compartment Boundary. Curr. Biol. *22*, 967–976.

Amit, S., Hatzubai, A., Birman, Y., Andersen, J.S., Ben-Shushan, E., Mann, M., Ben-Neriah, Y., and Alkalay, I. (2002). Axin-mediated CKI phosphorylation of beta-catenin at Ser 45: a molecular switch for the Wnt pathway. Genes Dev. *16*, 1066–1076.

Atcha, F.A., Syed, A., Wu, B., Hoverter, N.P., Yokoyama, N.N., Ting, J.-H.T., Munguia, J.E., Mangalam, H.J., Marsh, J.L., and Waterman, M.L. (2007). A unique DNA binding domain converts T-cell factors into strong Wnt effectors. Mol. Cell. Biol. *27*, 8352–8363.

Axelrod, J.D. (2010). Delivering the Lateral Inhibition Punchline: It's All About the Timing. Sci. Signal. *3*, pe38-pe38.

Baeg, G.H., Lin, X., Khare, N., Baumgartner, S., and Perrimon, N. (2001). Heparan sulfate proteoglycans are critical for the organization of the extracellular distribution of Wingless. Development *128*, 87–94.

Bafico, A., Gazit, A., Pramila, T., Finch, P.W., Yaniv, A., and Aaronson, S.A. (1999). Interaction of frizzled related protein (FRP) with Wnt ligands and the frizzled receptor suggests alternative mechanisms for FRP inhibition of Wnt signaling. J. Biol. Chem. *274*, 16180–16187.

Bajpai, S., Correia, J., Feng, Y., Figueiredo, J., Sun, S.X., Longmore, G.D., Suriano, G., and Wirtz, D. (2008). {alpha}-Catenin mediates initial E-cadherin-dependent cell-cell recognition and subsequent bond strengthening. Proc. Natl. Acad. Sci. U. S. A. *105*, 18331–18336.

Baker, N.E. (1988). Embryonic and imaginal requirements for wingless, a segment-polarity gene in Drosophila. Dev. Biol. *125*, 96–108.

Bänziger, C., Soldini, D., Schütt, C., Zipperlen, P., Hausmann, G., and Basler, K. (2006). Wntless, a Conserved Membrane Protein Dedicated to the Secretion of Wnt Proteins from Signaling Cells. Cell *125*, 509–522.

Baonza, A., and Garcia-Bellido, A. (2000). Notch signaling directly controls cell proliferation in the Drosophila wing disc. Proc. Natl. Acad. Sci. *97*, 2609–2614.

Baonza, a, Roch, F., and Martin-Blanco, E. (2000). DER signaling restricts the boundaries of the wing field during Drosophila development. Proc. Natl. Acad. Sci. U. S. A. *97*, 7331–7335.

Barolo, S., and Posakony, J.W. (2002). Three habits of highly effective signaling pathways: principles of transcriptional control by developmental cell signaling. Genes Dev. *16*, 1167–1181.

Bartscherer, K., Pelte, N., Ingelfinger, D., and Boutros, M. (2006). Secretion of Wnt Ligands Requires Evi, a Conserved Transmembrane Protein. Cell *125*, 523–533.

Basu, S., Haase, G., and Ben-Ze'ev, A. (2016). Wnt signaling in cancer stem cells and colon cancer metastasis. F1000Research *5*.

Bate, M., and Arias, A.M. (1991). The embryonic origin of imaginal discs in Drosophila. Development *112*, 755–761.

de Beco, S., Gueudry, C., Amblard, F., and Coscoy, S. (2009). Endocytosis is required for E-cadherin redistribution at mature adherens junctions. Proc. Natl. Acad. Sci. U. S. A. *106*, 7010–7015.

Behrens, J., von Kries, J.P., Kühl, M., Bruhn, L., Wedlich, D., Grosschedl, R., and Birchmeier, W. (1996). Functional interaction of β-catenin with the transcription factor LEF-1. Nature *382*, 638–642.

Bejsovec, A. (2006). Flying at the head of the pack: Wnt biology in Drosophila. Oncogene *25*, 7442–7449.

Bejsovec, A., and Martinez Arias, A. (1991). Roles of wingless in patterning the larval epidermis of Drosophila. Development *113*, 471–485.

Bejsovec, A., Cavallo, R.A., Cox, R.T., Moline, M.M., Roose, J., Polevoy, G.A., Clevers, H., and Peifer, M. (1998). Drosophila Tcf and Groucho interact to repress Wingless signalling activity. Nature *395*, 604–608.

Belenkaya, T.Y., Wu, Y., Tang, X., Zhou, B., Cheng, L., Sharma, Y. V., Yan, D., Selva, E.M., and Lin, X. (2008). The Retromer Complex Influences Wnt Secretion by Recycling Wntless from Endosomes to the Trans-Golgi Network. Dev. Cell *14*, 120–131.

Bell, S.M., Schreiner, C.M., Wert, S.E., Mucenski, M.L., Scott, W.J., and Whitsett, J.A. (2008). R-spondin 2 is required for normal laryngeal-tracheal, lung and limb morphogenesis. Development *135*, 1049–1058.

Benham-Pyle, B.W., Pruitt, B.L., and Nelson, W.J. (2015). Cell adhesion. Mechanical strain induces E-cadherin-dependent Yap1 and β-catenin activation to drive cell cycle entry. Science *348*, 1024–1027.

Benjamin, J.M., Kwiatkowski, A. V., Yang, C., Korobova, F., Pokutta, S., Svitkina, T., Weis, W.I., and Nelson, W.J. (2010). αE-catenin regulates actin dynamics independently of cadherin-mediated cell–cell adhesion. J. Cell Biol. *189*, 339–352.

Berster, J.M., and Göke, B. (2008). Type 2 diabetes mellitus as risk factor for colorectal cancer. Arch. Physiol. Biochem. *114*, 84–98.

Bhanot, P., Brink, M., Samos, C.H., Hsieh, J.-C., Wang, Y., Macke, J.P., Andrew, D., Nathans, J., and Nusse, R. (1996). A new member of the frizzled family from Drosophila functions as a Wingless receptor. Nature *382*, 225–230.

Bilic, J., Huang, Y.-L., Davidson, G., Zimmermann, T., Cruciat, C.-M., Bienz, M., and Niehrs, C. (2007). Wnt induces LRP6 signalosomes and promotes dishevelled-dependent LRP6 phosphorylation. Science *316*, 1619–1622.

Blair, S.S. (2003). Genetic mosaic techniques for studying Drosophila development. Development *130*.

Blitzer, J.T., and Nusse, R. (2006). A critical role for endocytosis in Wnt signaling. BMC Cell Biol. *7*, 28.

Bradley, R.S., Cowin, P., and Brown, A.M. (1993). Expression of Wnt-1 in PC12 cells results in modulation of plakoglobin and E-cadherin and increased cellular adhesion. J. Cell Biol. *123*, 1857–1865.

Brand, A.H., and Perrimon, N. (1993). Targeted gene expression as a means of altering cell fates and generating dominant phenotypes. Development *118*, 401–415.

Bray, S.J. (2016). Notch signalling in context. Nat. Rev. Mol. Cell Biol. *17*, 722–735.

Briscoe, J., and Thérond, P.P. (2013). The mechanisms of Hedgehog signalling and its roles in development and disease. Nat. Rev. Mol. Cell Biol. *14*, 418–431.

Brown, N.H. (1993). Integrins holdDrosophila together. BioEssays *15*, 383–390.

Brunner, D. (1994). A gain-of-function mutation in Drosophila MAP kinase activates multiple receptor tyrosine kinase signaling pathways. Cell *76*, 875–888.

Buechling, T., Chaudhary, V., Spirohn, K., Weiss, M., and Boutros, M. (2011). p24 proteins are required for secretion of Wnt ligands. EMBO Rep. *12*, 1265–1272.

BURNETT, G., and KENNEDY, E.P. (1954). The enzymatic phosphorylation of proteins. J. Biol. Chem. *211*, 969–980.

Buske, P., Przybilla, J., Loeffler, M., Sachs, N., Sato, T., Clevers, H., and Galle, J. (2012). On the biomechanics of stem cell niche formation in the gut - modelling growing organoids. FEBS J. *279*, 3475–3487.

Butler, M.T., and Wallingford, J.B. (2017). Planar cell polarity in development and disease. Nat. Rev. Mol. Cell Biol. *18*, 375–388.

Caca, K., Kolligs, F.T., Ji, X., Hayes, M., Qian, J., Yahanda, A., Rimm, D.L., Costa, J., and Fearon, E.R. (1999). Beta- and gamma-catenin mutations, but not E-cadherin inactivation, underlie T-cell factor/lymphoid enhancer factor transcriptional deregulation in gastric and pancreatic cancer. Cell Growth Differ. *10*, 369–376.

Calil, I., Tineli, R.A., Vicente, W.V. de A., Rodrigues, A.J., and Evora, P.R.B. (2007). The concept of crosstalk and its implications for cardiovascular function and disease. Arq. Bras. Cardiol. *88*, e26-31.

Campbell, G. (2002). Distalization of the Drosophila leg by graded EGF-receptor activity. Nature *418*, 781–785.

Carmon, K.S., Gong, X., Lin, Q., Thomas, A., and Liu, Q. (2011). R-spondins function as ligands of the orphan receptors LGR4 and LGR5 to regulate Wnt/ -catenin signaling. Proc. Natl. Acad. Sci. *108*, 11452–11457.

Cavey, M., Rauzi, M., Lenne, P.-F., and Lecuit, T. (2008). A two-tiered mechanism for stabilization and immobilization of E-cadherin. Nature *453*, 751–756.

de Celis, J.F., Garcia-Bellido, A., and Bray, S.J. (1996). Activation and function of Notch at the dorsal-ventral boundary of the wing imaginal disc. Development *122*, 359–369.

Červenka, I., Wolf, J., Mašek, J., Krejci, P., Wilcox, W.R., Kozubík, A., Schulte, G., Gutkind, J.S., and Bryja, V. (2011). Mitogen-activated protein kinases promote WNT/beta-catenin signaling via phosphorylation of LRP6. Mol. Cell. Biol. *31*, 179–189.

Chen, L., Fu, Y., Ren, M., Xiao, B., and Rubin, C.S. (2011). A RasGRP, C. elegans RGEF-1b, couples external stimuli to behavior by activating LET-60 (Ras) in sensory neurons. Neuron *70*, 51–65.

Cieśla, J., Frączyk, T., and Rode, W. (2011). Phosphorylation of basic amino acid residues in proteins: important but easily missed. Acta Biochim. Pol. *58*, 137–148.

Ciruna, B., and Rossant, J. (2001). FGF signaling regulates mesoderm cell fate specification and morphogenetic movement at the primitive streak. Dev. Cell *1*, 37–49.

Clevers, H., and Nusse, R. (2012). Wnt/β-catenin signaling and disease. Cell *149*, 1192–1205.

Clevers, H., Roose, J., Molenaar, M., Peterson, J., Hurenkamp, J., Brantjes, H., Moerer, P., van de Wetering, M., and Destrée, O. (1998). The Xenopus Wnt effector XTcf-3 interacts with Groucho-related transcriptional repressors. Nature *395*, 608–612.

Codelia, V.A., Sun, G., and Irvine, K.D. (2014). Regulation of YAP by Mechanical Strain through Jnk and Hippo Signaling. Curr. Biol. *24*, 2012–2017.

Cohen, B., Wimmer, E.A., and Cohen, S.M. (1991). Early development of leg and wing primordia in the Drosophila embryo. Mech. Dev. *33*, 229–240.

Cohen, B., McGuffin, M.E., Pfeifle, C., Segal, D., and Cohen, S.M. (1992). apterous, a gene required for imaginal disc development in Drosophila encodes a member of the LIM family of developmental regulatory proteins. Genes Dev. *6*, 715–729.

Cohen, B., Simcox, A.A., and Cohen, S.M. (1993). Allocation of the thoracic imaginal primordia in the Drosophila embryo. Development *117*, 597–608.

Cohen, P.T.W., Philp, A., and Vázquez-Martin, C. (2005). Protein phosphatase 4 – from obscurity to vital functions. FEBS Lett. *579*, 3278–3286.

Collu, G.M., Hidalgo-Sastre, A., and Brennan, K. (2014). Wnt-Notch signalling crosstalk in development and disease. Cell. Mol. Life Sci. *71*, 3553–3567.

Cong, F., Schweizer, L., and Varmus, H. (2004). Wnt signals across the plasma membrane to activate the -catenin pathway by forming oligomers containing its receptors, Frizzled and LRP. Development *131*, 5103–5115.

Cooper, G.M. (2000a). Signaling Molecules and Their Receptors.

Cooper, G.M. (2000b). Signaling in Development and Differentiation.

Coudreuse, D.Y.M., Roël, G., Betist, M.C., Destrée, O., and Korswagen, H.C. (2006). Wnt Gradient Formation Requires Retromer Function in Wnt-Producing Cells. Science (80-.). *312*, 921–924.

Courcelles, M., Frémin, C., Voisin, L., Lemieux, S., Meloche, S., and Thibault, P. (2013). Phosphoproteome dynamics reveal novel ERK1/2 MAP kinase substrates with broad spectrum of functions. Mol. Syst. Biol. *9*, 669.

Couso, J.P., Bishop, S.A., and Martinez Arias, A. (1994). The wingless signalling pathway and the patterning of the wing margin in Drosophila. Development *120*, 621–636.

Cox, R.T., Kirkpatrick, C., and Peifer, M. (1996). Armadillo is required for adherens junction assembly, cell polarity, and morphogenesis during Drosophila embryogenesis. J. Cell Biol. *134*, 133–148.

Crampton, S.P., Wu, B., Park, E.J., Kim, J.-H., Solomon, C., Waterman, M.L., and Hughes, C.C.W. (2009). Integration of the β-Catenin-Dependent Wnt Pathway with Integrin Signaling through the Adaptor Molecule Grb2. PLoS One *4*, e7841.

Daniels, D.L., and Weis, W.I. (2005). Beta-catenin directly displaces Groucho/TLE repressors from Tcf/Lef in Wnt-mediated transcription activation. Nat. Struct. Mol. Biol. *12*, 364–371.

Davidson, G., Wu, W., Shen, J., Bilic, J., Fenger, U., Stannek, P., Glinka, A., and Niehrs, C. (2005). Casein kinase 1 γ couples Wnt receptor activation to cytoplasmic signal transduction. Nature *438*, 867–872.

Davis, M.A., Ireton, R.C., and Reynolds, A.B. (2003). A core function for p120-catenin in cadherin turnover. J. Cell Biol. *163*, 525–534.

Delva, E., and Kowalczyk, A.P. (2009). Regulation of Cadherin Trafficking. Traffic *10*, 259–267.

Desai, R., Sarpal, R., Ishiyama, N., Pellikka, M., Ikura, M., and Tepass, U. (2013). Monomeric α-catenin links cadherin to the actin cytoskeleton. Nat. Cell Biol. *15*, 261–273.

Diaz-Benjumea, F.J., and Cohen, S.M. (1993). Interaction between dorsal and ventral cells in the imaginal disc directs wing development in Drosophila. Cell *75*, 741–752.

Diaz-Benjumea, F.J., and Cohen, S.M. (1995). Serrate signals through Notch to establish a Wingless-dependent organizer at the dorsal/ventral compartment boundary of the Drosophila wing. Development *121*, 4215–4225.

Diaz-Benjumea, F.J., and Hafen, E. (1994). The sevenless signalling cassette mediates Drosophila EGF receptor function during epidermal development. Development *120*, 569–578.

DiNardo, S., Wehrli, M., Dougan, S.T., Caldwell, K., O'Keefe, L., Schwartz, S., Vaizel-Ohayon, D., Schejter, E., and Tomlinson, A. (2000). arrow encodes an LDL-receptor-related protein essential for Wingless signalling. Nature *407*, 527–530.

Ding, Q., Xia, W., Liu, J.-C., Yang, J.-Y., Lee, D.-F., Xia, J., Bartholomeusz, G., Li, Y., Pan, Y., Li, Z., et al. (2005). Erk associates with and primes GSK-3beta for its inactivation resulting in upregulation of beta-catenin. Mol. Cell *19*, 159–170.

Doble, B.W., and Woodgett, J.R. (2003). GSK-3: tricks of the trade for a multi-tasking kinase. J. Cell Sci. *116*, 1175–1186.

Doubravska, L., Krausova, M., Gradl, D., Vojtechova, M., Tumova, L., Lukas, J., Valenta, T., Pospichalova, V., Fafilek, B., Plachy, J., et al. (2011). Fatty acid modification of Wnt1 and Wnt3a at serine is prerequisite for lipidation at cysteine and is essential for Wnt signalling. Cell. Signal. *23*, 837–848.

Duffy, J.B. GAL4 system in Drosophila: a fly geneticist's Swiss army knife. Genesis *34*, 1–15.

DuFort, C.C., Paszek, M.J., and Weaver, V.M. (2011). Balancing forces: architectural control of mechanotransduction. Nat. Rev. Mol. Cell Biol. *12*, 308–319.

Dufour, S., Mège, R.-M., and Thiery, J.P. (2013). α-catenin, vinculin, and F-actin in strengthening E-cadherin cell-cell adhesions and mechanosensing. Cell Adh. Migr. *7*, 345–350.

Ellwanger, K., Saito, H., Clement-Lacroix, P., Maltry, N., Niedermeyer, J., Lee, W.K., Baron, R., Rawadi, G., Westphal, H., and Niehrs, C. (2008). Targeted Disruption of the Wnt Regulator Kremen Induces Limb Defects and High Bone Density. Mol. Cell. Biol. *28*, 4875–4882.

Emrick, M.A., Hoofnagle, A.N., Miller, A.S., Ten Eyck, L.F., and Ahn, N.G. (2001). Constitutive activation of extracellular signal-regulated kinase 2 by synergistic point mutations. J. Biol. Chem. *276*, 46469–46479.

Emrick, M.A., Lee, T., Starkey, P.J., Mumby, M.C., Resing, K.A., and Ahn, N.G. (2006). The gatekeeper residue controls autoactivation of ERK2 via a pathway of intramolecular connectivity. Proc. Natl. Acad. Sci. U. S. A. *103*, 18101–18106.

Engl, W., Arasi, B., Yap, L.L., Thiery, J.P., and Viasnoff, V. (2014). Actin dynamics modulate mechanosensitive immobilization of E-cadherin at adherens junctions. Nat. Cell Biol. *16*, 587–594.

Fagotto, F., Funayama, N., Gluck, U., and Gumbiner, B.M. (1996). Binding to cadherins antagonizes the signaling activity of beta-catenin during axis formation in Xenopus. J. Cell Biol. *132*, 1105–1114.

Fagotto, F., Glück, U., and Gumbiner, B.M. (1998). Nuclear localization signal-independent and importin/karyopherin-independent nuclear import of beta-catenin. Curr. Biol. *8*, 181–190.

Fagotto, F., Jho, E. h, Zeng, L., Kurth, T., Joos, T., Kaufmann, C., and Costantini, F. (1999). Domains of axin involved in protein-protein interactions, Wnt pathway inhibition, and intracellular localization. J. Cell Biol. *145*, 741–756.

Farge, E. (2011). Mechanotransduction in Development. pp. 243–265.

Feig, L.A., and Cooper, G.M. (1988). Inhibition of NIH 3T3 cell proliferation by a mutant ras protein with preferential affinity for GDP. Mol. Cell. Biol. *8*, 3235–3243.

Feng, Q., and Gao, N. (2015). Keeping Wnt Signalosome in Check by Vesicular Traffic. J. Cell. Physiol. *230*, 1170–1180.

Fernández-Sánchez, M.E., Barbier, S., Whitehead, J., Béalle, G., Michel, A., Latorre-Ossa, H., Rey, C., Fouassier, L., Claperon, A., Brullé, L., et al. (2015). Mechanical induction of the tumorigenic β-catenin pathway by tumour growth pressure. Nature *523*, 92–95.

Fiedler, M., Mendoza-Topaz, C., Rutherford, T.J., Mieszczanek, J., and Bienz, M. (2011). Dishevelled interacts with the DIX domain polymerization interface of Axin to interfere with its function in down-regulating β-catenin. Proc. Natl. Acad. Sci. U. S. A. *108*, 1937–1942.

Fischer, J.A., Giniger, E., Maniatis, T., and Ptashne, M. (1988). GAL4 activates transcription in Drosophila. Nature *332*, 853–856.

FISCHER, E.H., and KREBS, E.G. (1955). Conversion of phosphorylase b to phosphorylase a in muscle extracts. J. Biol. Chem. *216*, 121–132.

Fortini, M.E. (2009). Notch Signaling: The Core Pathway and Its Posttranslational Regulation. Dev. Cell *16*, 633–647.

Fragoso, M.A., Patel, A.K., Nakamura, R.E.I., Yi, H., Surapaneni, K., and Hackam, A.S. (2012). The Wnt/β-Catenin Pathway Cross-Talks with STAT3 Signaling to Regulate Survival of Retinal Pigment Epithelium Cells. PLoS One *7*, e46892.

Franch-Marro, X., Wendler, F., Griffith, J., Maurice, M.M., and Vincent, J.-P. (2008). In vivo role of lipid adducts on Wingless. J. Cell Sci. *121*, 1587–1592.

Freeman, M., and Bienz, M. (2001). EGF receptor/Rolled MAP kinase signalling protects cells against activated Armadillo in the Drosophila eye. EMBO Rep. *2*, 157–162.

Frise, E., Knoblich, J.A., Younger-Shepherd, S., Jan, L.Y., and Jan, Y.N. (1996). The Drosophila Numb protein inhibits signaling of the Notch receptor during cell-cell interaction in sensory organ lineage. Proc. Natl. Acad. Sci. U. S. A. *93*, 11925–11932.

Fristrom, D., Gotwals, P., Eaton, S., Kornberg, T.B., Sturtevant, M., Bier, E., and Fristrom, J.W. (1994). Blistered: a gene required for vein/intervein formation in wings of Drosophila. Development *120*, 2661–2671.

Fujioka, A., Terai, K., Itoh, R.E., Aoki, K., Nakamura, T., Kuroda, S., Nishida, E., and Matsuda, M. (2006). Dynamics of the Ras/ERK MAPK cascade as monitored by fluorescent probes. J. Biol. Chem. *281*, 8917–8926.

Gagliardi, M., Piddini, E., and Vincent, J.-P. (2008). Endocytosis: a positive or a negative influence on Wnt signalling? Traffic *9*, 1–9.

Galindo, M.I., Bishop, S.A., Greig, S., and Couso, J.P. (2002). Leg patterning driven by proximal-distal interactions and EGFR signaling. Science *297*, 256–259.

Gao, C., Xiao, G., and Hu, J. (2014). Regulation of Wnt/β-catenin signaling by posttranslational modifications. Cell Biosci. *4*, 13.

Gardner, A.M., Vaillancourt, R.R., Lange-Carter, C.A., and Johnson, G.L. (1994). MEK-1 phosphorylation by MEK kinase, Raf, and mitogen-activated protein kinase: analysis of phosphopeptides and regulation of activity. Mol. Biol. Cell *5*, 193–201.

Giancotti, F.G., and Ruoslahti, E. (1999). Integrin Signaling. Science (80-.). *285*.

Gingras, A.-C., Caballero, M., Zarske, M., Sanchez, A., Hazbun, T.R., Fields, S., Sonenberg, N., Hafen, E., Raught, B., and Aebersold, R. (2005). A novel, evolutionarily conserved protein phosphatase complex involved in cisplatin sensitivity. Mol. Cell. Proteomics *4*, 1725–1740.

Giorgianni, M.W., and Mann, R.S. (2011). Establishment of medial fates along the proximodistal axis of the Drosophila leg through direct activation of dachshund by Distalless. Dev. Cell *20*, 455–468.

Giraldez, A.J., and Cohen, S.M. (2003). Wingless and Notch signaling provide cell survival cues and control cell proliferation during wing development. Development *130*, 6533–6543.

Go, M.J., Eastman, D.S., and Artavanis-Tsakonas, S. (1998). Cell proliferation control by Notch signaling in Drosophila development. Development *125*, 2031–2040.

Godt, D., and Tepass, U. (1998). Drosophila oocyte localization is mediated by differential cadherin-based adhesion. Nature *395*, 387–391.

Goldenberg, G., Harris, T.J.C., Wu, C., Duncan, K., and Korn, E. (2013). Adherens Junction Distribution Mechanisms during Cell-Cell Contact Elongation in Drosophila. PLoS One *8*, e79613.

Gomez, G.A., McLachlan, R.W., and Yap, A.S. (2011). Productive tension: force-sensing and homeostasis of cell–cell junctions. Trends Cell Biol. *21*, 499–505.

Green, J.L., Kuntz, S.G., and Sternberg, P.W. (2008). Ror receptor tyrosine kinases: orphans no more. Trends Cell Biol. *18*, 536–544.

Green, J.L., La, J., Yum, K.W., Desai, P., Rodewald, L.-W., Zhang, X., Leblanc, M., Nusse, R., Lewis, M.T., and Wahl, G.M. (2013). Paracrine Wnt signaling both promotes and inhibits human breast tumor growth. Proc. Natl. Acad. Sci. *110*, 6991–6996.

Greer, E.R., Chao, A.T., and Bejsovec, A. (2013). Pebble/ECT2 RhoGEF negatively regulates the Wingless/Wnt signaling pathway. Development *140*, 4937–4946.

Grenier, J.K., and Carroll, S.B. (2000). Functional evolution of the Ultrabithorax protein. Proc. Natl. Acad. Sci. *97*, 704–709.

Gumbiner, B.M., and Kim, N.-G. (2014). The Hippo-YAP signaling pathway and contact inhibition of growth. J. Cell Sci. *127*, 709–717.

Guo, M., Jan, L.Y., and Jan, Y.N. (1996). Control of daughter cell fates during asymmetric division: interaction of Numb and Notch. Neuron *17*, 27–41.

Guturi, K.K.N., Mandal, T., Chatterjee, A., Sarkar, M., Bhattacharya, S., Chatterjee, U., and Ghosh, M.K. (2012). Mechanism of β-catenin-mediated transcriptional regulation of epidermal growth factor receptor expression in glycogen synthase kinase 3 β-inactivated prostate cancer cells. J. Biol. Chem. *287*, 18287–18296.

Hall, E.T., and Verheyen, E.M. (2015). Ras-activated Dsor1 promotes Wnt signaling in Drosophila development. J. Cell Sci.

Hamada, F., Tomoyasu, Y., Takatsu, Y., Nakamura, M., Nagai, S., Suzuki, A., Fujita, F., Shibuya, H., Toyoshima, K., Ueno, N., et al. (1999). Negative regulation of Wingless signaling by D-axin, a Drosophila homolog of axin. Science *283*, 1739–1742.

Han, C., Yan, D., Belenkaya, T.Y., and Lin, X. (2005). Drosophila glypicans Dally and Dally-like shape the extracellular Wingless morphogen gradient in the wing disc. Development *132*, 667–679.

Happe, C.L., and Engler, A.J. (2016). Mechanical Forces Reshape Differentiation Cues That Guide Cardiomyogenesis. Circ. Res. *118*, 296–310.

Harris, T.J.C., and Tepass, U. (2010). Adherens junctions: from molecules to morphogenesis. Nat. Rev. Mol. Cell Biol. *11*, 502–514.

Hart, M., Concordet, J.P., Lassot, I., Albert, I., del los Santos, R., Durand, H., Perret, C., Rubinfeld, B., Margottin, F., Benarous, R., et al. (1999). The F-box protein beta-TrCP associates with phosphorylated beta-catenin and regulates its activity in the cell. Curr. Biol. *9*, 207–210.

Hartenstein, V., and Posakony, J.W. (1990). A dual function of the Notch gene in Drosophila sensillum development. Dev. Biol. *142*, 13–30.

Harterink, M., Port, F., Lorenowicz, M.J., McGough, I.J., Silhankova, M., Betist, M.C., van Weering, J.R.T., van Heesbeen, R.G.H.P., Middelkoop, T.C., Basler, K., et al. (2011). A SNX3-dependent retromer pathway mediates retrograde transport of the Wnt sorting receptor Wntless and is required for Wnt secretion. Nat. Cell Biol. *13*, 914–923.

Hatzis, P., van der Flier, L.G., van Driel, M.A., Guryev, V., Nielsen, F., Denissov, S., Nijman, I.J., Koster, J., Santo, E.E., Welboren, W., et al. (2008). Genome-Wide Pattern of TCF7L2/TCF4 Chromatin Occupancy in Colorectal Cancer Cells. Mol. Cell. Biol. *28*, 2732–2744.

Hay, B.A., Wolff, T., and Rubin, G.M. (1994). Expression of baculovirus P35 prevents cell death in Drosophila. Development *120*, 2121–2129.

Haÿ, E., Nouraud, A., Marie, P.J., Bouvet, S., and Jacquel, A. (2009). N-Cadherin Negatively Regulates Osteoblast Proliferation and Survival by Antagonizing Wnt, ERK and PI3K/Akt Signalling. PLoS One *4*, e8284.

He, X., Saint-Jeannet, J.P., Wang, Y., Nathans, J., Dawid, I., and Varmus, H. (1997). A member of the Frizzled protein family mediating axis induction by Wnt-5A. Science *275*, 1652–1654.

He, X., Tamai, K., Semenov, M., Kato, Y., Spokony, R., Liu, C., Katsuyama, Y., Hess, F., and Saint-Jeannet, J.-P. (2000). LDL-receptor-related proteins in Wnt signal transduction. Nature *407*, 530–535.

Helps, N.R., Brewis, N.D., Lineruth, K., Davis, T., Kaiser, K., and Cohen, P.T. (1998). Protein phosphatase 4 is an essential enzyme required for organisation of microtubules at centrosomes in Drosophila embryos. J. Cell Sci. *111 (Pt 10)*, 1331–1340.

Hendriksen, J., Jansen, M., Brown, C.M., van der Velde, H., van Ham, M., Galjart, N., Offerhaus, G.J., Fagotto, F., and Fornerod, M. (2008). Plasma membrane recruitment of dephosphorylated -catenin upon activation of the Wnt pathway. J. Cell Sci. *121*, 1793–1802.

Hendzel, M.J., Wei, Y., Mancini, M.A., Van Hooser, A., Ranalli, T., Brinkley, B.R., Bazett-Jones, D.P., and Allis, C.D. (1997). Mitosis-specific phosphorylation of histone H3 initiates primarily within pericentromeric heterochromatin during G2 and spreads in an ordered fashion coincident with mitotic chromosome condensation. Chromosoma *106*, 348–360.

Herr, P., and Basler, K. (2012). Porcupine-mediated lipidation is required for Wnt recognition by Wls. Dev. Biol. *361*, 392–402.

Herzig, M., Savarese, F., Novatchkova, M., Semb, H., and Christofori, G. (2007). Tumor progression induced by the loss of E-cadherin independent of β-catenin/Tcf-mediated Wnt signaling. Oncogene *26*, 2290–2298.

Heuberger, J., and Birchmeier, W. (2010). Interplay of Cadherin-Mediated Cell Adhesion and Canonical Wnt Signaling. Cold Spring Harb. Perspect. Biol. *2*, a002915–a002915.

van den Heuvel, M., Harryman-Samos, C., Klingensmith, J., Perrimon, N., and Nusse, R. (1993). Mutations in the segment polarity genes wingless and porcupine impair secretion of the wingless protein. EMBO J. *12*, 5293–5302.

Hikasa, H., and Sokol, S.Y. (2011). Phosphorylation of TCF Proteins by Homeodomain-interacting Protein Kinase 2. J. Biol. Chem. *286*, 12093–12100.

Hikasa, H., Ezan, J., Itoh, K., Li, X., Klymkowsky, M.W., and Sokol, S.Y. (2010). Regulation of TCF3 by Wnt-Dependent Phosphorylation during Vertebrate Axis Specification. Dev. Cell *19*, 521–532.

Hing, H.K., Sun, X., and Artavanis-Tsakonas, S. (1994). Modulation of wingless signaling by Notch in Drosophila. Mech. Dev. *47*, 261–268.

Hirata, N., Takahashi, M., and Yazawa, M. (2009). Diphosphorylation of regulatory light chain of myosin IIA is responsible for proper cell spreading. Biochem. Biophys. Res. Commun. *381*, 682–687.

Holmen, S.L., Robertson, S.A., Zylstra, C.R., and Williams, B.O. (2005). Wnt-independent activation of β-catenin mediated by a Dkk1-Fz5 fusion protein. Biochem. Biophys. Res. Commun. *328*, 533–539.

Hong, S., Troyanovsky, R.B., and Troyanovsky, S.M. (2013). Binding to F-actin guides cadherin cluster assembly, stability, and movement. J. Cell Biol. *201*, 131–143.

Hoppler, S., and Bienz, M. (1995). Two different thresholds of wingless signalling with distinct developmental consequences in the Drosophila midgut. EMBO J. *14*, 5016–5026.

Hoschuetzky, H., Aberle, H., and Kemler, R. (1994). Beta-catenin mediates the interaction of the cadherin-catenin complex with epidermal growth factor receptor. J. Cell Biol. *127*, 1375–1380.

Hsieh, J.C., Kodjabachian, L., Rebbert, M.L., Rattner, A., Smallwood, P.M., Samos, C.H., Nusse, R., Dawid, I.B., and Nathans, J. (1999). A new secreted protein that binds to Wnt proteins and inhibits their activities. Nature *398*, 431–436.

Huang, J., and Xue, L. (2015). Loss of flfl Triggers JNK-Dependent Cell Death in Drosophila. Biomed Res. Int. *2015*, 623573.

Huang, X., Liu, J., Shen, T., Meng, X., Dou, L., Lin, Y., and Li, J. (2016). Protein phosphatase 4 plays dual roles during cell proliferation. Cell Prolif. *49*, 219–235.

Huber, A.H., and Weis, W.I. (2001). The structure of the beta-catenin/E-cadherin complex and the molecular basis of diverse ligand recognition by beta-catenin. Cell *105*, 391–402.

Huber, A.H., Stewart, D.B., Laurents, D. V., Nelson, W.J., and Weis, W.I. (2001). The Cadherin Cytoplasmic Domain Is Unstructured in the Absence of β-Catenin. J. Biol. Chem. *276*, 12301–12309.

Hunter, T. (2012). Why nature chose phosphate to modify proteins. Philos. Trans. R. Soc. B Biol. Sci. *367*, 2513–2516.

Huppert, S.S., Jacobsen, T.L., and Muskavitch, M.A. (1997). Feedback regulation is central to Delta-Notch signalling required for Drosophila wing vein morphogenesis. Development *124*, 3283–3291.

Ikeda, S., Kishida, S., Yamamoto, H., Murai, H., Koyama, S., and Kikuchi, A. (1998). Axin, a negative regulator of the Wnt signaling pathway, forms a complex with GSK-3beta and beta-catenin and promotes GSK-3beta-dependent phosphorylation of beta-catenin. EMBO J. *17*, 1371–1384.

Ingber, D.E. (2006a). Cellular mechanotransduction: putting all the pieces together again. FASEB J. *20*, 811–827.

Ingber, D.E. (2006b). Mechanical control of tissue morphogenesis during embryological development. Int. J. Dev. Biol. *50*, 255–266.

Ireton, R.C., Davis, M.A., van Hengel, J., Mariner, D.J., Barnes, K., Thoreson, M.A., Anastasiadis, P.Z., Matrisian, L., Bundy, L.M., Sealy, L., et al. (2002). A novel role for p120 catenin in E-cadherin function. J. Cell Biol. *159*, 465–476.

Ishitani, T., Kishida, S., Hyodo-Miura, J., Ueno, N., Yasuda, J., Waterman, M., Shibuya, H., Moon, R.T., Ninomiya-Tsuji, J., and Matsumoto, K. (2003). The TAK1-NLK mitogen-activated protein kinase cascade functions in the Wnt-5a/Ca(2+) pathway to antagonize Wnt/beta-catenin signaling. Mol. Cell. Biol. *23*, 131–139.

Ishiyama, N., Lee, S.-H., Liu, S., Li, G.-Y., Smith, M.J., Reichardt, L.F., and Ikura, M. (2010). Dynamic and Static Interactions between p120 Catenin and E-Cadherin Regulate the Stability of Cell-Cell Adhesion. Cell *141*, 117–128.

Itasaki, N., and Hoppler, S. (2010). Crosstalk between Wnt and bone morphogenic protein signaling: a turbulent relationship. Dev. Dyn. *239*, 16–33.

Janda, C.Y., Waghray, D., Levin, A.M., Thomas, C., and Garcia, K.C. (2012). Structural basis of Wnt recognition by Frizzled. Science *337*, 59–64.

Janssen, R., Le Gouar, M., Pechmann, M., Poulin, F., Bolognesi, R., Schwager, E.E., Hopfen, C., Colbourne, J.K., Budd, G.E., Brown, S.J., et al. (2010). Conservation, loss, and redeployment of Wnt ligands in protostomes: implications for understanding the evolution of segment formation. BMC Evol. Biol. *10*, 374.

Jia, H., Liu, Y., Yan, W., and Jia, J. (2009). PP4 and PP2A regulate Hedgehog signaling by controlling Smo and Ci phosphorylation. Development *136*, 307–316.

Jo, C., Cho, S.-J., and Jo, S.A. (2011). Mitogen-activated Protein Kinase Kinase 1 (MEK1) Stabilizes MyoD through Direct Phosphorylation at Tyrosine 156 During Myogenic Differentiation. J. Biol. Chem. *286*, 18903–18913.

Johnson, L.N., and Barford, D. (1993). The Effects of Phosphorylation on the Structure and Function of Proteins. Annu. Rev. Biophys. Biomol. Struct. *22*, 199–232.

Jurgens, G., Wieschaus, E., Nusslein-Volhard, C., and Kluding, H. (1984). Mutations affecting the pattern of the larval cuticle inDrosophila melanogaster. Wilhelm Roux's Arch. Dev. Biol. *193*, 283–295.

Kadowaki, T., Wilder, E., Klingensmith, J., Zachary, K., and Perrimon, N. (1996). The segment polarity gene porcupine encodes a putative multitransmembrane protein involved in Wingless processing. Genes Dev. *10*, 3116–3128.

Kadoya, T., Kishida, S., Fukui, A., Hinoi, T., Michiue, T., Asashima, M., and Kikuchi, A. (2000). Inhibition of Wnt Signaling Pathway by a Novel Axin-binding Protein. J. Biol. Chem. *275*, 37030–37037.

Kaemmerer, E., and Gassler, N. (2016). Wnt Lipidation and Modifiers in Intestinal Carcinogenesis and Cancer. Cancers (Basel). *8*.

Kandachar, V., and Roegiers, F. (2012). Endocytosis and control of Notch signaling. Curr. Opin. Cell Biol. *24*, 534–540.

Kao, H.Y., Ordentlich, P., Koyano-Nakagawa, N., Tang, Z., Downes, M., Kintner, C.R., Evans, R.M., and Kadesch, T. (1998). A histone deacetylase corepressor complex regulates the Notch signal transduction pathway. Genes Dev. *12*, 2269–2277.

Karess, R.E., Chang, X.J., Edwards, K.A., Kulkarni, S., Aguilera, I., and Kiehart, D.P. (1991). The regulatory light chain of nonmuscle myosin is encoded by spaghetti-squash, a gene required for cytokinesis in Drosophila. Cell *65*, 1177–1189.

Kassis, J. a, Noll, E., VanSickle, E.P., Odenwald, W.F., and Perrimon, N. (1992). Altering the insertional specificity of a Drosophila transposable element. Proc. Natl. Acad. Sci. U. S. A. *89*, 1919–1923.

Katanaev, V.L., Solis, G.P., Hausmann, G., Buestorf, S., Katanayeva, N., Schrock, Y., Stuermer, C.A.O., and Basler, K. (2008). Reggie-1/flotillin-2 promotes secretion of the long-range signalling forms of Wingless and Hedgehog in Drosophila. EMBO J. *27*, 509–521.

Katoh, M., and Katoh, M. (2017). Molecular genetics and targeted therapy of WNT-related human diseases (Review). Int. J. Mol. Med. *40*, 587–606.

Kazanskaya, O., Glinka, A., del Barco Barrantes, I., Stannek, P., Niehrs, C., and Wu, W. (2004). R-Spondin2 Is a Secreted Activator of Wnt/β-Catenin Signaling and Is Required for Xenopus Myogenesis. Dev. Cell *7*, 525–534.

Khoo, P., Allan, K., Willoughby, L., Brumby, A.M., and Richardson, H.E. (2013). In Drosophila, RhoGEF2 cooperates with activated Ras in tumorigenesis through a pathway involving Rho1-Rok-Myosin-II and JNK signalling. Dis. Model. Mech. *6*, 661–678.

Kikuchi, A., Yamamoto, H., Sato, A., and Matsumoto, S. (2011). New Insights into the Mechanism of Wnt Signaling Pathway Activation. In International Review of Cell and Molecular Biology, pp. 21–71.

Kim, M., and Jho, E.-H. (2014). Cross-talk between Wnt/β-catenin and Hippo signaling pathways: a brief review. BMB Rep. *47*, 540–545.

Kim, M.J., Chia, I. V, and Costantini, F. (2008). SUMOylation target sites at the C terminus protect Axin from ubiquitination and confer protein stability. FASEB J. *22*, 3785–3794.

Kimelman, D., and Xu, W. (2006). beta-catenin destruction complex: insights and questions from a structural perspective. Oncogene *25*, 7482–7491.

Kirchner, J., Gross, S., Bennett, D., and Alphey, L. (2007). The nonmuscle myosin phosphatase PP1beta (flapwing) negatively regulates Jun N-terminal kinase in wing imaginal discs of Drosophila. Genetics *175*, 1741–1749.

Klingensmith, J., Nusse, R., and Perrimon, N. (1994). The Drosophila segment polarity gene dishevelled encodes a novel protein required for response to the wingless signal. Genes Dev. *8*, 118–130.

Knoblich, J.A. (2008). Mechanisms of asymmetric stem cell division. Cell *132*, 583–597.

Kobielak, A., and Fuchs, E. (2004). α-catenin: at the junction of intercellular adhesion and actin dynamics. Nat. Rev. Mol. Cell Biol. *5*, 614–625.

Komekado, H., Yamamoto, H., Chiba, T., and Kikuchi, A. (2007). Glycosylation and palmitoylation of Wnt-3a are coupled to produce an active form of Wnt-3a. Genes to Cells *12*, 521–534.

Korinek, V., Barker, N., Morin, P.J., van Wichen, D., de Weger, R., Kinzler, K.W., Vogelstein, B., and Clevers, H. (1997). Constitutive transcriptional activation by a beta-catenin-Tcf complex in APC-/- colon carcinoma. Science *275*, 1784–1787.

Kramps, T., Peter, O., Brunner, E., Nellen, D., Froesch, B., Chatterjee, S., Murone, M., Züllig, S., and Basler, K. (2002). Wnt/wingless signaling requires BCL9/legless-mediated recruitment of pygopus to the nuclear beta-catenin-TCF complex. Cell *109*, 47–60.

KREBS, E.G., and FISCHER, E.H. (1955). Phosphorylase activity of skeletal muscle extracts. J. Biol. Chem. *216*, 113–120.

Krejci, P., Aklian, A., Kaucka, M., Sevcikova, E., Prochazkova, J., Masek, J.K., Mikolka, P., Pospisilova, T., Spoustova, T., Weis, M., et al. (2012). Receptor tyrosine kinases activate canonical WNT/β-catenin signaling via MAP kinase/LRP6 pathway and direct β-catenin phosphorylation. PLoS One *7*, e35826.

Krüger, R., Kübler, D., Pallissé, R., Burkovski, A., and Lehmann, W.D. (2006). Protein and Proteome Phosphorylation Stoichiometry Analysis by Element Mass Spectrometry. Anal. Chem. *78*, 1987–1994.

Kuo, Y.M., Jones, N., Zhou, B., Panzer, S., Larson, V., and Beckendorf, S.K. (1996). Salivary duct determination in Drosophila: roles of the EGF receptor signalling pathway and the transcription factors fork head and trachealess. Development *122*, 1909–1917.

Kurayoshi, M., Yamamoto, H., Izumi, S., and Kikuchi, A. (2007). Post-translational palmitoylation and glycosylation of Wnt-5a are necessary for its signalling. Biochem. J. *402*, 515–523.

Kusserow, A., Pang, K., Sturm, C., Hrouda, M., Lentfer, J., Schmidt, H.A., Technau, U., von Haeseler, A., Hobmayer, B., Martindale, M.Q., et al. (2005). Unexpected complexity of the Wnt gene family in a sea anemone. Nature *433*, 156–160.

Landsberg, K.P., Farhadifar, R., Ranft, J., Umetsu, D., Widmann, T.J., Bittig, T., Said, A., Jülicher, F., Dahmann, C., Maekawa, M., et al. (2009). Increased cell bond tension governs cell sorting at the Drosophila anteroposterior compartment boundary. Curr. Biol. *19*, 1950–1955.

Langevin, J., Morgan, M.J., Sibarita, J.-B., Aresta, S., Murthy, M., Schwarz, T., Camonis, J., Bellaïche, Y., Tepass, U., Crair, M.C., et al. (2005). Drosophila exocyst components Sec5, Sec6, and Sec15 regulate DE-Cadherin trafficking from recycling endosomes to the plasma membrane. Dev. Cell *9*, 365–376.

Lecuit, T., and Yap, A.S. (2015). E-cadherin junctions as active mechanical integrators in tissue dynamics. Nat. Cell Biol. *17*, 533–539.

Lee, C.-H., Hung, H.-W., Hung, P.-H., and Shieh, Y.-S. (2010). Epidermal growth factor receptor regulates beta-catenin location, stability, and transcriptional activity in oral cancer. Mol. Cancer *9*, 64.

Lee, J.S., Ishimoto, A., and Yanagawa, S. (1999). Characterization of mouse dishevelled (Dvl) proteins in Wnt/Wingless signaling pathway. J. Biol. Chem. *274*, 21464–21470.

LeGoff, L., Rouault, H., and Lecuit, T. (2013). A global pattern of mechanical stress polarizes cell divisions and cell shape in the growing Drosophila wing disc. Development *140*.

Lemmon, M.A., and Schlessinger, J. (2010). Cell signaling by receptor tyrosine kinases. Cell *141*, 1117–1134.

Li, X., Yost, H.J., Virshup, D.M., and Seeling, J.M. (2001). Protein phosphatase 2A and its B56 regulatory subunit inhibit Wnt signaling in Xenopus. EMBO J. *20*, 4122–4131.

Liu, C., Li, Y., Semenov, M., Han, C., Baeg, G.-H., Tan, Y., Zhang, Z., Lin, X., and He, X. (2002). Control of β-Catenin Phosphorylation/Degradation by a Dual-Kinase Mechanism. Cell *108*, 837–847.

Lu, W., Yamamoto, V., Ortega, B., and Baltimore, D. (2004). Mammalian Ryk Is a Wnt Coreceptor Required for Stimulation of Neurite Outgrowth. Cell *119*, 97–108.

Luo, W., Peterson, A., Garcia, B.A., Coombs, G., Kofahl, B., Heinrich, R., Shabanowitz, J., Hunt, D.F., Yost, H.J., and Virshup, D.M. (2007). Protein phosphatase 1 regulates assembly and function of the β-catenin degradation complex. EMBO J. *26*, 1511–1521.

MacDonald, B.T., Yokota, C., Tamai, K., Zeng, X., and He, X. (2008). Wnt signal amplification via activity, cooperativity, and regulation of multiple intracellular PPPSP motifs in the Wnt co-receptor LRP6. J. Biol. Chem. *283*, 16115–16123.

Maher, M.T., Flozak, A.S., Stocker, A.M., Chenn, A., and Gottardi, C.J. (2009). Activity of the beta-catenin phosphodestruction complex at cell-cell contacts is enhanced by cadherin-based adhesion. J. Cell Biol. *186*, 219–228.

Mansour, S.J., Matten, W.T., Hermann, A.S., Candia, J.M., Rong, S., Fukasawa, K., Vande Woude, G.F., and Ahn, N.G. (1994). Transformation of mammalian cells by constitutively active MAP kinase kinase. Science *265*, 966–970.

Martín-Blanco, E., Gampel, A., Ring, J., Virdee, K., Kirov, N., Tolkovsky, A.M., and Martinez-Arias, A. (1998). puckered encodes a phosphatase that mediates a feedback loop regulating JNK activity during dorsal closure in Drosophila. Genes Dev. *12*, 557–570.

Martín-Blanco, E., Roch, F., Noll, E., Baonza, A., Duffy, J.B., and Perrimon, N. (1999). A temporal switch in DER signaling controls the specification and differentiation of veins and interveins in the Drosophila wing. Development *126*, 5739–5747.

Martin-Granados, C., Philp, A., Oxenham, S.K., Prescott, A.R., and Cohen, P.T.W. (2008). Depletion of protein phosphatase 4 in human cells reveals essential roles in centrosome maturation, cell migration and the regulation of Rho GTPases. Int. J. Biochem. Cell Biol. *40*, 2315–2332.

Marygold, S.J., and Vincent, J.-P. (2003). Armadillo levels are reduced during mitosis in Drosophila. Mech. Dev. *120*, 157–165.

Masiakowski, P., and Carroll, R.D. (1992). A novel family of cell surface receptors with tyrosine kinase-like domain. J. Biol. Chem. *267*, 26181–26190.

McCrea, P.D., Turck, C.W., and Gumbiner, B. (1991). A homolog of the armadillo protein in Drosophila (plakoglobin) associated with E-cadherin. Science *254*, 1359–1361.

McMahon, A.P., and Moon, R.T. (1989). Ectopic expression of the proto-oncogene int-1 in Xenopus embryos leads to duplication of the embryonic axis. Cell *58*, 1075–1084.

Mendez, M.G., and Janmey, P.A. (2012). Transcription factor regulation by mechanical stress. Int. J. Biochem. Cell Biol. *44*, 728–732.

Mendoza, M.C., Booth, E.O., Shaulsky, G., and Firtel, R.A. (2007). MEK1 and Protein Phosphatase 4 Coordinate Dictyostelium Development and Chemotaxis. Mol. Cell. Biol. *27*, 3817–3827.

Meng, W., Mushika, Y., Ichii, T., and Takeichi, M. (2008). Anchorage of Microtubule Minus Ends to Adherens Junctions Regulates Epithelial Cell-Cell Contacts. Cell *135*, 948–959.

Metcalfe, C., Mendoza-Topaz, C., Mieszczanek, J., and Bienz, M. (2010). Stability elements in the LRP6 cytoplasmic tail confer efficient signalling upon DIX-dependent polymerization. J. Cell Sci. *123*, 1588–1599.

Mihindukulasuriya, K.A., Zhou, G., Qin, J., and Tan, T.-H. (2004). Protein Phosphatase 4 Interacts with and Down-regulates Insulin Receptor Substrate 4 following Tumor Necrosis Factor- Stimulation. J. Biol. Chem. *279*, 46588–46594.

Mikels, A.J., and Nusse, R. (2006). Purified Wnt5a protein activates or inhibits beta-catenin-TCF signaling depending on receptor context. PLoS Biol. *4*, e115.

Molenaar, M., van de Wetering, M., Oosterwegel, M., Peterson-Maduro, J., Godsave, S., Korinek, V., Roose, J., Destrée, O., and Clevers, H. (1996). XTcf-3 transcription factor mediates beta-catenin-induced axis formation in Xenopus embryos. Cell *86*, 391–399.

Moon, R.T., Slusarski, D.C., and Corces, V.G. (1997). Interaction of Wnt and a Frizzled homologue triggers G-protein-linked phosphatidylinositol signalling. Nature *390*, 410–413.

Morrell, N.T., Leucht, P., Zhao, L., Kim, J.-B., ten Berge, D., Ponnusamy, K., Carre, A.L., Dudek, H., Zachlederova, M., McElhaney, M., et al. (2008). Liposomal Packaging Generates Wnt Protein with In Vivo Biological Activity. PLoS One *3*, e2930.

Morris, S.-A.L., and Huang, S. (2016). Crosstalk of the Wnt/β-catenin pathway with other pathways in cancer cells. Genes Dis. *3*, 41–47.

Mosimann, C., Hausmann, G., and Basler, K. (2006). Parafibromin/Hyrax Activates Wnt/Wg Target Gene Transcription by Direct Association with β-catenin/Armadillo. Cell *125*, 327–341.

Mosimann, C., Hausmann, G., and Basler, K. (2009). β-Catenin hits chromatin: regulation of Wnt target gene activation. Nat. Rev. Mol. Cell Biol. *10*, 276–286.

Murthy, K., Wadsworth, P., Marquis, H., Hostos, E.L. de, Nelson, W.J., Roques, S., Martel, V., Breton-Douillon, M., Perret, B., and Chap, H. (2005). Myosin-II-Dependent Localization and Dynamics of F-Actin during Cytokinesis. Curr. Biol. *15*, 724–731.

Nagafuchi, A., and Takeichi, M. (1989). Transmembrane control of cadherin-mediated cell adhesion: a 94 kDa protein functionally associated with a specific region of the cytoplasmic domain of E-cadherin. Cell Regul. *1*, 37–44.

Najdi, R., Holcombe, R.F., and Waterman, M.L. (2011). Wnt signaling and colon carcinogenesis: beyond APC. J. Carcinog. *10*, 5.

Nam, J.-S., Turcotte, T.J., Smith, P.F., Choi, S., and Yoon, J.K. (2006). Mouse Cristin/R-spondin Family Proteins Are Novel Ligands for the Frizzled 8 and LRP6 Receptors and Activate β-Catenin-dependent Gene Expression. J. Biol. Chem. *281*, 13247–13257.

Neumann, C.J., and Cohen, S.M. (1996). A hierarchy of cross-regulation involving Notch, wingless, vestigial and cut organizes the dorsal/ventral axis of the Drosophila wing. Development *122*, 3477–3485.

Neumann, C.J., and Cohen, S.M. (1997). Long-range action of Wingless organizes the dorsal-ventral axis of the Drosophila wing. Development *124*, 871–880.

Niehrs, C., Glinka, A., Wu, W., Delius, H., Monaghan, A.P., and Blumenstock, C. (1998). Dickkopf-1 is a member of a new family of secreted proteins and functions in head induction. Nature *391*, 357–362.

Nienhaus, U., Aegerter-Wilmsen, T., and Aegerter, C.M. (2009). Determination of mechanical stress distribution in Drosophila wing discs using photoelasticity. Mech. Dev.

Nolo, R., Abbott, L.A., and Bellen, H.J. (2000). Senseless, a Zn finger transcription factor, is necessary and sufficient for sensory organ development in Drosophila. Cell *102*, 349–362.

Noordermeer, J., Klingensmith, J., Perrimon, N., and Nusse, R. (1994). dishevelled and armadillo act in the Wingless signalling pathway in Drosophila. Nature *367*, 80–83.

Nusse, R., and Varmus, H. (2012). Three decades of Wnts: a personal perspective on how a scientific field developed. EMBO J. *31*, 2670–2684.

Nusse, R., and Varmus, H.E. (1982). Many tumors induced by the mouse mammary tumor virus contain a provirus integrated in the same region of the host genome. Cell *31*, 99–109.

Nusse, R., Brown, A., Papkoff, J., Scambler, P., Shackleford, G., McMahon, A., Moon, R., and Varmus, H. (1991). A new nomenclature for int-1 and related genes: the Wnt gene family. Cell *64*, 231.

Nusslein-Volhard, C., Wieschaus, E., and Kluding, H. (1984). Mutations affecting the pattern of the larval cuticle inDrosophila melanogaster. Wilhelm Roux's Arch. Dev. Biol. *193*, 267–282.

Nüsslein-Volhard, C., and Wieschaus, E. (1980). Mutations affecting segment number and polarity in Drosophila. Nature *287*, 795–801.

O'Connell, M.P., Fiori, J.L., Baugher, K.M., Indig, F.E., French, A.D., Camilli, T.C., Frank, B.P., Earley, R., Hoek, K.S., Hasskamp, J.H., et al. (2009). Wnt5A Activates the Calpain-Mediated Cleavage of Filamin A. J. Invest. Dermatol. *129*, 1782–1789.

Oldham, S., Stocker, H., Laffargue, M., Wittwer, F., Wymann, M., and Hafen, E. (2002). The Drosophila insulin/IGF receptor controls growth and size by modulating PtdInsP(3) levels. Development *129*, 4103–4109.

Oloumi, A., Syam, S., and Dedhar, S. (2006). Modulation of Wnt3a-mediated nuclear β-catenin accumulation and activation by integrin-linked kinase in mammalian cells. Oncogene *25*, 7747–7757.

Orsulic, S., and Peifer, M. (1996). An in vivo structure-function study of armadillo, the beta-catenin homologue, reveals both separate and overlapping regions of the protein required for cell adhesion and for wingless signaling. J. Cell Biol. *134*, 1283–1300.

Ota, S., Ishitani, S., Shimizu, N., Matsumoto, K., Itoh, M., and Ishitani, T. (2012). NLK positively regulates Wnt/β-catenin signalling by phosphorylating LEF1 in neural progenitor cells. EMBO J. *31*, 1904–1915.

Ozawa, M., Baribault, H., and Kemler, R. (1989). The cytoplasmic domain of the cell adhesion molecule uvomorulin associates with three independent proteins structurally related in different species. EMBO J. *8*, 1711–1717.

Pacquelet, A., Lin, L., and Rørth, P. (2003). Binding site for p120/δ-catenin is not required for *Drosophila* E-cadherin function in vivo. J. Cell Biol. *160*, 313–319.

Pai, L.M., Orsulic, S., Bejsovec, A., and Peifer, M. (1997). Negative regulation of Armadillo, a Wingless effector in Drosophila. Development *124*.

Panáková, D., Sprong, H., Marois, E., Thiele, C., and Eaton, S. (2005). Lipoprotein particles are required for Hedgehog and Wingless signalling. Nature *435*, 58–65.

Parker, D.S., Jemison, J., and Cadigan, K.M. (2002). Pygopus, a nuclear PHD-finger protein required for Wingless signaling in Drosophila. Development *129*.

Paul, I., Bhattacharya, S., Chatterjee, A., and Ghosh, M.K. (2013). Current Understanding on EGFR and Wnt/β-Catenin Signaling in Glioma and Their Possible Crosstalk. Genes Cancer *4*, 427–446.

Peifer, M., and Wieschaus, E. (1990). The segment polarity gene armadillo encodes a functionally modular protein that is the Drosophila homolog of human plakoglobin. Cell *63*, 1167–1176.

Peifer, M., Rauskolb, C., Williams, M., Riggleman, B., and Wieschaus, E. (1991). The segment polarity gene armadillo interacts with the wingless signaling pathway in both embryonic and adult pattern formation. Development *111*, 1029–1043.

Peifer, M., Pai, L.-M., and Casey, M. (1994). Phosphorylation of the Drosophila Adherens Junction Protein Armadillo: Roles for Wingless Signal and Zeste-white 3 Kinase. Dev. Biol. *166*, 543–556.

Perrimon, N., and Lin, X. (1999). Dally cooperates with Drosophila Frizzled 2 to transduce Wingless signalling. Nature *400*, 281–284.

Peters, J.M., McKay, R.M., McKay, J.P., and Graff, J.M. (1999). Casein kinase I transduces Wnt signals. Nature *401*, 345–350.

Phillips, R.G., and Whittle, J.R. (1993). wingless expression mediates determination of peripheral nervous system elements in late stages of Drosophila wing disc development. Development *118*, 427–438.

Port, F., and Basler, K. (2010). Wnt trafficking: new insights into Wnt maturation, secretion and spreading. Traffic *11*, 1265–1271.

Port, F., Hausmann, G., and Basler, K. (2011). A genome-wide RNA interference screen uncovers two p24 proteins as regulators of Wingless secretion. EMBO Rep. *12*, 1144–1152.

Posakony, J.W. (1994). Nature versus nurture: asymmetric cell divisions in Drosophila bristle development. Cell *76*, 415–418.

Przybyla, L., Lakins, J.N., and Weaver, V.M. (2016). Tissue Mechanics Orchestrate Wnt-Dependent Human Embryonic Stem Cell Differentiation. Cell Stem Cell *19*, 462–475.

Qian, D., Jones, C., Rzadzinska, A., Mark, S., Zhang, X., Steel, K.P., Dai, X., and Chen, P. (2007). Wnt5a functions in planar cell polarity regulation in mice. Dev. Biol. *306*, 121–133.

Raught, B., Gingras, A.-C., and Sonenberg, N. (2001). The target of rapamycin (TOR) proteins. Proc. Natl. Acad. Sci. *98*, 7037–7044.

Rauskolb, C., Sun, S., Sun, G., Pan, Y., and Irvine, K.D. (2014). Cytoskeletal tension inhibits Hippo signaling through an Ajuba-Warts complex. Cell *158*, 143–156.

Rebay, I., Fehon, R.G., and Artavanis-Tsakonas, S. (1993). Specific truncations of Drosophila Notch define dominant activated and dominant negative forms of the receptor. Cell *74*, 319–329.

Rijsewijk, F., Schuermann, M., Wagenaar, E., Parren, P., Weigel, D., and Nusse, R. (1987). The Drosophila homolog of the mouse mammary oncogene int-1 is identical to the segment polarity gene wingless. Cell *50*, 649–657.

Rimm, D.L., Koslov, E.R., Kebriaei, P., Cianci, C.D., and Morrow, J.S. (1995). Alpha 1(E)-catenin is an actin-binding and -bundling protein mediating the attachment of F-actin to the membrane adhesion complex. Proc. Natl. Acad. Sci. U. S. A. *92*, 8813–8817.

Rodriguez, J., Esteve, P., Weinl, C., Ruiz, J.M., Fermin, Y., Trousse, F., Dwivedy, A., Holt, C., and Bovolenta, P. (2005). SFRP1 regulates the growth of retinal ganglion cell axons through the Fz2 receptor. Nat. Neurosci. *8*, 1301–1309.

Rodríguez, D. del A., Terriente, J., Galindo, M.I., Couso, J.P., and Díaz-Benjumea, F.J. (2002). Different mechanisms initiate and maintain wingless expression in the Drosophila wing hinge. Development *129*, 3995–4004.

Rothbächer, U., Laurent, M.N., Deardorff, M.A., Klein, P.S., Cho, K.W., and Fraser, S.E. (2000). Dishevelled phosphorylation, subcellular localization and multimerization regulate its role in early embryogenesis. EMBO J. *19*, 1010–1022.

Roux, K.J., Kim, D.I., and Burke, B. (2013). BioID: A Screen for Protein-Protein Interactions. In Current Protocols in Protein Science, (Hoboken, NJ, USA: John Wiley & Sons, Inc.), p. 19.23.1-19.23.14.

Rubinfeld, B., Souza, B., Albert, I., Müller, O., Chamberlain, S.H., Masiarz, F.R., Munemitsu, S., and Polakis, P. (1993). Association of the APC gene product with beta-catenin. Science *262*, 1731–1734.

Rulifson, E.J., and Blair, S.S. (1995). Notch regulates wingless expression and is not required for reception of the paracrine wingless signal during wing margin neurogenesis in Drosophila. Development *121*, 2813–2824.

Salomon, D., Sacco, P.A., Roy, S.G., Simcha, I., Johnson, K.R., Wheelock, M.J., and Ben-Ze'ev, A. (1997). Regulation of beta-catenin levels and localization by overexpression of plakoglobin and inhibition of the ubiquitin-proteasome system. J. Cell Biol. *139*, 1325–1335.

Samuel, M.S., Lopez, J.I., McGhee, E.J., Croft, D.R., Strachan, D., Timpson, P., Munro, J., Schröder, E., Zhou, J., Brunton, V.G., et al. (2011). Actomyosin-Mediated Cellular Tension Drives Increased Tissue Stiffness and β-Catenin Activation to Induce Epidermal Hyperplasia and Tumor Growth. Cancer Cell *19*, 776–791.

Sanson, B., White, P., and Vincent, J.-P. (1996). Uncoupling cadherin-based adhesion from wingless signalling in Drosophila. Nature *383*, 627–630.

Sarrazin, S., Lamanna, W.C., and Esko, J.D. (2011). Heparan sulfate proteoglycans. Cold Spring Harb. Perspect. Biol. *3*.

Schatoff, E.M., Leach, B.I., and Dow, L.E. (2017). WNT Signaling and Colorectal Cancer. Curr. Colorectal Cancer Rep. *13*, 101–110.

Schlessinger, K., Hall, A., and Tolwinski, N. (2009). Wnt signaling pathways meet Rho GTPases. Genes Dev. *23*, 265–277.

Schmidt-Ott, U., and Technau, G.M. (1992). Expression of en and wg in the embryonic head and brain of Drosophila indicates a refolded band of seven segment remnants. Development *116*, 111–125.

Schwartz, M.A. (2010). Integrins and extracellular matrix in mechanotransduction. Cold Spring Harb. Perspect. Biol. *2*, a005066.

Schwarz-Romond, T., Fiedler, M., Shibata, N., Butler, P.J.G., Kikuchi, A., Higuchi, Y., and Bienz, M. (2007). The DIX domain of Dishevelled confers Wnt signaling by dynamic polymerization. Nat. Struct. Mol. Biol. *14*, 484–492.

Sebolt-Leopold, J.S. (2008). Advances in the Development of Cancer Therapeutics Directed against the RAS-Mitogen-Activated Protein Kinase Pathway. Clin. Cancer Res. *14*.

Seeling, J.M., Miller, J.R., Gil, R., Moon, R.T., White, R., and Virshup, D.M. (1999). Regulation of beta-catenin signaling by the B56 subunit of protein phosphatase 2A. Science *283*, 2089–2091.

Semënov, M. V, Tamai, K., Brott, B.K., Kühl, M., Sokol, S., and He, X. (2001). Head inducer Dickkopf-1 is a ligand for Wnt coreceptor LRP6. Curr. Biol. *11*, 951–961.

Sharma, R.P., and Chopra, V.L. (1976). Effect of the Wingless (wg1) mutation on wing and haltere development in Drosophila melanogaster. Dev. Biol. *48*, 461–465.

Sheehy, S.P., and Parker, K.K. (2011). The Role of Mechanical Forces in Guiding Tissue Differentiation. In Tissue Engineering in Regenerative Medicine, (Totowa, NJ: Humana Press), pp. 77–97.

Shilo, B. (2003). Signaling by the Drosophila epidermal growth factor receptor pathway during development. Exp. Cell Res. *284*, 140–149.

Siegfried, E., Wilder, E.L., and Perrimon, N. (1994). Components of wingless signalling in Drosophila. Nature *367*, 76–80.

Skarnes, W.C., Pinson, K.I., Brennan, J., Monkley, S., and Avery, B.J. (2000). An LDL-receptor-related protein mediates Wnt signalling in mice. Nature *407*, 535–538.

Smith, C.A., Lau, K.M., Rahmani, Z., Dho, S.E., Brothers, G., She, Y.M., Berry, D.M., Bonneil, E., Thibault, P., Schweisguth, F., et al. (2007). aPKC-mediated phosphorylation regulates asymmetric membrane localization of the cell fate determinant Numb. EMBO J. *26*, 468–480.

Song, L., Li, Z.-Y., Liu, W.-P., and Zhao, M.-R. (2015). Crosstalk between Wnt/β-catenin and Hedgehog/Gli signaling pathways in colon cancer and implications for therapy. Cancer Biol. Ther. *16*, 1–7.

Sonoda, J., Pei, L., and Evans, R.M. (2008). Nuclear receptors: decoding metabolic disease. FEBS Lett. *582*, 2–9.

Sopko, R., and Perrimon, N. (2013). Receptor tyrosine kinases in Drosophila development. Cold Spring Harb. Perspect. Biol. *5*.

Sousa-Nunes, R., Chia, W., and Somers, W.G. (2009). Protein Phosphatase 4 mediates localization of the Miranda complex during Drosophila neuroblast asymmetric divisions. Genes Dev. *23*, 359–372.

Sturtevant, M.A., Roark, M., and Bier, E. (1993). The Drosophila rhomboid gene mediates the localized formation of wing veins and interacts genetically with components of the EGF-R signaling pathway. Genes Dev. *7*, 961–973.

Su, L.K., Vogelstein, B., and Kinzler, K.W. (1993). Association of the APC tumor suppressor protein with catenins. Science *262*, 1734–1737.

Su, Y., Fu, C., Ishikawa, S., Stella, A., Kojima, M., Shitoh, K., Schreiber, E.M., Day, B.W., and Liu, B. (2008). APC Is Essential for Targeting Phosphorylated β-Catenin to the SCFβ-TrCP Ubiquitin Ligase. Mol. Cell *32*, 652–661.

Sun, J., and Jin, T. (2008). Both Wnt and mTOR signaling pathways are involved in insulin-stimulated proto-oncogene expression in intestinal cells. Cell. Signal. *20*, 219–229.

Sun, J., Khalid, S., Rozakis-Adcock, M., Fantus, I.G., and Jin, T. (2009). P-21-activated protein kinase-1 functions as a linker between insulin and Wnt signaling pathways in the intestine. Oncogene *28*, 3132–3144.

Sun, J., Wang, D., and Jin, T. (2010). Insulin alters the expression of components of the Wnt signaling pathway including TCF-4 in the intestinal cells. Biochim. Biophys. Acta *1800*, 344–351.

Sun, T.-Q., Lu, B., Feng, J.-J., Reinhard, C., Jan, Y.N., Fantl, W.J., and Williams, L.T. (2001). PAR-1 is a Dishevelled-associated kinase and a positive regulator of Wnt signalling. Nat. Cell Biol. *3*, 628–636.

Sun, Y., Chen, C.S., and Fu, J. (2012). Forcing stem cells to behave: a biophysical perspective of the cellular microenvironment. Annu. Rev. Biophys. *41*, 519–542.

Swarup, S., and Verheyen, E.M. (2012). Wnt/Wingless signaling in Drosophila. Cold Spring Harb. Perspect. Biol. *4*.

Swarup, S., Pradhan-Sundd, T., and Verheyen, E.M. (2015). Genome-wide identification of phospho-regulators of Wnt signaling in Drosophila. Development *142*, 1502–1515.

Tai, D., Wells, K., Arcaroli, J., Vanderbilt, C., Aisner, D.L., Messersmith, W.A., and Lieu, C.H. (2015). Targeting the WNT Signaling Pathway in Cancer Therapeutics. Oncologist *20*, 1189–1198.

Takada, R., Satomi, Y., Kurata, T., Ueno, N., Norioka, S., Kondoh, H., Takao, T., and Takada, S. (2006). Monounsaturated Fatty Acid Modification of Wnt Protein: Its Role in Wnt Secretion. Dev. Cell *11*, 791–801.

Takahashi-Yanaga, F., Shiraishi, F., Hirata, M., Miwa, Y., Morimoto, S., and Sasaguri, T. (2004). Glycogen synthase kinase-3beta is tyrosine-phosphorylated by MEK1 in human skin fibroblasts. Biochem. Biophys. Res. Commun. *316*, 411–415.

Talora, C., Campese, A.F., Bellavia, D., Felli, M.P., Vacca, A., Gulino, A., and Screpanti, I. (2008). Notch signaling and diseases: An evolutionary journey from a simple beginning to complex outcomes. Biochim. Biophys. Acta - Mol. Basis Dis. *1782*, 489–497.

Tamai, K., Zeng, X., Liu, C., Zhang, X., Harada, Y., Chang, Z., and He, X. (2004). A mechanism for Wnt coreceptor activation. Mol. Cell *13*, 149–156.

Tanaka, K., Kitagawa, Y., and Kadowaki, T. (2002). Drosophila Segment Polarity Gene Product Porcupine Stimulates the Posttranslational N-Glycosylation of Wingless in the Endoplasmic Reticulum. J. Biol. Chem. *277*, 12816–12823.

Tang, X., Fan, X., and Lin, X. (2011). Regulation of Wnt Secretion and Distribution. In Targeting the Wnt Pathway in Cancer, (New York, NY: Springer New York), pp. 19–33.

Tang, X., Wu, Y., Belenkaya, T.Y., Huang, Q., Ray, L., Qu, J., and Lin, X. (2012). Roles of N-glycosylation and lipidation in Wg secretion and signaling. Dev. Biol. *364*, 32–41.

Tang, Z., Dai, S., He, Y., Doty, R.A., Shultz, L.D., Sampson, S.B., and Dai, C. (2015). MEK Guards Proteome Stability and Inhibits Tumor-Suppressive Amyloidogenesis via HSF1. Cell *160*, 729–744.

Taniue, K., Nishida, A., Hamada, F., Sugie, A., Oda, T., Ui-Tei, K., Tabata, T., and Akiyama, T. (2010). Sunspot, a link between Wingless signaling and endoreplication in Drosophila. Development *137*, 1755–1764.

Tauriello, D.V.F., and Maurice, M.M. (2010). The various roles of ubiquitin in Wnt pathway regulation. Cell Cycle *9*, 3724–3733.

Thompson, B., Townsley, F., Rosin-Arbesfeld, R., Musisi, H., and Bienz, M. (2002). A new nuclear component of the Wnt signalling pathway. Nat. Cell Biol. *4*, 367–373.

Torres, V.A., Tapia, J.C., Rodriguez, D.A., Lladser, A., Arredondo, C., Leyton, L., and Quest, A.F.G. (2007). E-cadherin is required for caveolin-1-mediated down-regulation of the inhibitor of apoptosis protein survivin via reduced beta-catenin-Tcf/Lef-dependent transcription. Mol. Cell. Biol. *27*, 7703–7717.

Umbhauer, M., Djiane, A., Goisset, C., Penzo-Méndez, A., Riou, J.F., Boucaut, J.C., and Shi, D.L. (2000). The C-terminal cytoplasmic Lys-thr-X-X-X-Trp motif in frizzled receptors mediates Wnt/beta-catenin signalling. EMBO J. *19*, 4944–4954.

Umetsu, D., Aigouy, B., Aliee, M., Sui, L., Eaton, S., Jülicher, F., and Dahmann, C. (2014). Local Increases in Mechanical Tension Shape Compartment Boundaries by Biasing Cell Intercalations. Curr. Biol. *24*, 1798–1805.

Uren, A., Reichsman, F., Anest, V., Taylor, W.G., Muraiso, K., Bottaro, D.P., Cumberledge, S., and Rubin, J.S. (2000). Secreted frizzled-related protein-1 binds directly to Wingless and is a biphasic modulator of Wnt signaling. J. Biol. Chem. *275*, 4374–4382.

Valenta, T., Hausmann, G., and Basler, K. (2012). The many faces and functions of β-catenin. EMBO J. *31*, 2714–2736.

Vereshchagina, N., Bennett, D., Szöor, B., Kirchner, J., Gross, S., Vissi, E., White-Cooper, H., and Alphey, L. (2004). The essential role of PP1beta in Drosophila is to regulate nonmuscle myosin. Mol. Biol. Cell *15*, 4395–4405.

Verheyen, E.M., and Gottardi, C.J. (2010). Regulation of Wnt/beta-catenin signaling by protein kinases. Dev. Dyn. *239*, 34–44.

Vicente-Manzanares, M., Ma, X., Adelstein, R.S., and Horwitz, A.R. (2009). Non-muscle myosin II takes centre stage in cell adhesion and migration. Nat. Rev. Mol. Cell Biol. *10*, 778–790.

Villarino, A. V, Kanno, Y., Ferdinand, J.R., and O'Shea, J.J. (2015). Mechanisms of Jak/STAT signaling in immunity and disease. J. Immunol. *194*, 21–27.

Vlastaridis, P., Kyriakidou, P., Chaliotis, A., Van de Peer, Y., Oliver, S.G., and Amoutzias, G.D. (2017). Estimating the total number of phosphoproteins and phosphorylation sites in eukaryotic proteomes. Gigascience *6*, 1–11.

Voronkov, A., and Krauss, S. (2013). Wnt/beta-catenin signaling and small molecule inhibitors. Curr. Pharm. Des. *19*, 634–664.

Wang, H., Liu, T., and Malbon, C.C. (2006a). Structure-function analysis of Frizzleds. Cell. Signal. *18*, 934–941.

Wang, H., Somers, G.W., Bashirullah, A., Heberlein, U., Yu, F., and Chia, W. (2006b). Aurora-A acts as a tumor suppressor and regulates self-renewal of Drosophila neuroblasts. Genes Dev. *20*, 3453–3463.

Wang, N., Butler, J.P., and Ingber, D.E. (1993). Mechanotransduction across the cell surface and through the cytoskeleton. Science *260*, 1124–1127.

Wang, S., Krinks, M., Lin, K., Luyten, F.P., and Moos, M. (1997). Frzb, a secreted protein expressed in the Spemann organizer, binds and inhibits Wnt-8. Cell *88*, 757–766.

Weeraratna, A.T., Jiang, Y., Hostetter, G., Rosenblatt, K., Duray, P., Bittner, M., and Trent, J.M. (2002). Wnt5a signaling directly affects cell motility and invasion of metastatic melanoma. Cancer Cell *1*, 279–288.

Wei, Q., Yokota, C., Semenov, M. V., Doble, B., Woodgett, J., and He, X. (2007). R-spondin1 Is a High Affinity Ligand for LRP6 and Induces LRP6 Phosphorylation and β-Catenin Signaling. J. Biol. Chem. *282*, 15903–15911.

van de Wetering, M., Barker, N., Harkes, I.C., van der Heyden, M., Dijk, N.J., Hollestelle, A., Klijn, J.G., Clevers, H., and Schutte, M. (2001). Mutant E-cadherin breast cancer cells do not display constitutive Wnt signaling. Cancer Res. *61*, 278–284.

Whittle, J.R. (1990). Pattern formation in imaginal discs. Semin. Cell Biol. *1*, 241–252.

Widmann, T.J., and Dahmann, C. (2009). Wingless signaling and the control of cell shape in Drosophila wing imaginal discs. Dev. Biol. *334*, 161–173.

Wieschaus, E., Nusslein-Volhard, C., and Jurgens, G. (1984). Mutations affecting the pattern of the larval cuticle inDrosophila melanogaster. Wilhelm Roux's Arch. Dev. Biol. *193*, 296–307.

Willert, K., and Nusse, R. (2012). Wnt proteins. Cold Spring Harb. Perspect. Biol. *4*, a007864.

Willert, K., Brink, M., Wodarz, A., Varmus, H., and Nusse, R. (1997). Casein kinase 2associates with and phosphorylates Dishevelled. EMBO J. *16*, 3089–3096.

Willert, K., Brown, J.D., Danenberg, E., Duncan, A.W., Weissman, I.L., Reya, T., Yates, J.R., and Nusse, R. (2003). Wnt proteins are lipid-modified and can act as stem cell growth factors. Nature *423*, 448–452.

Williams, J.A., Paddock, S.W., and Carroll, S.B. (1993). Pattern formation in a secondary field: a hierarchy of regulatory genes subdivides the developing Drosophila wing disc into discrete subregions. Development *117*, 571–584.

Winston, J.T., Strack, P., Beer-Romero, P., Chu, C.Y., Elledge, S.J., and Harper, J.W. (1999). The SCFbeta-TRCP-ubiquitin ligase complex associates specifically with phosphorylated destruction motifs in IkappaBalpha and beta-catenin and stimulates IkappaBalpha ubiquitination in vitro. Genes Dev. *13*, 270–283.

Wong, L.L., and Adler, P.N. (1993). Tissue polarity genes of Drosophila regulate the subcellular location for prehair initiation in pupal wing cells. J. Cell Biol. *123*, 209–221.

Wong, G.T., Gavin, B.J., and McMahon, A.P. (1994). Differential transformation of mammary epithelial cells by Wnt genes. Mol. Cell. Biol. *14*, 6278–6286.

Wong, H.-C., Bourdelas, A., Krauss, A., Lee, H.-J., Shao, Y., Wu, D., Mlodzik, M., Shi, D.-L., and Zheng, J. (2003). Direct binding of the PDZ domain of Dishevelled to a conserved internal sequence in the C-terminal region of Frizzled. Mol. Cell *12*, 1251–1260.

Wu, G., Xu, G., Schulman, B.A., Jeffrey, P.D., Harper, J.W., and Pavletich, N.P. (2003). Structure of a beta-TrCP1-Skp1-beta-catenin complex: destruction motif binding and lysine specificity of the SCF(beta-TrCP1) ubiquitin ligase. Mol. Cell *11*, 1445–1456.

Wu, S.K., Gomez, G.A., Michael, M., Verma, S., Cox, H.L., Lefevre, J.G., Parton, R.G., Hamilton, N.A., Neufeld, Z., and Yap, A.S. (2014). Cortical F-actin stabilization generates apical-lateral patterns of junctional contractility that integrate cells into epithelia. Nat. Cell Biol. *16*, 167–178.

Wu, X., Tu, X., Joeng, K.S., Hilton, M.J., Williams, D.A., and Long, F. (2008). Rac1 Activation Controls Nuclear Localization of β-catenin during Canonical Wnt Signaling. Cell *133*, 340–353.

Xie, S., and Martin, A.C. (2015). Intracellular signalling and intercellular coupling coordinate heterogeneous contractile events to facilitate tissue folding. Nat. Commun. *6*, 7161.

Xu, C., Kim, N.-G., and Gumbiner, B.M. (2009). Regulation of protein stability by GSK3 mediated phosphorylation. Cell Cycle *8*, 4032–4039.

Xu, Q., Wang, Y., Dabdoub, A., Smallwood, P.M., Williams, J., Woods, C., Kelley, M.W., Jiang, L., Tasman, W., Zhang, K., et al. (2004). Vascular development in the retina and inner ear: control by Norrin and Frizzled-4, a high-affinity ligand-receptor pair. Cell *116*, 883–895.

Yamamoto, H., Kishida, S., Kishida, M., Ikeda, S., Takada, S., and Kikuchi, A. (1999). Phosphorylation of axin, a Wnt signal negative regulator, by glycogen synthase kinase-3beta regulates its stability. J. Biol. Chem. *274*, 10681–10684.

Yanagawa, S., van Leeuwen, F., Wodarz, A., Klingensmith, J., and Nusse, R. (1995). The dishevelled protein is modified by wingless signaling in Drosophila. Genes Dev. *9*, 1087–1097.

Yanfeng, W.A., Berhane, H., Mola, M., Singh, J., Jenny, A., and Mlodzik, M. (2011). Functional dissection of phosphorylation of Disheveled in Drosophila. Dev. Biol. *360*, 132–142.

Yang, E., Tacchelly-Benites, O., Wang, Z., Randall, M.P., Tian, A., Benchabane, H., Freemantle, S., Pikielny, C., Tolwinski, N.S., Lee, E., et al. (2016). Wnt pathway activation by ADP-ribosylation. Nat. Commun. *7*, 11430.

Yang, P.-T., Lorenowicz, M.J., Silhankova, M., Coudreuse, D.Y.M., Betist, M.C., and Korswagen, H.C. (2008). Wnt Signaling Requires Retromer-Dependent Recycling of MIG-14/Wntless in Wnt-Producing Cells.

Yao, M., Qiu, W., Liu, R., Efremov, A.K., Cong, P., Seddiki, R., Payre, M., Lim, C.T., Ladoux, B., Mège, R.-M., et al. (2014). Force-dependent conformational switch of α-catenin controls vinculin binding. Nat. Commun. *5*, 4525.

Yenush, L., and White, M.F. (1997). The IRS-signalling system during insulin and cytokine action. Bioessays *19*, 491–500.

Zallen, J.A. (2007). Planar polarity and tissue morphogenesis. Cell *129*, 1051–1063.

Zecca, M., Basler, K., and Struhl, G. (1996). Direct and long-range action of a wingless morphogen gradient. Cell *87*, 833–844.

Zeller, E., Hammer, K., Kirschnick, M., and Braeuning, A. (2013). Mechanisms of RAS/β-catenin interactions. Arch. Toxicol. *87*, 611–632.

Zeng, L., Fagotto, F., Zhang, T., Hsu, W., Vasicek, T.J., Perry, W.L., Lee, J.J., Tilghman, S.M., Gumbiner, B.M., and Costantini, F. (1997). The Mouse Fused Locus Encodes Axin, an Inhibitor of the Wnt Signaling Pathway That Regulates Embryonic Axis Formation. Cell *90*, 181–192.

Zeng, X., Goetz, J.A., Suber, L.M., Scott, W.J., Schreiner, C.M., and Robbins, D.J. (2001). A freely diffusible form of Sonic hedgehog mediates long-range signalling. Nature *411*, 716–720.

Zeng, X., Tamai, K., Doble, B., Li, S., Huang, H., Habas, R., Okamura, H., Woodgett, J., and He, X. (2005). A dual-kinase mechanism for Wnt co-receptor phosphorylation and activation. Nature *438*, 873–877.

Zeng, X., Huang, H., Tamai, K., Zhang, X., Harada, Y., Yokota, C., Almeida, K., Wang, J., Doble, B., Woodgett, J., et al. (2007). Initiation of Wnt signaling: control of Wnt coreceptor Lrp6 phosphorylation/activation via frizzled, dishevelled and axin functions. Development *135*, 367–375.

Zhang, F., Huang, Z.-X., Bao, H., Cong, F., Wang, H., Chai, P.C., Xi, Y., Ge, W., Somers, W.G., Yang, Y., et al. (2016). Phosphotyrosyl phosphatase activator facilitates localization of Miranda through dephosphorylation in dividing neuroblasts. Development *143*, 35–44.

Zhang, X., Ozawa, Y., Lee, H., Wen, Y.-D., Tan, T.-H., Wadzinski, B.E., and Seto, E. (2005). Histone deacetylase 3 (HDAC3) activity is regulated by interaction with protein serine/threonine phosphatase 4. Genes Dev. *19*, 827–839.

Zhou, G., Mihindukulasuriya, K.A., MacCorkle-Chosnek, R.A., Van Hooser, A., Hu, M.C.-T., Brinkley, B.R., and Tan, T.-H. (2002). Protein Phosphatase 4 Is Involved in Tumor Necrosis Factor- -induced Activation of c-Jun N-terminal Kinase. J. Biol. Chem. *277*, 6391–6398.

Zhuang, X., Semenova, E., Maric, D., and Craigie, R. (2014). Dephosphorylation of Barrier-to-autointegration Factor by Protein Phosphatase 4 and Its Role in Cell Mitosis. J. Biol. Chem. *289*, 1119–1127.

Zimmerman, S.G., Thorpe, L.M., Medrano, V.R., Mallozzi, C.A., and McCartney, B.M. (2010). Apical constriction and invagination downstream of the canonical Wnt signaling pathway require Rho1 and Myosin II. Dev. Biol. *340*, 54–66.